STELLINGEN

behorende bij het proefschrift

CHARACTERIZATION OF DELTAIC ROCKS FOR NUMERICAL RESERVOIR SIMULATION

van

F.C.J. Mijnssen

14 Oktober 1991

STELLING 1: In zijn klassifikatie van deltas onderschat Galloway (1975) het effect van getijde.

GALLOWAY, W.E. (1975) Process framework for describing morphologic and stratigraphic evolution of deltaic depositional systems. In *Deltas, Models for Exploration* (ed by M.L. Broussard), pp. 87-98. Houston Geological Society, Houston.

STELLING 2: Geologische variabiliteit gedraagt zich vooral probabilistisch op de schaal waarop koolwaterstofreservoirs moeten worden beschreven voor numerieke vloeistofsimulaties.

STELLING 3: Statistische interpolatie technieken gebaseerd op de theorie van "regionalized variables" zijn in het algemeen slecht bruikbaar voor het beschrijven van permeabiliteitsverdelingen in koolwaterstofreservoirs.

STELLING 4: Vertikale permeabiliteiten in schaliehoudende zandstenen worden in de methode van Begg, Chang en Haldorsen (1985) berekend met:

$$K_{ve} = \frac{(1 - F_s)\, h^2}{n_s} \sum_{i=1}^{n_s} \frac{K_{ei}}{s_i^2} \qquad (4.1)$$

In deze vergelijking is K_{ve} de effectieve verticale permeabiliteit, F_s de schalie fractie, h de hoogte van het gesteente volume onder beschouwing, n_s het aantal stroomlijnen, K_{ei} de effectieve permeabiliteit van stroomlijn i en s_i de lengte van stroomlijn i Gebruikt men nu, zoals wordt voorgesteld door Begg et al., gemiddelde stroomlijnlengtes, dan geldt:

$$\sum_{i=1}^{n_s} \frac{K_{ei}}{s_i^2} = \sum_{i=1}^{n_s} \frac{K_{ei}}{\bar{s}^2} \qquad (4.2)$$

Bij lage schaliedichtheden zal dit leiden tot een onderschatting van de vertikale permeabiliteit.

BEGG, S.H., CHANG, D.M. & HALDORSEN, H.H. (1985) A simple statistical method for calculating the effective permeability of a reservoir containing discontinuous shales. Paper presented at the 60th Annual Technical Conference and Exhibition of the

Society of Petroleum Engineers held in Las Vegas, Nevada, September 22-25.

STELLING 5: De opmerking van Desbarats (1987) dat de stroombuisbenadering van Begg en King (1985) voor het berekenen van verticale permeabiliteiten in zandsteen/schalie sequenties alleen betrouwbare resultaten geeft in het geval van kleine schaliefracties, dit vanwege de aanname van "noninteractie", is onjuist.

BEGG, S.H. & KING, P.R. (1985) Modelling the effects of shales on reservoir performance: Calculation of effective vertical permeability. Paper presented at the Society of Petroleum Engineers 1985 Reservoir Simulation Symposium held in Dallas, Texas, February 10-13.

DESBARATS, A.J. (1987) Numerical estimation of effective permeability in sand-shale formations. *Water Resources Research*, **23**, 273-286.

STELLING 6: De gepubliceerde schalielengte histogrammen gemeten aan ontsluitingen zijn misleidend, omdat geen rekening is gehouden met de orientatie van de schalies ten opzichte van de orientie van de ontsluiting.

STELLING 7: De verhouding van de volumina clastische en carbonaat sedimenten in de Nederlandse ondergrond is omgekeerd evenredig met het aantal professoren aan nederlandse universiteiten die de sedimentologie van deze afzettingen doceren.

STELLING 8: Door het verhogen van het aantal uren wiskundeonderwijs aan studenten geologie en het aantal veldwerkdagen voor studenten in de mijnbouwkunde en petroleumwinning, zullen de bewezen Nederlandse olie en gasreserves waarschijnlijk evenredig toenemen.

STELLING 9: Eerstejaars wedstrijdroeiers die aan het begin van het studiejaar meer dan 77,5 kg wegen moet worden afgeraden deel te nemen aan de selectie voor lichte ploegen.

STELLING 10: Het selectief contracteren van relatief licht gebouwde coureurs (het zogenaamde klimmerstype) door de grote nederlandse profploegen heeft tot gevolg dat de nederlandse inbreng in de grote ééndaagse koersen (klassiekers) zal afnemen.

CHARACTERIZATION OF DELTAIC ROCKS FOR NUMERICAL RESERVOIR SIMULATION

CHARACTERIZATION OF DELTAIC ROCKS FOR NUMERICAL RESERVOIR SIMULATION

PROEFSCHRIFT

ter verkrijging van de graad van doctor
aan de Technische Universiteit Delft,
op gezag van de Rector Magnificus,
prof. drs P.A. Schenck,
in het openbaar te verdedigen
ten overstaan van een commissie,
aangewezen door het College van Decanen
op maandag 14 oktober te 16.00 uur

door

FRANS CHRISTIAAN JACOBUS MIJNSSEN

geboren te Amsterdam
doctorandus in de wis- en natuurwetenschappen

Dit proefschrift is goedgekeurd door de promotor prof. ir K.J. Weber

CIP-DATA KONINKLIJKE BIBLIOTHEEK, DEN HAAG

Mijnssen, Frans Christiaan Jacobus

Characterization of deltaic rocks for numerical reservoir simulation / Frans Christiaan Jacobus Mijnssen. – [S.L. : s.n.]. – Ill.
Thesis Delft. – with ref. – With summary in Dutch.
ISBN 90-9004418-3
Subject headings: geology / deltas ; reservoir characterization

cover design: Jos Rietstap & Chris Mijnssen
typesetting and layout: Chris Mijnssen
typeset system: Apple Macintosh and Microsoft Word
graphing system: Claris MacDraw
text type: Courier and Symbol

TABLE OF CONTENTS

ACKNOWLEDGEMENT

PREFACE

1. INTRODUCTION 1

1.1 Statement of the problem 1
1.2 Reservoir characterization 2
1.3 Outline of this thesis 5

2. DELTAIC SEDIMENTS 6

2.1 Overall framework for sedimentation in deltaic systems 6
2.1.1 HINTERLAND CHARACTERISTICS 8
2.1.2 RECEIVING BASIN CHARACTERISTICS 9
2.2 Delta types 13
2.2.1 THE DELTA CLASSIFICATION OF FISHER ET AL. (1969) 13
2.2.2 THE DELTA CLASSIFICATION OF COLEMAN AND WRIGHT (1975) 13
2.2.3 THE DELTA CLASSIFICATION OF GALLOWAY (1975) 16
2.2.4 THE DELTA CLASSIFICATION OF SNEIDER, TINKER AND MECKEL (1978) 22
2.2.5 CLASSIFICATION OF DELTA TYPES FOR RESERVOIR CHARACTERIZATION 22
2.3 Genetic units 27
2.3.1 FLUVIAL DOMINATED DELTAS 27
2.3.1.1 Delta front silts and prodelta clays 27
2.3.1.2 Distributary mouth bar sands 29
2.3.1.3 Distributary channel and levees 29
2.3.1.4 Interdistributary bay deposits 30
2.3.2 TIDE-DOMINATED DELTAS 31
2.3.2.1 Prodelta fines 31
2.3.2.2 Tidal sand bar 32

2.3.2.3 Estuarine channel fill 33
2.3.2.4 Tidal flat fines 34
2.3.3 DELTAS WITH FLUVIAL/WAVE/TIDE INTERACTION 35
2.3.3.1 Barrier deposits 35
2.3.3.2 Tidal channel sands 36
2.3.3.3 Tidal flat sediments 37
2.3.4 WAVE DOMINATED DELTAS 37
2.3.4.1 Foreshore 37
2.3.4.2 Strandplain and distributary channel fill 38
2.3.5 DELTAS WITH WAVE/CURRENT INTERACTION 39
2.3.5.1 Distributary mouth bar and beach ridge complex 40
2.3.5.2 Channel fill facies 40
2.3.6 FAN DELTAS 40
2.3.6.1 Distributary channel fill 41
2.3.6.2 Nearshore deposits 42
2.3.6.3 Submarine deposits 42
2.3.7 LACUSTRINE DELTAS 42
2.3.7.1 Distributary mouth bar 43
2.3.7.2 Channel fill and levee sediments 43
2.3.7.3 Interdistributary bay sediments 44
2.4 Composition of deltaic deposits 44
2.4.1 TRAILING EDGE COASTS 46
2.4.2 COLLISION AND MARGINAL SEA COASTS 47
2.4.3 INTERMONTANE BASINS 48
2.5 Common diagenetic patterns in deltaic rocks 48
2.5.1 PHYSICAL DIAGENETIC PROCESSES 49
2.5.2 CHEMICAL DIAGENETIC PROCESSES 49
2.5.2.1 Precipitation 50
2.5.2.2 Dissolution 50
2.5.2.3 Partial dissolution and alteration 52
2.5.2.4 Recrystallization 52
2.5.2.5 The influence of depositional environment on chemical diagenetic processes 53
2.5.3 THE EFFECT OF DIAGENETIC PROCESSES ON POROSITY AND PERMEABILITY 54

3. DESCRIPTION OF RESERVOIR ARCHITECTURE IN DELTAIC ROCKS 62

3.1 Basic types of reservoir architecture in deltaic systems 62

3.2 Description of reservoir architecture 63

3.2.1 RESERVOIR DATA 63

3.2.1.2 Cuttings 65

3.2.1.1 Cores 67

3.2.1.3 Sidewall samples 67

3.2.1.4 Well logs 68

3.2.1.5 Well testing 68

3.2.1.6 Seismic data 69

3.2.2 MODELLING TECHNIQUES 69

3.2.2.1 Deterministic modelling 70

3.2.2.2 Simulating geological processes 72

3.2.2.3 Geostatistical techniques 73

3.3 Developing a knowledge base 98

3.3.1 STRUCTURE OF THE KNOWLEDGE BASE 99

3.3.2 ANALOGUE CRITERIA 99

3.3.3 ANALOGUE TYPES 101

3.4 Case studies 106

3.4.1 THE NORTH MARKHAM-NORTH BAY CITY, A DENSELY DRILLED FIELD 108

3.4.2 THE ATCHAFALAYA DELTA, A RECENT ENVIRONMENT 120

3.4.2.1 Geological setting 120

3.4.2.2 Data extraction 123

3.5 Practical approach to reservoir modelling 125

4. INCORPORATING SEDIMENTOLOGICAL VARIABILITY IN RESERVOIR SIMULATION GRIDS 128

4.1 Sedimentologically defined flow unit configurations for the construction of reservoir models 128

4.2 Sorting trends 139

4.3 Sedimentary structures 140

4.4 Shales 143

4.4.1 DIRECT ESTIMATION OF VERTICAL PERMEABILITY 144

4.4.2 LENGTH OF SHALE BODIES 145
4.4.3 EVALUATION OF PUBLISHED SHALE MODELS 147
4.4.3.1 Shale models with a repetitive pattern 148
4.4.3.2 Shale models with a random pattern 155
4.4.3.3 Comparison and application of shale models 163
4.4.4 EVALUATION OF SHALE MODELS 164
4.4.4.1 Repetitive versus random patterns 164
4.4.4.2 Permeability of shales 164
4.4.4.3 Effect of vertically varying shale densities 165
4.4.4.4 Introduction of a Poisson distribution 166
4.4.4.5 Calculation of streamline lengths 167
4.4.4.6 2-D versus 3-D modelling 168
4.4.4.7 Comparison of calculated streamline lengths with numerical fluid flow simulation 170
4.4.5 VERTICAL PERMEABILITIES IN BIOTURBATED SAND/SHALE SEQUENCES 173
4.4.5.1 Types of bioturbation 174
4.4.5.2 Method for determining vertical permeability in bioturbated sand/shale sequences 174
4.5 Simulation experiments on configurations of common flow units 177
4.5.1 PREVIOUS WORK ON AVERAGING PERMEABILITY 177
4.5.2 PERMEABILITY ANISOTROPIES 178
4.5.2.1 Fine grid simulations 178
4.5.2.2 Results of the simulations using a fine-meshed grid 181
4.5.3 PSEUDO RELATIVE PERMEABILITY AND CAPILLARY PRESSURE CURVES 181
4.5.4 TWO-PHASE FLOW SIMULATIONS ON CONFIGURATIONS OF COMMON FLOW UNITS 184
4.5.5 DISCUSSION 194

5. CONCLUSIONS 196

6. RECOMMENDATIONS 199

NOMENCLATURE 200

REFERENCES 202

ABSTRACT 219

SAMENVATTING 221

CURRICULUM VITAE 223

ACKNOWLEDGEMENT

I thank my supervisor prof.ir K.J. Weber for his guidance during my Ph.D. study and his never failing interest in any of its aspects. I will always remember the stimulating questions he raised and the numerous discussions we had.

I thank drs L. Vasak for his guidance and assistance during my Ph.D. study. I will never forget his support at the moments my research seemed to be at a dead end.

I thank ir F.J.T. Floris for his assistance especially with the mathematical and numerical flow simulation aspects of this thesis.

I thank ir H. Kool, ir J.D.N. Vonck, ir S. Rozendal and ir E.J. Pelt for their M.Sci. work, which was carried out in the framework of my Ph.D. study. Their results form significant contributions to this thesis.

I appreciate the interest of my colleagues at the TNO Institute of Applied Geoscience and my fellow Ph.D. students at the Department of Mining and Petroleum Engineering. The fruitful discussions we had and their comments on my work were very helpful.

I thank Jos Rietstap and Wim Immers for their drafting work, especially for incorporating my last minute changes in Figures 4.28 to 4.34.

I thank the TNO Institute of Applied Geoscience for sponsoring my Ph.D Study.

Finally, special thanks go to my family, friends and of course Elien for their support and patience during my Ph.D. study, especially during the time I wrote this thesis.

PREFACE

The research that I present in this thesis was initiated by the Geo-energy Department of the TNO Institute of Applied Geoscience, because they encountered major problems during the construction of geological models for their reservoir simulation studies. During my study I have focused on most aspects of characterization of reservoir rocks for numerical reservoir simulation. Main emphasis is on deltaic sediments, because these form an important class of hydrocarbon reservoirs. I hope that my work can serve as basis for further research in the area of reservoir characterization.

1. INTRODUCTION

1.1 Statement of the problem

To predict the production behaviour of a hydrocarbon reservoir the fluid flow through the reservoir is often numerically simulated. This numerical simulation has three ingredients:

- *Fluid flow equations*: These can be considered universal. They will not introduce major uncertainties in conventional simulation studies.

- *Fluid properties*: these are constant or vary only regionally through the reservoir. They will not introduce major uncertainties in most simulations.

- *Rock properties*: These can vary rapidly in space. They will introduce major uncertainties in simulation studies.

Because rock properties introduce major uncertainties into reservoir simulation studies, the rock properties must be characterized adequately. Three major problems occur when doing this:

- *Determination of geology from reservoir data*: Only a limited amount of data is available from the reservoir. Most of these data give only indirect information about the rocks present (Figure 1.1).

- *Description of reservoir architecture*: Detailed information on the rock succession is only available at wells in the vertical direction (Figure 1.2).

- *Averaging of geological variability over grid block volumes*: Much geological variation takes place on a much smaller scale than conventional grid block sizes (Figure 1.3).

This thesis will concentrate on the last two problems, the description of reservoir architecture and the averaging of geological variability over grid block volumes. It will focus on deltaic rocks because these frequently contain hydrocarbons and much has already been published on these rocks which can be used as basis for this study.

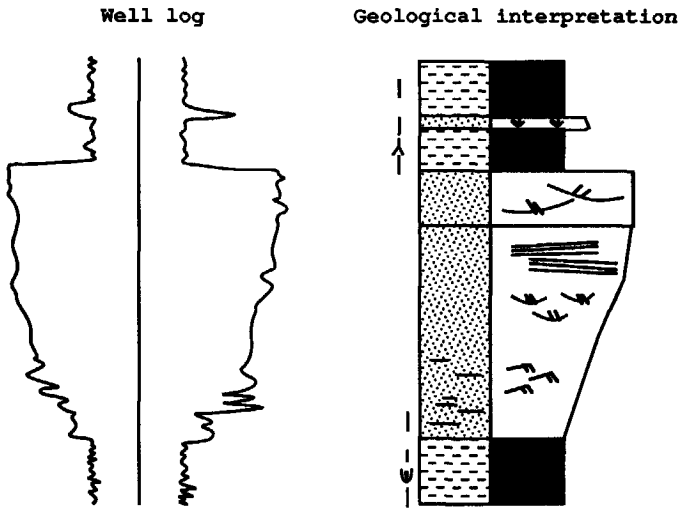

Figure 1.1 Determination of geology from reservoir data.

1.2 Reservoir characterization

Until the late seventies geological characterization of reservoirs was not very important in hydrocarbon production. However, high oil prices and increasingly depleted reservoirs resulted in the

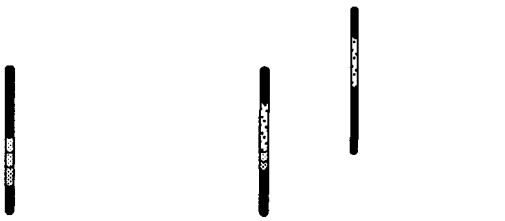

RESERVOIR DATA

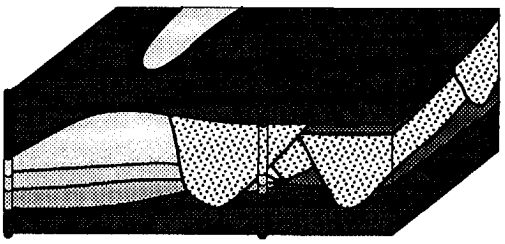

RESERVOIR MODEL

Figure 1.2 Illustration of the limited amount of data from the reservoir that is available for the description of reservoir architecture.

introduction of enhanced oil recovery schemes like steam drive and polymer injection. This in turn resulted in an growing interest in more accurate geological characterizations of hydrocarbon reservoirs. The explosive growth of reservoir characterization research was triggered by the work of Haldorsen (1983) who gave an extensive overview of reservoir characterization procedures. The research concentrated on methods for the stochastic description of reservoir architecture, modelling shales for the calculation of vertical permeability anisotropies and on improving seismic methods for data acquisition. Much of this work was presented at the Reservoir Characterization Technical Conference, April 29-May 1, 1985 and was compiled by Lake and Carroll (1986). After this conference several new lines of research were initiated. It was demonstrated that

sequence-based stochastic techniques[1] had limitations for simply estimating permeability (Tomutsa, Jackson and Szpakiewicz, 1986). Therefore object-based techniques[2] were proposed (i.e. Augedal, Omre and Stanley, 1986). However, it soon became apparent that there are insufficient quantitative geological data to enable accurate reservoir modelling with these techniques. This resulted in various outcrop studies to obtain such data (Flint, Van Rossem and Williams, 1989; Walderhaug and Mjos, 1991; Lowry and Raheim, 1991). Also, techniques were developed to obtain a reservoir description by sequence-based lithofacies estimation (Matheron et al., 1987; Ravenne et al., 1989; Guérillot et al., 1990) and the limits of enhanced data acquisition techniques were investigated (Quint, 1990).

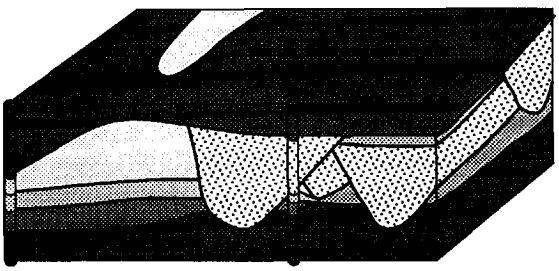

RESERVOIR MODEL

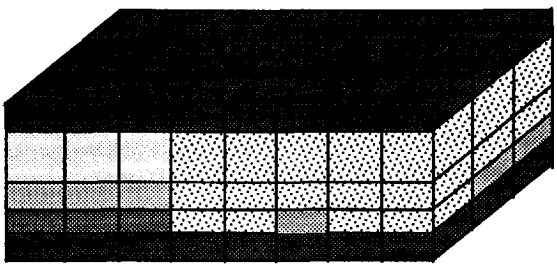

SIMULATION MODEL

Figure 1.3 Translation of a reservoir model into a simulation model.

[1]Sequence-based methods generate values of a property at individual grid blocks, based on statistical information about relationships between values at neighbouring locations (Dubrule, 1989).

[2]Object-based methods generate the distribution of objects (e.g. sand bodies) in space, based on statistical information about the size and shape of these objects (Dubrule, 1989).

1.3 Outline of this thesis

To be able to understand what variability occurs in deltaic depositional systems, this thesis will start with a basic description of sedimentation in such systems. To evaluate the use of reservoir data for geological modelling, an overview is given of the data-acquisition techniques presently used in the development of hydrocarbon reservoirs. Also an analysis is given of the most common techniques for hydrocarbon reservoir modelling to be able to asses which techniques are most appropriate. Finally, to be capable to determine accurate simulator input parameters, those sedimentological characteristics of deltaic rocks are studied which have the most impact on fluid flow.

2. DELTAIC SEDIMENTS

2.1 Overall framework for sedimentation in deltaic systems

To make it easier to understand how modern and ancient deltas vary, the interactions between the variables that control the development of deltas and define causal relationships between these variables must be summarized in a framework (Elliott, 1986). The framework adopted in this chapter regards delta regime as a general expression of the overall setting and relates this regime to the delta's morphology and distribution of sediments (Figure 2.1).

The variables affecting deltas stem from the characteristics of the hinterland and receiving basin (Elliott, 1986). Since hinterland supplies sediment, hinterland characteristics are largely reflected in the fluvial regime and the transported sediment load. The most important feature of the receiving basin is the energy regime which controls the introduction of river-borne sediment. The basinal regime depends on several major features of the basin such as shape, size, bathymetry and climatic settings.

An important feature which emerged from comparisons between modern deltas is the relationship between delta regime and morphology. Initially, the classic birdfoot-lobate-arcuate-cuspate spectrum of delta types was related to increasing wave influence over fluvial processes (Bernard, 1965). This relationship has since been extended by using data from a wide range of modern deltas, including those significantly influenced by tidal processes (Fisher et al, 1969; Wright and Coleman, 1973; Coleman and Wright, 1975).

The framework for deltaic sedimentation derived from modern deltas can also be applied to ancient deltaic successions, where studies are

based on a partial record of the sediment distribution gained from measured sections, subsurface cores or borehole logs (Elliott, 1986).

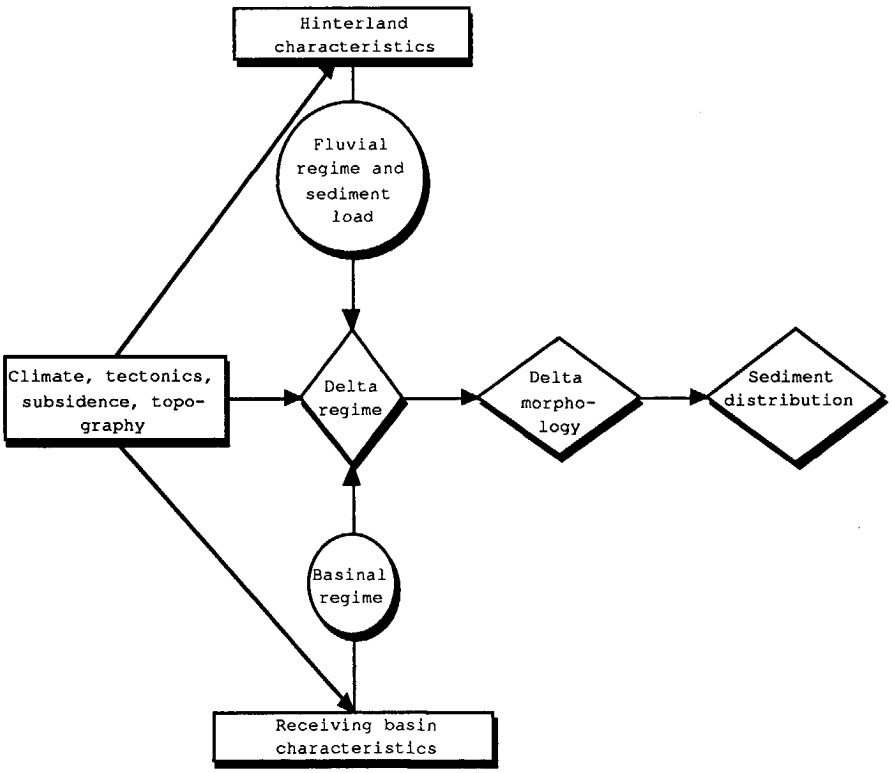

Figure 2.1 Factors influencing sedimentation in deltaic systems (modified after Elliott, 1986).

Recognition of sub-environments and the processes that operate in them permits the nature of the delta to be reconstructed. In thick basinal successions that comprise a series of delta complexes, it may be possible to detect temporal variations in delta type, reflecting the evolution of the hinterland and/or receiving basin (Belt, 1975; Galloway, 1975; Whitbread and Kelling, 1982).

The nature of the delta is inferred from a partial record of the sediment distribution. Once the delta type is known the remainder of

the sediment distribution in unexposed or unexplored areas can be predicted. This is important in the exploration and development of hydrocarbons located in deltaic sand bodies (Elliott, 1986).

2.1.1 HINTERLAND CHARACTERISTICS

The hinterland comprises the drainage basin and the fluvial system where variables such as relief, geology, climate and tectonic behaviour interact to determine the fluvial regime and sediment supply which feed the delta. There are two important features: the total amount of sediment supplied in relation to the reworking ability of the basinal processes, and the grain size distribution, which influences the dispersion and depositional patterns (Elliott, 1986). Coarse-grained bedload tends to be deposited in the immediate vicinity of the distributary mouth bars, or is reworked by wave and tidal processes into beach barrier systems or tidal current ridge complexes. In contrast, finer grained suspended load is generally transported offshore and dispersed with the aid of basinal processes over a wide area of the basin. Deposition produces an extensive mud-dominated platform in front of the delta which may be over-ridden by delta front sands as progradation continues. This results in extensive synsedimentary deformation of the succession by clay diapirism and growth faulting (Elliott, 1986).

Fluctuations in discharge can be significant in determining the grain size of the sediment supply. For example, rivers with erratic or 'flashy' regimes characterized by brief, episodic periods of high discharge are more likely to supply coarse sediment to the delta than more stable regimes which tend to sort sediment prior to its reaching the delta (Elliott, 1986).

The timing of fluctuations in fluvial discharge relative to fluctuations in basinal energy regime also influences deposition in the delta area. If the maxima are in phase, basinal processes continually redistribute the river-borne sediment; if the maxima are out of phase, periods of virtually uncontested delta progradation

alternate with periods of reworking by basinal processes (Wright and Coleman, 1973).

Tectonic events can control sediment supply from the hinterland. For example, in the Gulf of Mexico, Tertiary tectonic events in the Rocky Mountains caused periodic, large-scale reorganization of the drainage basins supplying streams bound for the Gulf Coast. These changes produced a series of major depositional centres of differing age in the Gulf Coast region, each with a distinctive bulk petrography and perhaps unique assemblage of delta types (Winker, 1982).

2.1.2 RECEIVING BASIN CHARACTERISTICS

The characteristics of the receiving basin that influence the development of deltas include water depth and salinity, as well as the shape, size, bathymetry and energy regime of the basin. The overall basin behaviour in terms of subsidence rates and tectonic activity is also important (Elliott, 1986).

The relative density of river and basin waters is an important primary factor controlling the manner in which the sediment-laden river discharge is dispersed after it enters the basin. This is partly a function of the salinity of the basin waters (Bates, 1953). Where rivers enter freshwater basins, the water bodies either mix immediately at the river mouth, or the river discharge flows beneath the basin waters as density currents. In contrast, where rivers enter a saline basin the river waters may extend into the basin as a plume whose buoyancy is supported by the denser sea water.

The basinal energy includes the effects of tidal processes, and wave-induced processes. Semi-permanent currents, oceanic currents and wind effects are less important. The type of basin (Figure 2.2) is a major factor controlling the nature of the basinal regime. For example, at ocean-facing continental margins (Figure 2.2: Type III), the full range of basinal processes affects deltas (e.g. the Niger delta), whereas in semi-enclosed and enclosed seas (Figure 2.2: Types IV and

V), wave energy can be limited due to reduced fetch, and tidal influence is minimal (e.g. the Danube, Ebro, Mississippi and Po deltas) (Elliott, 1986). Deltas located in narrow elongated basins or gulfs connected to an ocean (Figure 2.2: Types I and II) experience considerable tidal effects as tidal currents are amplified, and may therefore transport considerable volumes of sediment (e.g. the Klang delta). Smaller scale deltas prograding into lagoons or lakes are commonly dominated by fluvial processes as the influence of basinal processes is limited (Donaldsen, Martin, and Kanes, 1970; Kanes, 1970; Van Heerden and Roberts, 1988). Basin water depth and the presence or absence of a shelf influence the basinal regime, particularly in terms of the extent of wave attenuation and tidal current amplification.

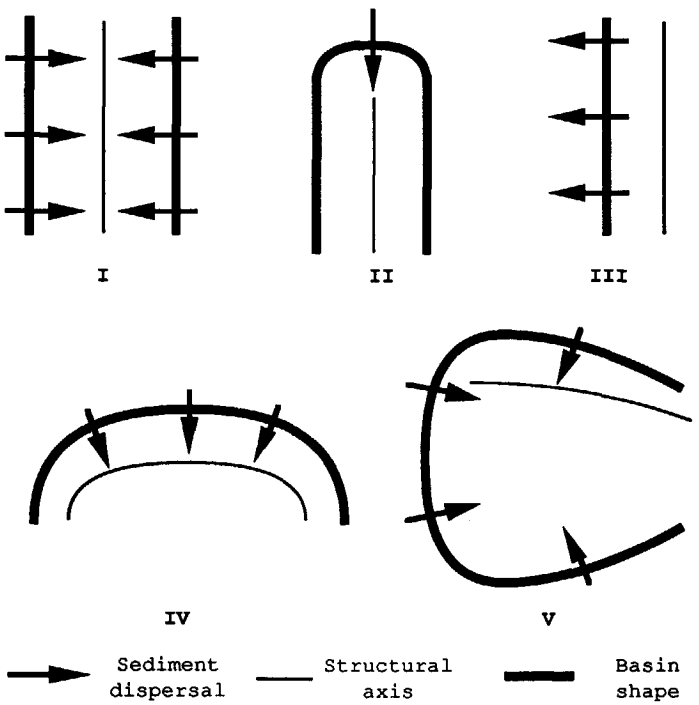

Figure 2.2 Outline and tectonic setting of receiving basins (after Coleman and Wright, 1975).

Because deltas are areas of low relief at the margins of basins, they are extremely sensitive to subsidence trends and basin tectonics (Elliott, 1986). Delta sites may be affected by basement related tectonics, as in the Ganges-Brahmaputra delta which is located in a downwarped basin with numerous active faults, and the Tertiary Niger delta which developed in an aulacogene (Morgan and McIntire, 1959; Coleman, 1969; Burke, Dessauvagie and Whiteman, 1971). They may also be affected by sediment-induced or 'substrate' tectonics involving overpressured shales which induce deep-seated lateral clay flowage, diapirism and faulting as in the Mississippi and Niger deltas (Weber, 1971; Coleman et al., 1974; Weber and Daukoru, 1975; Weber, 1987).

Finally, two more factors influence delta formation: global eustatic fluctuation and the setting of the basin margin in terms of global tectonics. Vail, Mitchum and Thompson (1977) demonstrated that sea-level fluctuates through time. Periods of relative highstand of sea-level alternate with periods of relative lowstand of sea-level. This is probably reflected in the thickness of deltaic cycles (van Wagoner et al., 1990). For example, the Jurassic Brent delta in the North Sea, which represent one deltaic cycle, was formed during a continued slow rise of sea-level. This cycle is much thicker, than deltaic cycles formed in the Niger delta during the Tertiary, a period of rapid fluctuations of sea-level.

Inman and Nordstrom (1971) differentiated three types of coasts based on the global tectonic setting of these coasts: collision coasts, trailing edge coasts and marginal sea coasts. Collision coasts are subdivided into coasts where a continental plate is colliding with an oceanic plate (i.e. west coast of the Americas), and island arc coasts were two oceanic plates are colliding. In both cases rivers entering the basin will have small drainage areas, resulting in a low sediment yield. This makes the rivers unable to produce significant deltas. Furthermore, the preservation potential of these deltas is small, because they are likely to be destroyed by subduction.

Trailing edge coasts are subdivided into Afro-trailing edge coasts, neo-trailing edge coasts and Amero-trailing edge coasts. Afro-trailing edge coasts form along continents with another trailing edge

coast on the opposite side of the continent (i.e. Atlantic and Indian coast of Africa). Such continents are devoid of active mountain ranges formed by plate collision. Therefore erosion is slight, which result in a relatively small input of sediment along the coast (Inman and Nordstrom, 1971). However, the long-living nature of these coast and the stable tectonic regime may result in the formation of extensive deltaic successions (i.e. Niger delta). The preservation potential of deltas formed in these areas is large.

New trailing-edge coasts form near beginning separation centres and rifts (i.e Red Sea, Gulf of California). Because such coasts are relatively young, deltas formed in these areas are usually relatively small. However, if separation continues, these coasts become Amero- or Afro-trailing edge coasts and extensive deltaic successions may form.

Amero-trailing edge coasts form along continents characterized by a collision coast on the other side of the continent (i.e. east coast of the Americas). Such continents are characterized by active mountain ranges (i.e. Rocky Mountains) and the rivers bound for the trailing edge coast usually have enormous catchments. This favours the development of extensive deltaic successions (i.e. Mississippi delta) along these coasts, if littoral currents do not transport sediments away from the river mouth as in the case of the Amazon.

Marginal sea coasts are found on the continental side of back arc basins. If active mountain ranges are present in the bordering continent, significant delta development occurs. However, the preservation potential of marginal seas, and therefore deltas formed in these settings, is limited, because the subductional regime might shift from extensional to compressional as a result of the decrease in the age of the subducting plate. For example, remnants of a destroyed back arc basin are described in the Southern Andes by Dalziel, De Wit and Palmer (1974).

2.2 Delta types

A number of papers have been written on the classification of deltas in relation to their genesis. In this section the most commonly used classifications are discussed. Also a classification scheme is proposed, especially for reservoir characterization.

2.2.1 THE DELTA CLASSIFICATION OF FISHER ET AL. (1969)

Fisher et al. (1969) distinguish highly-constructive deltas dominated by fluvial processes from highly-destructive deltas dominated by basinal processes. Lobate and birdfoot types are recognized in the highly-constructive class, and wave-dominated and tide-dominated types in the highly-destructive class (Figure 2.3). Each type has a characteristic morphology and facies pattern. These are described in terms of vertical sequences, areal facies distribution and sand body geometry. Because facies relationships are emphasized, the classification can easily be applied to subsurface data (Elliott, 1986).

A disadvantage is that this classification concentrates on end-members of what is in reality a continuous spectrum. Also only deltas of mature river systems entering marine basins are discussed. Fan deltas and lacustrine deltas cannot be incorporated in this classification scheme. Furthermore, the term 'highly-destructive' is misleading in this context since all deltas are by definition constructive whilst active (Elliott, 1986).

2.2.2 THE DELTA CLASSIFICATION OF COLEMAN AND WRIGHT (1975)

Coleman and Wright (1975) compared 36 deltas based on quantitative and semi-quantitative data on a number of physical processes which control sedimentation in deltaic systems. First they did a

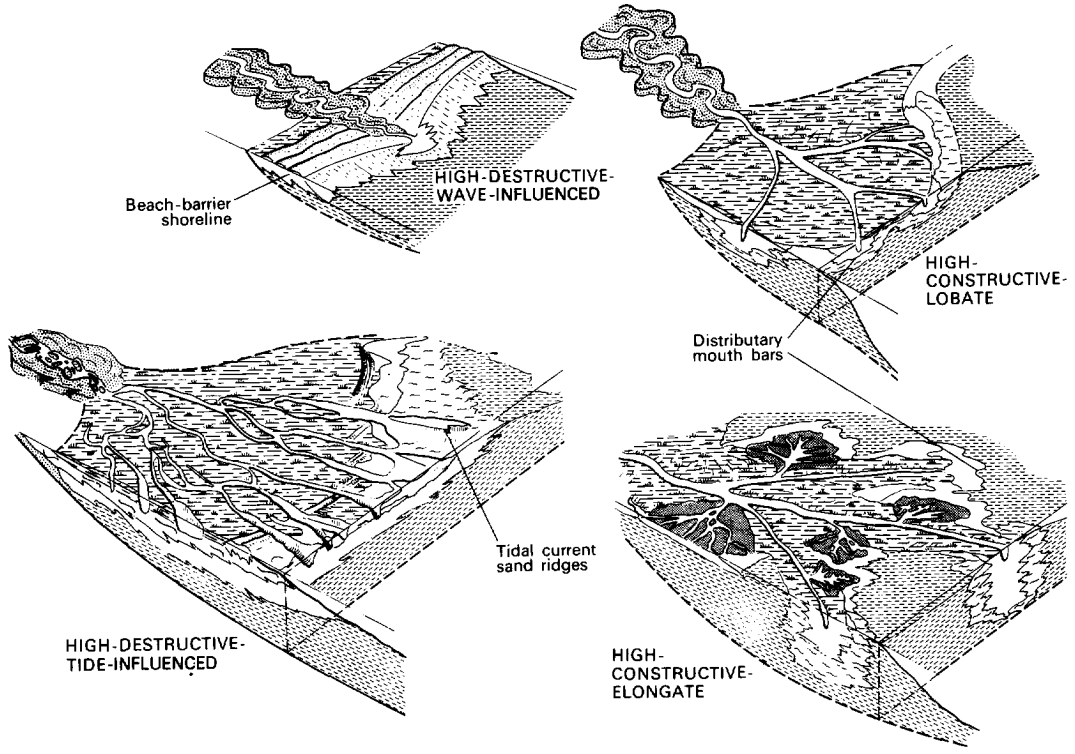

Figure 2.3 Delta types as differentiated by Fisher et al. (1969) (after Elliott, 1986).

hierarchical cluster analysis on the data from 30 of these deltas. This led to a subdivision into 6 groups. Two deltas (Grijalva and Ebro deltas) could not be incorporated in any of these groups (Table 2.1).

Table 2.1 Delta classes as found by Coleman and Wright (1975) by hierarchical clustering. The Ebro and Grijalva deltas could not be classified in any of the six groups.

Class 1	Class 2	Class 3	Class 4	Class 5	Class 6	other
Amazon	Godavari	Hwang Ho	Colville	Parana	Chao Praya	Grijalva
Senegal	Lena	Irriwady	Shatt el Arab	Sagavar-nitok	Tana	Ebro
Magdalena	Missis-sippi	Niger	Ganges			
Burdekin	Danube	Nile	Ord			
	Mekong	Orinoco				
	Indus	Red				
	Yangtze	São Fransisco				
	Klang					
	Po					

Later they described 12 processes that control sedimentation in deltaic systems (Table 2.2). They also differentiated 6 types of sand distribution models. Based on these sand distribution patterns and the differentiated delta control processes they proposed six delta classes in which most of the modern deltas can be grouped. A modern delta was chosen from each group, to illustrate the relationship between the process setting and the resulting sedimentary sequence.

Table 2.2 Delta control processes differentiated by Coleman and Wright (1975).

climate	tidal processes
relief in drainage basin	wind systems
water discharge regime	currents
sediment yield	shelf slope
river mouth processes	tectonics of receiving basin
wave power	receiving basin geometry

Table 2.3 lists the main characteristics for each group, and the modern examples given by Coleman and Wright (1975). The subdivision of deltas based on the hierarchical clustering is significantly different from that based on delta control processes and sand distribution. Coleman and Wright (1975) do not give an explanation for this, nor do they state which parameters were used in the cluster analysis. So it is impossible to ascertain the cause of this discrepancy.

Coleman and Wright (1975) give vertical sections and sand distribution patterns for the groups they differentiated. Their classification can therefore be used for subsurface data. However, yet again they only discuss deltas of mature river systems entering marine basins and ignore fan deltas and lacustrine deltas.

2.2.3 THE DELTA CLASSIFICATION OF GALLOWAY (1975)

Galloway (1975) classifies deltaic systems according to the relative importance of fluvial processes, wave induced processes and tidal processes. He uses a ternary diagram in which deltas can be plotted according to the relative importance of these processes (Figure 2.5 A). This has the advantage that deltas can be classified according to a sliding scale, in contrast with the classification of Fisher et al. (1969) and Coleman and Wright (1975).

Table 2.3 Main characteristics and modern example of the delta classes differentiated by Coleman and Wright (1975).

	Type 1	Type 2	Type 3	Type 4	Type 5	Type 6
fluvial energy	high	low	low	low	low	low
wave energy	low	low	low	inter-mediate	high	extreme
tidal energy	low	high	extreme	high	inter-mediate	inter-mediate
sand distri-bution pattern (Figure 2.4)	Type A	Type B	Type B	Type C	Type D	Type E
offshore slope	low	low	low	low	steep	steep
littoral currents	low	high	low	low	low	high
receiving basin geometry (Figure 2.2)	Type V	Type I	Type II	Type V	Type IV	Type IV
modern example	Missis-sippi	Klang	Ord	Burdekin	São Francisco	Senegal

Elliott (1986) distinguishes several classes of deltaic systems on the basis of Galloway's (1975) diagram. He illustrates the relation between delta control processes and delta morphology with some modern examples (Table 2.4). His delta classes correspond with Types 1, 3, 4 and 5 of Coleman and Wright (1975). Types 2 and 6 of Coleman and Wright (1975) are not found in Elliott's (1986) classification,

because littoral currents are not incorporated in Galloway's (1975) original classification.

Figure 2.4 Sand distribution patterns occurring in most common deltaic systems (modified after Coleman and Wright, 1975).

In his original diagram Galloway (1975) plotted some modern deltas qualitatively. Based on information from Coleman and Wright (1975) I took a more quantitative approach (Figure 2.5 B). Water discharge was used to represent sediment input, average wave power to represent wave energy flux, and tidal range to represent tidal energy flux. Water discharge was used instead of sediment input, because Coleman and Wright (1975) gave no data for this parameter and water discharge and sediment input are closely related.

The parameters were normalized according to Equation 2.1:

$$\hat{u} = \frac{u - \min(u)}{\max(u) - \min(u)} \qquad (2.1).$$

In this equation $\hat{u}$ is the normalized variable of u, min(u) the minimal value of u and max(u) the maximal value of u. The relative importance of the parameters was calculated, and the deltas were plotted in the diagram of Figure 2.5B.

Most of the deltas plotted in Figure 2.5B are formed where rivers enter marine basins. This is why most of the deltas are concentrated in the tide-dominated area of the diagram. The position of the modern Mississippi delta is interesting. Generally this delta is considered to be almost completely fluvially dominated. However, Figure 2.5B

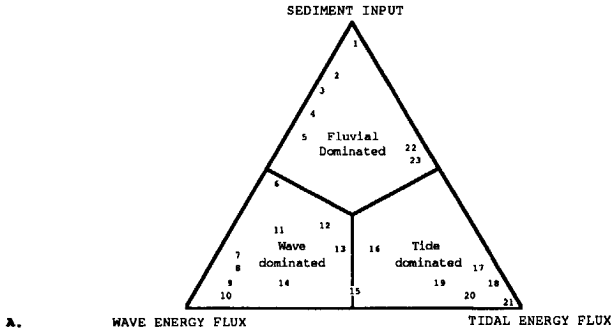

1 = Recent Mississippi delta
2 = St. Bernard lobe (Mississippi delta)
3 = Po delta
4 = Danube delta
5 = LaFourche lobe (Mississippi delta)
6 = Ebro delta
7 = Rhône delta
8 = Kelantan delta
9 = Brazos delta
10 = Sao Francisco delta
11 = Nile delta
12 = Orinoco delta
13 = Niger delta
14 = Burdekin delta
15 = Copper delta
16 = Mekong delta
17 = Yolu delta
18 = Fly delta
19 = Colorado delta
20 = Ganges-Brahmaputra delta
21 = Klang-Langat delta
22 = Yukon delta
23 = Mahakam delta
24 = Amazon delta
25 = Chao Phraya delta
26 = Colville delta
27 = Hwang-Ho delta
28 = Indus delta
29 = Irriwady delta
30 = Magdalena delta
31 = Ord delta
32 = Senegal delta

Figure 2.5 Ternary diagram in which delta systems can be plotted according to the relative importance of fluvial processes, tidal processes and wave induced processes: A) Diagram in which a number of modern deltas have been plotted qualitatively (modified after Galloway, 1975); B) Diagram in which quantitative data on water discharge, tidal range and average wave power are used.

shows a considerable tidal component. This might partly be caused by the water discharge being taken instead of the sediment discharge.

However, the modern Mississippi delta can never be plotted in the uppermost corner of the diagram (Figure 2.5A), because deltas that form in basins without tides (i.e. Danube delta) would then have to be plotted outside the diagram. Comparison of Figure 2.5A and B indicates that the position of several other deltas in the original diagram given by Galloway (1975) might also be questionable.

Table 2.4 Comparison of delta classes defined by Elliott (1986) and Coleman and Wright (1975).

delta class (Elliott, 1986)	**modern examples**	**delta class** (Coleman and Wright, 1975)
fluvial dominance	Mississippi	Type 1
fluvial/wave interaction	Danube, Nile	Type 4
wave dominance	São Francisco	Type 5
fluvial/wave/tide interaction	Niger, Burdekin	Type 4
tide dominance	Ord	Type 3

Galloway's (1975) method is an elegant way of classifying deltas according to the relative importance of fluvial, tidal and wave induced processes. A disadvantage is that the effect of littoral currents cannot be incorporated in this scheme. To be able to incorporate such currents in the classification scheme, Galloway's diagram should be extended in the third dimension (Figure 2.6). In this figure the importance of littoral currents can be given in relation to the cumulative importance of fluvial processes, wave induced processes, and tidal processes. Some of the deltas listed by Coleman and Wright (1975) have been plotted in this diagram. This has been done qualitatively, because of the absence of quantitative data on littoral currents.

Galloway's (1975) classification is applicable to subsurface data if it is combined with the work of Elliott (1986). However, Elliott's (1986) nomenclature is misleading, because it is based on the original diagram by Galloway (1975) (Table 2.4). Furthermore, littoral currents should be incorporated in the classification scheme. Also, Elliott considered only mature river systems entering marine basins and gave no model for fan deltas and lacustrine deltas.

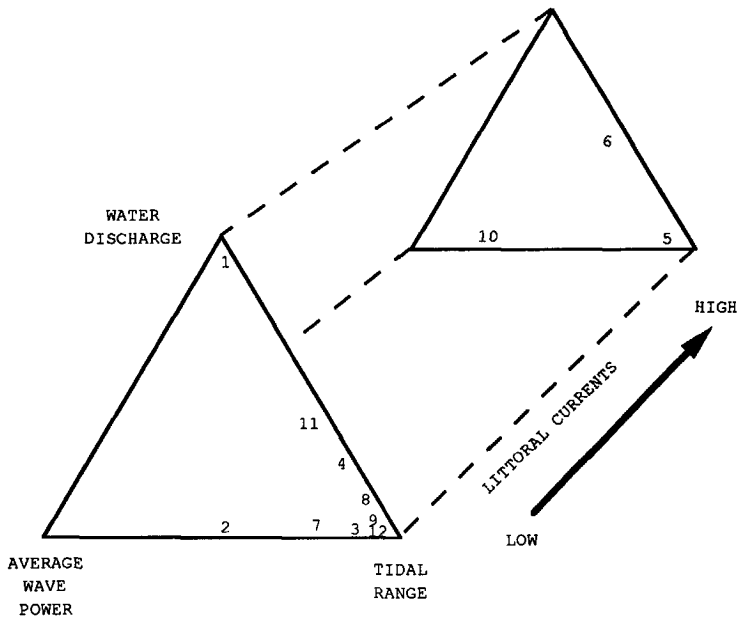

1 = Danube delta
2 = Sao Francisco delta
3 = Burdekin delta
4 = Ganges-Brahmaputra delta
5 = Klang-Langat delta
6 = Amazon delta
7 = Indus delta
8 = Irriwady delta
9 = Ord delta
10 = Senegal delta
11 = Mississippi delta

Figure 2.6 Classification scheme of Galloway (1975) extended for littoral currents with some modern examples. Because of the lack of quantitative and qualitative data on the importance of littoral currents, only a few deltas could be plotted in the diagram.

2.2.4 THE DELTA CLASSIFICATION OF SNEIDER, TINKER AND MECKEL (1978)

Sneider et al. (1978) describe two delta classes which form the extremes of a continuous spectrum. These are mud-rich deltas and sand-rich deltas. According to Sneider et al. (1978) mud-rich deltas are formed where basinal energy is low, sand-rich deltas where basinal energy is high.

Mud-rich deltas have many bifurcating distributary channels. Distributary channels are straight to sinuous, and shorelines are discontinuous sands and muds. As examples Sneider et al. (1978) mention the Mississippi delta, Orinoco delta, Lena delta and Volga delta. Sand-rich deltas have few active distributary channels. Distributary channels are meandering, and shorelines are continuous sand. As modern examples Sneider et al. (1978) mention the Nile delta, Rhône delta and the Brazos-Colorado delta. They describe the two delta types in terms of continuity of major sands and pore space distribution and continuity. This approach of relating these properties to delta types is very useful for reservoir characterization. However, their subdivision of the deltaic environments into two classes is too simple.

2.2.5 CLASSIFICATION OF DELTA TYPES FOR RESERVOIR CHARACTERIZATION

A delta classification for reservoir characterization should be based on parameters that can be inferred from subsurface data. These parameters include the net sand distribution and the vertical succession of rock types as seen in well logs and cores, and as detectable in seismic sections. These requisites are best met by the classification proposed by Coleman and Wright (1975).

Coleman and Wright's (1975) classification can be improved. Although they differentiate two tide-dominated delta types, they characterize these two deltas by a similar sand distribution pattern and more or less the same vertical rock succession. Therefore, I considered the

differences between the two types not sufficient for reservoir characterization and I have combined the two delta types (Type 2 in Figure 2.7). Secondly, Coleman and Wright (1975) only discuss marine deltas of mature river systems and ignore fan deltas and lacustrine deltas, both of which are important in hydrocarbon production (for example, hydrocarbons are found in fan delta deposits in the Jurassic of the North Sea (Brown, 1984), and in lacustrine deltaic deposits in China (Zhiwu et al., 1982)). Therefore I have added both types to the classification proposed in this thesis.

These modifications result in seven delta types. In Figure 2.7 they are represented by a composite vertical column and sand distribution pattern. Table 2.5 lists the depositional characteristics of each delta type. This table also gives a modern example of each delta type and areas where hydrocarbons are produced from such deposits.

I classified thirty modern deltas according to the proposed classification (Table 2.6). All deltas could be grouped in the classification. Note the few examples of deltas with wave/current interaction, fan deltas and lacustrine deltas. This suggests that these deltas could be incorporated in the other classes. However, deltas with wave/current interaction represent deltas which form under an extreme energy regime. Therefore, the internal configuration and sediment distribution in these deltas differs significantly from the other groups. The paucity of fan deltas and lacustrine deltas is caused by the limited amount of published data on these kinds of deltas. Many of the modern deltas are classified as deltas with fluvial/wave/tide interaction. This suggest that a further subdivision could be made. However, the internal configuration and sediment distribution of these deltas does not justify such a further subdivision.

The different delta types differentiated in the proposed classification are illustrated with modern examples. This makes it possible to obtain sound relationships between delta-forming processes and sediment configuration and distribution. However, the present situation is not very representative for most of the geological history, because of rapid fluctuations of sea-level

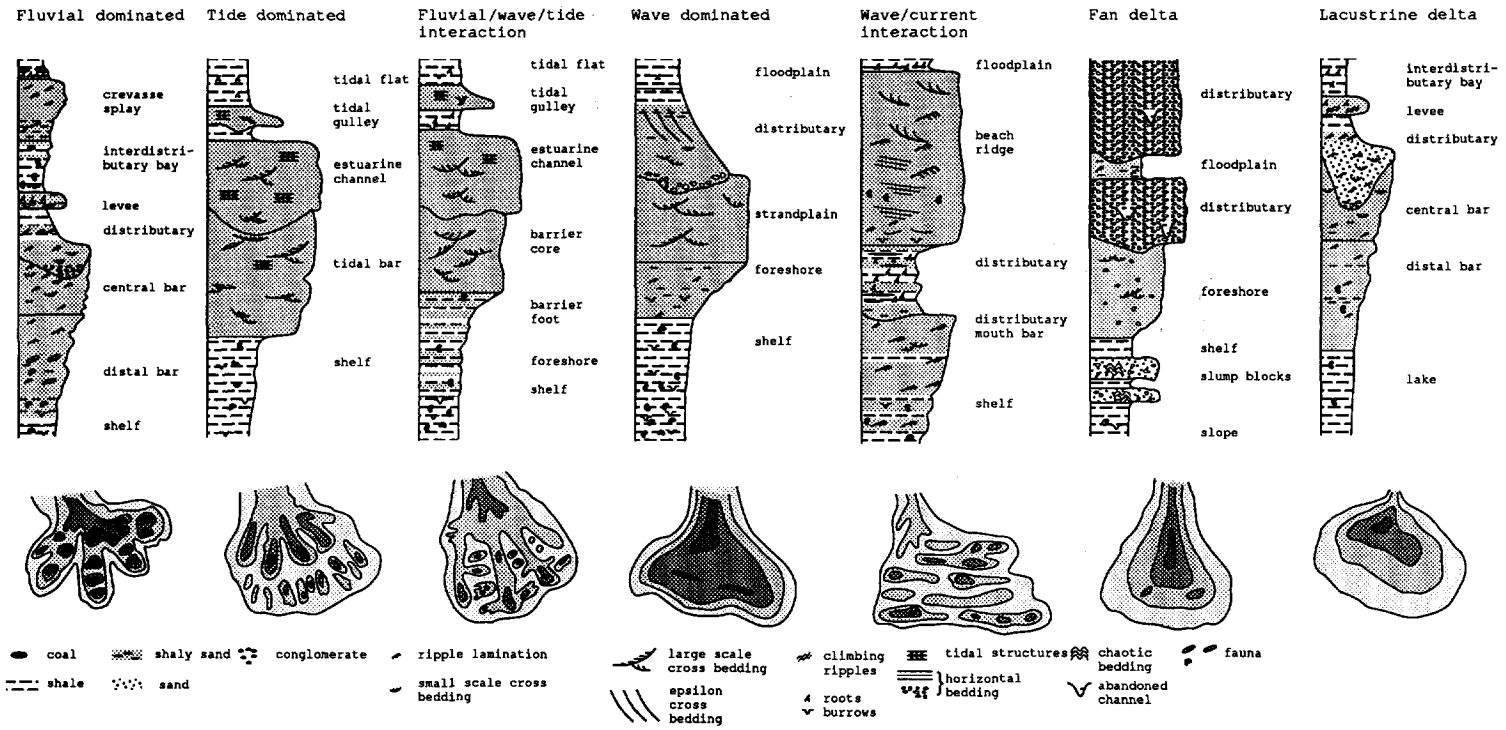

Figure 2.7 Common delta types characterized by composite vertical rock successions and sand distribution patterns (modified after Coleman and Wright, 1975).

Table 2.5 Depositional characteristics of delta types.

	fluvial dominated deltas	tide dominated deltas	deltas with fluvial/wave/tide interaction	wave dominated	deltas with wave/current interaction	fan deltas	lacustrine deltas
fluvial energy	high	low	low	low	low	high	high
wave power	low	low	intermediate	high	high	intermediate	low
tidal range	low	high	intermediate	intermediate	intermediate	intermediate	low
littoral current	low	low	low	low	high	low	low
recent example	Mississippi	Colorado	Niger	Nayarit	Senegal	Yallahs	Catatumbo
hydrocarbon play	Texas Gulf Coast	East Borneo	Nigeria	Texas Gulf Coast	Texas Gulf Coast	North Sea	China

during the Pleistocene. Nevertheless, I concluded from the literature that most phenomena found in Holocene deltas can also be found in ancient deltaic sequences. For example, the Booch sandstone of Oklahoma (Lower Pennsylvanian) shows the same characteristics as sediments of the fluvial dominated Modern Mississippi delta (Fisk, 1961). Fossil tide-dominated deltas are reported from East Borneo, while fossil deltaic successions described from the Gulf Coast by Weise (1980), show the same characteristics as modern deltas with fluvial/wave/tide interaction, wave/current interaction, or which are wave dominated. Wescott and Ethridge (1980) demonstrated

similarities between Holocene and fossil fan delta successions and Hyne, Cooper and Dickey (1979) did the same for lacustrine deltas.

Table 2.6 Thirty modern deltas classified according to a modified version of Coleman and Wright's classification.

fluvial dominated deltas	tide dominated deltas	deltas with fluvial/wave/current interaction	wave dominated delta	deltas with wave/current interaction	fan deltas	lacustrine deltas
Dneiper	Amazon	Burdekin	Grijalva	Senegal	Yallahs	Catatumbo
MacKenzie	Chao Praya	Colville	Magdalena			
Mississippi	Ganges	Danube	São Francisco			
Volga	Indus	Ebro	Tana			
	Klang	Irriwady	Nayarit			
	Ord	Mekong				
	Shatt el Arab	Niger				
		Nile				
		Orinoco				
		Red				
		Sagavarnitok				

2.3 Genetic units[1]

2.3.1 FLUVIAL DOMINATED DELTAS

Fluvial dominated deltas are characterized by fingerlike mouth bar/channel sands encased in delta front fines. These 'bar-finger sands' (Fisk, 1961) consist of an overall coarsening upward sequence starting with silty sands and clayey muds of the distal bar environment shifting to clean sands of the distributary mouth bar, which is cut by distributary channel sediments. On top of the sequence one finds sandy levee and crevasse deposits, and marsh and interdistributary bay fines (Figure 2.8). All genetic units differentiated in fluvial dominated deltas are listed in Table 2.7.

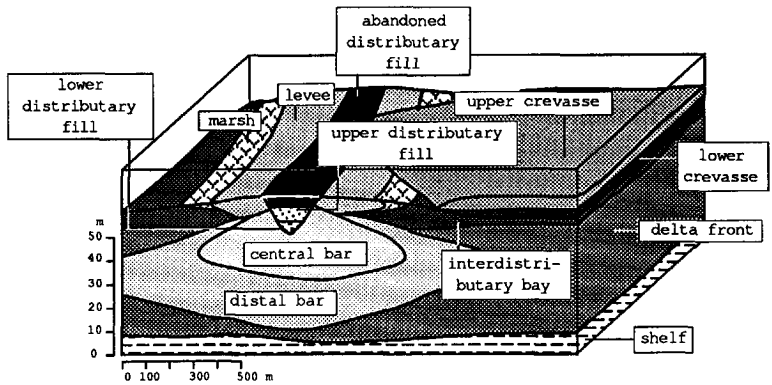

Figure 2.8 Internal configuration of fluvial dominated deltas.

2.3.1.1 Delta front silts and prodelta clays

Delta front fines are deposited in front and on either side of the bar finger sands. They are mainly deposited from suspension and

[1]A genetic unit is defined as a sedimentary body composed during a single occurrence of a particular depositional process (Sneider et al., 1977).

consist of clayey silts (Fisk, 1961). These sediments are often strongly bioturbated. The delta front silts are underlain by the prodelta clays deposited even further away from the river mouth (Figure 2.8).

Table 2.7 Genetic units occurring in deltaic depositional systems.

fluvial dominated deltas	tide dominated deltas	deltas with fluvial/wave/tide interaction	wave dominated deltas	deltas with wave/current interaction	fan deltas	lacustrine deltas
delta front	prodelta	barrier	foreshore	distributary mouth bar	floodplain	distributary marsh
distributary mouth bar	tidal sand bar	tidal channel	strandplain	distributary channel	nearshore	distributary mouth bar
levees	estuarine channel complex	tidal flat	distributary channel	beach ridge	distributary channel	levee
crevasse splay	tidal flat	tidal gully				interdistributary bay
distributary channel	tidal gully					
marsh						
interdistributary bay						

Rapid deposition of sand in the overlying bar-finger sands cause the penecontemporeneous deformation structures to develop in the delta front and prodelta fines. Coleman (1981) described several types of synsedimentary deformation structures in the delta front of the Mississippi delta, i.e. slumping, mud diapirism, mudflows etc. Mud diapirism is most important for the reservoir characterization because it disturbs the bar-finger sequence.

2.3.1.2 Distributary mouth bar sands

Distributary mouth bar sands have lens-like geometries. In the Mississippi delta these bar-fingers reach lengths of about 23 kilometres. The sands can be up to 8 kilometres wide and attain thicknesses of 81 metres (Fisk, 1961).

For reservoir characterization, two sub-units can be differentiated within bar-finger sands (Figure 2.8). The distal bar forms the transition between the delta front clays and silts and the sands of the central bar. In the Mississippi delta the distal bar is characterized by alternating layers of clayey silts and silty sands (Fisk, 1961) that can be up to 40 metres thick. The sedimentary structures occurring in the distal bar sediments include festoon cross-beds; these are found in sandy layers that have a thickness 5 centimetres or less.

Central bar sediments consist of clean sands. In the Mississippi delta they can be up to 40 metres thick. This part of the bar finger is usually the most permeable (Fisk, 1961). Planar and festoon cross-bedding occur in the central bar.

2.3.1.3 Distributary channel and levees

Distributary channels in fluvial dominated deltas are usually straight because of the low gradient of the channels, the cohesive bank material (interdistributary bay fines) and the low tidal energy. Channel size can vary considerably, from a few metres wide and only

about 1 metre deep to up 1 kilometre wide and 30 metres deep (Coleman, 1981). For reservoir characterization, I have subdivided the distributary channel fill into three parts (Figure 2.8). The lower distributary consist of poorly sorted sandy material. The upper distributary shows a fining upwards from silty sands to sandy silts with numerous shale breaks, especially at the top of the unit. The distributary top consists mainly of silty clays with abundant root structures.

Levees are formed on the banks of the distributary channels. Sedimentation on levees takes place during overbank flooding. Levee sediments consist of alternating silty sand and clayey silt layers. They form the transition between the distributary channel sediments and the interdistributary bay sediments.

2.3.1.4 Interdistributary bay deposits

Two modes of sedimentation can be differentiated in the distributary bay area: sedimentation out of suspension in the aftermath of flooding events, and sedimentation by crevassing.

Crevassing occurs when a channel breaches its banks. Generally two mechanisms for the development of a crevasse splay can be differentiated (Elliott, 1986): 1) a sudden incursion of sediment-laden river water into the interdistributary bay area; 2) the development of a semi-permanent crevasse channel.

In the first case, a lobate sand body is formed on the lower flanks of the levees and the bay floor. These lobes are about 1 to 2 metres thick, and in the order of a few square kilometres in area (Arndorfer, 1973). In the second case river water is discharged semi-permanently into the interdistributary bay area, and the crevasse splay evolves into a sub-delta. Coleman and Gagliano (1964) describe several of these sub-deltas in the Mississippi deltaic plain. As a sub-delta progrades into the bay, proximal facies progressively overlie distal facies resulting in small coarsening upward sequences that are 2 to 10 metres thick (Elliott, 1974).

Fine-grained sediments are deposited in the interdistributary bay area out of suspension during and after overbank flooding events. Fine-grained laminated sediment is deposited over the entire area, although lamination is often destroyed by subsequent bioturbation.

2.3.2 TIDE-DOMINATED DELTAS

Tide-dominated deltas are characterized by wedge shaped sandy estuarine channel fill cross-cutting sheetlike tidal sand bar complexes and tidal flat fines. The distribution of genetic units is given in Figure 2.9. Genetic units differentiated in tide-dominated deltas are given in Table 2.7.

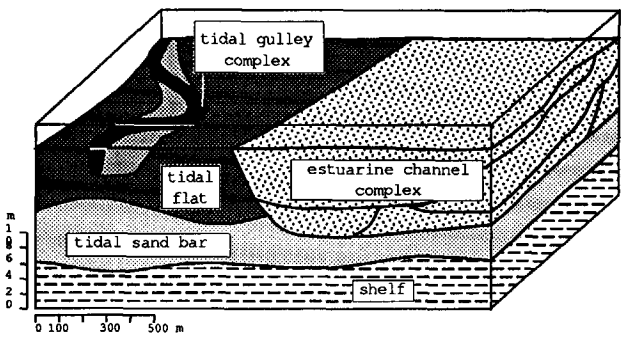

Figure 2.9 Internal configuration of tide dominated deltas.

2.3.2.1 Prodelta fines

In tide-dominated deltas, suspended sediment is preferentially trapped around the margin of the delta as a result of the strong tidal currents in and near the estuarine channel. These sediments form the prodelta mud facies. In deep basins the prodelta mud accumulates and forms a broad seaward-extending subtidal platform, onto which tidal sand ridge and tidal flat deposits advance. In shallow basins sediment is dispersed, and merges with proximal marine

facies. Sediments consist of mud, silt, and muddy sand. Minor constituents include plant and scattered shell debris. Though not documented by studies of modern tidal deltas, mass gravity transport processes and growth faulting probably modify prodelta and overlying delta margin deposits (Galloway and Hobday, 1983).

2.3.2.2 Tidal sand bar

Elongated tidal ridges or bars occur on the marginal shelf or broad delta platform of tide-dominated deltas and are produced by the complete remoulding of channel-mouth deposits by tide-generated currents. They are oriented parallel to the tidal current directions. So they can be oriented parallel to the coast, as described for the Klang-Langat delta (Coleman, Gagliano and Smith, 1970), or perpendicular to the coast, as described for the Colorado delta (Meckel, 1975). The bars occur in fields or swarms as part of a widespread but irregularly distributed subaqueous sand sheet that breaks up into isolated bars in deep water. In the Colorado delta, sand ridges have a maximum amplitude of about 10 metres and are regularly spaced at intervals of several miles (Meckel, 1975). In the Colorado delta the total tidal sand bar 40 kilometres long, varies in width from 7 to 15 kilometres and is 3 to 12 metres thick (Meckel, 1975).

The internal features of a complete tidal ridge sequence are summarized in Figure 2.10. Interbar and distal bar deposits consist of interbedded mud, silt, and sand. An coarsening upward sequence is produced as well-sorted mid- and upper-bar sands are deposited. However, the common presence of discontinuous mud lenses, beds, and clast zones suggests that delta-associated tidal sand ridges contain an erratic vertical sequence (Galloway and Hobday, 1983). Sedimentary structures are dominated by parallel stratification and low- to high-angle stratification. The presence of large dunes and sand waves on submerged bars suggests that both trough and tabular cross stratification might be abundant. Thin sand and silty beds in the lower bar sequence exhibit wavy and ripple lamination and burrows.

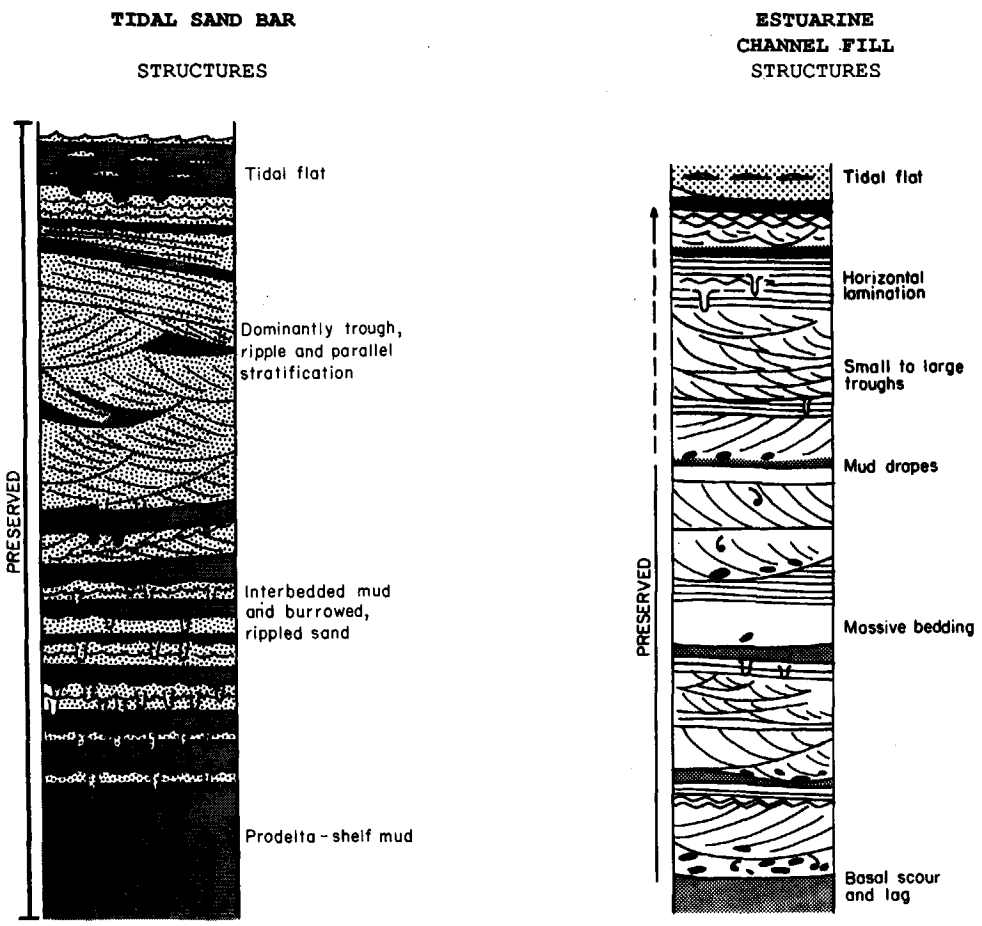

Figure 2.10 Vertical succession of a tidal sand bar and estuarine channel in tide dominated deltas (after Galloway and Hobday, 1983).

2.3.2.3 Estuarine channel fill

Because the channel mouth is a locus of bed load deposition and tidal transport has a dominant up-channel component, estuarine distributaries tend to fill with sand, forming lenses that thicken and widen seawards (Galloway and Hobday, 1983).

The channel fill deposit is composed of multiple, superimposed and variably preserved upward-fining depositional units. In the Colorado delta, internal depositional sequences range from 1 to 8 metres thick. The composite estuarine sand body may be 25 to 30 metres thick (Meckel, 1975). Well-sorted sand constitutes most of the channel fill and contains many discontinuous mud and silt drapes. Primary structures are diverse, and show little regularity in vertical distribution. Cross stratification, predominantly of both trough and tabular types, is abundant. Well developed herringbone cross-stratification is uncommon, but bidirectional dips are apparent. Parallel and ripple lamination are common throughout the sequence. Scattered burrows may also occur, particularly in the muddier intervals. The overall sequence of estuarine channel fills is characterized by bundle sequences (Visser, 1980). A generalized vertical section of an estuarine channel fill is given in Figure 2.10.

2.3.2.4 Tidal flat fines

The subareal part of a tide-dominated delta consists of tidal flat sediments and their associated tidal channel and gully, and salt marsh sediments. The tidal flat complex consists predominantly of mud with some interbedded thin sands and cross-cutting tidal channels and gullies, filled with mud and silt.

Periodic channel shifting and changing sediment supply along the delta margin results in periods of destruction and erosion of portions of the tidal flat. Thin, transgressive sand and shell ridges, which are interbedded with tidal flat muds, reflect such alternations of constructional and destructional phases. In wet climates, extensive marsh or swamp deposits cover the supratidal flats, depositing beds of peat and organic-rich mud. This is for example illustrated by the Klang-Langat delta (Coleman et al., 1970). In arid settings such as the Colorado delta (Meckel, 1975), or the Ord delta (Wright, Coleman and Thom, 1975), supratidal flats are the site of evaporite deposition.

2.3.3 DELTAS WITH FLUVIAL/WAVE/TIDE INTERACTION

The term delta was originally defined by Herodotus (454 B.C.) based on the typical triangular shape of the Nile delta, which is a typical example of a delta with fluvial/wave/tide interaction. This delta shape is also very characteristic of other deltas with fluvial/wave/tide interaction (i.e. Niger delta). Four genetic units can generally be differentiated in this type of delta (Table 2.7). The overall distribution of these genetic units is given in Figure 2.11.

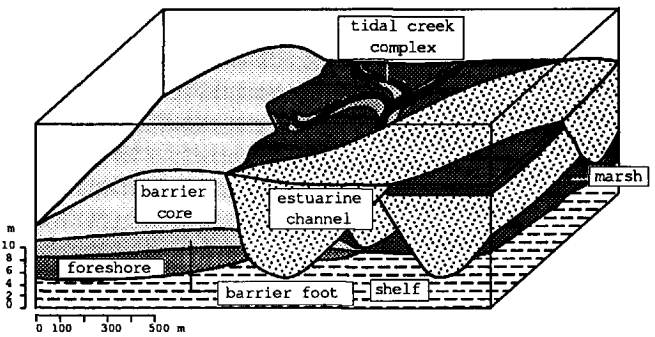

Figure 2.11 Internal configuration of deltas characterized by fluvial/wave/tide interaction.

2.3.3.1 Barrier deposits

The lowermost deposits of deltas with fluvial/wave/tide interaction consist of alternating beds of silts and clays deposited in a shallow marine environment. Lamination is often destroyed by bioturbation. The silt beds are sometimes cross-bedded on a centimetre scale. Plant fragments are commonly interbedded. The marine fauna content is generally poor in terms of specimens and species. These sediments grade upward into more sandy sediments of the barrier bar.

The barrier bar sequence is subdivided into three parts: foreshore deposits, barrier foot deposits and barrier core deposits. Foreshore

deposits consist of severely bioturbated clays with some thin sands The barrier foot consists of alternating sand, silt and clay layers. The sand layers increase in number and thickness upward (Weber, 1971). The barrier foot is overlain by clean and coarser sands of the barrier bar deposited in the zone of wave action (Weber, 1971). The main part of the barrier bar is usually parallel bedded with occasional small scale cross-bedding in the lower part and a limited number of burrows. Silty clay and lignite beds may occur. These are formed in the swampy depressions between successive beach ridges.

Allen (1965) describes erosion of the landward side of the barrier bars by tidal channels. Oomkens (1974) states that most of the sands that will be preserved are the tidal channel sands. Weber (1971), however, reports a significant amount of barrier bar sands that are preserved in the Tertiary Niger delta. In fact, several oil fields in the Niger delta produce from barrier sands. Weber (1971) states that barrier sands attain lengths of 5-37 kilometres parallel to the coast and are up to 5 kilometres wide in the modern Niger delta.

2.3.3.2 Tidal channel sands

Tidal channel fill sequences are deposited as a result of a decrease of flow velocity in a tidal channel. Tidal channel fill sequences are described by Oomkens (1974) from excavations and core holes in recent tidal deposits from the Netherlands. He reports a sharp erosional base. There is generally a bed of very coarse-grained 'lag' deposits concentrated at the base of the channel. The lower interval of most tidal channels consists of festoon cross-bedded sands. An upward change in sedimentary structures is often observed, from predominantly decimetre-scale cross-bedding in the lower part to centimetre scale cross-bedding in the upper part of the channel fill.

Weber (1971) reports a upward decrease of grain size in tidal channel fill sequences in the Niger delta. He also reports numerous clay breaks in the sequence, giving the spontaneous potential log response of the tidal channel sequence a serrated character.

2.3.3.3 Tidal flat sediments

Tidal flat sediments consist of alternations of silt and clay. Usually however, the laminated nature of these sediments is destroyed by plant roots and burrowing organisms. Brackish to fresh molluscs are sometimes preserved in the clay, microfauna is notably absent (Oomkens, 1974). The tidal flat fines are often hard to differentiate from shallow marine sediments deposited at the base of the barrier bar sequence (Oomkens, 1974).

Usually a dense system of meandering tidal gullies is present in the tidal flat area. Gully fills usually have a small amount of coarse-grained material at the base of the fill. This material grades rapidly upward into bioturbated and rooted sandy clays (Oomkens, 1974).

2.3.4 WAVE DOMINATED DELTAS

In wave dominated deltas, most of the sediment is transported laterally from the distributary mouth, resulting in the development of an extensive strandplain adjacent to the river mouth.

A good description of a recent wave dominated delta, the Nayarit coastal plain (Mexico), is given by Curray, Emmel and Crampton (1969). Tyler and Ambrose (1983) describe a fossil example from an oil reservoir in the Texas Gulf Coast in a wave dominated delta system. Based on these examples I have differentiated three genetic units for reservoir characterization (Table 2.7). The internal structure of wave dominated deltas is illustrated in Figure 2.12.

2.3.4.1 Foreshore

The distributary mouth bar forms a sheetlike body of sediment that underlies the whole deltaic sequence. It consist of bioturbated fossiliferous muds at the base which grade upward into alternating

mud, silt and sand beds with wave-indicative scouring, grading and cross-lamination (Coleman and Wright, 1975). The bedding and primary structures are wholly to partially destroyed by burrowing. Slumped or contorted bedding indicate sporadic gravity mass flow of sediment down the sloping surface (Galloway and Hobday, 1983).

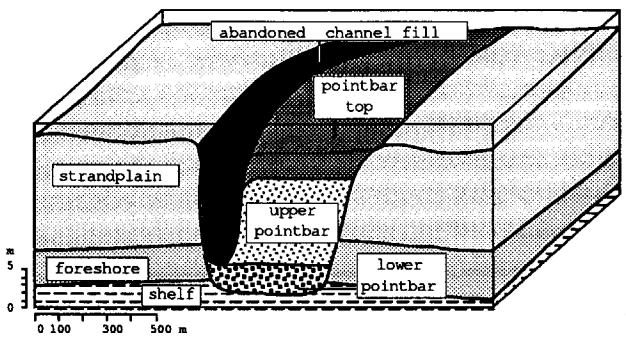

Figure 2.12 Internal configuration of wave dominated deltas.

2.3.4.2 Strandplain and distributary channel fill

The interbedded sediments of the distributary mouth bar grade upward into massive sands of the strandplain. These sands show planar or low angle trough stratification containing scattered burrows and discontinuous mud beds and lenses. At the top of the sequence low angle planar beach stratification is often found. The uppermost beds sometimes show root marks, indicating subareal exposure (Galloway and Hobday, 1983).

Distributary channels in wave dominated deltas are usually moderately sinuous, as is demonstrated by the Nayarit coastal plain (Curray et al., 1969). These channels form broad meander belts up to 5 kilometres wide. Width/thickness ratios range from 100:1 to 1000:1 in the Rhône delta (Oomkens, 1970).

Meandering of the channels results in the formation of point bars with characteristic point bar phenomena like lateral accretion

surfaces, fining upwards and the typical sequence of sedimentary structures from large-scale trough cross-bedding via parallel bedding up to small scale cross-bedding and parallel lamination.

For reservoir characterization, I have divided the point bar sequence into three parts. The lower point bar corresponds with the part of the point bar where epsilon bedding is absent. The upper point bar is characterized by parallel bedding and small scale cross-bedding. The top of the point bar is characterized by sandy silts and clays, characterized by parallel lamination and root structures. An abandoned channel plug is often clearly visible due to the sandy nature of the surrounding sediments (strandplain and point bar) (Figure 2.12).

2.3.5 DELTAS WITH WAVE/CURRENT INTERACTION

The Senegal delta is an example of a delta with wave/current interaction. This delta is described by Coleman and Wright (1975). For reservoir characterization, I have differentiated three genetic units (Table 2.7). In Figure 2.13 the internal configuration of deltas with wave/current interaction is illustrated.

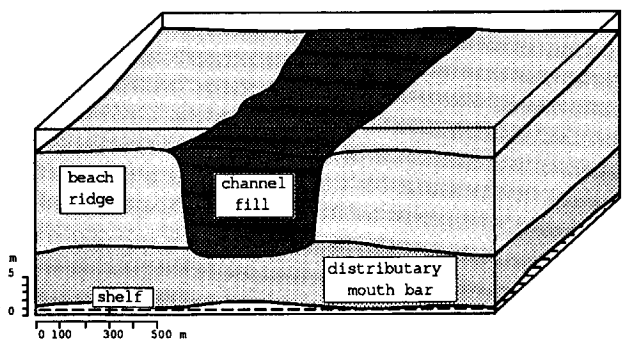

Figure 2.13 Internal configuration of deltas characterized by wave/current interaction.

2.3.5.1 Distributary mouth bar and beach ridge complex

In the Senegal delta the mouth bar has a sheetlike geometry and consists of sand and silt that is moderately sorted, with occasional mud drapes, especially in the lower part of the unit. Small scale cross-bedding is abundant. Grain size tends to increase upward. Near the top gently dipping parallel laminations can be found (Coleman and Wright, 1975).

Beach ridges consist of well-sorted clean sand displaying gently dipping parallel lamination which grade into well-sorted clean sandy units displaying large-scale low angle cross-bedding with root structures at the top. These sands are of beach barrier to aeolian origin (Coleman and Wright, 1975).

2.3.5.2 Channel fill facies

Abandoned channel fills occur in between the sandy beach barrier ridges (Figure 2.13). Within the Senegal delta these channel fills consist of alternating sand, silt and coal layers. The sands are more common near the base of the unit. These sand layers usually have a scoured base. Root and animal burrows are abundant, especially at the top of the unit (Coleman and Wright, 1975). These channel fills are oriented more or less parallel to the coast.

2.3.6 FAN DELTAS

Fan deltas have been defined as alluvial fans that prograde into a standing body of water from an adjacent highland (Holmes, 1965; MacGowen, 1970). The essential elements for the development of fan deltas are high relief adjacent to the coastal zone and steep gradient, bed-load streams that are braided to the coast. This results in the deposition of a fan-shaped sediment body. These conditions and the resulting sedimentary deposits are common along several Holocene coasts and throughout a large segment of geological

history (Wescott and Ethridge, 1980). A good description of a fan delta complex is given by Wescott and Ethridge (1980) on the Yallahs fan delta in Jamaica; below, this delta will be used as a model of fan deltas.

2.3.6.1 Distributary channel fill

The distributary channel fill of the Yallahs fan delta consists predominantly of poorly sorted, well-imbricated gravels. These gravels represent longitudinal bars deposited in active channels (Figure 2.14). The matrix of the gravels is coarse sand. Silt and clay content is low (Wescott and Ethridge, 1980).

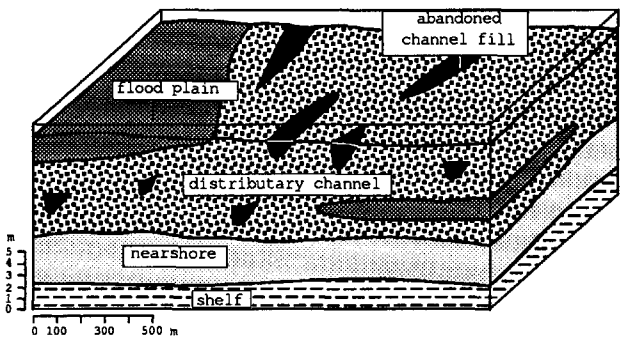

Figure 2.14 Internal configuration of fan deltas.

In addition to the conglomerates of the active channel fill, more sandy intercalations occur. These correspond with floodplain deposition adjacent to the active channel (Figure 2.14). The sediments consist of silty, very fine sand with ripple cross-lamination, ripple drift lamination, small scale cut and fill structures and abundant burrows and roots (Wescott and Ethridge, 1980).

Abandoned channels are common, but are not laterally extensive features in the distributary channel fill of the Yallahs fan (Wescott

and Ethridge, 1980) (Figure 2.14). A core taken in an abandoned channel in the Yallahs fan is characterized by muddy, rooted sands with isolated pebbles overlying homogeneous muds. The coarser sediment at the top of the core is probably introduced by overwash from the beach (Wescott and Ethridge, 1980).

2.3.6.2 Nearshore deposits

In the nearshore deposits the fluvial deposits are modified by marine processes and interfinger with marine deposits. Generally the nearshore is more sandy than the distributary channel area. If gradients are relatively steep, resulting in shelves being absent or only marginally developed, gravels are quite common in the nearshore deposits (Wescott and Ethridge, 1980). The predominant sedimentary structures are low angle cross beds. Occasional burrows occur.

2.3.6.3 Submarine deposits

If gradients are relatively steep the submarine deposits consist of fine sand, silt and clay. Coarser material is introduced in such areas by turbidity currents and slumps. Burrowing is abundant (Wescott and Ethridge, 1980). If gradients are not steep the submarine deposits are mainly sandy becoming finer and eventually muddy basinwards. Slumping and turbidity currents do not occur because of the relatively gentle gradients. Therefore coarse material will not be deposited.

2.3.7 LACUSTRINE DELTAS

Where rivers flow into shallow lakes frictional forces between entering river waters and lake waters dominate (Hyne et al., 1979). This causes a coarse-grained sand bar to be deposited in front of the river mouth, which diverts the flow. This results in sandy sediment being deposited over a large area, which produces a relatively thin

but very continuous sand sheet intersected by sandy channel fills. Figure 2.15 gives the distribution of genetic units within lacustrine deltas.

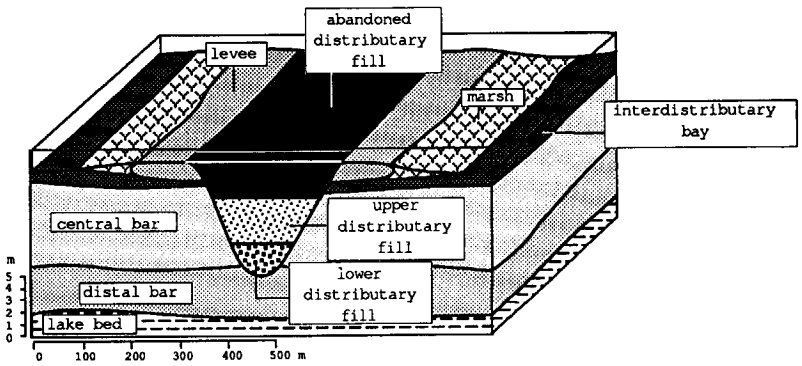

Figure 2.15 Internal configuration of lacustrine deltas.

2.3.7.1 Distributary mouth bar

The distributary mouth bar is subdivided into the distal bar and the central bar (Figure 2.15). The distal bar consists of alternating sand, silt and clay layers. The number and thickness of the sand layers increase upward. The sedimentary structures that occur in the distal bar are ripple and small-scale cross-lamination.

The central bar consists of clean sands. These sands are usually moderately to well-sorted. Occasionally thin and discontinuous mud drapes and lenses occur. The most prominent sedimentary structures are large-scale cross-bedding and horizontal bedding (Hyne et al., 1979).

2.3.7.2 Channel fill and levee sediments

The channel fill is subdivided into three parts (Figure 2.15). The lower distributary is characterized by massive sands with a basal

layer of gravel. The main sedimentary structures are trough cross-bedding. The lower distributary grades upward into the upper distributary which consists of alternating sand and silt layers. The sand layers become fewer and thinner upward. The main sedimentary structures are small-scale trough cross-bedding and ripple lamination. The abandoned distributary fill consist mainly of mud. Root structures are common in this part of the fill (Hyne et al., 1979). The distributary top grades laterally into levee sediments. These are characterized by alternating sand and shale layers. The sands contain ripple lamination. Original lamination might be disturbed by vegetation.

2.3.7.3 Interdistributary bay sediments

The interdistributary bay is the site of sedimentation out of suspension and dense vegetation leading to peat formation. The sediments are initially horizontally laminated, but this lamination is usually disturbed by the plant growth. Crevasse splays are rare, because of the absence of tides in lacustrine environments (Hyne et al., 1979).

2.4 Composition of deltaic deposits

The composition of deltaic sandstones depends on the composition of the parent rocks from which the sand grains originate, the mode of transportation of the sand grains to the site of deposition, the depositional mode, weathering at the parent rock location, during transport and at the site of deposition, and diagenetic processes.

The type of parent rock determines the mineral species that are available. The types of rocks in the source area are mainly dependent of the tectonic setting of that area. This will determine if the source area is mainly volcanic, consists of metamorphic or igneous

rocks, or contains sedimentary rocks. These different types of source terrains will provide different types of mineral suites.

Transportation will modify the composition of the material derived from the source area. The overall grain size will decrease, and crystal aggregates will disintegrate, giving a relative enrichment in single crystal grains.

Deposition can result in the preferential concentration of mineral types. For example, heavy minerals can be concentrated in coarse-grained fluvial deposits (Witwatersrand placers, South Africa) (Minter, 1978), or in beach sands (garnet rich beach sands, The Netherlands) (Schuiling et al., 1985).

Weathering processes play a role from the moment a particle is eroded until it is buried. One can differentiate between physical weathering and chemical weathering. Physical weathering is the breaking down of the parent rocks into progressively smaller grains. The main result of physical weathering is the reduction in grain size, the decrease of multi-crystal grains vis-à-vis single crystal grains, and the relative depletion of well cleaving minerals in the coarse grain fraction, in relation to badly cleaving minerals. On the other hand, the fine grain fraction will be enriched with well cleaving minerals. Physical weathering will not change the overall mineralogical composition of the rocks.

Physical weathering is mainly dependent on the mode and duration of transportation. It is most severe in steep gradient streams and tidal areas. In the latter the oscillating character of the water movements can result in tremendous transport distances (Swett, Klein and Smith, 1971).

Sometimes climate can also be important for physical weathering. This is especially the case in areas where temperature fluctuates around 0 °C. In this case alternating freezing and thawing result in significant physical weathering (Pannekoek, 1973).

Chemical weathering is the alteration of the minerals that are unstable under atmospheric conditions. New minerals may be formed (i.e. kaolinite in feldspar rich rocks), or minerals may be lost by solution (i.e. pyroxenes and amphiboles). The severity of chemical weathering is mainly determined by the prevailing climate. Chemical weathering is most severe in humid tropical climates, and the least in arid polar climates.

Finally, diagenetic processes can significantly change the composition of sand. Minerals can be replaced by more stable forms (i.e. calcite replacement of aragonite). New minerals can be precipitated from solution forming a cement between the sand grains. On the other hand, other minerals can be dissolved. For a more detailed discussion of diagenetic processes, see § 2.5.

All factors that influence the composition of sediments are related to climate and tectonic setting. The tectonic setting is thought to have an especially important influence on the composition of sediments (Johnson, 1990; Maynard, 1984; Potter, 1984; Dickinson et al., 1983; Valloni and Maynard, 1981; Dickinson and Valloni, 1980; Dickinson and Suczek, 1979) Therefore, in this thesis the composition of deltaic sediments is discussed in relation to the tectonic setting in which they were deposited. In this thesis the classification of Inman and Nordstrom (1971) is used to classify different tectonic settings.

2.4.1 TRAILING EDGE COASTS

Inman and Nordstrom (1971) differentiate three types of trailing edge coasts (see § 2.1). Deltaic sediments formed along Amero- and Afro-trailing edge coasts probably have more or less the same mineralogical composition. In these settings the deltas are all formed by mature river systems draining a predominantly cratonic area. In these cases the majority of the parent rocks will consist of older sediments. Mountainous areas are so far away from the depositional site that most multi-crystal fragments will be broken

down into the component crystals. Also, most of the unstable minerals will disappear because of weathering processes. Quartz is the main constituent of these deltaic sediments. Some K-Feldspars will usually be present, because only under extreme conditions will all feldspars be removed from the sediment by weathering (Suttner, Basu and Mack, 1981). This is illustrated by the composition of the Mississippi delta, which contains 75 to 93 per cent quartz with the remainder consisting mainly of feldspar and some rock fragments (Ethridge, 1970).

Fan deltas and lacustrine deltas are the most common delta types in new trailing edge coasts. The sediments in these deltas are from nearby, often volcanic sources, and are therefore much less mature than deltaic sediments formed along Amero and Afro trailing edge coasts. For example, the sediments of Lake Turkana in the African Rift System do not contain very much quartz. Feldspars are abundant. Biotite, amphiboles, pyroxenes and magnetite are common, even in the sand-silt fraction (Yuretich, 1986). The mineral assemblages of fan deltas are thought to be even less mature, because transport distances will be even shorter.

2.4.2 COLLISION AND MARGINAL SEA COASTS

The most common deltas along these kinds of coasts are fan deltas (Wescott and Ethridge, 1980). At some distance from the subduction zone more mature river systems can develop deltaic sequences (i.e. Mahakam delta, Indonesia). These are usually tide-dominated, because of the large number of small straits in these areas.

Because most river systems of collision and marginal sea coasts are relatively immature, the composition of the sediments deposited in their deltas will resemble the composition of the rocks in their catchments. In these tectonic settings the main parent rock is usually volcanic. Therefore the sediments consist mainly of volcanic rock fragments or their alteration products. The type of rock fragments depends on the exact locality of the main source area,

because the nature of the vulcanism depends on the relative position to the subduction trough. Johnson (1990) showed that subtle differences between source locality are visible in the sediments.

2.4.3 INTERMONTANE BASINS

A special category of deltas are those formed in intermontane basins. in these settings only fan deltas and lacustrine deltas are found. Because their source areas are not usually characterized by active vulcanism the sediments will consist mostly of quartz and feldspars. The amount of rock fragments and unstable minerals will mainly dependent on the duration and mode of transportation to the site of deposition.

2.5 Common diagenetic patterns in deltaic rocks

Diagenesis is defined as all the mechanical, chemical, mineralogical and biogenical processes and changes in a sediment and its interstitial water after its deposition that take place at temperatures below those leading to metamorphism (below 300 °C). It excludes changes brought about by vulcanism, weathering and tectonism (Van Straaten et al., 1980). So it includes processes like compaction, recrystallization and replacement, cementation and pressure solution. The nature of diagenesis is determined by geothermal gradient, depth of burial, original mineralogies and texture, the nature and distribution of diagenetic minerals and textures, types and amount of pore space, nature of migration and convexion of pore fluids and depositional environment (Pettijohn, Potter and Siever, 1987; Blatt, Middleton and Murray, 1980).

2.5.1 PHYSICAL DIAGENETIC PROCESSES

Physical diagenetic processes lead to a loss of pore volume and an increase in bulk density as a result of an adjustment to the force of gravitation. The major process is compaction of the sediment through an increase in packing density, fracturing and plastic deformation. In sediments consisting of minerals resistant to fracturing and cleavage, compaction is often not very significant, as is illustrated by unconsolidated Tertiary sandstones of the Texas Gulf Coast which have more or less the same permeabilities as equivalent modern sands, although they are buried under 3226 metres of younger sediments (Dickinson, 1953). If, however, the sediment is rich in labile rock fragments, squeezing of the rock fragments result in significant compaction. Sometimes the soft rock fragments are able to form a kind of pseudo-matrix in which the more resistant grains float.

Because deltaic sediments are usually rather mature and therefore do not contain abundant labile rock fragments, physical compaction will not be of major importance in deltaic sediments. Exceptions might be sediments of fan deltas, because of the short transport distances in these settings and therefore the relative immaturity of these sediments.

2.5.2 CHEMICAL DIAGENETIC PROCESSES

Several chemical processes take place during diagenesis of a sediment. The most important are precipitation, dissolution, recrystallization, and partial dissolution and alteration. Chemical changes are more important than physical changes in altering the character of many sandstones after deposition. Cementation and lithification are mainly the result of chemical precipitation of a binding agent or the chemical welding of adjacent detrital grains. Chemical processes, especially those involving complex alterations of labile rock fragments, involve the interaction between solid mineral grains and pore fluids. The bulk and mineral composition of the

solids change slowly during diagenesis in response to changes in pore water chemistry.

2.5.2.1 Precipitation

Precipitation of various minerals takes place directly from the interstitial solutions onto the surfaces of the same or different mineral grains. Many minerals have been identified as authogenetic precipitates (Table 2.8). The most common diagenetic silicates and oxides are precipitates of minerals present in the primary detrital assemblage, such as quartz, feldspar, clays, zircon, and tourmaline. Diagenetic minerals may be of the same chemical composition but are sometimes different in their crystal structure, as illustrated by the precipitation of opal on quartz surfaces and anatase overgrowths on brookite. Other diagenetically precipitated minerals may be of phases not originally present in the detrital mix. Secondary carbonate is typically of this kind. Others are anhydrite, iron oxides, halite, pyrite, and other normally non-detrital minerals. These minerals show crystalline forms impinging on, or growing from detrital grain surfaces in encrusting, coating, or spiky outgrowths that would be difficult to explain as detrital (Pettijohn et al., 1987).

2.5.2.2 Dissolution

Dissolution can take place according to two mechanisms. The solid phase can dissolve homogeneously, always leaving behind a fresh surface of the as yet undissolved solid unaltered in composition. This is called congruent dissolution. The solid can also dissolve selectively, whereby the the solid that is left undissolved is changed in composition. This is called incongruent dissolution (Pettijohn et al., 1987).

Dissolution is an integral part of the recrystallization process, because dry recrystallization, that is, a restructuring of the mineral by solid diffusion without mediation of a surrounding fluid, would take so long under diagenetic temperatures that great lengths of geological time would be needed for most transformations

(Pettijohn et al., 1987). Most recrystallization takes place by dissolution of the precursor and precipitation of the final crystal. The whole process may take place in a thin film of solution immediately adjacent to the solid surface in such a way that the dissolved ions are immediately reprecipitated with restricted communication with interstitial water at large.

Table 2.8 Mineral species formed as precipitates in sandstones during diagenesis (data from Blatt et al., 1980).

silica minerals	zeolites	feldspars	clay minerals	iron oxides	titanium minerals	carbonates	sulphates	others
opal-a	phillipsite	k-feldspar	kaolinite	hematite	anatase	calcite	gypsum	tourmaline
opal-ct	clinoptilolite	albite	illite	goethite	brookite	dolomite	anhydrite	zircon
chalcedony	heulandite		smectite			ferroandolomite	barite	
quartz	laumontite		chlorite			siderite		
	analcime							

Dissolution will also be of major importance in the replacement process, for the same reasons as with recrystallization. Dissolution will take place in an exceedingly thin film of water between the boundary surfaces. The transport process within the film must be

adequate to move the dissolved material out and the precipitating material in from the interstitial waters (Pettijohn et al., 1987).

2.5.2.3 Partial dissolution and alteration

Partial dissolution and alteration occur in a great number of rock-forming minerals. The solid dissolves and reacts with water in such a way that both the solute and the residual solid are different in composition from the original solid phase. The kaolinization of feldspar is a well known partial dissolution and alteration process. During this process aluminium will not go into solution but is conserved as a solid in the alumino-silicate structure (Pettijohn et al., 1987).

In addition to kaolinite formation from feldspar, most other diagenetic clay minerals are not formed by simple dissolution and precipitation processes. In these processes the alumino-silicate is also preserved in solid form. One can simply visualize the process as one in which cations are exchanged, lost, or gained, and silica is gained or lost relative to aluminium, by the detrital solid reacting with the surrounding solution.

2.5.2.4 Recrystallization

The driving force behind any recrystallization of a substance from one form to another other more stable form is the tendency towards a minimum in the Gibbs free energy of the chemical system (Pettijohn et al., 1987). Recrystallization includes the formation of a larger crystals from an aggregate of small ones to minimize the interfacial energy of each crystal (Guggenheim, 1967). This might be expected to cause sandstones to become single large crystals, but this does not happen because the interfacial energy is negligible for crystals larger than 0.1 millimetre (Pettijohn et al., 1987).

In more complex recrystallizations one polymorph will invert to another without a change in chemical composition. An example of a

recrystallization process is the transformation of opal-a, via opal-ct to quartz. Opal-a is the amorphous form of silica that can be precipitated both biogenetically and abiogenetically. Opal-ct is a form of disordered cristobalite. The individual steps in the recrystallization are the dissolution of opal-a, reprecipitation of opal-ct, gradual ordering of opal-ct, precipitation as chalcedony (micro-crystalline quartz) and finally crystal growth and the formation of macro-crystalline quartz (Pettijohn et al., 1987).

Another well known example of a recrystallization process is the recrystallization of aragonite to calcite. Aragonite is not a stable mineral under most surface and subsurface conditions. Therefore, aragonite formed in modern sands, where both biological and non-biological processes seem to ignore chemical equilibrium over short time scales, is rapidly transformed to calcite after deposition.

2.5.2.5 The influence of depositional environment on chemical diagenetic processes

Some papers discuss the relation between depositional and compositional aspects of a sediment, and diagenetic processes. Füchtbauer (1967a) documented a dominant environmental control on cementation patterns in the feldspathic Buntsandstein sandstone (Lower Triassic, northern Germany). Precipitation of autogenetic minerals was controlled by depositional environment, although diagenesis occurred at burial depths of 1000 to 1200 metres. In brackish-marine to evaporite environment cementing minerals were anhydrite, calcite, ferrous dolomite, albite, halite, analcite, barite and celestite. In fluvial deposits potassium-feldspar and dolomite were the cementing minerals. Chlorite and vermiculite were restricted to estuarine deposits, while quartz and micas were formed autogenetically in all environments.

In a subsequent paper Füchtbauer (1974) generalized his observations of fluvial, marine and evaporitic sandstone of Triassic and Upper Carboniferous age in Germany and concluded that kaolinite, sudoite (dioctahedral chlorite), and K-feldspar cements can be regarded as

characteristic to freshwater sandstones. Early chlorite, analcime and albite cements are found mainly in marine and evaporitic sandstones, provided that the influence of the influx of meteoric water during diagenesis can be excluded.

Almon, Fullerton and Davies (1976) studied vulcano-clastic sandstones from the Horsethief Formation (Upper Cretaceous, Montana), a deltaic-nearshore marine sequence. Autogenesis had occurred at depths of 500 to 1000 metres. Autogenetic corrensite (mixed layer montmorillonite-chlorite) and dolomite were found to be restricted to delta distributary channel and distributary mouth bar sediments; montmorillonite to bay-beach, crevasse, lagoon, barrier island, and shallow sub-tidal settings. Calcite cement occurred in all environments.

Preferential quartz cementation is reported by Stonecipher, Winn and Bishop (1984) for the Frontier Formation of Wyoming. They found very low permeabilities as a result of extensive quartz cementation in marine sand ridge and beach sediments, the most quartz-rich genetic units in the system. In the less mature distributary channel sands higher permeabilities were found because clay fragments and other non-quartz clasts prevented extensive quartz cementation.

2.5.3 THE EFFECT OF DIAGENETIC PROCESSES ON POROSITY AND PERMEABILITY

Diagenetic processes can have a significant effect on porosity and permeability. In a general way permeability and porosity tend to decrease with increased burial as a result of compaction and cementation. However, material that has been cemented earlier or was originally present can also dissolve increasing the permeability and porosity.

The effects of burial diagenesis on various types of sandstones are discussed by Nagtegaal (1978). He has stated that burial diagenesis of sandstones normally results in partial framework collapse through mechanical compaction, plastic deformation, pressure solution and

mineralogical alteration of framework constituents. He studied the effect of these processes on the porosity and permeability of sandstones of varying mineralogical composition.

To effectively study the influence of the sandstone framework Nagtegaal (1978) only considered arenites. He differentiated three types:

- *Quartz arenites* (less than 10 % feldspar and less than 10% lithic fragments)
- *Arkosic arenites* (more than 10 % feldspar and more feldspar than lithic fragments)
- *Lithic arenites* (more than 10 % lithic fragments and more lithic fragments than feldspar fragments)

Arkosic arenites and lithic arenites can be subdivided further into pure arkosic and lithic arenites (the former contain less than 10 % lithic fragments, the latter contain less than 10 % feldspar fragments), and arkosic-lithic arenites (more than 10 % lithic fragments) and lithic-arkosic arenites (more than 10 % feldspar fragments) (Figure 2.16).

Nagtegaal (1978) measured the porosity and permeability for each of the three arenite groups from a number of samples and compared the results with estimated initial porosity and permeability values. These latter values were determined by measuring the grain size and sorting of the samples and fitting these data into a data set that Beard and Weyl (1973) obtained for artificial grain size and sorting mixes whose porosity and permeability they had determined. The results are shown in Figure 2.17.

The quartz arenite samples used in this study contain an average of 95 % quartz and polycrystalline quartz, 3 % feldspars and 1 % of other constituents, which classifies these rocks as very pure quartz arenites (Figure 2.16). The grain size of the samples varies between very fine to fine (coastal barrier sands) and medium to coarse

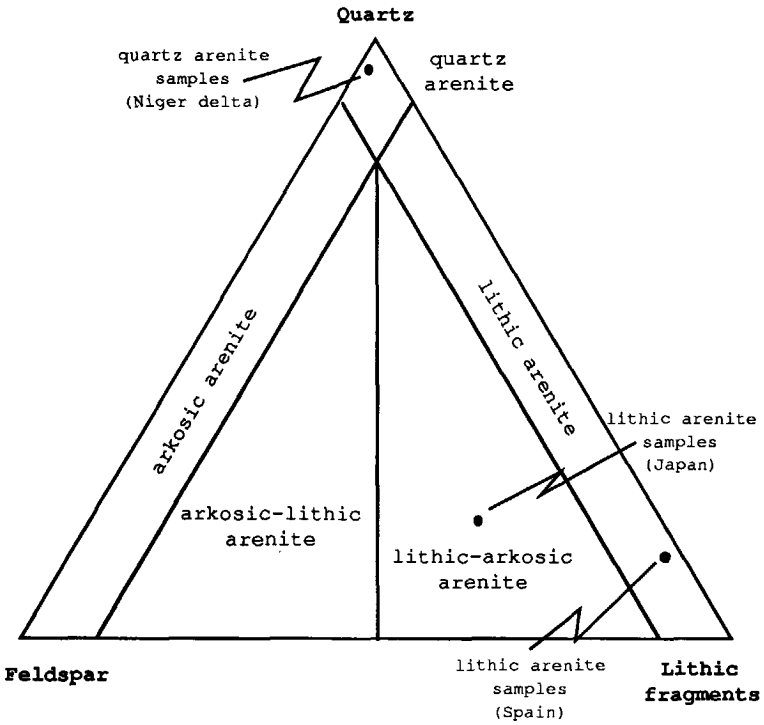

Figure 2.16 Classification of arenites according to Nagtegaal (1978). The average compositions of the quartz arenite and the lithic arenite samples used by Nagtegaal (1978) are indicated. The average composition of the arkosic arenite samples could not be plotted because Nagtegaal gave no data on the amounts of quartz and lithic fragments in these samples.

(channel fill and crevasse splay sands) (Figure 2.17B). The samples were taken from depths of 3596 to 3657 metres. From Figure 2.17B it is apparent that the very fine to fine-grained sandstones show a somewhat larger diagenetic shift than the medium to coarse-grained sandstones. This is probably the result of pressure solution which, according to Füchtbauer (1967b), has a more severe effect on fine-grained sands.

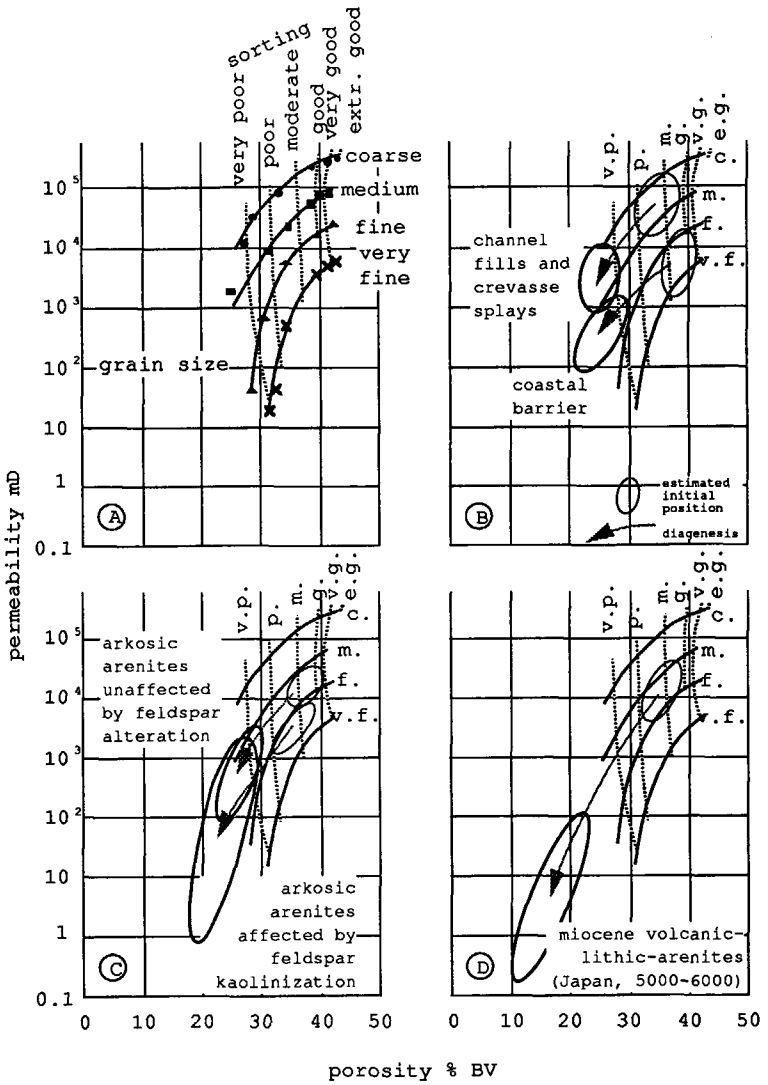

Figure 2.17 Porosity and permeability values: A) unconsolidated sands (based on Beard and Weyl, 1973), B) Miocene quartz arenites at 3596-3657 m burial (12 samples), Niger delta, C) Jurassic arkosic arenites with kaolinization at 2743-3047 m burial (20 samples) and without kaolinization at 3048-3352 m burial (34 samples), North Sea and D) Miocene volcanic lithic arenites at 1524-1828 m burial (18 samples), Japan (after Nagtegaal, 1978).

Nagtegaal (1978) studied two sets of pure arkosic arenite samples. The first set contained an average of 20 % unaltered feldspar. The second set contained an average of 7.8 % feldspar, but this must have been much higher before diagenesis. In this set many feldspars had been altered to varying degrees and there was abundant authigenic interstitial kaolinite, both fine crystalline and in the form of large vermicules. The samples were taken from depths of 2743 to 3352 metres. The porosity/permeability plots showed an overlap for both sets to a certain extent. However, the field for the kaolinized samples extended into regions of low porosity/permeability (Figure 2.17C). This effect can directly be attributed to the widespread autogenesis of kaolinite. The wide range in permeabilities was caused by the variation in degree of feldspar alteration among the samples.

Nagtegaal (1978) also studied two sets of lithic arenite samples. The first set of samples was from exposed Westphalian D strata in the South Central Spanish Pyrenees and contained on average 14 % quartz and 2 % feldspar. The remainder comprised non-volcanic lithics (mainly phyllites). The second set was lithic-arkosic arenites from Japan containing on average 55 % lithic fragments (predominantly of andesitic volcanic origin), 20 % quartz, 13 % feldspar and 12 % undifferentiated components (Figure 2.16). In the Spanish samples no diagenesis was observed other than extreme plastic deformation of the phyllite fragments. Porosities were less than 10 % and permeabilities less than 0.1 mD. Maximum burial depths as determined from interbedded coals must have been around 4500 to 6000 metres. According to Nagtegaal (1978) the absence of authigenic minerals, except for some late replacive calcite, suggest that plastic deformation of the soft lithics set in very early and proceeded rapidly. In the Japanese samples a sharp reduction of porosity and permeability is visible (Figure 2.17D) although they were buried to relatively shallow depths (1524 to 1828 metres).

When the kaolinized arkosic samples from the Jurassic of the North Sea are compared with the lithic arenite samples from the Miocene of Japan the latter samples display a much more rapid reduction in porosity and permeability although autogenesis of clay minerals has occurred in both sets of samples. According to Nagtegaal (1978) this

is because in the lithic-arkosic arenites of Japan, in addition to widespread mineralogical alteration, plastic deformation of soft lithics is a major process reducing porosity and permeability.

The difference between permeability and porosity in the North Sea and Japanese samples might also be explained by the kinds of clay minerals that are found in the samples. Neasham (1977) pointed out that the kind of authigenic clay minerals strongly determines the reduction in porosity and permeability that takes place. He differentiated three types of dispersed autogenetic clays:

- *Discrete particle clays*: pseudohexagonal, platy crystals attached as discrete particles to pore walls or occupying intergranular pores (i.e. kaolinite) (Figure 2.18A),

- *Pore lining clays*: relatively continuous and thin clay mineral coatings (i.e. illite, chlorite and montmorillonite) (Figure 2.18B),

- *Pore bridging clays*: minerals attached to the pore walls and extending far into or completely across a pore or pore throat (i.e. illite, chlorite and montmorillonite) (Figure 2.18C).

Neasham (1977) categorized 14 sandstone samples with similar textural properties (very fine to fine and well to very well-sorted) according to the three abovementioned classes and characterized these samples according to their fluid flow properties. He demonstrated that there is a clear effect of dispersed clay type on permeability and porosity (Figure 2.19). Sands with discrete particle clays have the greatest porosities and permeabilities. With the same weight class, sands with pore lining clays have porosities comparable with those of discrete particle clays. However, their permeabilities are much smaller. Sands with pore bridging clays have the smallest porosities and permeabilities.

The cementation of minerals from invading pore waters is very effective in reducing sandstone porosity and permeability by blocking

pores and pore throats. This can be concluded, for example, from the earlier mentioned study done by Stonecipher et al. (1984) on the Frontier Formation of Wyoming, where the extensively cemented quartz-rich basal zones had much smaller permeabilities than the more clay-rich and therefore less cemented upper zones.

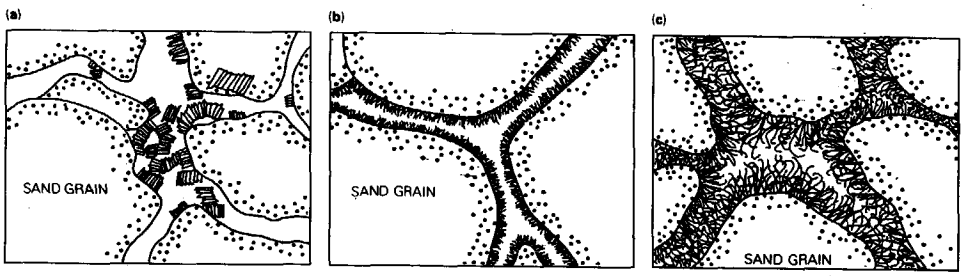

Figure 2.18 Morphologies of dispersed clays in sandstone reservoir rock: A) discrete particle clays, B) pore lining clays and C) pore bridging clays (after Neasham, 1977).

At greater depths decementation (the dissolution of earlier precipitated material) can take place, resulting in the development of secondary porosity. Decementation under deep burial conditions has been given as the cause of secondary porosity in many sandstones (Schmidt and MacDonald, 1979a,b). Secondary porosity, especially that produced by dissolution of calcite cement, may be the result of increases in calcite solubility controlled by decreases in temperature or increases in the salinity of pore waters. If a sandstone is uplifted from a deeply buried position to more shallow depths the pore water may change from a slightly supersaturated or saturated brine to a cooler, less concentrated brine. If the temperature effect is larger than the brine salinity effect, calcite will dissolve. Invasion by undersaturated meteoric waters would have the same result (Pettijohn et al., 1987). In addition to decementation the dissolution of detrital grains can cause secondary porosity. The most commonly dissolved detrital grains are the non-quartz constituents like carbonates, feldspars, rock fragments, etc.

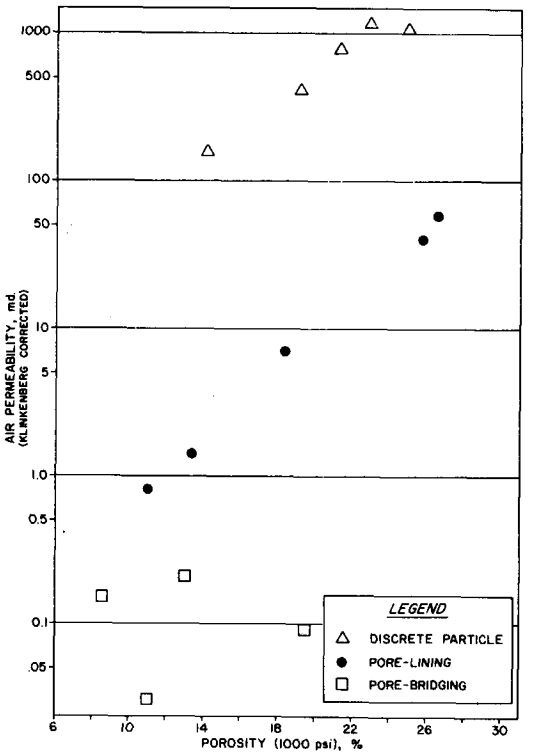

Figure 2.19 Cross-plot of porosity and air permeability of selected sandstone samples which have contrasting dispersed clay morphology (after Neasham, 1977).

3. DESCRIPTION OF RESERVOIR ARCHITECTURE IN DELTAIC ROCKS

3.1 Basic types of reservoir architecture in deltaic systems

One of the main prerequisites for accurate reservoir simulation is a sound description of the reservoir architecture with respect to fluid flow (see Chapter 1). Weber and Van Geuns (1990) were among the first to relate reservoir architecture to fluid flow. They differentiated three basic reservoir types (Figure 3.1). The following definitions were proposed:

1. Layer cake reservoirs (Figure 3.1A) consist of a package of very extensive sandstones which individually have rock properties that can be represented realistically in maps without showing major discontinuities or changes in horizontal permeability. The layers do not have to be of constant thickness, but changes in thickness should be gradual. The boundaries between layers should coincide with major changes in properties or baffles to flow. The vertical permeability in each layer should also show only gradual changes laterally.

2. Jigsaw-puzzle reservoirs (Figure 3.1B) are composed of a series of sand bodies that fit together without major gaps between the units. An occasional poorly permeable or impermeable body may be embedded in the reservoir. Also there may be impermeable baffles between certain superimposed sand bodies. Rock properties may change abruptly between sand units. Internally certain units may have very heterogeneous properties which should be quantified through modelling. Good reservoir definition should be obtainable from a detailed fence diagram.

3. Labyrinth reservoirs (Figure 3.1C) are typically complex arrangements of sand pods and lenses. The reservoir does not have to be strictly discontinuous, but this will often appear to be the case in sections. Also, the interconnectedness consists partly of thin sheets of poorly permeable sandstone. Detailed correlations are only possible where wells are closely spaced. The sand continuity is often direction dependent. Accurate three-dimensional models can rarely be made, but probabilistic modelling can be attempted.

Weber and Van Geuns (1990) gave a rough estimate of the minimum well spacing that is needed to obtain a reliable description of the reservoir architecture from deterministic correlation (Table 3.1). If the wells are spaced too far apart, modelling techniques have to be used to describe the reservoir architecture.

I characterized the seven delta types differentiated in Chapter 2 according to the above-mentioned reservoir classes. The geological models for the various delta types (Figures 2.8, 2.9 and 2.11 to 2.15) were transformed into fluid conduit models (Figure 3.2). In these models only the sand-rich units are indicated. From Figure 3.2 it becomes apparent that most deltas form jigsaw-puzzle types of reservoir. Some deltas form a mixture between layer-cake and jigsaw-puzzle type reservoirs (Table 3.2).

3.2 Description of reservoir architecture

3.2.1 RESERVOIR DATA

Several data sources from the reservoir are available for the description of the reservoir architecture: physical samples, petrophysical measurements, production data and seismic data.

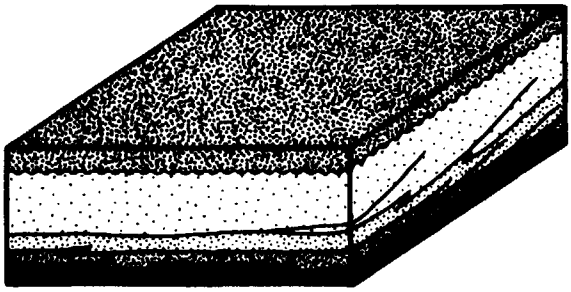

A) Layercake: layers represent sands deposited in same environment of deposition.

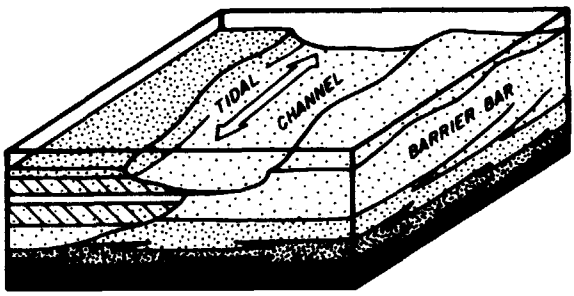

B) Jigsaw puzzle: reservoir architecture determination requires detailed sedimentological analysis.

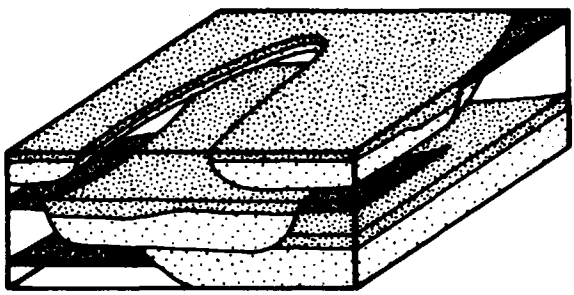

C) Labyrinth: in 3D interconnectedness exist locally but in part only via thin low permeable sheet sands.

Figure 3.1 Basic reservoir types (modified after Weber and Van Geuns, 1990).

Physical samples are collected as cuttings, cores and side wall samples. The petrophysical properties of formations intersected by the bore-hole are measured by various well logging tools.

Table 3.1 Approximate average well spacing required for deterministic correlation of major sand units (after Weber and Van Geuns, 1990).

well pattern	layer-cake reservoirs		jigsaw puzzle reservoirs		labyrinth reservoirs	
	spacing (m)	wells (km^{-1})	spacing (m)	wells (km^{-1})	spacing (m)	wells (km^{-1})
rectangular	1000	1	600	3	200	25
triangular	1200	0.8	800	2	300	13
random		1.3		4		32

Often additional permeability measurements are taken using a mini-permeameter. This technique is ideal for taking large numbers of permeability measurements from cores which can then be averaged and compared with measurements from core plugs and well logs. The advantages of measuring on cores over other sampling methods are that good physical data are recovered and a good depth control is maintained if the core recovery is good.

3.2.1.2 Cuttings

Cuttings are samples of the formation rock that have been drilled away by the bit and are circulated up to the surface by drilling fluid. As they form a waste product, cuttings' analysis is a cheap way of obtaining information on the type of formations being penetrated by the bore-hole; a further advantage is that they are continuous. The major disadvantage is that the exact depth from which

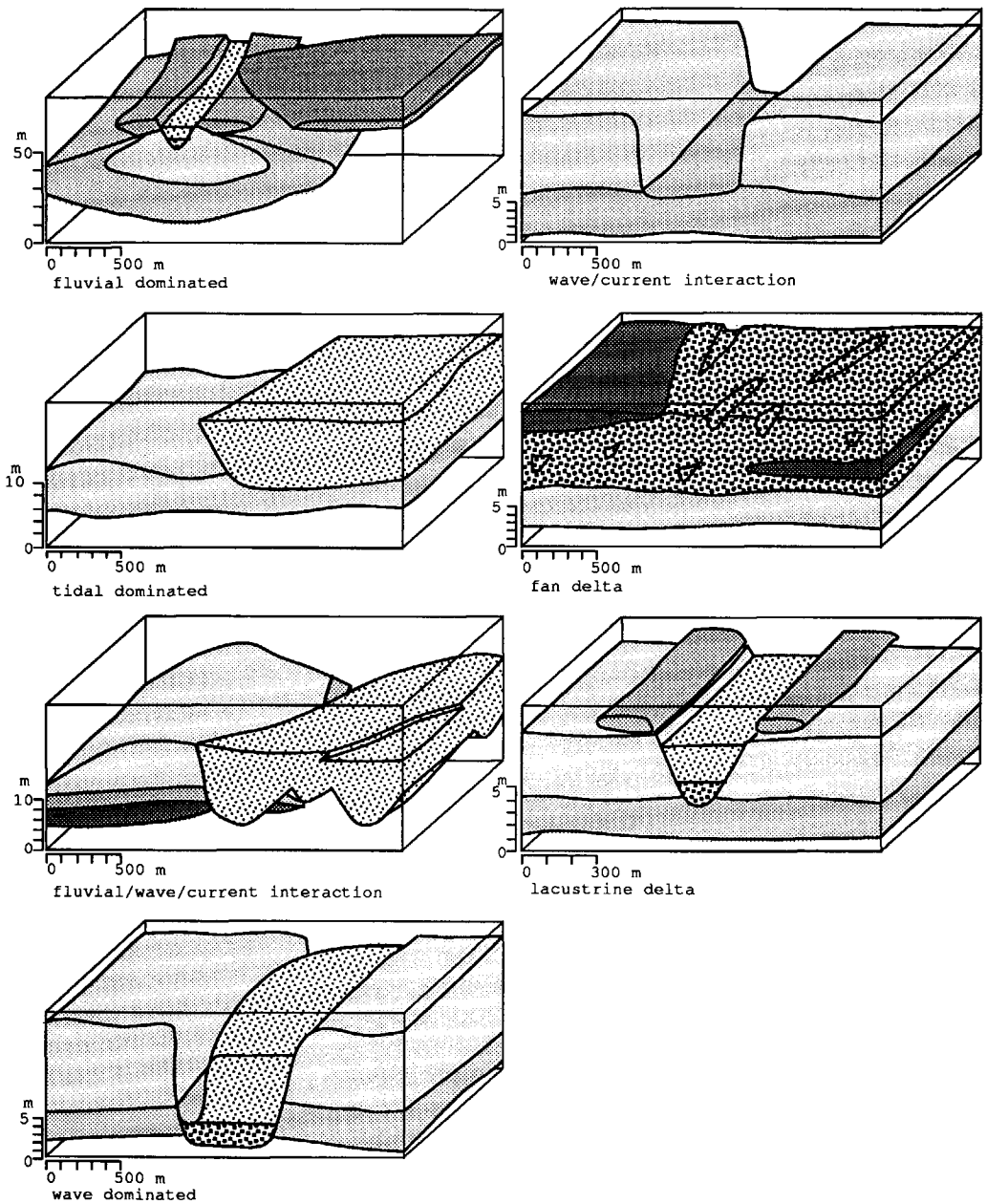

Figure 3.2 Reservoir architecture in deltaic depositional systems.

the cuttings originate cannot be established because of mixing during transportation in the drilling fluid.

3.2.1.1 Cores

Cores represent actual segments of the subsurface. Cores give information on the vertical rock succession in the bore-hole. Cores are very important in gaining insight into the environment in which the sediments were deposited. Furthermore, porosity and permeability can be determined from core plugs.

Table 3.2 Classification of delta types according to the reservoir classes differentiated by Weber and Van Geuns (1990).

layer-cake	layer-cake to jigsaw puzzle	jigsaw puzzle	jigsaw puzzle to labyrinth	labyrinth
	tide-dominated deltas wave dominated deltas deltas with wave/current interaction fan deltas	fluvial dominated deltas deltas with fluvial/wave/ tide interaction lacustrine deltas		

3.2.1.3 Sidewall samples

Sidewall samples are as the name implies, samples collected from the wall of the bore-hole. A large number of these samples can be taken. These samples are analysed in order to detect the various sedimentary bodies present in the bore-hole. Porosity and permeability

measurements are usually not very realistic because the samples are compacted during acquisition. The advantage of this method is that the samples are relatively cheap and can be collected during a logging operation.

3.2.1.4 Well logs

The use of well logs for determining reservoir properties has become a very widespread and sophisticated technique in recent decades. Well logs measure physical properties which are related to the characteristics of the rock types penetrated by a bore-hole.

Log responses are influenced by formation properties such as grain size distribution, sorting, packing, mineral composition and clay content. The output of well logging tools thus consists of a record of formation data versus depth.

The main advantages of this technique are that the measurements are continuous, with good depth control and reasonable vertical resolution; beds down to a few centimetres thick can be differentiated. The horizontal resolution varies between a few centimetres and several metres, depending on the type of log.

Well log data can be used to determine rock properties like porosity and permeability and to give an indication of the environments of deposition in which the rocks penetrated by the bore-hole were deposited. The main drawback of data gathered by well logs is the limited horizontal resolution, making the data representative for only a small volume of reservoir in the immediate vicinity of the well.

3.2.1.5 Well testing

When a productive formation has been found the flow characteristics can be determined by means of a well test. This information can be used by the production geologist to roughly determine the

permeability of the producing layer. The same procedure can also be done on a smaller scale using a wire-line formation tester which detects pressure differentials during and after a certain production time. The data found using these techniques is not very detailed, as flow characteristics are determined by many factors in a large area surrounding the well.

3.2.1.6 Seismic data

In most cases, seismic sections are available of the area where exploration wells are to be drilled. Possible reservoir structures and faults can be determined from the regional seismic information. These seismic sections give an indication of the geometry of a possible reservoir and reveal large faults and other large structural features. At normal reservoir depth however, the vertical resolution of regional seismic data is not sufficiently good to enable individual layers or heterogeneities to be detected. The quantitative resolution depends on the technique used to acquire, process and interpret the data. If the data are very good the smallest possible features that can be detected must often be at least 10 metres thick. This minimum thickness is valid for good quality seismic data.

High resolution seismic techniques such as well to well seismic surveys are relatively new to the industry and are not yet routinely used in reservoir development. However, some promising results have been presented (Cramer, 1988; Gallagher, 1991; Lawson, 1991; Paulsson, 1991; Robertson, 1991; Mondt, 1990; Quint, 1990).

3.2.2 MODELLING TECHNIQUES

From the previous section it can be concluded that data available from the reservoir does not usually yield enough information to be able to construct an accurate reservoir model. The data are only valid in the immediate vicinity of the well (i.e. well logs and

cores), or not detailed enough (i.e. seismic data and well tests). Therefore modelling techniques must often be used to obtain a better description of the reservoir. These modelling techniques should incorporate the data from the reservoir and general geological knowledge.

3.2.2.1 Deterministic modelling

Deterministic modelling as described in this thesis is defined as a modelling technique which uses quantitative and qualitative input data to produce an explicit geological model of a reservoir. This means that when a model has been created each location in the reservoir being modelled has been allocated a certain set of values for the different rock properties. The reservoir is thereby delineated into manageable parts. The sizes of these parts depend on the detail required, the reservoir complexity and the amount of reservoir data available.

There are several case studies on deterministic modelling in the literature. For example, Johnson and Krol (1984) studied the geology of a heterogeneous sandstone reservoir in the Lower Jurassic Statfjord Formation of the Brent field in the North Sea. Their study describes the geological characteristics of the reservoir and illustrates how these features were incorporated into a detailed computer simulation model. They constructed a framework to obtain a detailed description of the reservoir with particular emphasis on the size, shape and trend of sand bodies, the dimensions of shale bodies, well log response to genetic units and porosity/permeability distribution. The data were from 14 wells spaced 1 to 6 kilometres apart and consisted of 700 metres of core material, mainly from 4 extensively cored wells.

Two main facies types were recognized within the Statfjord Formation: transgressive shallow marine sandstones and fluvial sandstones and shales. The shallow marine sandstones are 30 metres thick sheet-like sandstones, well-sorted and coarsely grained. They contained no shale intercalations (Unit 1). The fluvial sediments could be divided into

4 groups with a total thickness of 230 metres, active channel fills, inactive channel fills, floodplain sheet sands and floodplain shales. Only the active channel fills formed significant hydrocarbon-bearing genetic bodies. Figure 3.3 shows the individual sedimentary units. Unit 1 is fully correlatable across the section and poses no problem. Unit 2 consists of shale-dominated extensive floodplain deposits. Unit 3.1 is mainly sand-dominated with multi-story channel bodies. Reservoir pressure confirms good interconnectedness. Unit 3.2 consists of channel bodies that are less stacked than in unit 3.1. Because the sediments formed extensive sheets and there was good interconnectedness Johnson and Krol were able to construct correlation panels and a deterministic model. Reservoir simulation studies later confirmed the reliability of the model (Johnson and Krol, 1984).

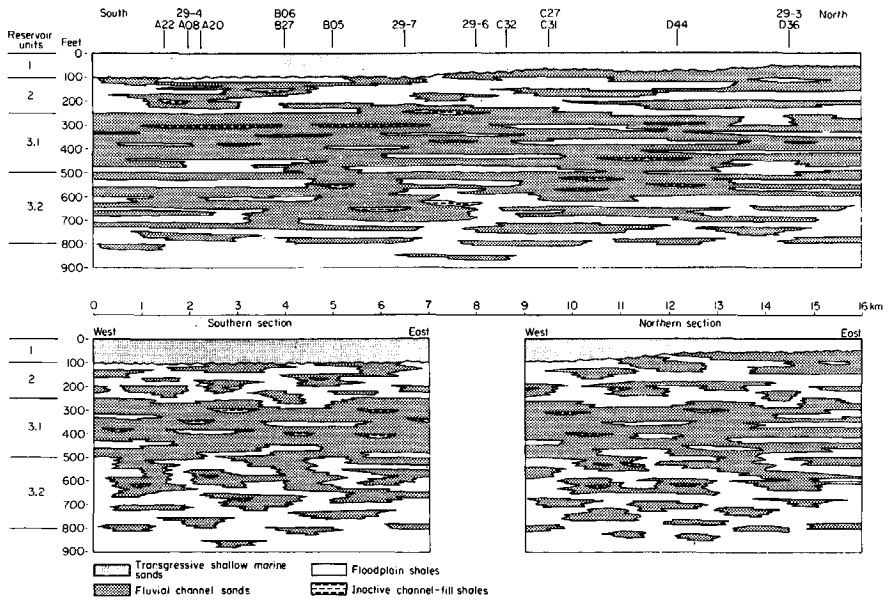

1 ft = 0.3048 m

Figure 3.3 Conceptual reservoir model of the Statfjord Formation in the Brent field (after Johnson and Krol, 1984).

Martin and Evans (1988) studied marginal aeolian/sabkha sequences in the Southern North Sea, based on 16 exploration wells, 8 of which were extensively cored, and 16 production wells. The area described is the North Viking field situated in the Leman/Silverpit Formation transition zone. Martin and Evans located aeolian dune, inter-dune sabkha and lacustrine sabkha facies. The aeolian dune facies consisted of fine to medium grained cross-bedded sandstones, 0.2-0.3 metres thick. The inter-dune facies consisted of very fine to fine-grained sandstone with silty laminations. The lacustrine sabkha facies were very fine-grained sand lenses in a muddy siltstone matrix. Aeolian dune and inter-dune sequences alternated every 1 to 3 metres, occasionally punctuated with 0.2-0.3 metres thick lacustrine sabkha siltstone.

The facies had clear diagnostic log responses. Therefore, uncored wells could be interpreted with confidence. Because the beds are thin Martin and Evans opted to perform a mini-permeameter study on the cores, the conventional core analysis spacing of 0.3 metres would not accurately represent the reservoir heterogeneity. Detailed correlation was established and a clear picture of the sequence becoming more muddy and evaporitic could be constructed for the transition of the Leman Formation into the Silverpit Formation.

Both these studies (Johnson and Krol, 1984 and Martin and Evans, 1988) make it clear that deterministic modelling is possible when sufficient information is available on the formation structures. Lateral homogeneity relative to the well spacing is essential for good correlation. The main advantage of deterministic modelling is that it is a relatively simple technique that has frequently been applied in practice. The main disadvantage is that correlations are often made too quickly, resulting in simplistic reservoir models.

3.2.2.2 Simulating geological processes

A geological model of the underground can be built by simulating geological processes. These techniques construct a geological model step by step just as the actual situation was formed. In order to

create such a model, all geological processes that play a role during and after deposition must be quantified. This makes such modelling techniques extremely difficult.

In the sixties models of various depositional environments were made. Examples are a simulation model for marine sedimentation (Harbaugh and Wahlstedt, 1967) and a simulation model for deltaic sedimentation (Bonham-Carter & Sutherland, 1968). However, none of those models were used frequently in reservoir characterization studies.

The reason most geological simulation models never left the experimental stage is that the geology they model is often too complex, resulting in far too many input parameters. The models that did become usable in practice are all based on fluviatile sedimentation. These models are described by Allen (1978), Leeder (1978), Bridge (1979) and Bridge and Leeder (1979).

3.2.2.3 Geostatistical techniques

The geostatistical techniques discussed in this thesis are divided into two groups, sequence-based techniques and object-based techniques. The sequence-based techniques are based on sequence-related data. This means that values of a property are modelled at individual grid-points, based on information about statistical relationships between values at neighbouring locations (Dubrule, 1989). The object-based methods I will discuss use statistical information about the size and shape and location of individual objects (genetic units) in space to model the distribution of these objects (Dubrule, 1989).

Sequence-based techniques

Sequence-based techniques were first introduced by the South-African mining engineer Krige (1951). The French mathematician Matheron (1963) gave a mathematical background to Krige's techniques and introduced this as the theory of regionalized variables. Regionalized variables are variables that have a certain distribution in a dimension of space. An example of a spatially correlated geological

phenomenon is thickness of a stratigraphic unit. Since their introduction geostatistics have been widely applied in the mining industry.

Da Costa E Silva (1984) was one of the first to apply sequence-based techniques incorporating semi-variograms and kriging to reservoir data. He used sequence-based techniques to calculate porosity and vertical permeability in a North Sea reservoir. Data for the calculations of porosity and horizontal permeability were obtained from well tests. Vertical permeability data were obtained from cores from 6 appraisal wells. In all, 30 wells were used in the study. The area covered by the reservoir is approximately 95 square kilometres. The wells were more or less randomly distributed in this area, with clusters in the East and South of the reservoir. The well spacing varied between 0.5 and 4 kilometres.

Da Costa E Silva calculated horizontal semi-variograms for the porosity data and natural logarithm of the permeability data shown in Figures 3.4 for E-W, NE-SW and N-S directions. In this figure there is a clear drift of porosity and permeability on the E-W axis. This implies a systematic increase in these two properties from West to East.

Based on the variograms shown in Figure 3.4, Da Costa E Silva (1984) postulated a range of influence[1]. The range of 4000 metres is questionable, as from Figure 3.4 it can be seen that a range of 2000 metres would also correlate with the data.

Each value of the input data was omitted from the data set and estimated by kriging the rest of the data set. Da Costa E Silva (1984) found a mean error of 1.84 %, between actual and estimated values for horizontal permeability. Pelt (1990) evaluated his results and found a mean error of approximately 13 %.

The method using geostatistics combined with kriging and cross validation presented by Da Costa E Silva (1984) is technically

[1]The range of influence of a semi-variogram is the distance over which the variance between neighbouring points is less than the population variance.

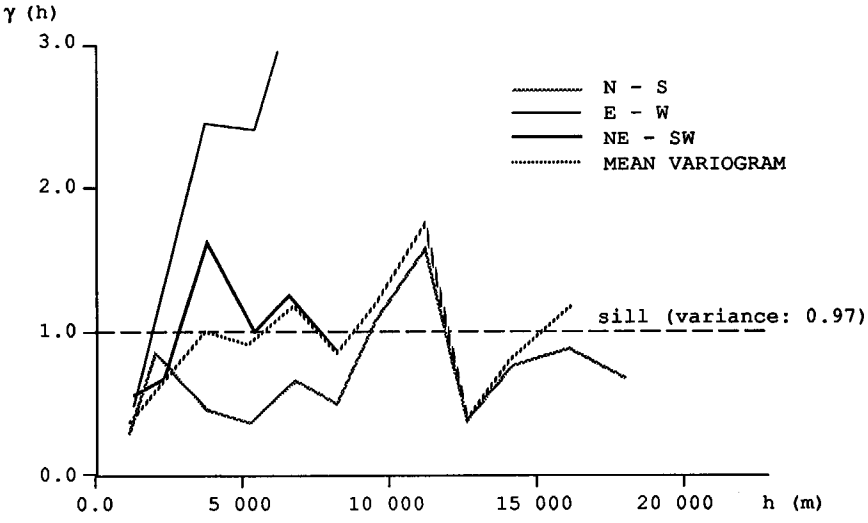

A.

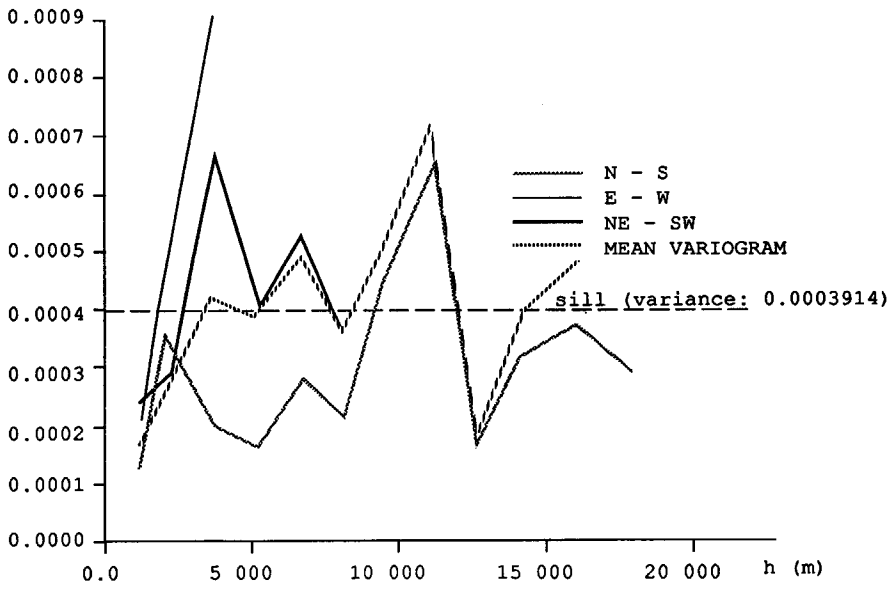

B.

Figure 3.4 Horizontal variograms for A: ln(K) and B: porosity (after Da Costa E Silva, 1984).

correct. The problem lies in the usefulness of the method for petroleum geologists. Data derived from well tests give averaged values over the area surrounding the well that provides production for that well. With such general data it was possible to apply geostatistical methods with little fear of large errors. The results are maps which probably do not vary much from reality, but can only be used as an indication of the average permeability and porosity in an area of 1 square kilometre. This is not very accurate and not very useful when trying to describe a reservoir in detail.

A further drawback of using geostatistics in the manner Da Costa E Silva (1984) did, is that he gave no consideration whatsoever to the geology of the reservoir. He used no information of the lithology, stratigraphy and structural geology to predict the reservoir properties.

Dubrule and Haldorsen (1986) studied the permeability variation of zone 4A of the Sadlerochit Formation of the Prudhoe Bay field, Alaska, USA. The dominant lithology was fine-grained sandstone with coarser sandstone and conglomerates near the base that was probably deposited in a braided fluvial environment. Semi-variograms were constructed based on arithmetic averages of the core permeability of 62 cored wells. Only wells with a core recovery of more than 50 % were used and non-pay intervals were not included. Using a basic mapping technique it was shown that the permeability systematically increases towards the NE.

They constructed variograms of the logarithm of permeability from the cored wells. In Figure 3.5 the semi-variograms are shown for SW-NE and SE-NW axes. The permeability increase towards the NE is visible in the variograms. The average well spacing is 2280 metres and results in a lag of the same distance in the semi-variograms. If the permeability trend is taken into account neither semi-variogram shows a range of influence for the permeability. Two wells 2280 metres apart are no better correlatable than wells 9150 metres apart. This indicates that the range for the variograms is less than 2280 metres. Dubrule and Haldorsen (1986) chose 750 metres as the range of influence, this is the average well spacing of cored and non-cored

wells. They do mention that the choice is arbitrary and probably too optimistic.

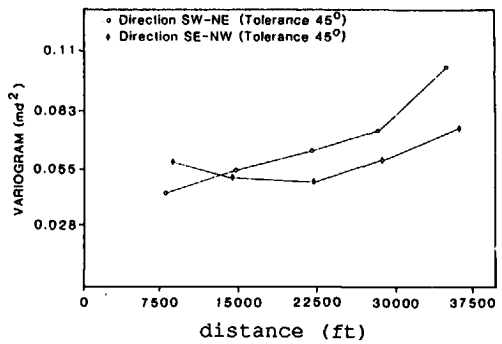

1 ft = 0.3048 m

Figure 3.5 Semi-variograms calculated for the logarithm of permeability (after Dubrule and Haldorsen, 1986).

In order to construct a reliable permeability map, they included additional permeability data from 631 uncored wells. At a point permeability was estimated by its 48 nearest neighbours. The end result of this mapping is shown in Figure 3.6. According to Dubrule and Haldorsen (1986) the permeability map created is a smoothed version of reality.

The study done by Dubrule and Haldorsen (1986) is again only geologically useful in so far that it gives a general overview of the permeability distributions. The range of influence of the semi-variograms was chosen to be 750 metres but is probably much less. Because of the large well spacing, the actual range of influence cannot be determined.

Tomutsa et al. (1986) studied outcrop (Salt Creek anticline) and subsurface (Teapot Dome reservoir and Hartzog Draw reservoir) facies of the Shannon sandstone in central Wyoming. The Teapot reservoir is located 8 kilometres southeast of the outcrop and 90 metres subsurface. The Hartzog Draw reservoir is 40 kilometres northwest of

the outcrop at 2740 metres subsurface. The facies examined in these three areas is a fine-grained sand which is predominantly trough and planar-tangentially cross-bedded. These sands are interpreted as a high energy marginal shelf ridge deposit.

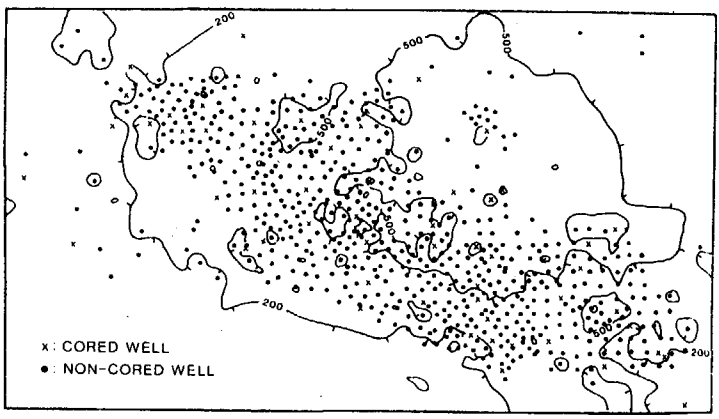

Figure 3.6 Map of permeability obtained from all wells in the Prudhoe Bay field (Alaska, USA) studied by Dubrule and Haldorsen (1986).

The outcrop data consisted of 278 core plugs taken from four main sampling sections varying from 12 to 24 metres in length. On average, the high energy marginal shelf ridge in the outcrop was 3 metres thick. Data taken from the Teapot reservoir consisted of routine core analysis on 10 cored wells; the average thickness of the high energy marginal shelf ridge was 3.6 metres. Comparison of logarithm permeability distributions of outcrop and Teapot data show a reasonable similarity between the distributions considering that the outcrop data were taken from lower Shannon and Teapot data from upper Shannon. These two depositional events are separated by approximately 9.1 metres of siltstone.

Vertical semi-variograms of outcrop and Teapot data are shown in Figure 3.7. The semi-variograms are reasonably similar except below 1 metre, this is probably because of the different sampling scale.

Outcrop data were sampled every 10-15 centimetres and Teapot data every 30 centimetres. The range for these semi-variograms is between 0.6 and 1 metres indicating that there are probably different permeability and porosity zones within the high energy marginal shelf ridge formation. If this had not been the case the range should have been near the total thickness of 3-4 metres. Closer inspection of the outcrop did indeed reveal 4 zones in the high energy marginal shelf ridge facies that differed in their lithology and bedding. Clay content, glauconite content and degree of cementation varied among zones. Core data supported this subdivision.

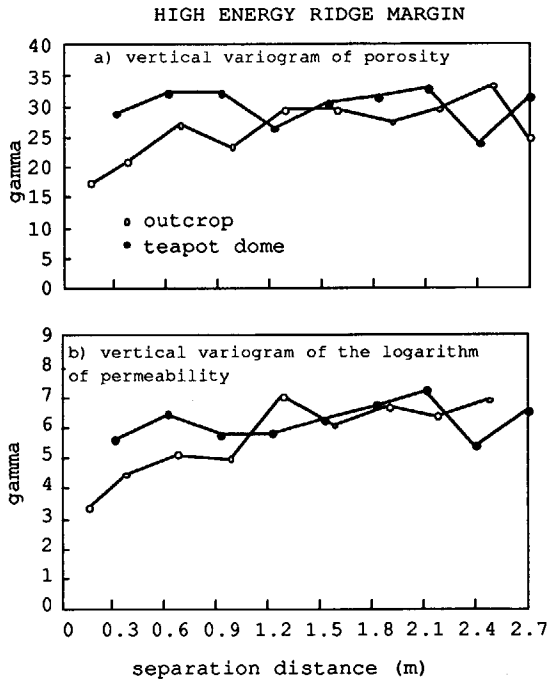

Figure 3.7 Vertical semi-variograms of permeability and porosity data (after Tomutsa et al., 1986).

The semi-variograms for lateral porosity and permeability in the outcrop (Figure 3.8) display a range of less than 3 metres. The

sampling distance for these data was 3 metres, which was insufficient to be able to calculate the range.

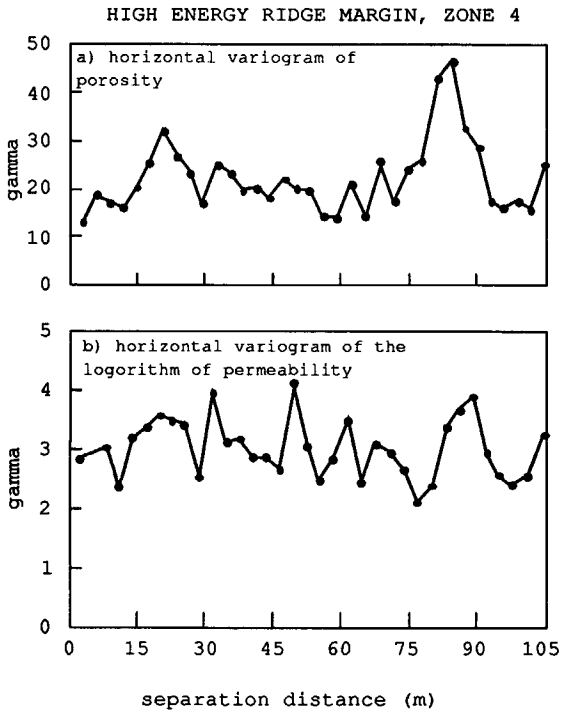

Figure 3.8 Horizontal semi-variograms of permeability data (after Tomutsa et al., 1986).

The data from the Hartzog Draw consisted of routine core analysis on 8 cored wells. Hartzog Draw permeability data peaked at much lower values, possibly because of diagenetic processes and compaction. As result of this and of the limited data available, Tomutsa et al. did not compare the Hartzog Draw and outcrop data further. Their study shows that within rather homogeneous shelf ridge sands the range of influence is very limited (less than 3 metres) making lateral geostatistical estimation of rock properties only possible over short distances.

Goggin et al. (1988) studied permeability patterns in aeolian Jurassic Page sandstone deposits in northeastern Arizona. The study was done on an outcrop showing dune and inter-dune deposits, exhibiting highly ordered heterogeneity, based on stratification types that are a direct result of depositional processes. The dominant stratification types were grain flow deposits (high permeability), wind ripple deposits (medium permeability) and inter-dune deposits (low permeability). These clearly have separate permeability distributions.

Five grids were used for actual measurements (OCROP1 to OCROP5). The grid size varied from 30.3 x 60.6 metres to 0.5 x 1 metres (horizontal x vertical) and the number of measurements per grid varied from 48 to 209. The grids were located at right angles to the direction of dune migration. In order to minimize the effect of weathering, a thin part of the outer rock was removed prior to taking a measurement.

Figure 3.9 shows a semi-variogram based on horizontal permeability data in OCROP1. The experimental values closely approximate the theoretical semi-variogram. In Figure 3.10 the anisotropy for each grid is shown. For OCROP1 the maximum range of influence is found along an inclination of 20° from horizontal. This is approximately equal to the angle of the cross bed sets in the outcrop. The data from OCROP4 were interpreted as having a pure nugget effect. This means that the measured data is considered to be random. An explanation for this is that heterogeneities occur on the same or smaller scale than sampling. With a smaller sampling scale (OCROP5) this randomness apparently disappears.

As a whole, changes from OCROP1 to OCROP5 show differences in the order of stratification, from dune/inter-dune stratification to within-dune stratification heterogeneities. In this study, the large number of measurements and the fact that measurements were taken from a visible surface resulted in the semi-variograms reliably reflecting the scale of heterogeneity and the periodicity in the outcrop area.

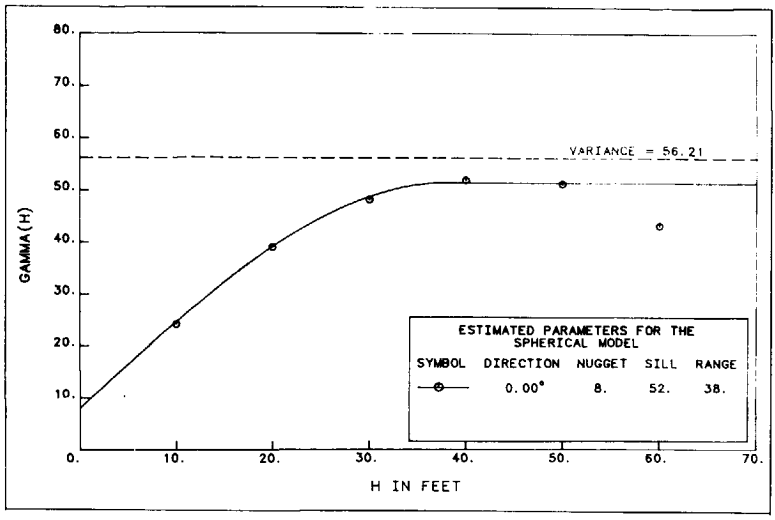

1 ft = 0.3048 m

Figure 3.9 Horizontal semi-variogram for OCROP 1 permeability data (after Goggin et al., 1988).

Kittridge et al. (1989) studied outcrop (Algerita escarpment) and subsurface (Wasson reservoir) heterogeneity of the San Andres Formation in New Mexico and Texas. The outcrop area studied can be divided into a lower portion containing massive bedded fusulinid litho-facies and intercalations of mud support dolomite. The upper portion contains oolitic grain-supportstones with trough cross-bedded dolograinstone units. The main pay zone in the reservoir is composed of open-marine packstones and wackestones.

Data from the outcrop consisted of measurements taken with a mini-permeameter in a large grid (A: 30.3 x 26 metres), 6 smaller grids (B, C, D, E, F and G) located within A and a vertical transect (VT). The largest sampling interval in A was 3.3 metres, sampling intervals in the smaller grids were 15 and 30 centimetres. In the B and E grids data were also collected at intervals of 1.25 and 2.50 centimetres. Vertical data were taken every 5 centimetres. The grid locations are shown in Figure 3.11. Outer weathering of the rocks was removed prior to measuring by grinding. This reduced the permeability by comparison

with that of several core plugs taken for calibration. Subsurface data consisted of core analysis of 10 closely spaced wells.

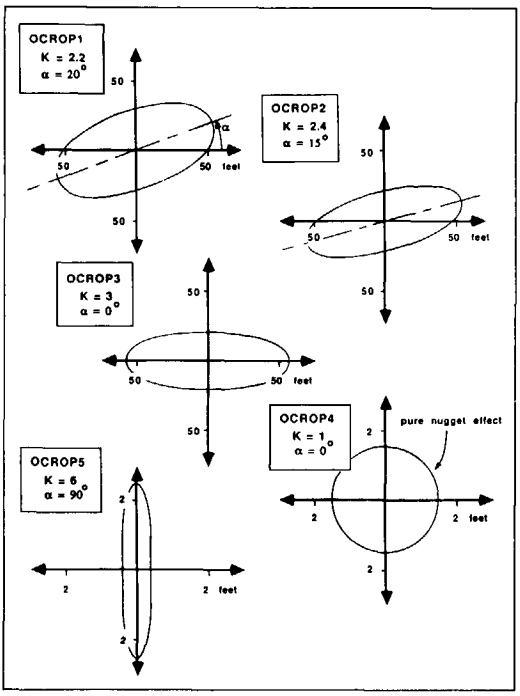

1 ft = 0.3048 m

Figure 3.10 Range of anisotropies for each grid used by Goggin et al. (1988).

The data used by Kittridge et al. in variograms was either log normally or power normally transformed to achieve normal distribution. Figure 3.12 shows the semi-variograms taken in grid B for sample spacings of 15 centimetres and 1.25 centimetres. The ranges of the figures differ, indicating various scales of heterogeneities. The 30 centimetres measurements showed a pure nugget effect (random data) and are not included in Figure 3.12. The reason for this apparent randomness is probably that heterogeneities occur on the same scale as the sampling.

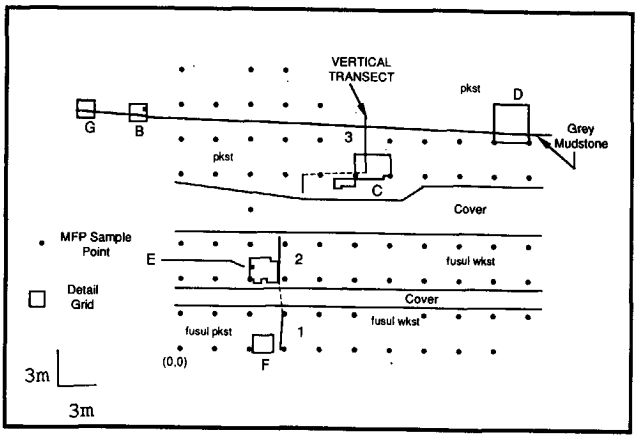

Figure 3.11 Grid locations used by Kittridge et al (1989).

An important aspect highlighted by this study is the observation of distinct scales of spatial correlation that depend on the spacing of the data. This indicates different order heterogeneities. Furthermore this study shows that the geology of the Algerita Escarpment appears to be reasonably similar to the producing interval in Wasson reservoir.

Brummert et al. (1989) present a comparison of four methods for interpolating and extrapolating reservoir data: simple averaging, fifth degree bi-cubic spline, inverse weighted distance squared, and kriging. They applied these methods to the horizontal permeability, vertical-horizontal permeability ratio, thickness and porosity of 5 producing reservoir layers and 1 non-producing layer. They used the various methods to estimate top of structure. They did not reveal the location of the reservoir and they have manipulated the data in order to disguise real values. They maintained that this did not distort the interpolation and extrapolation methods.

The producing zones Brummert et al. studied were composed of clear uniform, fine-grained sandstone grading into non-producing laminated shale and shaly sand sections. Sand/shale sequences occurred throughout the reservoir causing stratigraphic traps. They

characterized the depositional environment as a deep marine environment with mass flow deposits.

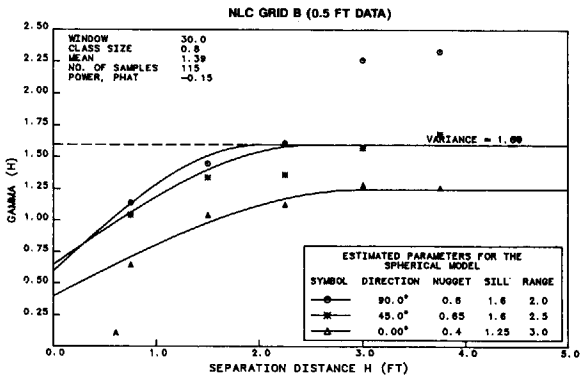

A.

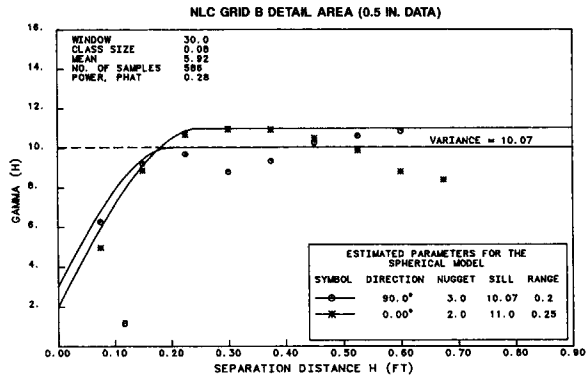

B.

1 in. = 2.54 cm
1 ft = 0.3048 m

Figure 3.12 Semi-variograms of permeabilities for grid B: A) 15 cm sample spacing; B) 1.25 cm sample spacing (after Kittridge et al., 1989).

The data they used were measured from cores. Data were available from 42 wells. The well spacing is not given by Brummert et al. (1989). In all the cores most of the layers studied were detectable. Brummert et al. compared the estimation methods by removing a value from the data

set and estimating it using one of the 4 methods. They calculated the error by:

$$E = \frac{|V_e - V_t|}{V_t} \times 100\ \% \qquad (3.1).$$

In this equation is E the absolute percentage error, V_e the estimated value and V_t the measured value.

Figure 3.13 shows the error comparison between the estimation methods. It can be seen that horizontal permeability cannot be realistically estimated in this reservoir by any method. The error varies between 45 % and 135 % depending on the layer. Using the fifth degree bi-cubic spline method thickness can be estimated with a mean error of around 4 %. Porosity can be estimated with an absolute mean error of around 7 % by all methods except the bi-cubic spline method, kriging is the best method for estimating porosity in this case.

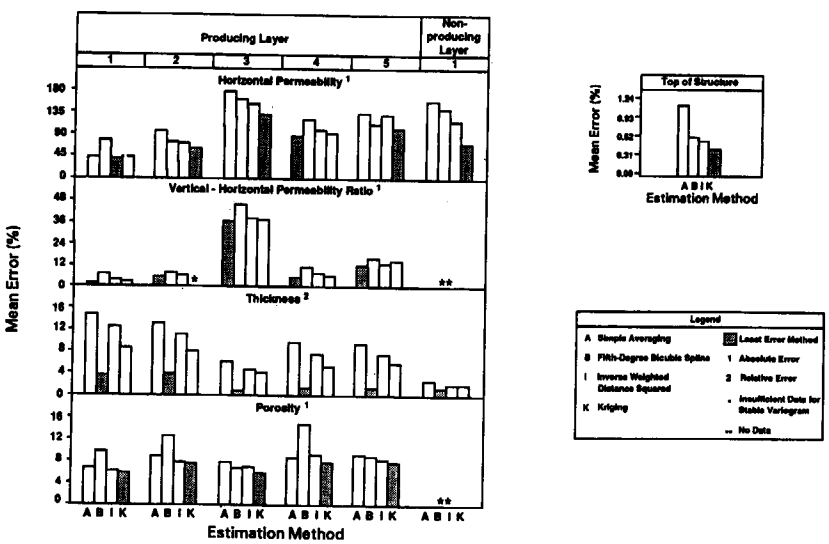

Figure 3.13 Error comparison between the four different methods of estimating various reservoir parameters evaluated by Brummert et al. (1989).

This sort of study is valuable for determining the usefulness of various techniques of estimating reservoir properties and should be carried out in other reservoirs. However, more geological information should be presented, so that the reservoir data and outcome of the estimation methods can be evaluated more objectively.

In addition to estimating rock properties like porosity and permeability, Matheron et al. (1987) developed a technique for modelling litho-facies in the inter-well area. This technique uses data on the horizontal cumulative proportions of each dominant lithology, plus well data. The data on cumulative proportions must be derived from analogue outcrops. The method was tested on a cliff face in Yorkshire (UK). Cumulative proportions were derived from outcrop by Ravenne et al. (1989). Based on this study the facies were assumed to display local stationarity, resulting in a horizontal range of influence for all three facies of 150 metres. Due to the layer-like structure of the facies vertically the range of influence calculated in this plane was only 6 metres. Using the average semi-variograms and a Gaussian threshold curve as a function of height, Matheron et al. simulated the cliff face based on 'well' data (vertical lines of data on the cliff). Comparison of the actual cliff and simulated sections showed that the lateral continuity in the simulated section seems to be somewhat greater. This might indicate an too over-optimistic range of influence.

In order to apply this technique to litho-facies description in each well, horizontal proportions of litho-facies and horizontal and vertical correlations between litho-facies (semi-variogram ranges) must be available (Guérillot et al., 1990). The horizontal proportions of litho-facies and horizontal and vertical correlation must be obtained from outcrops. Until an extensive data base has been constructed for these parameters this method will have a high degree of uncertainty.

Ravenne and Beucher (1988) published more results of the method of Matheron et al. (1987), using data from the Yorkshire cliff again. The cliff section was divided into 4 litho-facies (sandstone, shaly sandstone, silty clay, clay). The cliff data were digitized and used

to construct proportion curves, semi-variograms and cross-variograms of the 4 litho-facies. From the data from wells behind the cliff it was found that the proportions accumulated along the vertical axis were practically the same as those along the cliff.

Ravenne and Beucher (1988) investigated the influence of the number of conditioning wells, the semi-variogram range and the proportion curves for a 2-dimensional simulation of 1000 metres x 30 metres. Simulations using 11 conditioning wells in the 1000 metres section (ranges of influence were 175 metres horizontally and 10 metres vertically) give an image similar to the digitized litho-facies of the cliff. A simulation using only one conditioning well at each end (practically more realistic) resulted in a reasonably similar image, but was inaccurate in some parts.

The influence of the horizontal range of influence was examined using ranges of influence of 50, 500 and 1500 metres. The 50 metres range resulted in a fractionated image. The continuity was lost for a large part of the section. The larger ranges resulted in simulations with increasing continuity and more tabular bodies.

Ravenne and Beucher's study of the influences on simulations clearly shows that the horizontal range of influence is very important for the resulting simulation. However, this factor is also the most difficult to obtain. So far there are no reports of data from outcrops being used to model subsurface reservoirs according to the method of Matheron et al. (1987). Such case studies should show if this method is reliable and practical.

Object-based techniques

Object-based techniques for constructing reservoir models use stochastic variables. This means that instead of assigning explicit values to parameters, the parameters vary within a certain distribution.

By nature reservoirs are in themselves deterministic as there is only one correct configuration of the internal geometries and properties (Haldorsen, Brand and MacDonald, 1988). When data are scarce and

inconclusive, a shift from the deterministic approach to the stochastic approach is necessary. In such cases reservoirs can be called stochastic for modelling purposes. When a quantity cannot be measured or interpreted with a certain reliability, only the probability that certain properties will take on certain values given a probability distribution, can be used as a modelling criterion. Figure 3.14 shows the difference between deterministic and stochastic relationships. Unlike deterministic relationships, stochastic relationships display a trend and distribution of a property at different given (input) values. Hence, using a stochastic relationship makes it possible to have different results from the same input data each time the model is used. However, the possibilities are constrained by the probability distribution.

Object-based stochastic modelling of reservoir architecture uses stochastic means to generate possible representations of reservoir architecture. This is done using assumptions concerning the size of sedimentary bodies and rules of the disposition of these bodies. The model can be conditioned to comply with well observations and geological rules. Factors that can be addressed in the quantitative geological description of the reservoir include modelling of sand bodies, baffles and fractures (Haldorsen et al., 1988). In this thesis I will focus on the modelling of genetic units.

The simplest method for creating object-based stochastic representations of reservoir architecture is to randomly model sand bodies in a matrix of non-permeable material. This can be done in a 2-dimensional cross-section or 3-dimensional volume, the easiest case being a 2-dimensional cross-section. A modelling algorithm based on this simple method is described by Haldorsen et al. (1988). The method for 2-dimensions is as follows.

The algorithm is based on a given net sand fraction and given distributions for the thickness of the sand body (H_s) and its ratio of width to thickness (W/H_s). The following assumptions are made for this modelling technique. A cross-section area is chosen with dimensions L for the length and H for the thickness. The given/required net sand fraction is defined as the net area of sand

divided by the total area of the cross-section; overlapping sand bodies must be accounted for in order to get the actual net sand fraction. The net sand fraction is also referred to as the net to gross ratio or sand/shale ratio (F_s) describing the fraction of reservoir quality sand. The positions of the sand bodies (sand body centres) and the sand body sizes are independent of all other sand bodies. Sands generated entirely within another previously generated sand body are eliminated. Sands crossing the boundaries of the defined cross-section area are chopped off beyond these boundaries.

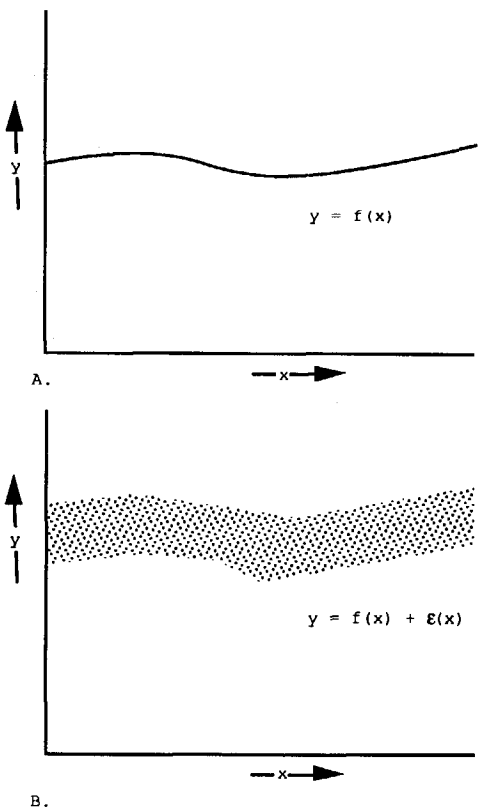

Figure 3.14 A) Deterministic relationship between x and y; B) stochastic relationship between x and y. (after Haldorsen, 1983)

The actual generation of a cross-section based on the previously discussed assumptions starts with the generation of a random sand body centre within the cross-section. This position is given as (x,z). From empirical cumulative distribution functions a thickness is randomly sampled. Next a width/thickness ratio is sampled from the W/H_s distribution and the width of the sand body is calculated. The sand body size and position have now been established. If the sand body is entirely located within an earlier generated sand body, its position is discarded and a new position is generated. After generation of each sand body the net sand fraction is calculated taking overlapping sand bodies into account. If the modelled sand fraction is smaller than the required fraction, the whole process of creating a sand body is repeated until the required fraction is achieved. Figure 3.15 shows the modelling algorithm in a flow diagram.

The modelling algorithm can easily be extended to 3-dimensional models (Haldorsen et al., 1988; Augedal et al., 1986). A generated 2-dimensional cross-section is then taken as the 'front' section of the reservoir volume being modelled. By adding an angle (for variability of orientations) to the input data the sand bodies can be extended into the volume at a certain angle sampled from the distribution, resulting in a 3-dimensional reservoir volume (Figure 3.16). Instead of straight channels the modelling algorithm can be adapted to change the direction of the channels locally. The direction then assumes values around the palaeo-current direction within the modelling volume; this will, however, make the modelling process more difficult computationally.

The first practical addition to the modelling algorithm presented by Haldorsen et al. (1988) is to condition the model to sand bodies found in the wells located in the modelling volume. The algorithm for generating a 2-dimensional cross-section must then begin by generating sand bodies located in the wells. The thickness of these sand bodies can be deduced from cores or well logs. Using the W/H_s distribution the width of the sand bodies is then calculated. As the vertical position of the sands is known from well data, only a horizontal location value (x) for the sand bodies must be generated.

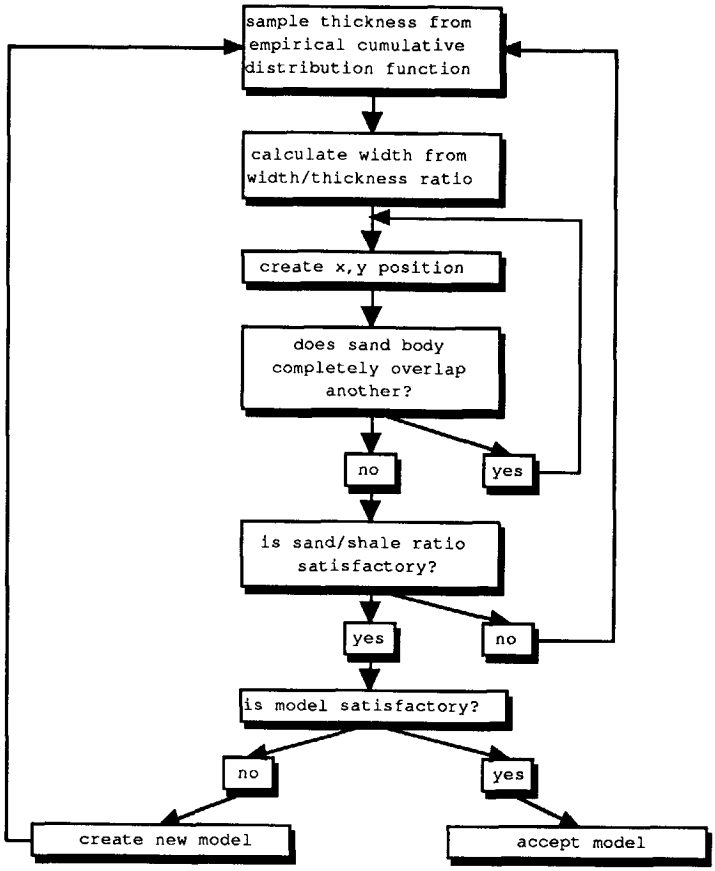

Figure 3.15 Flow chart of randomly modelling sands in a shaly matrix.

It is unlikely that the wells will pass through the centres of the sand bodies, so x is chosen randomly within the constraints given by the generated widths and the well location. The flow diagram in Figure 3.17 shows the algorithm for conditioned random simulation. This type of modelling still results in very crude geological models with only one type of sand body distributed in an impermeable shale matrix. This is not a very realistic situation compared with the actual geology of reservoirs. In order to further improve this modelling technique various types of related sand bodies should be

incorporated into the models. For example crevasse splays can be added to the model.

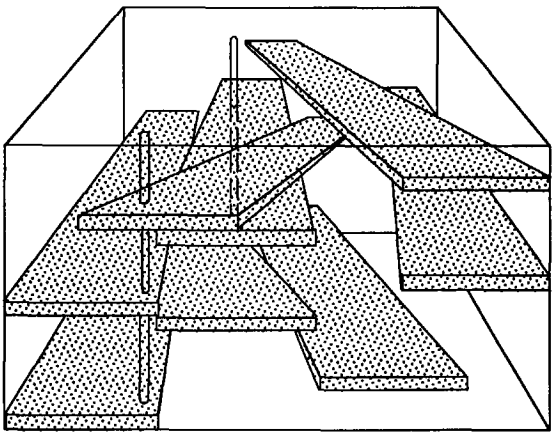

Figure 3.16 Object-based modelling in three dimensions: sand body orientation can vary a certain angle around the depositional dip (modified after Stanley et al., 1990).

The steps discussed above to create realistic geological models are shown in Figures 3.18 to 3.20. These figures are obviously very simplistic but illustrate the above-mentioned methods. Figure 3.18 shows two wells drilled in a heterogeneous reservoir. Sand bodies are not correlatable between the wells in this situation. Based on the net sand fraction found in the two wells a random model can be constructed as shown in Figure 3.19. This model is also conditioned to the sand bodies found in wells. Figure 3.20 shows a simulation that is both conditioned to well information and displays geological features normally associated with each other, in this case crevasse splays attached to channels. Using this geological knowledge specific environments of deposition can be modelled with their characteristic genetic units distributed according to geological rules. This modelling algorithm can be extended in three dimensions by taking into account three-dimensional size distributions and by allowing the orientation of the sand body to vary around the depositional dip direction by a certain angle.

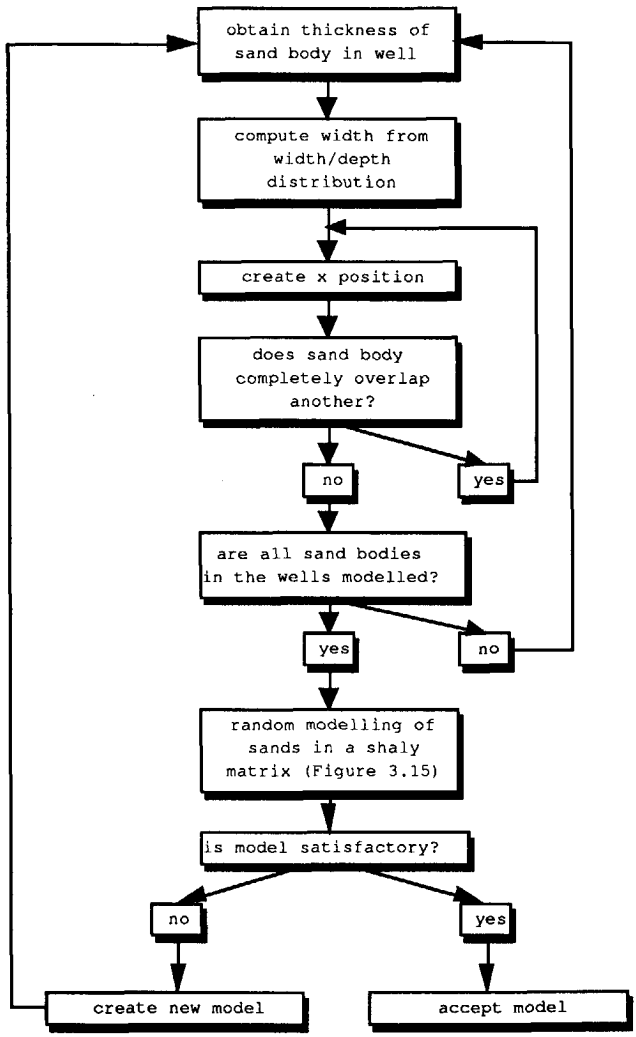

Figure 3.17 Randomly modelling sands in a shaly matrix, but conditioned to well data.

An example of modelling of reservoir architecture with object-based techniques is given by Silva, Niko and Van Den Bergh (1988). They studied the Eocene Lower C sands in the Lake Maracaibo area in Venezuela in order to achieve the best secondary recovery scheme. An area containing 22 wells was used as the pilot area for the water/gas injection study to keep reservoir pressure above the bubble point.

Within this fault block an area containing 14 wells with good core and log information was selected as study area.

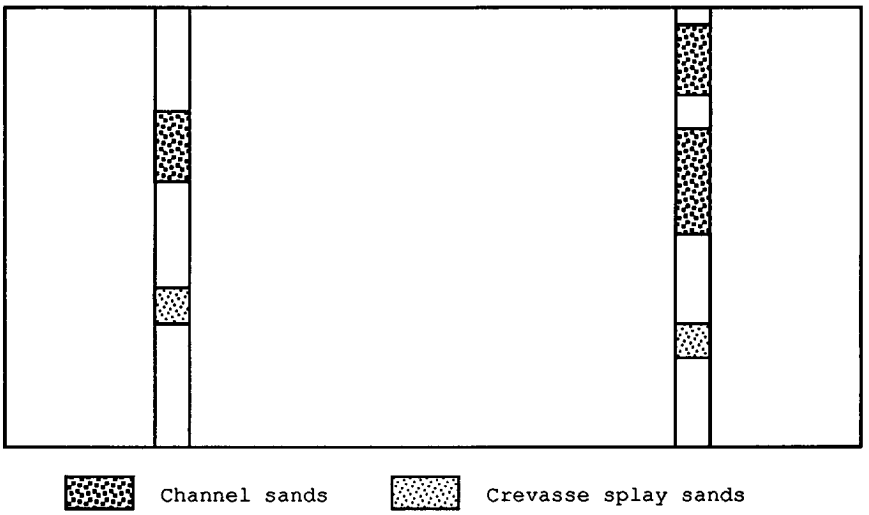

Figure 3.18 Two wells drilled in a heterogeneous reservoir.

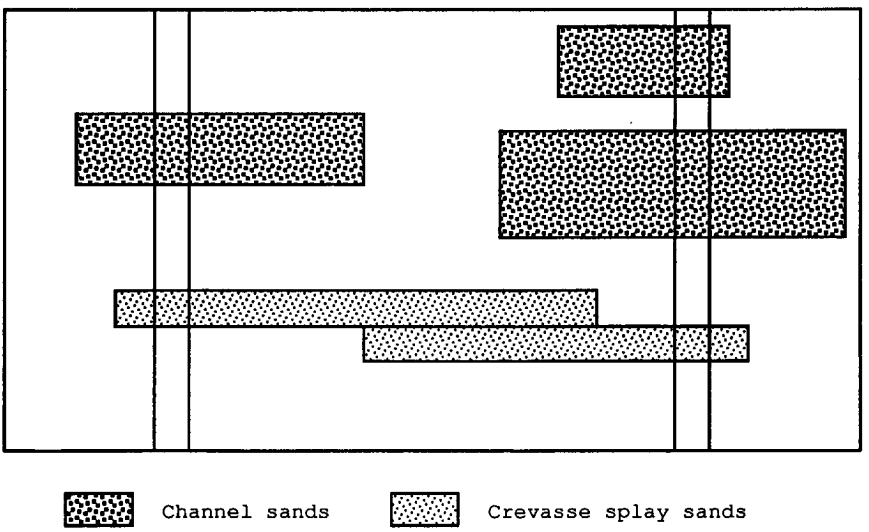

Figure 3.19 Random model conditioned to the wells.

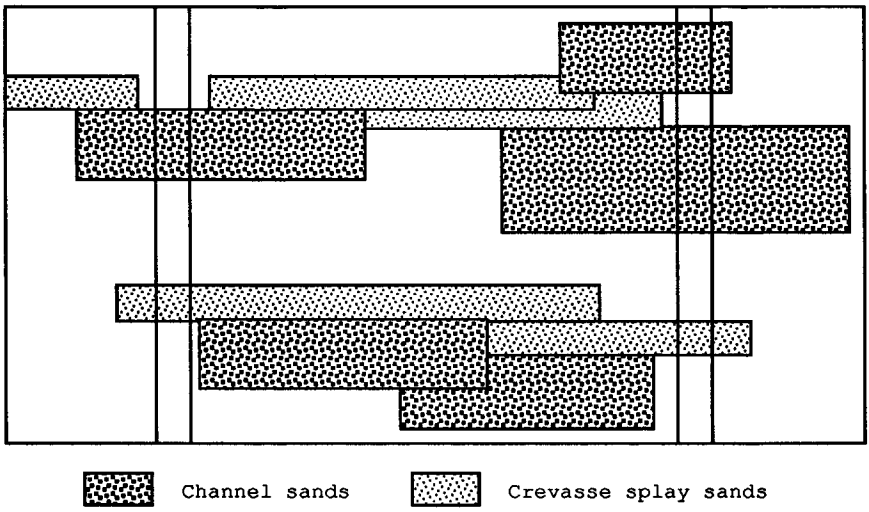

Figure 3.20 Random model conditioned to well data and geological rules.

From RFT pressure surveys they found that subunits of the Eocene Lower C sands (CLC) are geologically very complex. The largest problem in the reservoir was that the well spacing (1.2 kilometres) was larger than the dimensions of individual sand bodies. This made good well correlation impossible and so they adopted a probabilistic approach to describe the reservoir architecture in 2-dimensional sections.

The sediment sequence in the reservoir contains a number of sand-rich intervals separated by thick shales. These shales differentiate the reservoir into several isolated units. The environment of deposition has been defined as a fluvial or tidal dominated delta, with the sand-rich units being products of delta lobes progressing from an inferred southwestern source. Two main genetic units occur in the CLC reservoir: channel sands and bar sands.

The section chosen for probabilistic modelling was an extensively cored cross-section containing 3 wells. The data used for the construction of the probabilistic geological models consisted of

litho-facies descriptions in the wells, width/height distributions of the sand-body units based on information from non-meandering distributary channels. Net to gross ratios were taken from the conditioning wells and the long axes of the sand bodies were assumed to intersect the section at angles between 0 and 30 degrees. Two possible reservoir architectures were created, based on the 3 wells in the cross-section. These geological models are shown in Figure 3.21. Both models honour well data and contain equally probable sand-body distributions. The second reservoir model performed worse, mainly because of poorer sand connectedness. Qualitatively the drive performances were equal but the recovery for the second model was less. Comparison of gas to water drive performances showed a consistently better oil recovery for water drive. Silva et al. do not state if this is the result by the modelled reservoir architecture or by other causes.

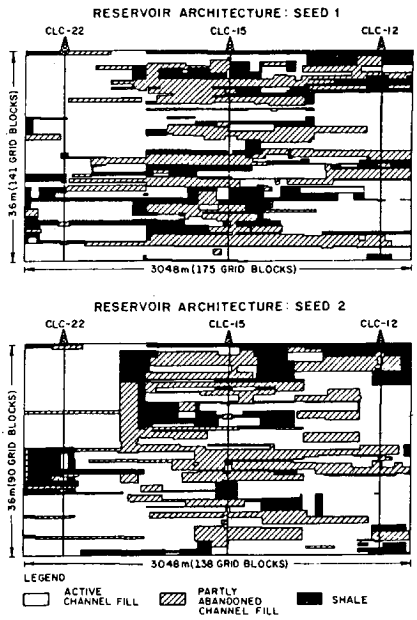

Figure 3.21 Reservoir architecture modelled by Silva et al.(1988) for the Eocene Lower C Sands in the Lake Maracaibo area of Venezuela.

Although the study was performed on a small-scale, it clearly demonstrates the usefulness of probabilistic modelling in such cases. It should be kept in mind, however, that if this technique is applied to 3-dimensional situations two other important phenomena should be taken into account. Firstly, flow that is forced through poorly permeable zones in 2-dimensional sections might flow more easily through a short circuit in 3-dimensions. This will then result in poorly permeable sands being bypassed. Secondly, oil that is trapped in dead ends in 2-dimensional sections might be more accessible in 3-dimensions. In this study the large net to gross ratio probably diminishes the chance of oil being trapping in dead ends, but the bypassing of oil in a 3-dimensional model can result in lower recoveries.

3.3 Developing a knowledge base

From § 3.2 it becomes clear that usually the data from the reservoir are insufficient for a reliable and accurate reservoir model. Modelling techniques should be used to create a reservoir model based on data from the reservoir and on general geological knowledge.

From the modelling techniques discussed in § 3.2.2 it becomes apparent that geological simulation models are often unpractical for reservoir modelling , because of the complexity of the processes that play a role during sedimentation. Sequence-based geostatistical techniques also seem to be of limited value, because of the limited range of influence of most rock parameters. Object-based techniques have most potential. However, there is a lack of quantitative geological information on the dimensions of genetic units and the relationships between them. A knowledge base containing such information must be developed.

3.3.1 STRUCTURE OF THE KNOWLEDGE BASE

In order to develop a knowledge base containing quantitative geological data, firstly I defined relevant geological relations on different scales. I distinguished three scales of geological variation: large-scale (variation between genetic units), medium-scale (variation within genetic units), and small-scale (variation due to textural and compositional features of the rocks). Variation on a large-scale is mainly concerned with geometries and internal configuration of sedimentary environments. Variation on an intermediate scale is concerned with geometries and internal configuration of genetic units. Examples are width/thickness ratios of genetic units, and sizes of baffles to flow. Variation on a small-scale features is concerned with variation in rock properties caused by the texture and composition of the rocks. Relations on this scale incorporated in the knowledge base are mainly concerned with porosity and permeability trends, for example those caused by sedimentary structures (Table 3.3).

3.3.2 ANALOGUE CRITERIA

One way of obtaining quantitative geological information for use in modelling of reservoir architecture is to measure, catalogue and statistically process facies attributes from geological analogues where the sedimentological configuration is well known. Analogue data has to be collected and applied with care. Not only the depositional environment but also other factors must be taken into account (Cross, 1991).

In general, analogue data must ideally satisfy four conditions which are in decreasing order of importance:

- the sedimentary facies must be similar.
- the tectonic regime must be similar.

Table 3.3 Knowledge base parameters.

LARGE-SCALE (variation between genetic units)	MEDIUM SCALE (variation within genetic units)	SMALL-SCALE (variation within sets)
internal architecture of depositional complexes[1]	internal configuration of genetic units	porosity anisotropies
shape of depositional complexes	shape of genetic units	permeability anisotropies
size of depositional complexes	size of genetic units	
relation between sizes of affiliated genetic units	textural trends within genetic units	
transition probability between genetic units	porosity trends within genetic units	
	permeability trends within genetic units	
	orientation of baffles to flow	
	size of baffles to flow	

- the grain size and mineral composition must be comparable.
- the palaeo-climate must be comparable.

Analogues can be very comparable even if not all abovementioned requirements are met. This is illustrated in Figures 3.22, 23 and 24. Figure 3.22 show a number of tidal bundle sequences from different localities and ages which are quite similar. In Figures 3.23 and 3.24

[1]A sedimentary complex is defined as a complex of genetically related units, which is the product of a set of specific sedimentary processes that acted at the surface of the earth.

this has been done for barrier island sequences and point bar deposits respectively.

3.3.3 ANALOGUE TYPES

Quantification of geological variation is possible where the rate of variation may be adequately sampled. Such opportunities are presented by outcrops, recent environments and densely drilled fields. Outcrops give continuous information on the distribution of rock properties in a cross-sectional view. However, outcrop studies are relatively expensive and time-consuming, the orientation of the sections is invariate and information on the areal distribution of the genetic units is limited. Data from recent environments yields continuous information on the areal distribution of rock properties, but for the distribution of rock properties in a cross-sectional view shallow wells have to be drilled (e.g. van Heerden and Roberts, 1988), or high resolution seismic data have to be available (e.g. Corsmit et al., 1987). A major problem in using analogue data from recent environments for reservoir modelling is that many depositional environments are reworked and not preserved in the same geometry. Also compactional and diagenetic features cannot be assessed from recent deposits. The gathering of data is again relatively time-consuming and expensive. Studies on densely-drilled fields are relatively less expensive and time-consuming than outcrop studies or studies on recent environments. Also the direction of the sections is less restricted and diagenetic and compactional features can be taken into account. On the other hand, a major problem is the limited continuity of the data. This causes uncertainties in the 3-dimensional distribution of genetic units. Also cores must usually be available to get reliable sedimentological interpretations of the genetic units.

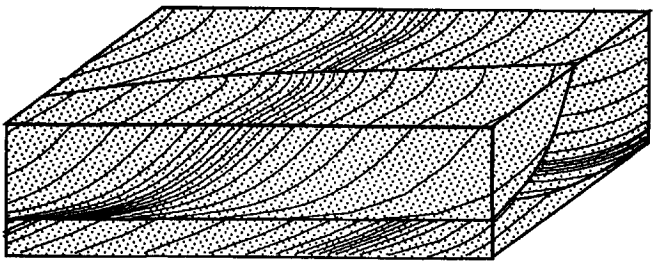

Block diagram showing tidal channel facies

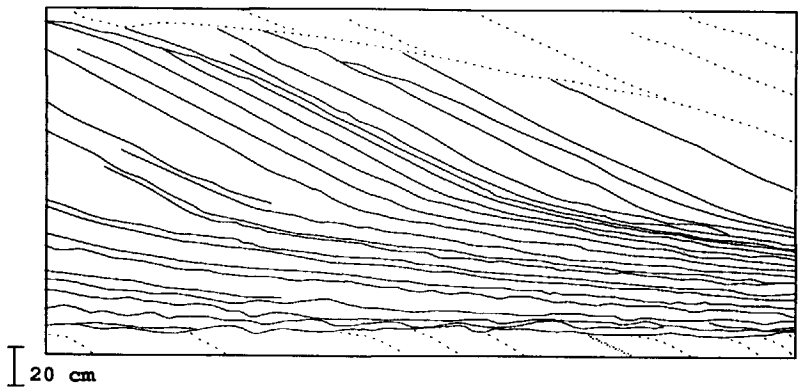

Oosterschelde, The Netherlands: Holocene (Drawn from lacquer peel)

Pyrenees, Spain: Tertiary (Courtesy A.W. Martinius, Delft University of Technology)

Figure 3.22 Tidal bundle sequences from different ages and localities.

Kelsim Pit, Belgium: Tertiary (Courtesy L.C. Van Geuns, Shell Research)

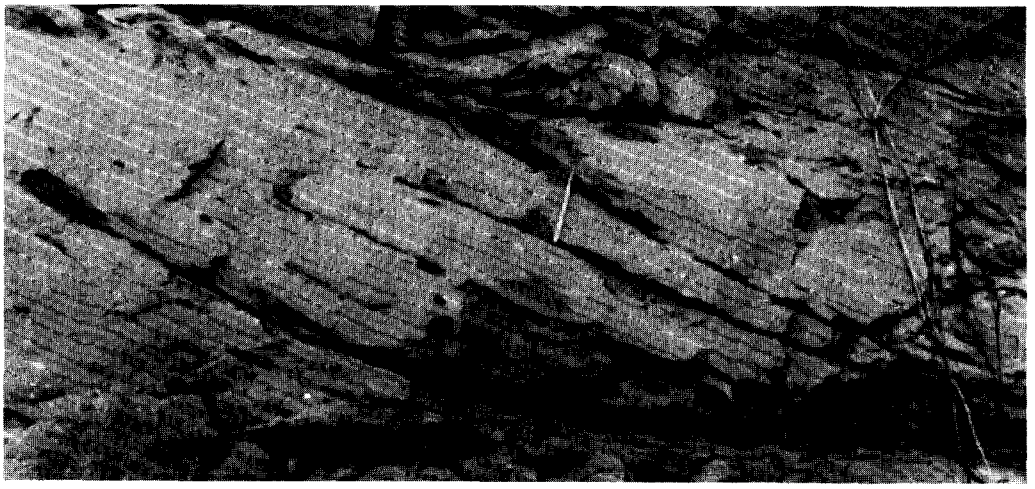

Miri Hill, Sarawak: Tertiary (Courtesy K.J. Weber, Delft University of Technology)

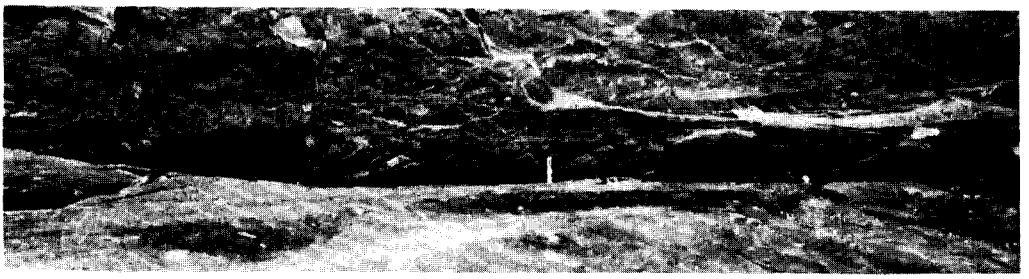

Kangaroo Island, Australia: Cambrium (Courtesy S.D. Nio, INTERGEOS)

Figure 3.22 Continued.

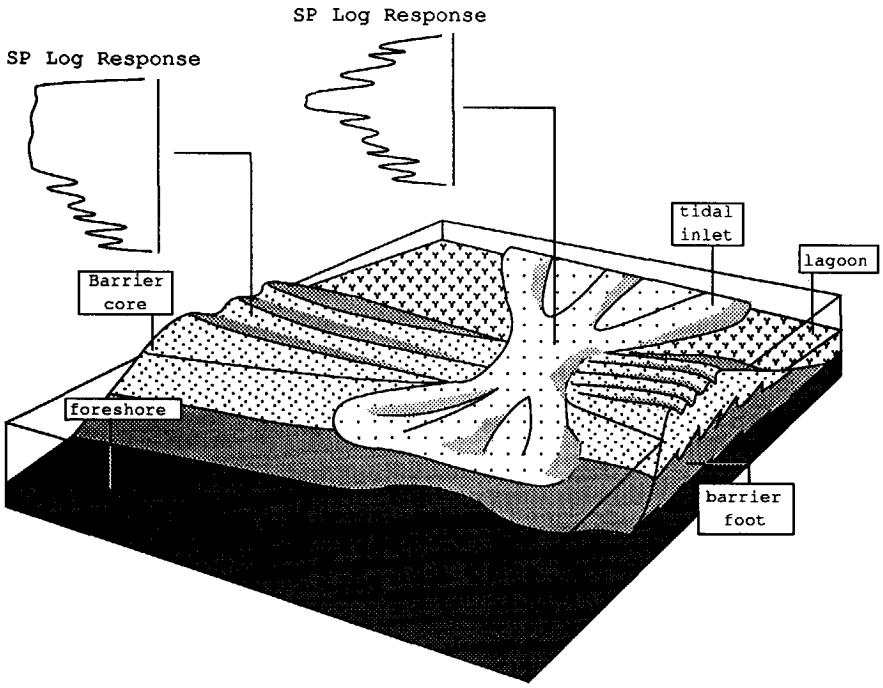

Block diagram showing barrier bar facies with corresponding SP - log response

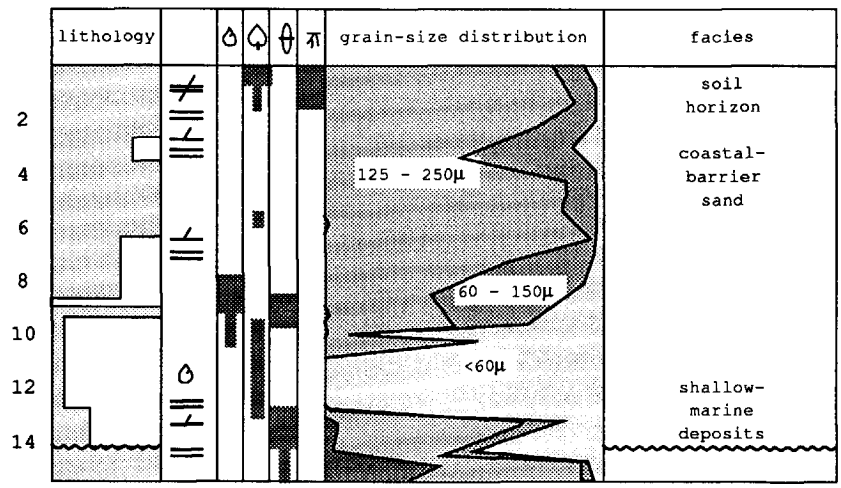

Niger delta, Nigeria: Holocene (after Oomkens, 1974)

Figure 3.23 Barrier bar sequences from different ages and localities.

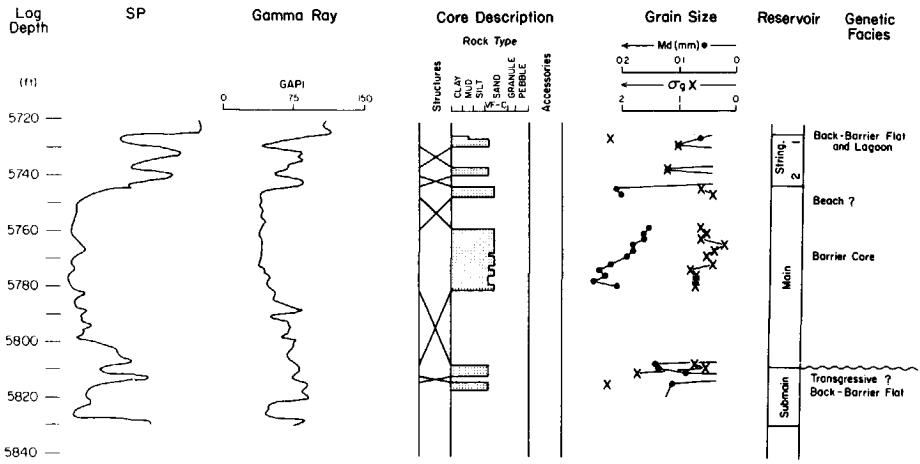

Frio Formation, Texas: Oligocene (modified after Galloway and Cheng, 1985)

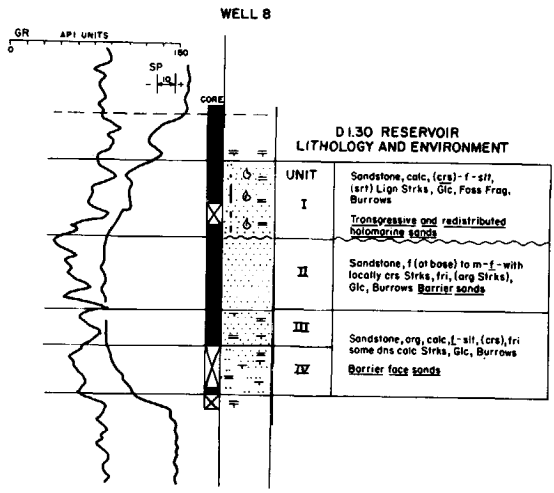

Niger delta, Nigeria: Tertiary (Modified after Weber et al., 1978)

Figure 3.23 Continued.

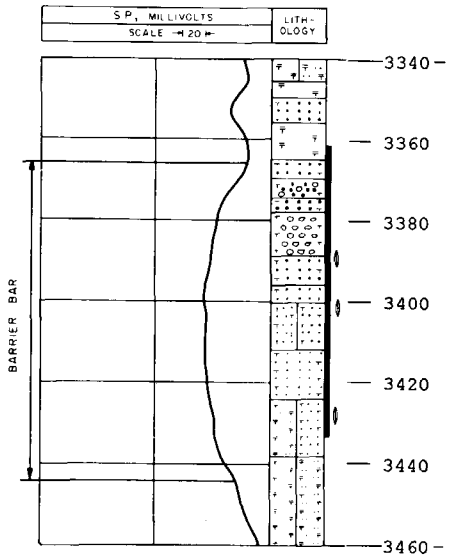

Elk Field, Oklahoma: Carboniferous (after Sneider et al., 1977)

Figure 3.23 Continued.

3.4 Case studies

Several examples of the use of outcrop studies for the development of a knowledge base have been published (e.g. Ravenne et al., 1989; Flint et al., 1989; Walderhaug and Mjos, 1991; Lowry and Raheim, 1991). Studies of recent environments or densely-drilled fields for the construction of a knowledge base are not generally available. In this chapter an evaluation is given of the possibilities for knowledge base development based on information from densely-drilled fields and Recent environments. This evaluation is based on three reservoirs from the North Markham-North Bay City field in the Texas Gulf Coast and the Recent Atchafalaya delta, Louisiana.

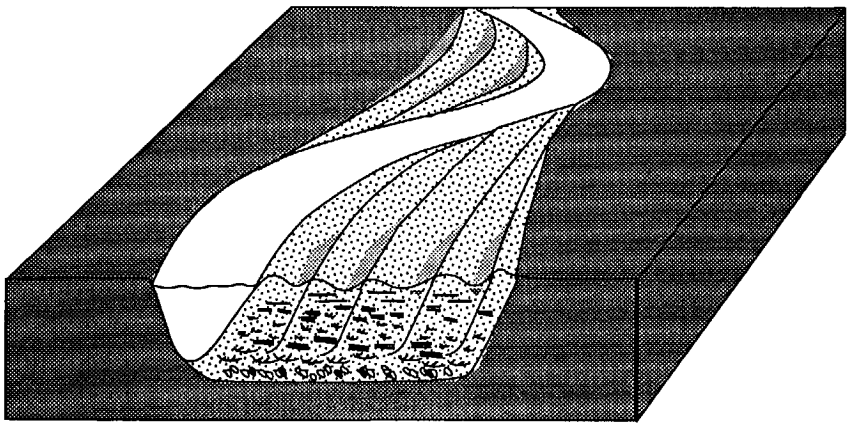

Block diagram showing point bar facies

LAS = Lateral Accretion Surface

Rio Puerco, New Mexico: Holocene (after Sheperd, 1987)

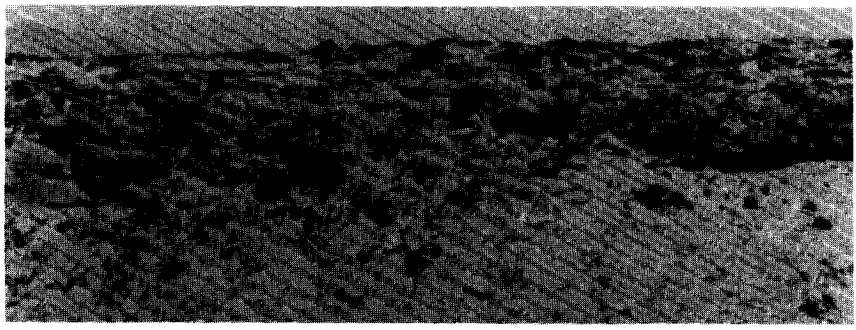

Willwood Formation, Wyoming: Eocene (after Kraus and Middleton, 1987)

Figure 3.24 Pointbar deposits from different ages and localities.

Monllobat Formation, Spain: Eocene (Courtesy A.W. Martinius, Delft University of Technology)

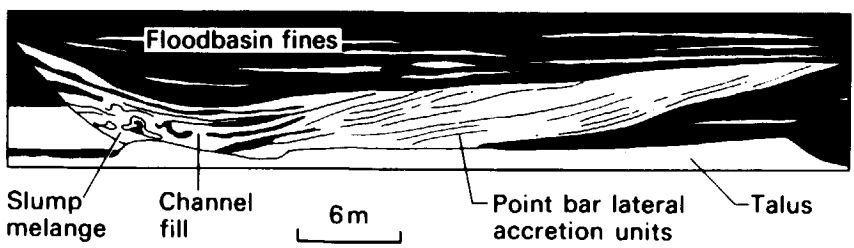

Scalby Formation, Yorkshire: Jurassic (After Nami and Leeder, 1978)

Figure 3.24 Continued.

3.4.1 THE NORTH MARKHAM-NORTH BAY CITY, A DENSELY DRILLED FIELD

The North Markham-North Bay City field is located in the eastern part of the Texas Gulf Coast, USA (Figure 3.25), and it produces oil and gas from multiple stacked shoreline sandstones of Oligocene Frio Formation (Tyler and Ambrose, 1983). Contemporaneous growth faulting was the dominant structural process during deposition of the North

Markham-North Bay City reservoirs. The faulting produced strike elongated roll over anticlines, which form the hydrocarbon traps (Tyler and Ambrose, 1983). By 1969 the Railroad Commission of Texas recognized 20 separate hydrocarbon reservoirs in the field, 9 are principally oil reservoirs and the remaining 11 are gas reservoirs. Cumulative oil production from the field by the end of 1982 was $7.1 \cdot 10^6$ m^3 and total gas production was $2.8 \cdot 10^6$ m^3 (Railroad Commission of Texas, 1983).

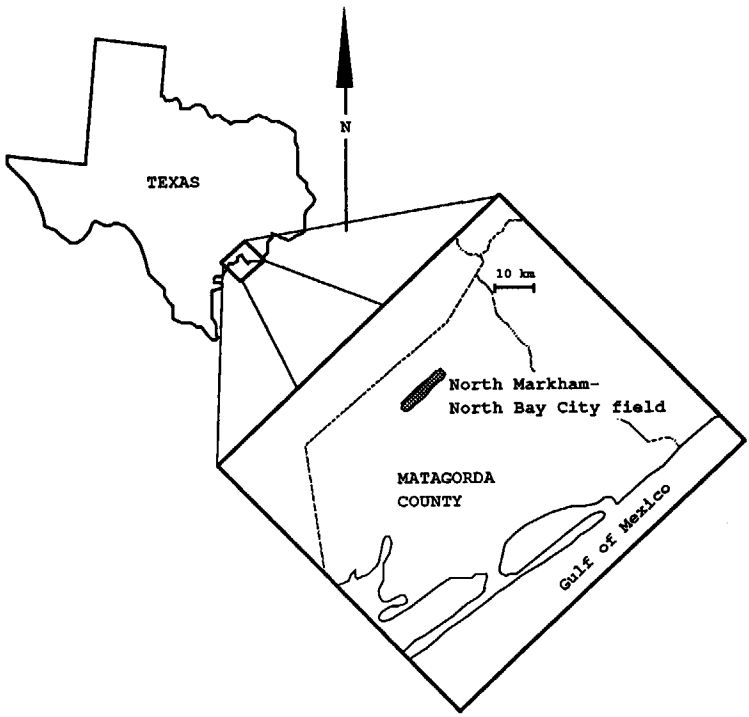

Figure 3.25 Location of the North Markham - North Bay City field.

The three main oil reservoirs of the field are the Carlson, Cornelius and Cayce reservoirs. Data available for these reservoirs are spontaneous potential (SP) logs, resistivity logs, water-cut data and well productivity data. Average well spacing in the North Markham-North Bay City field varies between 100 and 350 metres and most wells were drilled in the early forties. SP- and resistivity logs have

limited vertical resolution and only allow speculative sedimentological interpretation. Furthermore, the absence of cores hampers interpretation of the depositional environment. However, based on regional geological information, available production data and log shape mapping Tyler and Ambrose (1983) were able to interpret the Carlson, Cornelius and Cayce reservoirs as different types of strandplain deposits (Figures 3.26, 3.27 and 3.28).

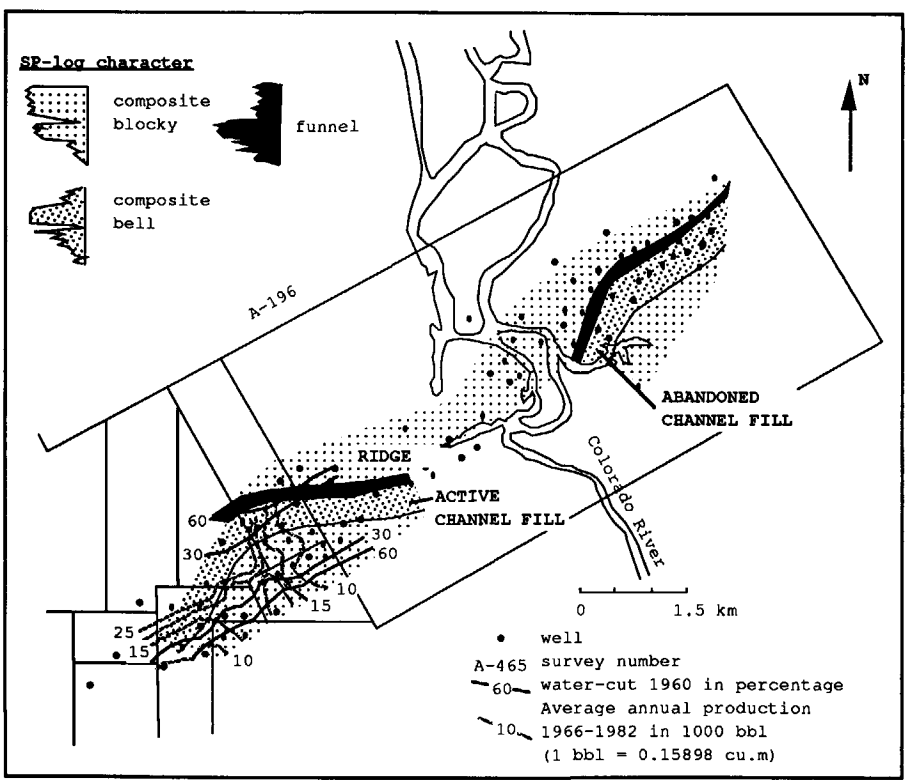

Figure 3.26 Palaeogeographic map of transgressed strandplain sandstones of the Carlson reservoir showing log-shape distribution, water-cut data and productivity data (modified from Tyler and Ambrose, 1983).

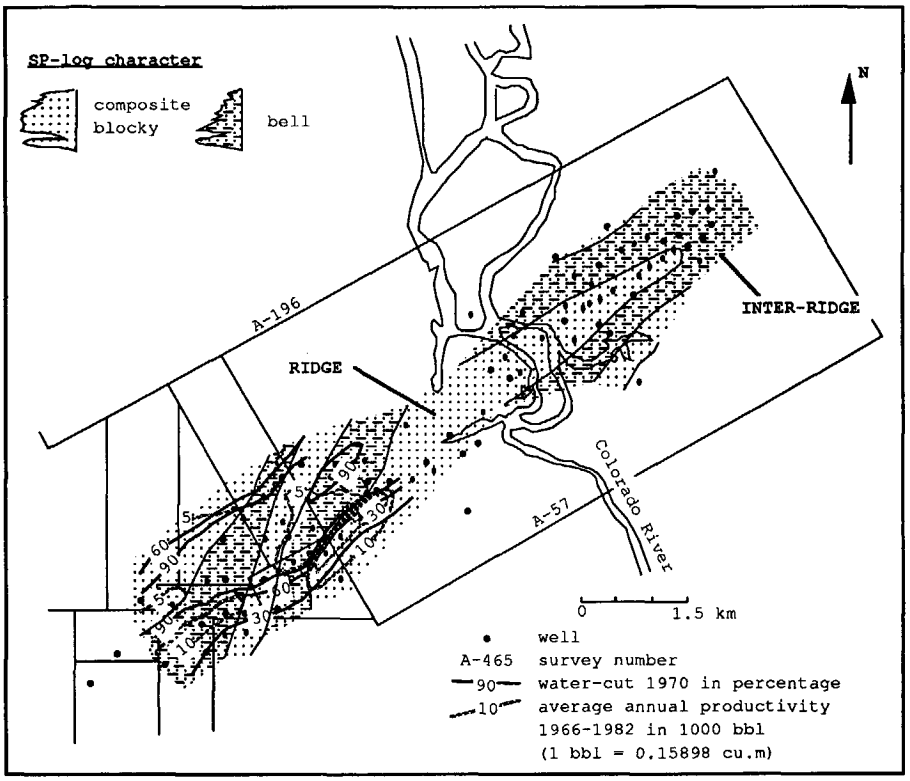

Figure 3.27 Palaeogeographic map of mud-rich strandplain deposits of the Cornelius reservoir showing log-shape distribution, water-cut data and productivity data (modified from Tyler and Ambrose, 1983).

For the purpose of knowledge base development I quantified the geological models of Tyler and Ambrose (1983). I used as much as possible of the details incorporated in the original maps of Tyler and Ambrose (Figures 3.26, 3.27 and 3.28) and constructed additional cross-sections. The grid of sections that I used is shown in Figure 3.29. An example of a cross-section is given in Figure 3.30. Orientation of the sections is parallel or perpendicular to depositional dip as inferred from the geological models. I overlaid a grid on the maps and cross-sections to obtain quantitative information on upward- and lateral transition probabilities between genetic units and on relative occurrence of genetic units (Figure

3.30). Lateral and vertical transition probabilities can be used in reservoir modelling to condition the position of genetic units to each other. The relative occurrence of genetic units can be used for conditioning of the relative abundance of various genetic units. Also I determined dimensions of individual genetic units. This geometrical data can be used to generate realistic dimensions for individual genetic units within a reservoir model.

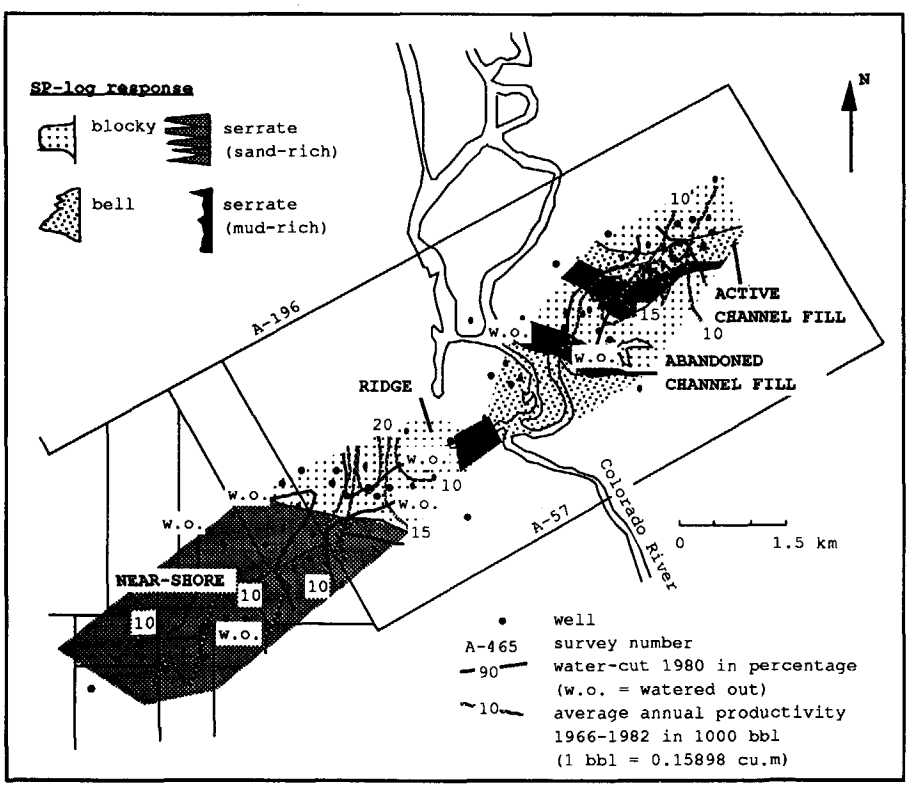

Figure 3.28 Palaeogeographic map of sand-rich strandplain sandstones of the Cayce reservoir showing log-shape distribution, water-cut data and productivity data (modified from Tyler and Ambrose, 1983).

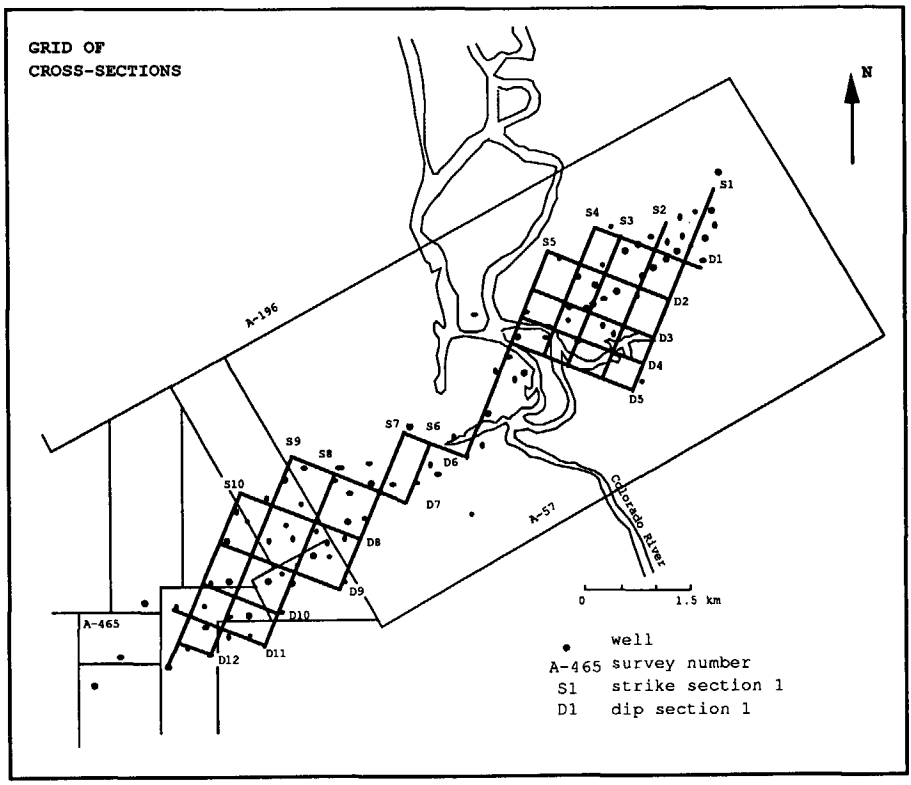

Figure 3.29 Base-map of the North Markham - North Bay City field showing grid of sections that was used for the quantification of the sedimentological models of Tyler and Ambrose (1983).

The results of the quantification are shown in Figure 3.28. Results are plotted separately for strike and dip lines to investigate if the results are direction dependent. There is no major difference in upward-transition probability between dip and strike sections in the transgressed sand-rich strandplain sandstones of the Carlson reservoir. Figure 3.31 shows that the largest variability in upward transition probabilities occurs in the upper part of the sequence. This can be explained by the limited lateral continuity of the genetic units in this part of the sequence (Figure 3.30). In the Cornelius reservoir there are minor differences in upward transition probabilities between strike and dip lines (Figure 3.31). The

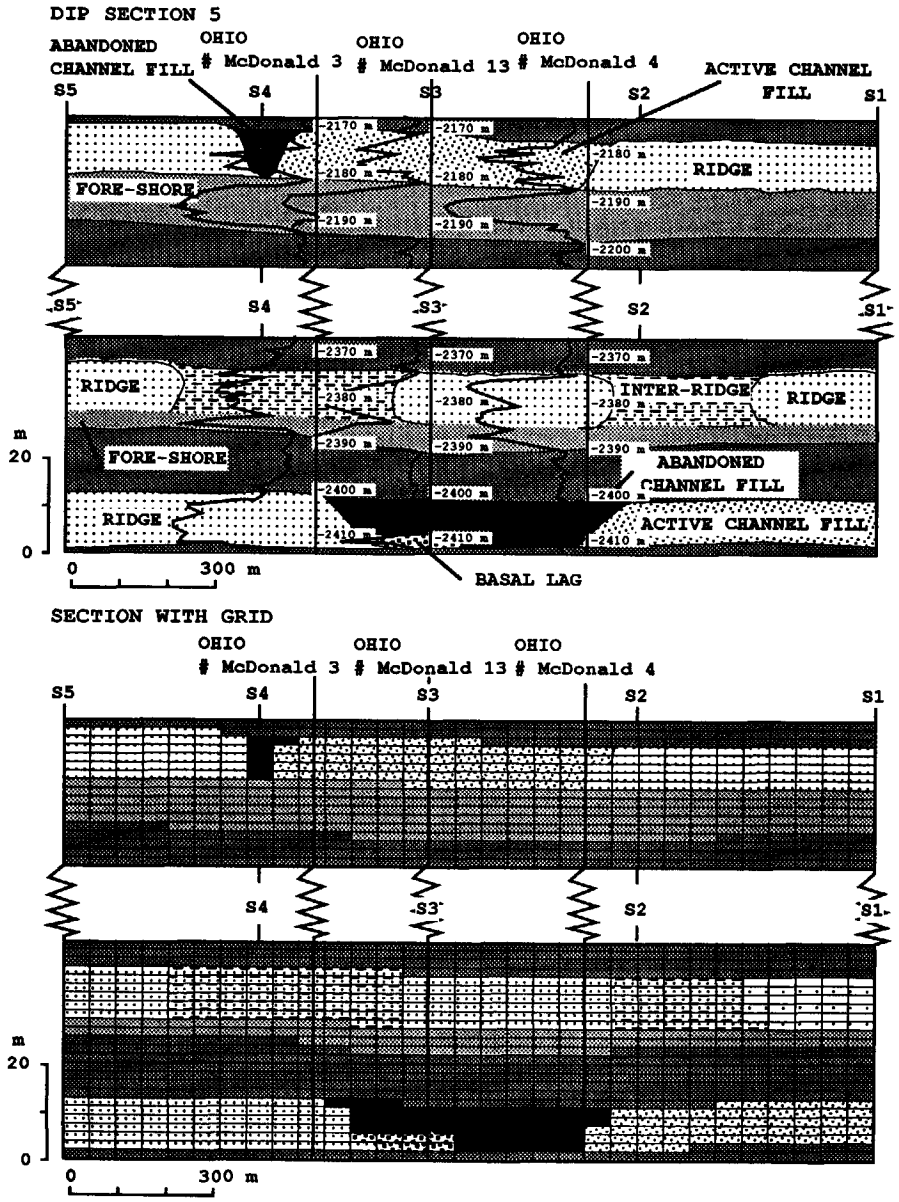

Figure 3.30 Sedimentological cross-section (Dip Section 5) through the Carlson, Cornelius and Cayce reservoirs showing SP-log responses. Also the same section is given with the grid overlain on it that was used for the quantification of the sedimentological models.

somewhat higher transition probability from fore-shore to inter-ridge sediments in the strike sections is caused by the fact that the orientation of the genetic units is more or less parallel to the strike lines, and the strike lines used in this study run predominantly through inter-ridge material. There is also no major difference in upward-transition probability between dip and strike sections in the Cayce reservoir (Figure 3.31).

CARLSON RESERVOIR

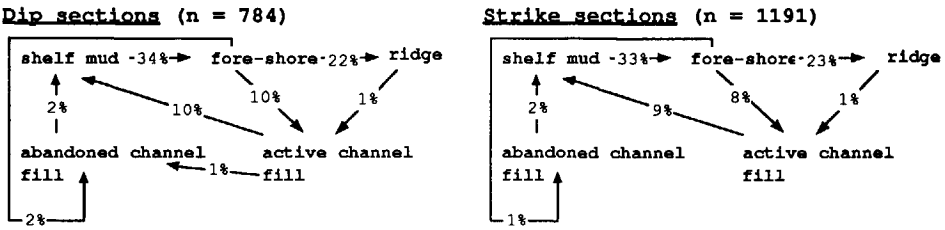

CORNELIUS RESERVOIR

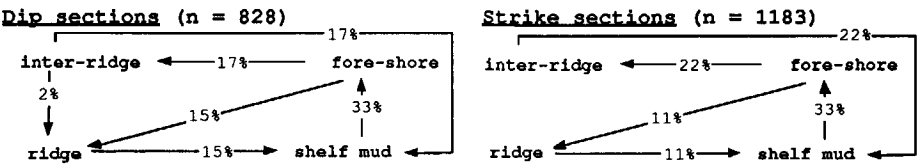

CAYCE RESERVOIR

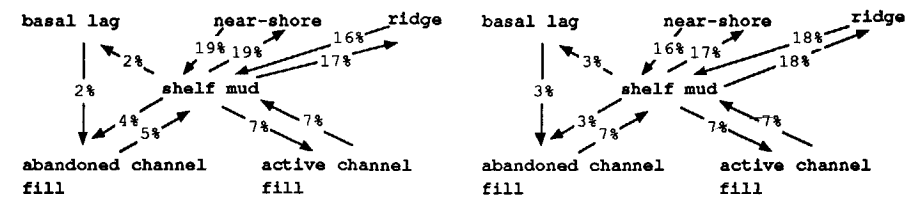

Figure 3.31 Upward transition probabilities in the Carlson, Cornelius and Cayce reservoirs.

Lateral transition probabilities in the Carlson reservoir show variation between dip and strike lines (Figure 3.32). Most remarkable

is the higher transition probability between active channel and ridge sediments in the dip sections. This is caused by the orientation of the channel which is more or less parallel to the strike lines. Lateral transition probabilities in the Cornelius reservoir also show some differences between dip and strike sections (Figure 3.32). This is partly caused by the limited number of transitions (n=227) and partly by the orientation of the genetic units within the Cornelius reservoir. For example, the relatively large number of inter-ridge to ridge transitions in the dip sections is caused by the fact that the genetic units are oriented perpendicular to the dip sections. Lateral transition probabilities in the Cayce reservoir show a major difference between dip and strike lines (Figure 3.32). This is probably caused by the relative limited number of considered transitions (n=133) coupled with a high variability in sediment types within the Cayce reservoir.

Comparison of relative occurrence of genetic units in the Carlson reservoir shows again no major difference between strike and dip lines (Figure 3.33). The relatively large amount of fore-shore deposits is caused by the occurrence of these deposits everywhere in the reservoir as a basal zone (Figure 3.30). From the genetic units in the upper part of the sequence the ridge sediments are most abundant. Comparison of relative occurrence of genetic units in the Cornelius reservoir shows that in the dip sections the ridge sediments are relatively more abundant than in the strike sections (Figure 3.33). This is explained by the orientation of the genetic units parallel to the strike sections, and because the strike sections run predominantly through inter-ridge sediments. Comparison of relative occurrence of genetic units in the Cayce reservoir shows again no major difference between strike and dip lines (Figure 3.33).

I determined relative occurrence of the genetic units in an areal view by overlying a grid on the palaeogeographic maps. The results are shown in Figure 3.33. The majority of the area in the Carlson reservoir is occupied by ridge sediments. Abandoned channel fill sediments occur about three times as little as active channel fill sediments. In the Cornelius reservoir inter-ridge and ridge sediments occur in more or less the same amount and that in the Cayce reservoir

strandplain and near-shore sediments occur in more or less the same amounts. The significance of the data on relative occurrence of genetic units both vertically and laterally as presented in Figure 3.33 is probably of limited use because the study area is relatively small in relation to the size of individual genetic units and is defined geologically in an arbitrary way by the field boundaries.

CARLSON RESERVOIR

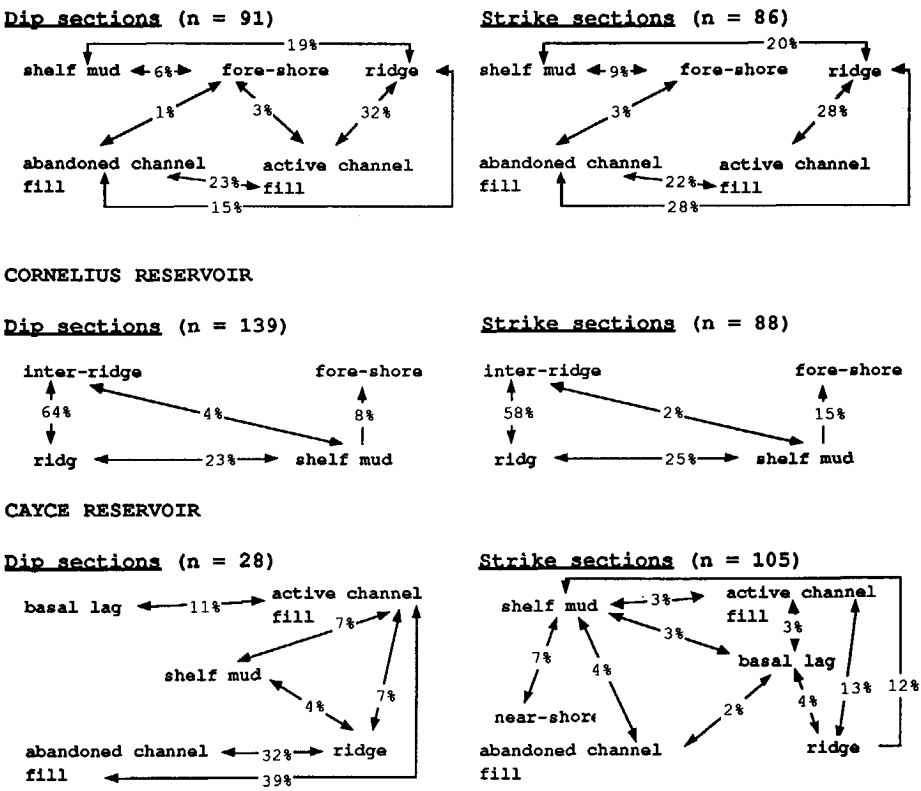

CORNELIUS RESERVOIR

CAYCE RESERVOIR

Figure 3.32 Lateral transition probabilities in the Carlson, Cornelius and Cayce reservoirs.

I measured width and thickness for individual genetic units within the three reservoirs under study. Width is defined as the width perpendicular to the orientation of the genetic unit under

consideration (as inferred from the geological model). Thickness is defined as the maximum thickness of the genetic unit at the location of the width measurement. In the Carlson and Cayce reservoirs I measured channel dimensions (Table 3.4) and in the Cornelius reservoir I measured ridge dimensions (Table 3.5). A remark must be made with respect to the dimensions of the channels measured in the Carlson and Cayce reservoirs. MacPherson and Miller (1990) reported that they could not correlate individual channels in the Bell Ridge Field, California (USA) despite of a 10 acre well spacing. The data on channel dimensions from the Carlson and Cayce reservoir might therefore reflect composite rather than single sediment bodies. Also dimensions could be measured for only a small number of genetic units because the area under study is small in relation to the sizes of individual genetic units. Additional data from other studies in similar sedimentological settings are required to obtain a statistical significant data set.

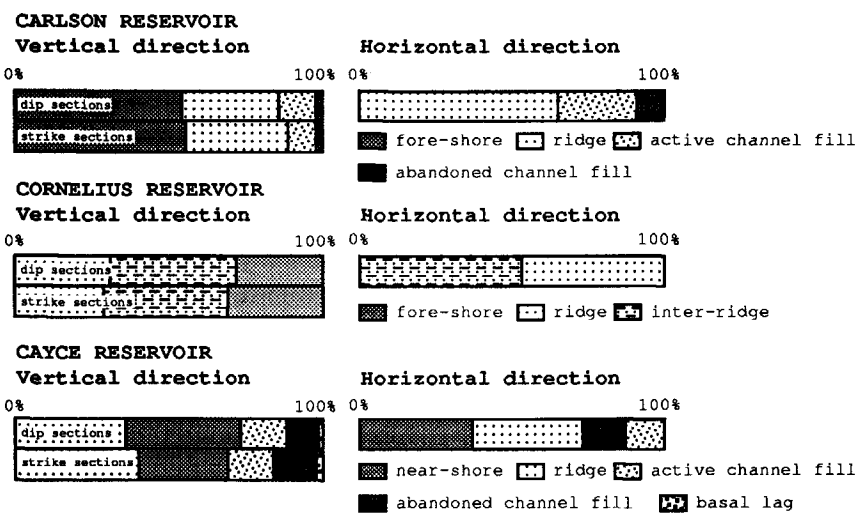

Figure 3.33 Relative occurrence of genetic units in the Carlson, Cornelius and Cayce reservoirs.

Table 3.4 Channel dimensions in the Carlson and Cayce reservoirs.

CARLSON RESERVOIR			
	average width	average thickness	width/thickness ratio
total channel fill	633 m	9 m	70
active channel fill	516 m	9 m	57
abandoned channel fill	117 m	9 m	13

CAYCE RESERVOIR			
	average width	average thickness	width/thickness ratio
total channel fill	882 m	12 m	69
active channel fill	373 m	12 m	31
abandoned channel fill	366 m	12 m	28

Table 3.5 Ridge dimensions in the Cornelius reservoir.

average width	average thickness	width/thickness ratio
390 m	14 m	28
438 m	12 m	37
323 m	11 m	29

3.4.2 THE ATCHAFALAYA DELTA, A RECENT ENVIRONMENT

3.4.2.1 Geological setting

The Atchafalaya river is the result of avulsion processes of the Mississippi river. Where the Atchafalaya river enters the Gulf of Mexico, a rapidly growing delta is formed. The bay in which the Atchafalaya delta develops is characterized by low wave energy, low tidal range, weak littoral drift and gentle offshore slope. The Atchafalaya delta can therefore be classified as a fluvial dominated delta system (see Chapter 2).

Van Heerden and Roberts (1988) published two detailed sedimentological sections through the Atchafalaya delta. One of these sections is shown in Figure 3.34. These two sections were used to obtain knowledge base parameters in the same way as was done for the North Markham-North Bay City field.

Van Heerden and Roberts (1988) differentiated 7 genetic units in the Atchafalaya delta (Table 3.6). The distribution of these genetic units is given in Figures 3.34. In the prodelta sediments a lower and a upper unit are differentiated. The lower prodelta sediments consists of clays. They represent the initial stages of delta growth. The sedimentation rate in this stage was very slow. Occasional shell layers occur. These shell layers are interpreted as storm lag deposits (Van Heerden and Roberts, 1988).

The upper prodelta sediments are somewhat coarser grained than the lower prodelta sediments. In addition to the clays they also contain some silt. The deposits show parallel lamination. Variations in the thickness of the prodelta unit suggest early establishment of sub-aqueous distributary channel systems (Van Heerden and Roberts, 1988). The distal bar sediments are coarser grained than the prodelta sediments. Therefore, together with the underlying prodelta sediments they form a wedge of sediment that coarsens upward. A clear pattern of channels is developed in this wedge.

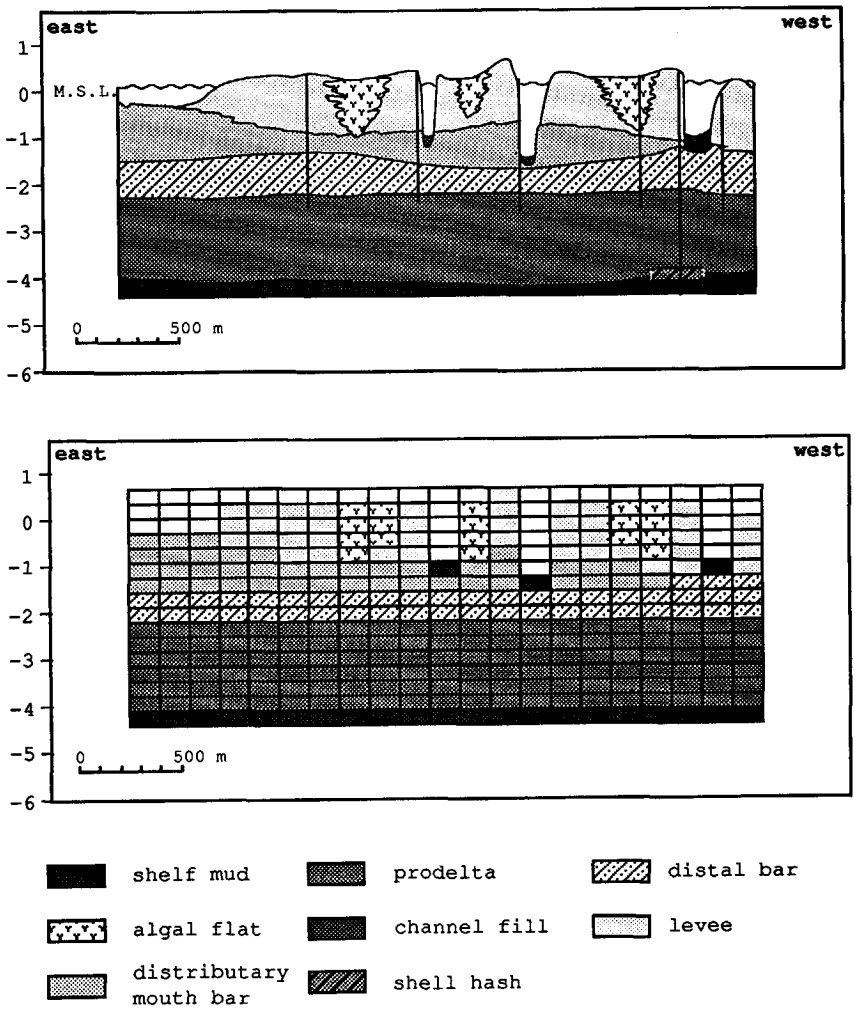

Figure 3.34 Cross-section through the Atchafalaya delta: A) sedimentological section (after Van Heerden and Roberts, 1988); B) gridded section.

The distributary mouth bar sediments are deposited as discrete subaqueous lobes in front of the river mouth. The sediments of the distributary mouth bar show an overall coarsening upward sequence consisting of repeated fining upward sequences of parallel and cross laminated sands and silts that pass upward into parallel-laminated clays (Van Heerden and Roberts, 1988). The sandy nature of the

distributary mouth bar probably makes it a potential reservoir unit. The many clay intercalations however, will act as serious baffles to flow.

Table 3.6 Genetic units within the Atchafalaya delta.

prodelta	levee
distal bar	back-barrier algal flat
distributary mouth bar	channel fill

The levees consist of sands and silts which show cross-lamination. Because of the sandy nature of the distributary mouth bar, this unit is a potential reservoir element. Sometimes the levees directly overlie distal bar sediments. This indicates high sedimentation rates.

The back-barrier algal flats are formed behind the levees on emerging delta lobes. Thin intercalations of coarser material (fine sand and silt) are introduced into these areas by overbank channels, levee overtopping during floods and redistribution of levee material during winter storms. Silt and clay can be transported in this environment by tides. These back-barrier flats form important barriers to flow.

The lithology of these genetic units is only marginally described by Van Heerden and Roberts (1988). According to general information on such deltaic sediments (Coleman and Prior, 1981), I assume that the channel fill sediments are mostly clayey to silty. Because of their clayey and silty nature, channel fill deposits will form lateral baffles to flow.

3.4.2.2 Data extraction

I superimposed a grid on the sections presented by Van Heerden and Roberts (1988) (Figure 3.34). From these gridded sections the relative occurrence of genetic units in a cross-sectional view and lateral and upward transition probabilities were derived. The results are shown in Figure 3.35. Width/depth-ratios were also derived for the channels within the Atchafalaya delta (Table 3.7).

From Figure 3.35 it can be seen that the variability increases upward. Upward transition probability from prodelta to distal bar and from distal bar to distributary mouth bar are largest, while transitions between genetic units higher in the section are relatively sparse. This is also illustrated by lateral transition probabilities (Figure 3.35). These show the opposite to the upward transition probabilities: A relatively large transition probability between the genetic units high in the section and a relatively small transition probability between genetic units low in the section.

Figure 3.35 shows that the prodelta sediments are most abundant. This is not unexpected, because the prodelta sediments form a broad flat on which the other sediments are deposited. Channel fill and algal flat sediments are the least common. This again illustrates the increase of variability upward. The small amount of channel fill sediments is also caused by the fact that the channels are still active and therefore as yet only partly filled.

Table 3.7 shows the width, depth and width/depth ratio of the various channels in the cross-sections. The width of the channels varies from 100 to 1000 metres. Depths vary from 0.25 to 1.5 metres. Width/depth ratios vary from 133 to 1333. Van Heerden and Roberts (1988) differentiated 3 types of channels. Tertiary channels have width/depth ratios of up to 150, secondary channels have width/depth ratios from 150 to 250 and primary channels have width/depth ratios larger than 250. This subdivision into three channel types can also be seen in Table 3.7.

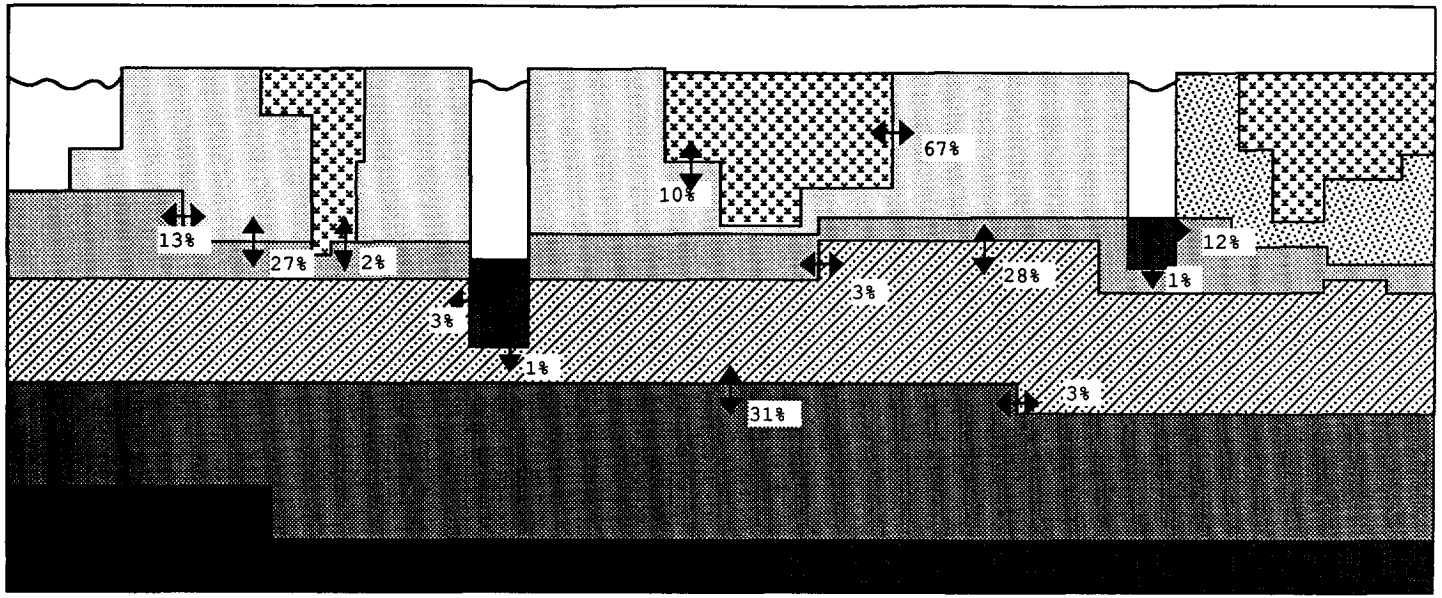

relative abundance: cross sectional view

upward transitions

sideward transitions

shelf mud

prodelta

distal bar

distributary mouth bar

algal flat

basal lag

levee

Figure 3.35 Statistics of the Atchafalaya delta.

Table 3.7 Channel dimensions within the Atchafalaya delta.

width (m)	depth (m)	width/depth
1000	0.8	1250
100	0.8	125
100	0.8	125
400	1.5	267
100	0.3	333
200	0.3	667

3.5 Practical approach to reservoir modelling

Of all the ingredients employed by reservoir simulators, rock properties vary the most. To obtain accurate simulation results, an accurate description of the distribution of rock properties must be available. Such a description of the reservoir cannot usually be solely obtained from reservoir data. Modelling techniques often have to be used. Of these modelling techniques, object-based techniques have the most potential. Object-based methods are well suited for assessing reservoir connectivity in relation to well pattern. Even at an early stage when only a few wells have been drilled, several runs can be done based on the information from the wells and width/length/thickness distributions found from analogue studies. These runs yield the average relations between well spacing, well pattern and sand body connectivity. Volumetric estimates and average distributions of the thickness of net sand can be obtained based on these models.

At a later stage, when more wells have been drilled (average well spacing about 1 kilometre) mixed probabilistic/deterministic models can be constructed. These models are often very detailed because they are built up from millions of voxels (volume elements). To prepare input for a reservoir simulation the number of volume elements will have to be reduced by a factor of between 100 and 1000. Two methods can be used for this. Firstly, groups of similar voxels can be combined and their properties averaged. Secondly, one can subdivide the reservoir into facies-related flow units for which average properties can be derived from limited information on controlling characteristics (see Chapter 4).

To obtain accurate object-based reservoir models a knowledge base containing quantitative geological information should be developed. Such a knowledge base must be based on data from geologically well known areas, like outcrops, recent environments and densely drilled fields.

Quantification of sedimentological parameters in the Carlson, Cornelius and Cayce reservoirs as described in § 3.4.1 demonstrates the use of densely drilled fields as analogues for the conditioning of reservoir models. If the sedimentological setting is characterized by lateral continuous sediment bodies (e.g. strandplain environment) data from densely drilled fields have significant use in addition to data from outcrops and recent environments. Data from densely drilled fields give three-dimensional information on the distribution of genetic units, while outcrops usually give only two-dimensional information. With respect to Recent environments, densely drilled fields can be easier sampled vertically and give information on the effects of burial. However, only if cores are available it is possible to quantify phenomena within genetic units. Also reliability of the sedimentological interpretations of the genetic units depends strongly on the availability of core data.

The results from data extraction from the Atchafalaya delta showed the utility of recent environments for knowledge base development. The main advantage is that the depositional setting and areal distribution of the genetic units are exactly known. However, the

distribution of genetic units in the vertical plane must be inferred from shallow wells. Also the genetic units are still developing. Therefore channel fill dimensions could not be accurately determined in the Atchafalaya delta. The dimensions of algal flat sediments could not be determined, because the sediments have not yet compacted. Furthermore, the Holocene Epoch is not representative for most other epochs due to a rapid sea-level rise.

4. INCORPORATING SEDIMENTOLOGICAL VARIABILITY IN RESERVOIR SIMULATION GRIDS

4.1 Sedimentologically defined flow unit configurations for the construction of reservoir models

Within deltaic deposits most sand bodies have their own characteristic shape. On the other hand, a number of sand bodies have more or less the same internal characteristics, although they are genetically different (Tables 4.1 to 4.7). For example, the central bar facies of fluvial-dominated deltas, the barrier core facies of fluvial/wave/tide-dominated deltas, the strandplain facies of wave dominated deltas, and the central bar facies of lacustrine deltas are all characterized by sands that have a uniform grain size distribution, are well-sorted, and contain a few thin shales. Because of this similarity, the fluid flow through these sediments will behave more or less the same.

Based on the resemblances of the internal configuration of different genetic sand bodies, I distinguished eight sedimentologically defined flow unit configurations (Table 4.8). These sedimentologically defined flow unit configurations can be described as volumes of rock which are homogeneous heterogeneous. In geological terms this means that the internal sedimentary structures and baffles are distributed in a similar pattern throughout the body and that the diagenetic overprint is the same everywhere. In Figure 4.1 the internal configuration of these 8 sedimentologically defined flow unit configurations is given.

In general three heterogeneity types within the flow units are important for fluid flow:

1. sorting trend,
2. sedimentary structures,

Table 4.1 Sedimentological characteristics of sandy genetic units in fluvial dominated deltas.

genetic unit	shape	size			baffles	sedimentary structures	grain size	sorting	normalized permeability	normalized porosity	GR response	elementary flow unit type
		length	width	thickness								
distal bar		25-30 km	2-4 km	10-24 m	horizontal shales (100-1000 m)	ripple lamination	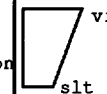		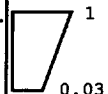	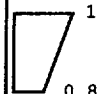		A
central bar		25-30 km	1-2 km	10-20 m	horizontal shales (0-50 m)	small-scale cross-bedding	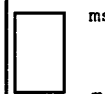					B
lower distributary		25-30 km	500-1000 m	2-10 m	horizontal shales (30-400 m)	small-scale cross-bedding		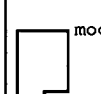			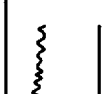	C
upper distributary		25-30 km	500-1000 m	3-10 m	horizontal shales	ripple lamination		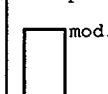				D
levee		25-30 km	500-2000 m	0.5-2 m	horizontal shales (500-1000 m)	ripple lamination root marks	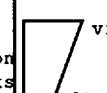	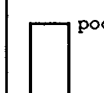				E
crevasse splay		1-7 km	5-20 km	3-15 m	horizontal shales (100-1000 m)	ripple lamination	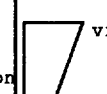					A

cly = clay; slt = silt; vfs = very fine sand; fs = fine sand; ms = medium sand; cs = coarse sand; vcs = very coarse sand; cgl = conglomerate

Table 4.2 Sedimentological characteristics of sandy genetic units in tide dominated deltas.

genetic unit	shape	size			baffles	sedimentary structures	grain size	sorting	normalized permeability	normalized porosity	GR response	elementary flow unit type
		length	width	thickness								
tidal sand bar		40 km	7-15 km	3-6 m	horizontal shales (100-1000 m)	ripple lamination	vfs / slt	mod. / poor	1 / 0.03	1 / 0.8		A
estuarine channel fill		40-45 km	1.5-8 km	20-30 m	Inclined shales	bundles	vfs / vfs	well / well	1 / 1	1 / 1		F

cly = clay; slt = silt; vfs = very fine sand; fs = fine sand; ms = medium sand; cs = coarse sand; vcs = very coarse sand; cgl = conglomerate

Table 4.3 Sedimentological characteristics of sandy genetic units in deltas with fluvial/wave/tide interaction.

genetic unit	shape	size			baffles	sedimentary structures	grain size	sorting	normalized permeability	normalized porosity	GR response	elementary flow unit type
		length	width	thickness								
barrier foot	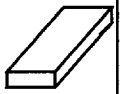	5-35 km	3-8 km	5-7 m	horizontal shales (100-1000 m)	ripple lamination	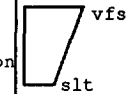	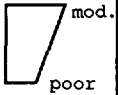	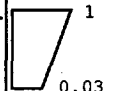	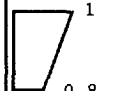		A
barrier core		5-35 km	3-8 km	8-20 m	horizontal shales (0-50 m)	small-scale cross-bedding	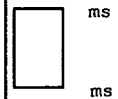	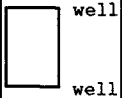	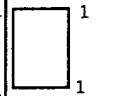	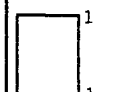		B
foreshore	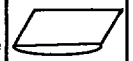	5-35 km	3-8 m	3-5 m	horizontal shales (500-1000 m)	ripple lamination root marks	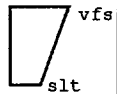	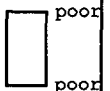	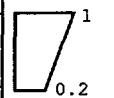	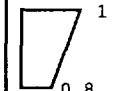		E
estuarine channel fill		40-45 km	1.5-8 km	20-30 m	Inclined shales	bundles	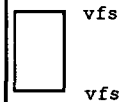	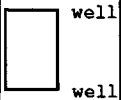	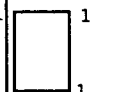	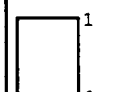		F

cly = clay; slt = silt; vfs = very fine sand; fs = fine sand; ms = medium sand; cs = coarse sand; vcs = very coarse sand; cgl = conglomerate

Table 4.4 Sedimentological characteristics of sandy genetic units in wave dominated deltas.

genetic unit	shape	size			baffles	sedimentary structures	grain size	sorting	normalized permeability	normalized porosity	GR response	elementary flow unit type
		length	width	thickness								
foreshore		35-60 km	10-20 km	3-5 m	horizontal shales (100-1000 m)	ripple lamination	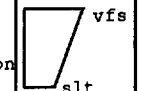	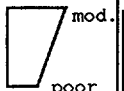	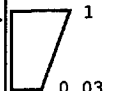	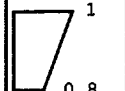	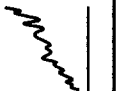	A
strand-plain		30-60 km	10-20 km	5-12 m	horizontal shales (0-50 m)	small-scale cross-bedding	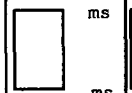		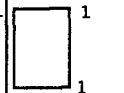	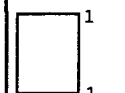		B
lower pointbar		10-20 km	5-10 km	1-3 m	horizontal shales (30-400 m)	small-scale cross-bedding	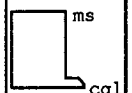	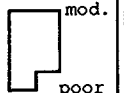	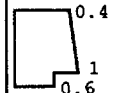	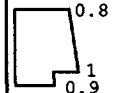		C
upper pointbar		2-7 km	2-5 km	5-12 m	inclined shales	ripple lamination epsilon bedding	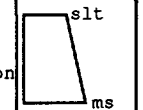	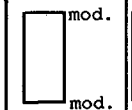	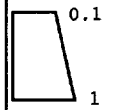	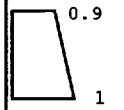		G

cly = clay; slt = silt; vfs = very fine sand; fs = fine sand; ms = medium sand; cs = coarse sand; vcs = very coarse sand; cgl = conglomerate

Table 4.5 Sedimentological characteristics of sandy genetic units in deltas with wave/current interaction.

genetic unit	shape	size			baffles	sedimentary structures	grain size	sorting	normalized permeability	normalized porosity	GR response	elementary flow unit type
		length	width	thickness								
distributary mouth bar		40-80 km	40-50 km	12-21 m	horizontal shales (100-1000 m)	ripple lamination	vfs / slt	mod. / poor	1 / 0.03	1 / 0.8		A
beach ridge		20-80 km	0.5-2.5 km	9-45 m	horizontal shales (0-50 m)	cross-bedding	ms / ms	well / well	1 / 1	1 / 1		B

cly = clay; slt = silt; vfs = very fine sand; fs = fine sand; ms = medium sand; cs = coarse sand; vcs = very coarse sand; cgl = conglomerate

Table 4.6 Sedimentological characteristics of sandy genetic units in fan deltas.

genetic unit	shape	size			baffles	sedimentary structures	grain size	sorting	normalized permeability	normalized porosity	GR response	elementary flow unit type
		length	width	thickness								
floodplain		0.5-3 km	0.5-3 km	1-3 m	horizontal shales (100-1000 m)	ripple lamination	vfs / slt	mod. / poor	1 / 0.03	1 / 0.8		A
nearshore	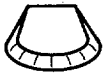	10-30 km	5-10 km	10-60 m	horizontal shales (0-50 m)	cross-bedding	ms / ms	well / well	1 / 1	1 / 1		B
distributary channel fill		10-30 km	5-20 km	10-60 m	abandoned channel	imbrication horizontal bedding	cgl / cgl	poor / poor	1 / 1	1 / 1		H

cly = clay; slt = silt; vfs = very fine sand; fs = fine sand; ms = medium sand; cs = coarse sand; vcs = very coarse sand; cgl = conglomerate

Table 4.7 Sedimentological characteristics of sandy genetic units in lacustrine deltas.

genetic unit	shape	size			baffles	sedimentary structures	grain size	sorting	normalized permeability	normalized porosity	GR response	elementary flow unit type
		length	width	thickness								
distal bar		5-8 km	2-4 km	10 m	horizontal shales (100-1000 m)	ripple lamination						A
central bar		5-8 km	1-2 km	10 m	horizontal shales (0-50 m)	small-scale cross-bedding						B
lower distributary		5-8 km	200-400 m	3-5 m	horizontal shales (30-400 m)	small-scale cross-bedding						C
upper distributary		5-8 km	200-400 m	0.5-1 m	horizontal shales	ripple lamination	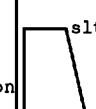			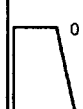		D
levee		5-8 km	500-2000 m	0.5-2 m	horizontal shales (500-1000 m)	ripple lamination root marks					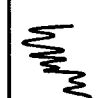	E

cly = clay; slt = silt; vfs = very fine sand; fs = fine sand; ms = medium sand; cs = coarse sand; vcs = very coarse sand; cgl = conglomerate

Table 4.8 Classification of genetic units in eight categories of sedimentologically defined flow unit configurations.

delta type	Type A	Type B	Type C	Type D	Type E	Type F	Type G	Type H
fluvial dominance	distal bar, crevasse splay	central bar	lower distributary	upper distributary	levee			
tide dominance	tidal sand bar					estuarine channel fill		
fluvial/wave/tide interaction	barrier foot	barrier core			fore shore	estuarine channel fill		
wave dominance	fore shore	strand-plain	lower point bar				upper point bar	
wave/current interaction	distributary mouth bar	beach ridge						
fan delta	flood-plain	near shore						distributary channel fill
lacustrine delta	distal bar	central bar	lower distributary	upper distributary	levee			

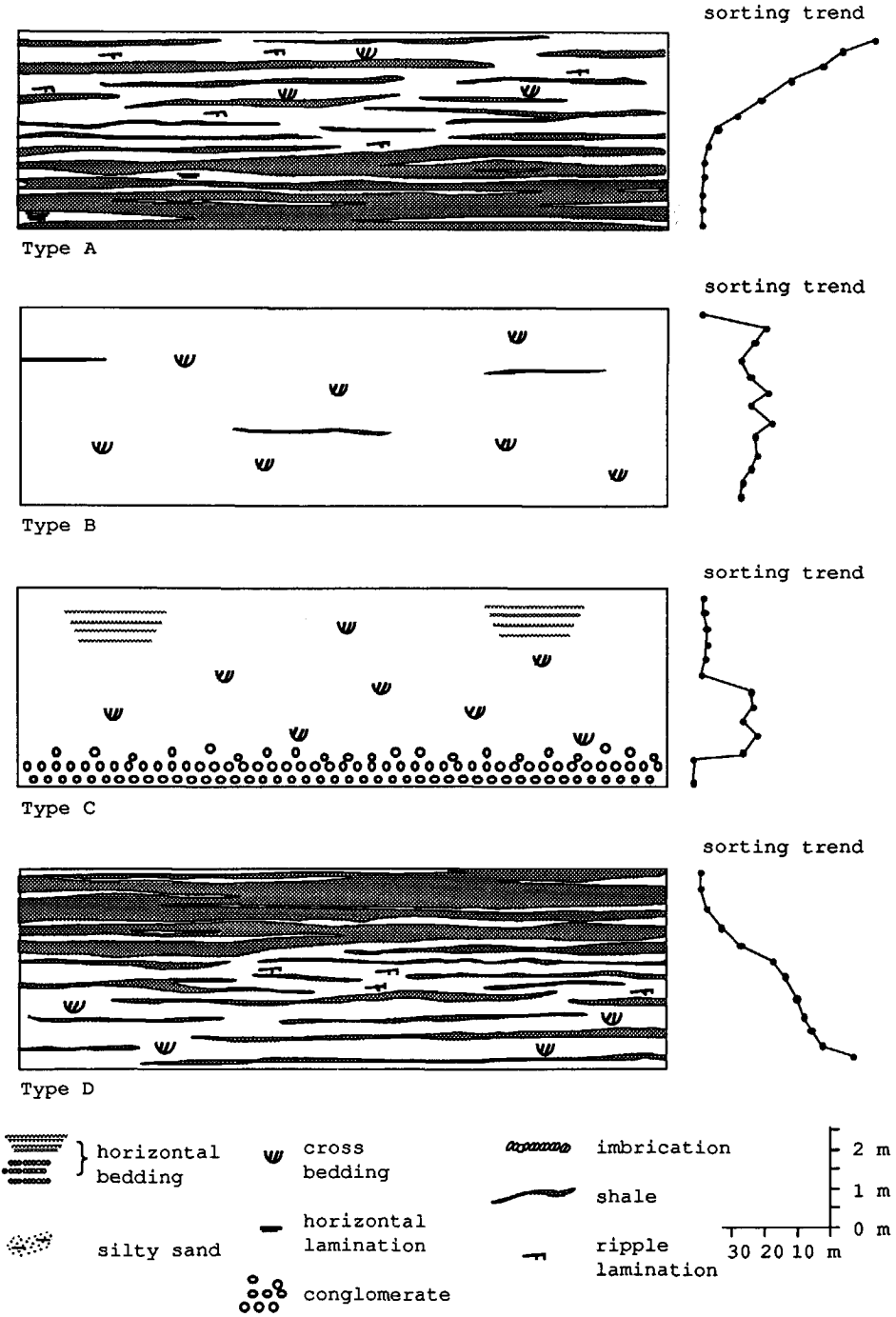

Figure 4.1 Sedimentologically defined flow unit configurations within deltaic depositional environments.

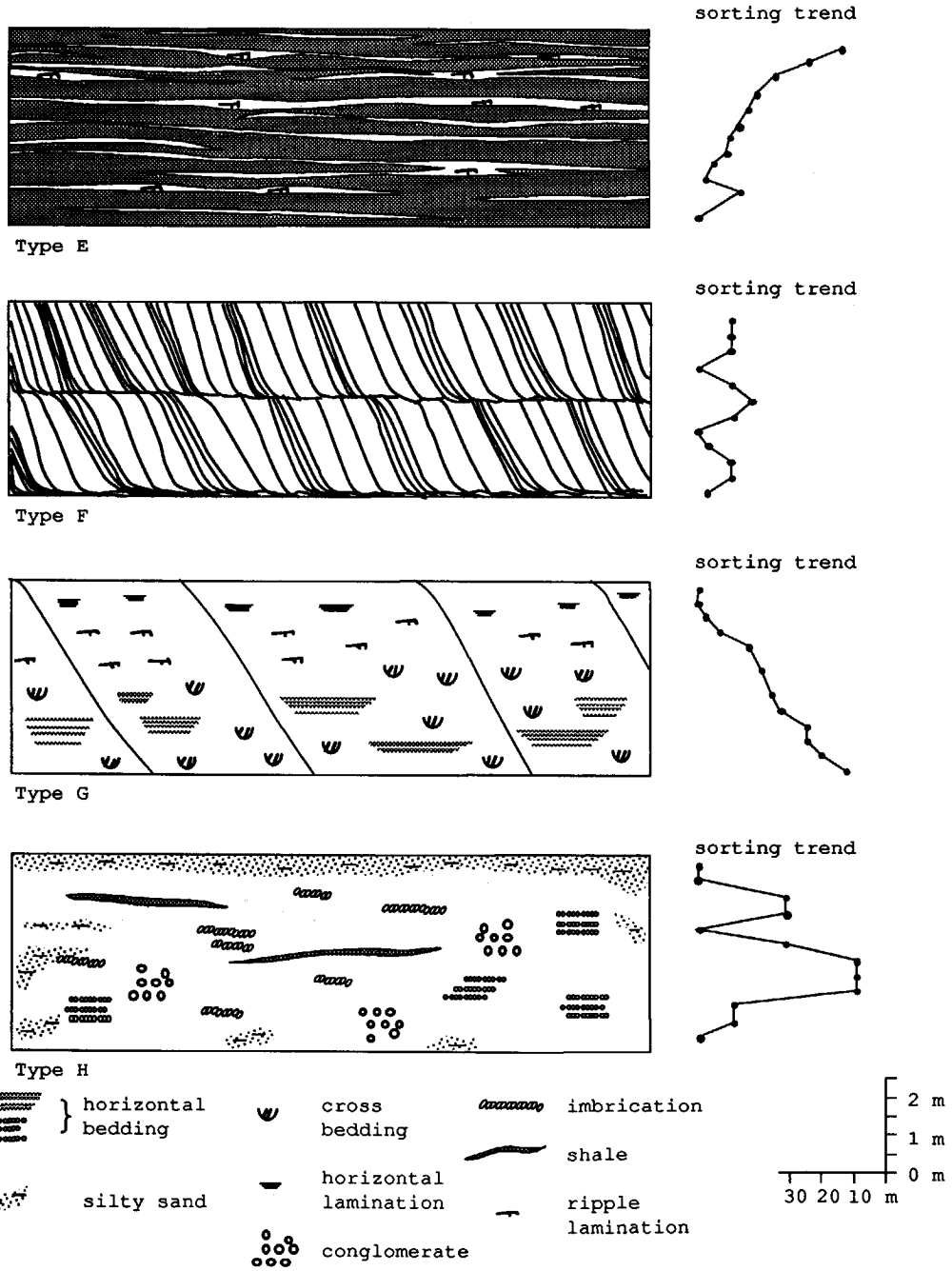

Figure 4.1 Continued.

3. shales.

The effect of sorting trend, sedimentary structures and shales on fluid flow will be discussed below.

4.2 Sorting trends

There are three types of sorting trend in sedimentary rocks. A reduction of sorting is visible when sediments are deposited in a regime of decreasing energy regime of the transporting medium. Examples are point bars formed in meander belts (Allen, 1970a), or distributaries in the lower deltaic plain (Coleman, 1981). Such rocks are characterized by an upward decrease of permeability and porosity (Tables 4.1 to 4.7).

Sorting increases when a sediment body progrades. Examples can be found in prograding barrier island systems, or distributary mouth bar systems. In these environments fine-grained distal sediments are overlain by progressively coarser material of more proximally deposited sediment. Such rocks are characterized by an upward increase of permeability and porosity (Tables 4.1 to 4.7).

Finally, a sedimentary sequence which shows no obvious trend in sorting can occur. In these cases, the flow regime is usually erratic. This results in a large variation in sorting, but without a significant trend. Examples are sediments deposited in braided river environments. Such rocks are characterized by an erratic permeability and porosity distribution (Tables 4.1 to 4.7).

4.3 Sedimentary structures

From Figure 4.1 it becomes apparent that sedimentary structures often occur in deltaic rocks. These sedimentary structures reflect the conditions under which the rocks are deposited. The type of sedimentary structure present depends on the flow characteristics of the transporting medium and the grain size of the available material (Figure 4.2).

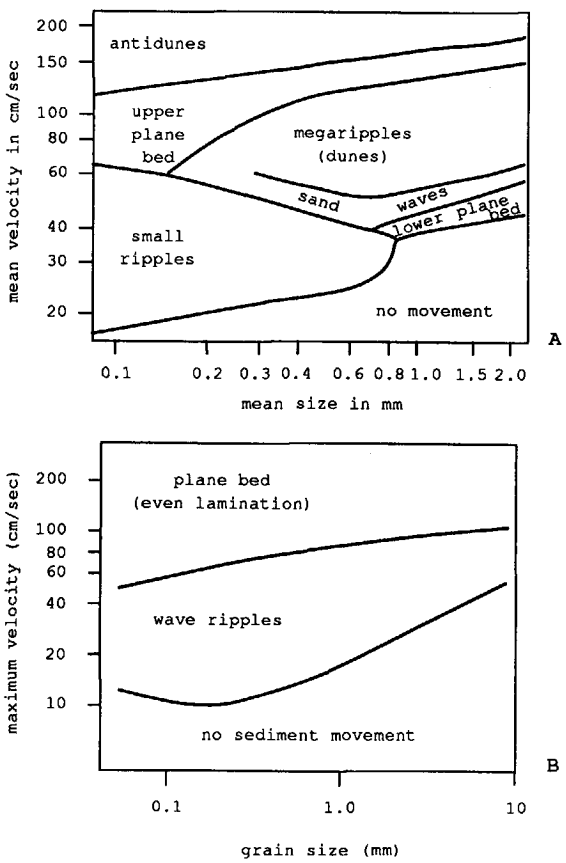

Figure 4.2 Bed form in relation to stream power and grain size: A) uni-directional flow (modified after Middleton and Southard, 1978), B) bi-directional flow (modified after Allen, 1970b).

Nearly all types of sedimentary structures can occur in deltaic sediments. However, most of the structures will consist of rhomboid small- and large-scale ripples and lower- and upper-stage plane beds. The internal structure of the dominant ripple types in deltaic deposits is given in Figure 4.3.

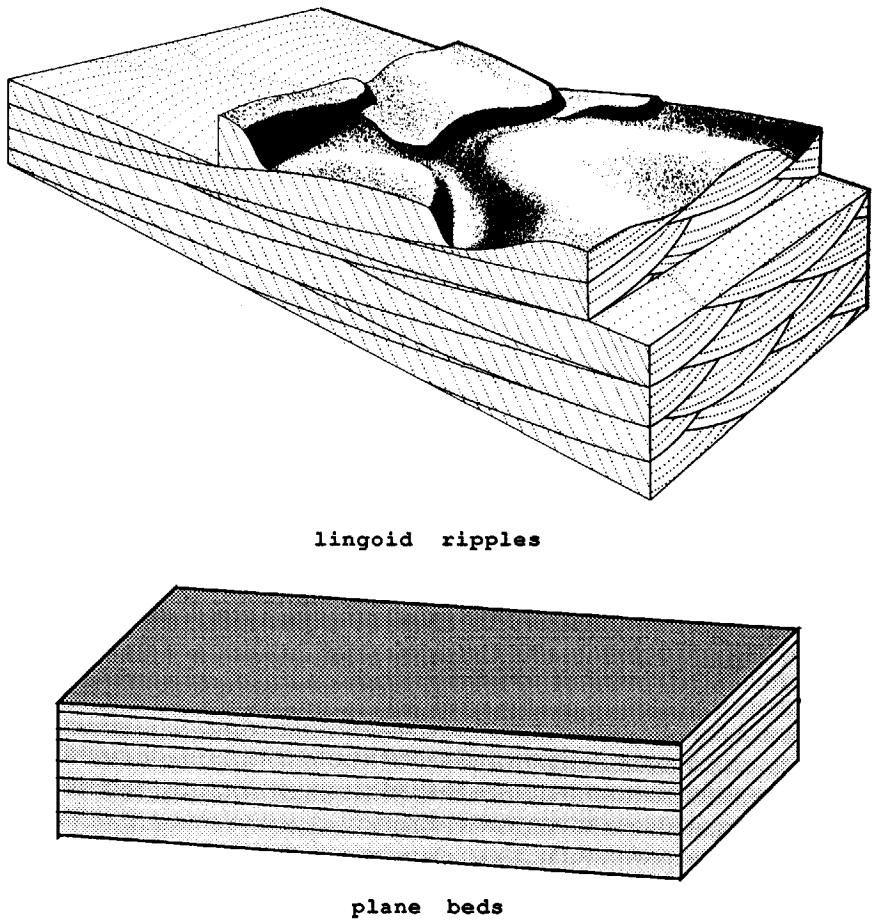

Figure 4.3 Block diagram showing internal configuration of common ripple types in deltaic rocks.

Various researchers have attempted to relate the type of cross-bedding to permeability (Weber et al., 1972; Pryor, 1973; Van Veen,

1977; Weber, 1982; Rose, 1983; Kortekaas, 1985; Stalkup, 1986; Dreyer, Scheie and Walderhaug, 1990). Of these, Weber et al. (1972), Weber (1982) and Kortekaas (1985) related sedimentary structures to permeability anisotropy. These authors paid particular attention to permeability anisotropies in trough cross-bedded sandstones. Weber et al. (1972) and Weber (1982) published nomograms from which horizontal permeability anisotropies for trough cross-bedded sandstones can be derived, when the ratio between bottom-set permeability and lamina permeability is known (Figure 4.4). These nomograms are valid for trough cross-bedded sets with length/width ratios of 4 and ratio of set length and bottom-set thickness of 300 (Figure 4.5). The dip angle of the laminae must be equal to 30°. According to Weber et al. (1972) and Weber (1982), these are values which are representative for most cross-bedded sandstones.

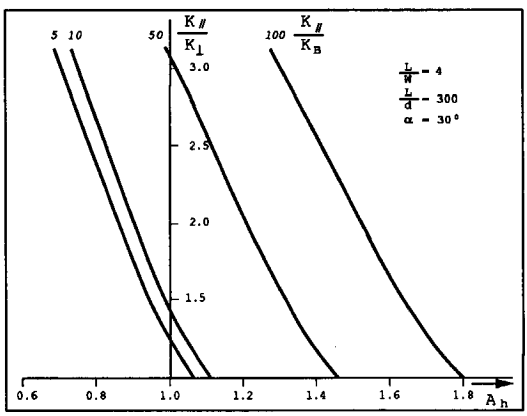

Figure 4.4 Nomograms for the estimation of horizontal permeability anisotropy in trough cross-bedded sandstones (after Weber, 1982).

Also according to Weber et al. (1972) and Weber (1982) horizontal permeability anisotropies in unconsolidated trough cross-bedded sands will rarely exceed 1.6 or be less than 0.7. However, in consolidated sands, anisotropies are more important because the ratio between lamina and bottom-set permeability is larger.

In horizontally laminated or bedded sands, the permeability anisotropies will be small. Obviously, horizontal permeability anisotropies are negligible. Vertical permeability anisotropies can occur because of vertical alternation of layers of different grain sizes and sorting.

4.4 Shales

Most deltaic rocks contain shale intercalations ranging in length from kilometres to decimetres. Only the major intercalations that straddle several wells can be correlated with some certainty. For the purpose of reservoir modelling, these can be called deterministic shales (Haldorsen, 1983). In reservoir simulation they often form the boundaries between overlying grid blocks. They occur, for example, in nearshore areas (barrier foot and distal bar environments).

Many of the shorter shales occur more randomly and in numerous forms, i.e. clay drapes in channel fills and flaser bedding. Very small clay lenses, like those in flaser bedding, can be modelled on a small-scale and can be considered as intrinsic rock characteristics when averaging permeability. Stochastic shales range between 1 and 100 metres long and are small compared with the average well spacing and are shorter than the usual simulation grid block. Such shales can only be modelled on the basis of analogue outcrops.

Several studies have been done on outcrops to find representative shale length distributions for a given facies (Weber, 1982; Martin and Cooper, 1984; Geehan et al., 1986). The resulting data have been used to design shale models that are used to calculate vertical permeability (K_{ve}). These models will be discussed below. Most of the 1-100 metres long shale bodies occur in fluviatile environments.

Below I will evaluate and compare techniques for directly estimating the vertical permeability and also various published shale models for

calculating this parameter. I will propose some modifications to cater for cases with less dense shale distributions and will critically examine data published on shale dimensions. Also I will discuss a method for the determination of vertical permeabilities in bioturbated sand/shale sequences (§ 4.4.5).

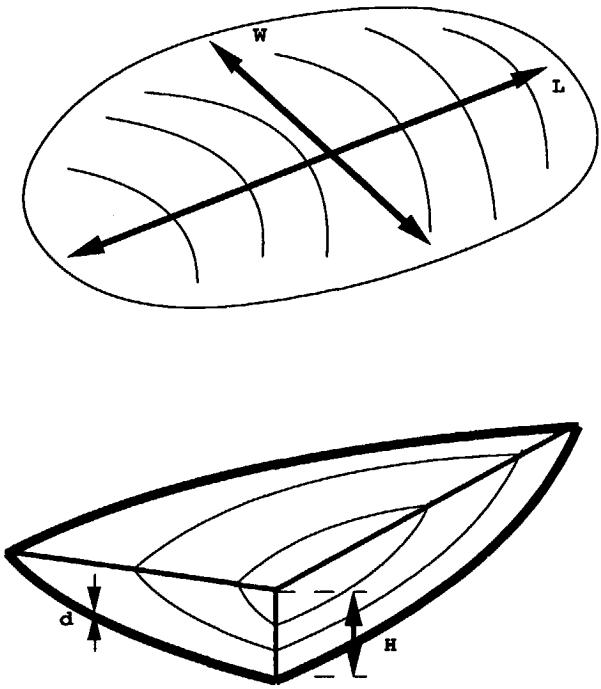

Figure 4.5 Cross-bed dimensions (after Weber, 1982).

4.4.1 DIRECT ESTIMATION OF VERTICAL PERMEABILITY

The vertical permeability can be estimated directly by vertical pulse tests. This is especially important in the case of fairly continuous but not completely impervious shales and silt layers which cannot be

assumed to be impermeable. However, this information cannot be extrapolated far from the wells.

Production tests involve large volumes of the reservoir. The information from such tests is difficult to interpret without a detailed and reliable reservoir model. Wire line formation tests obtained in infill wells after an appreciable production history may reveal pressure differences from which the effective vertical permeability can be derived.

4.4.2 LENGTH OF SHALE BODIES

Shale intercalations shorter than the sides of the grid block, i.e. less than 100-200 metres long, pose a problem when preparing input data for reservoir simulators. Published data from outcrops show that such shales are mainly restricted to fluviatile sand bodies (Figure 4.6). We collected additional data on fluviatile shales from the literature, from graphs or by taking measurements from photographs (Figure 4.7). The data were collected on distributary channels, point bars, braided rivers and fluvio-glacial deposits. In these facies the most numerous clay intercalations are drapes over bedforms ranging from 1-100 metres long. Except for epsilon bedding surfaces in point bars, the clay drapes are mostly horizontal.

Anastomosis of the clay drapes does occur, but in the shale models such complications are not accounted for. In practice this phenomenon will locally cause poor sweep efficiency and reduced horizontal permeability, but its influence on vertical permeability is probably limited.

The common clay drapes found in different fluviatile deposits are deposited by the same processes. Thus we may expect a large degree of correspondence between the histograms of shale lengths from different outcrops (Figure 4.7). A major problem with respect to horizontal shale dimensions is the absence of three-dimensional observations. Usually, outcrop studies only yield two-dimensional information.

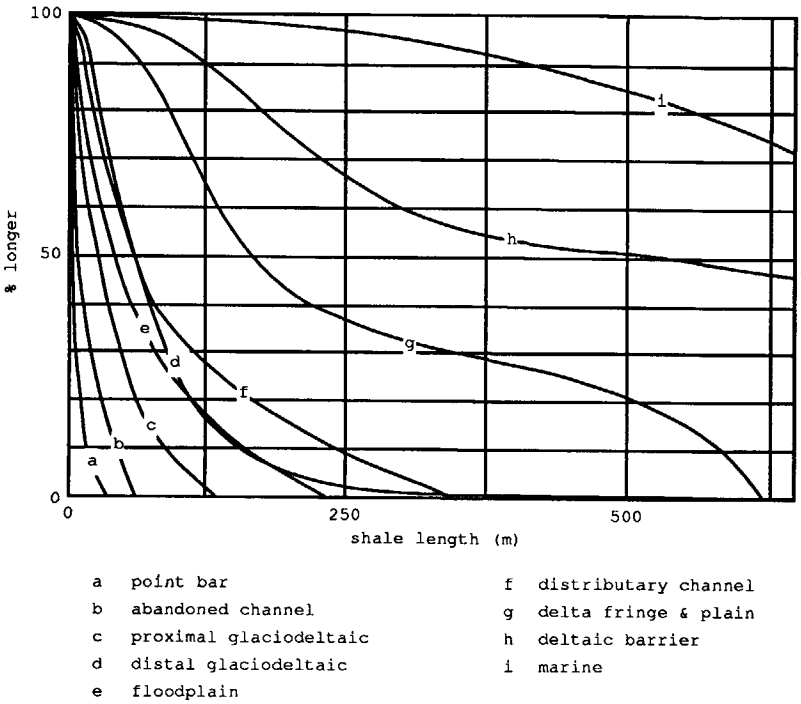

Figure 4.6 Cumulative distribution curves of shales lengths (based on data from Weber, 1982; Martin and Cooper, 1984 and Geehan et al. 1986).

In fluvial systems it is often assumed that clay drapes are roughly oval in shape, with the long axis oriented in the direction of flow (Haldorsen, 1989). Haldorsen also proposed a width/length ratio of 1:2 for stochastic shales but did not give the basis for this. As will be demonstrated below, it is the shortest dimension that controls effective vertical permeability.

Assuming that outcrop observations have been made in directions which are arbitrary with respect to the orientation of the shale bed, one can generate model histograms of shale length for different width/length ratios. This can be done by measuring the lengths of random cuts through rectangles with specific width/length ratios

(Figure 4.8). Typically we obtain a peak in the lower length region followed by a long tail and a small peak at the upper limit of the length distribution. The first peak represents approximately the average shale width, whereas the second peak indicates the length. The histograms derived from outcrops are similar in shape (Figure 4.7) and indicate a width/length ratio of roughly 1:3. Similar curves are also published by Geehan and Underwood (1990) for outcrop measurements in nearshore deposits. These curves indicate a width/length ratio of 1:6.

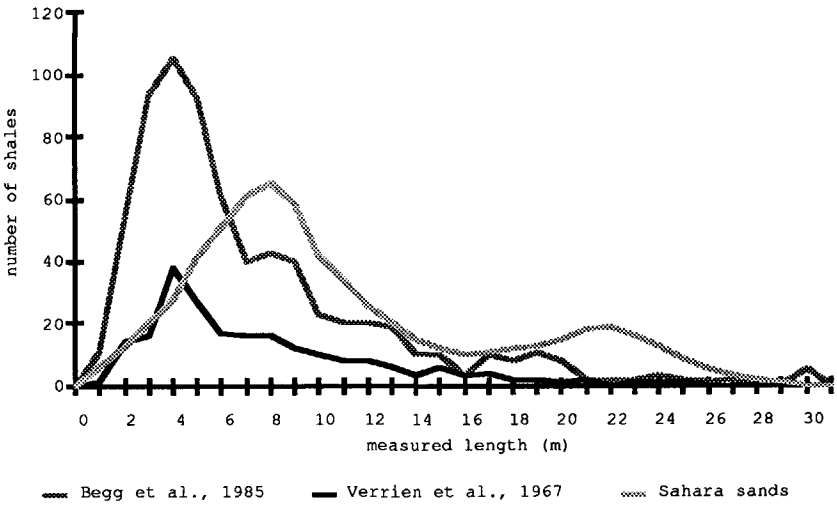

Figure 4.7 Distribution curves of shale lengths measured in outcrops. The distribution curve of the Sahara sands is based on photographs published by Beuf et al. (1971).

4.4.3 EVALUATION OF PUBLISHED SHALE MODELS

In this paragraph the shale models published in the literature are compared and evaluated, and it is suggested how they can be modified to cater for cases with fewer shale intercalations.

4.4.3.1 Shale models with a repetitive pattern

Dupuy and LeFebvre du Prey (1968) studied vertical permeability anisotropy of a medium with a repetitive pattern of impermeable flow barriers. They defined a two-dimensional flow element with two shales and transformed this flow element to a flow element without shales, but with similar flow characteristics (Figure 4.9). According to their method the permeability anisotropy can be calculated from the transformation operator (for the mathematical background to the transformation see the original paper by Dupuy and LeFebvre du Prey). The Dupuy and LeFebvre du Prey method works both in two and three dimensions (Table 4.9).

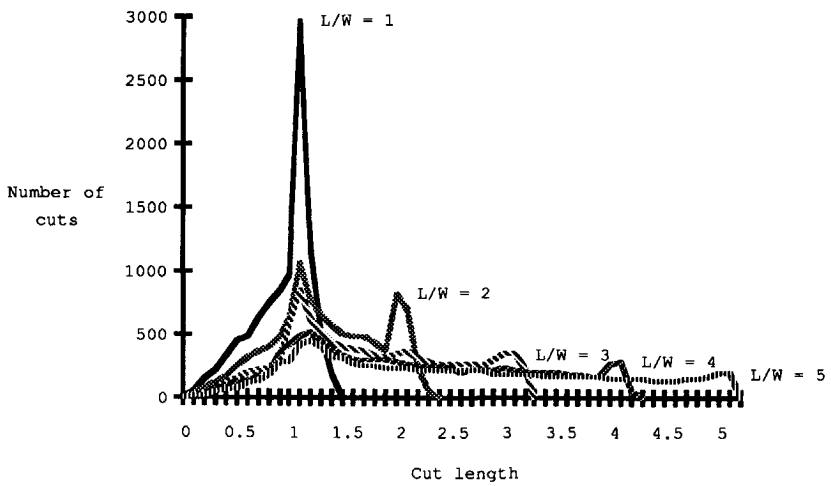

Figure 4.8 Distribution curves for length of cuts taken randomly through rectangles with different length/width ratios.

Dupuy and LeFebvre du Prey tested their method on data from a sandstone outcrop with numerous horizontal shale intercalations. They determined the length, horizontal and vertical spacing and horizontal overlap of the shales and used these data to construct an 'average' flow element for which they calculated the permeability anisotropy. They compared the outcome with results from resistivity measurements

of a scale model of the outcrop made from electro-conductive paper. The Dupuy and LeFebvre du Prey model gave a permeability anisotropy of 0.16, whereas the model made from electro-conductive paper gave a value of 0.20.

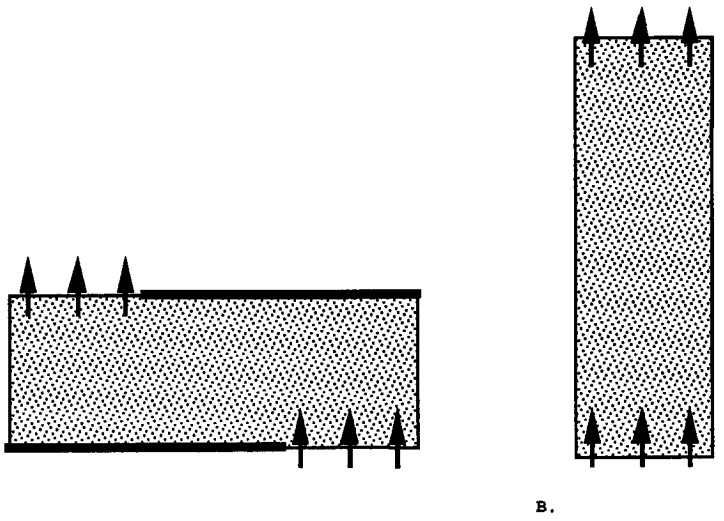

Figure 4.9 Transformation according to the method of Dupuy and LeFebvre du Prey (1968) of a flow element with two shales to a flow element without shales but with the same resistance to flow.

Prats (1972) also calculated permeability anisotropies by transforming a flow element with two shales to a flow element without shales, but with similar flow characteristics (for the mathematical background of the transformation see the original paper by Prats). Prats considered the two-dimensional case only (Table 4.9). In his paper he plotted vertical permeability anisotropy versus twice the width/height ratio of a flow element for several values of the fractional aperture α (half the horizontal spacing of the shales) (Figure 4.10).

Prats acknowledged that his model is too simple in several important respects. For example, the shales are assumed to be impermeable and

the shale distribution is repetitive; these assumptions are rarely met in real reservoir rocks. Also, Prats's model cannot be used in three dimensions (Table 4.9).

Table 4.9 Main characteristics of shale models.

Authors	applicable in 3-D	shale length	shale thickness	shale configuration	permeable shales	two phase	anisotropic matrix
Dupuy & LeFebvre du Prey (1968)	+	c	c	rp	-	-	-
Prats (1972)	-	c	c	rp	-	-	-
Brydges et al. (1975)	-	c	c	rp	-	-	-
Weber (1982)	-	c	c	rp	+	-	+
Martin & Cooper (1984)	-	v	v	rp	-	-	-
Haldorsen & Lake (1984)	-	v	v	rn	-	-	-
Begg & King (1985)	+	v	v	rn	-	-	-
Begg et al. (1985)	+	v	v	rn	-	-	+
Desbarats (1987)	+	v	v	rn	+	-	-
Deutsch (1989)	+	c	c	rn	+	-	-

+ = yes; - = no; c = constant; v = variable; rp = repetitive; rn = random

Chirlin (1985) proved that the transformation Prats used is not conformable. He gave a conformable transformation and presented graphs of the permeability anisotropy versus 2X/Y based on his

transformation operator. The permeability anisotropies found with Chirlin's method are smaller than those found with Prats's method, especially for small values of α (Table 4.10).

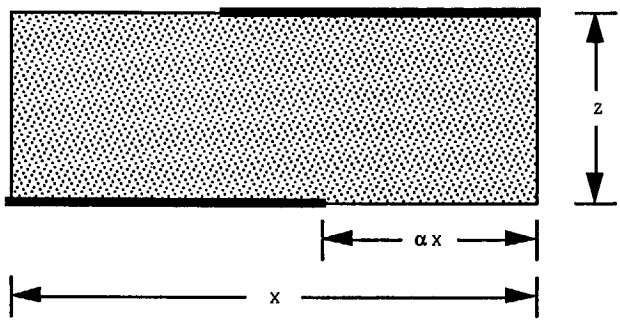

Figure 4.10 Flow element as defined by Prats (1972).

Brydges, Gulati, and Baum (1975) presented an analytical model for calculating the fluid permeability of organic matrix composites reinforced with glass ribbon. These composites consist of a very permeable matrix in which poorly permeable material is embedded in a regular fashion. Therefore, this model has obvious links with shale models. Brydges et al. considered the flow element given in Figure 4.11. In this flow element the ribbons are assumed to be impermeable. They calculated the permeability perpendicular to the ribbons by solving flow equations using Darcy's law. The following equation was found for this permeability normal to the ribbons:

$$K_{ve} = \frac{K_m}{1 + \frac{1}{2\alpha} + \frac{u_1}{S}\left(\frac{u_1 + 2\alpha}{H}\right)\left(\frac{S}{S + H}\right)\gamma(1 - \gamma)} \qquad (4.1).$$

In this equation K_{ve} is the permeability of the composite perpendicular to the ribbons, K_m the permeability of the organic matrix, α half the spacing between two glass ribbons (fractional aperture), S the ribbon thickness, u_1 the ribbon width, H the

vertical distance between the ribbons and γ the ratio between the overlap and the width of the glass ribbons (Figure 4.11).

Table 4.10 Comparison of permeabilities found by Prats (1972) and Chirlin (1985) for a flow element with $2\Delta X/\Delta X = 25$.

α	permeability anisotropy	
	Prats (1972)	Chirlin (1985)
0.2	0.001	0.010
0.3	0.007	0.014
0.4	0.014	0.023
0.45	0.025	0.038
0.5	0.060	0.077
0.55	0.15	0.17
0.6	0.25	0.26
0.7	0.44	0.45
0.8	0.62	0.63
0.9	0.81	0.82
0.95	0.91	0.91
1	1	1

Brydges et al. compared the outcomes of Equation 4.1 with experimental results. They determined permeability perpendicular to ribbons for several composites reinforced with glass ribbon and calculated the permeability anisotropy (K_{ve}/K_m). Comparison of the results with permeability anisotropies calculated with Equation 4.1

shows that Equation 4.1 overestimates the permeability anisotropy (Table 4.11).

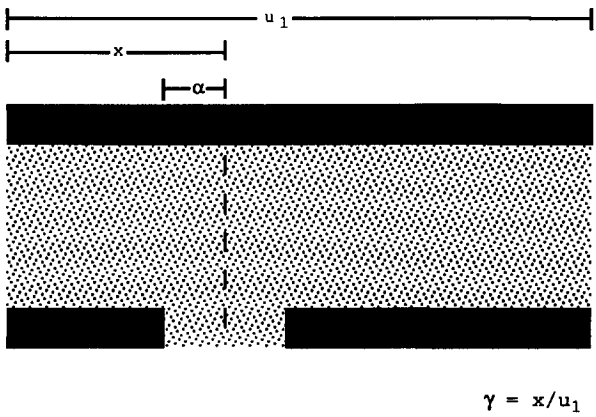

Figure 4.11 Flow element as defined by Brydges et al. (1975).

Table 4.11 Comparison of permeabilities calculated with Equation 4.1 and experimental results (based on Brydges et al., 1975).

composite characteristics	permeability anisotropy	
	measured	Equation 4.1
F_r = 0.62; γ = 0.5; u_1/α = 264	$7.9 \cdot 10^{-6}$	$5.7 \cdot 10^{-5}$
F_r = 0.22; γ = 0.5; u_1/α = 121	$9.2 \cdot 10^{-5}$	$4.6 \cdot 10^{-3}$
Fr = 0.54; γ = 0.5; u_1/α = 121	$5.7 \cdot 10^{-5}$	$4.4 \cdot 10^{-4}$

Weber (1982) used the same assumptions as Prats (1972), but also allowed for the possibility of permeable shales. His model is thus an extension of Prats's model. Weber presented a graph in which

permeability anisotropy is plotted against a dimensionless parameter. This parameter is defined as SK_{mv}/HK_s.

Martin and Cooper (1984) described the simulation of a steam flood in a glacio-deltaic reservoir (Marmul Field, South Oman). Conventional simulation using the harmonic average of measured vertical permeability values gave an unsatisfactory match. According to Martin and Cooper this was because these simulations could not explicitly model the tortuous flow path present within a system of non-continuous poorly permeable beds. Martin and Cooper therefore decided to investigate alternative approaches. They used the shale generation scheme of Haldorsen and Lake (1984) to obtain a geological model for the reservoir. This generation scheme models discontinuous shales between wells stochastically. In the resulting reservoir model Martin and Cooper (1984) defined four types of shale geometry elements on the basis of which they translated the original stochastic reservoir model into a model with repetitive shales. They then calculated the effective vertical permeabilities for each of the four types of shale geometry elements for the non-wetting phase:

$$(K_{ve})_{nw} = K \left(\frac{H - S}{L}\right) \frac{H}{T} \tag{4.2}$$

and also for the wetting phase:

$$(K_{ve})_{w} = K \left(\frac{H - S}{L}\right) \frac{H}{T} + \left(\frac{L - 2\alpha}{L}\right) \left(\frac{K_m K_s H}{S K + (H - S) K_s}\right) + \frac{2\alpha}{L} \left(\frac{K_m K_s H}{0.5 S K + (H - 0.5 S) K_s}\right) \tag{4.3}.$$

In this equation T is the tortuous flow path through the sand matrix, which is defined as:

$$T \approx L + 2H - 2l - S \tag{4.4}.$$

In this equation l is half the horizontal spacing between two shales. The results were used as reservoir simulation input. Martin and Cooper do not state if their method improved the simulation results.

4.4.3.2 Shale models with a random pattern

Haldorsen and Lake (1984) concentrated solely on stochastic shales. They assumed that the shales are randomly distributed in space, and that there is no correlation between shale length and thickness. This assumption is based on the work of Delhomme and Giannesini (1979), who assume that the thickness of a shale break is only related to the local topography prevailing at the time of deposition, and therefore independent of the length of the break. Haldorsen and Lake also assumed that a well is statistically representative of its drainage area. These assumptions can be seen as a first attempt to tackle the problem of shale modelling, but they are not always realistic. The main disadvantage of such an approach is that it ignores the reservoir geology. It reduces the problem to a statistical one. Possible geological trends will be overlooked, and are not accounted for in the model.

Haldorsen and Lake's model is based on determining the length of the effective flow path. This is used to find an expression for the effective vertical permeability. Haldorsen and Lake derived the following analytical expression for the length of the effective flow path:

$$\Delta z_e = \frac{1}{2} \sum_{i=1}^{n} \{\Delta x \, [1 - \xi(z)]_i\} \qquad (4.5).$$

The idea is that, on average, a fluid particle traversing the block vertically travels horizontally half the length of each shale body encountered. The average vertical permeability is then given by:

$$\frac{\bar{K}_{ve}}{K_m} = (1 - F_s) \frac{(\Delta z)^2}{(\Delta z_e)^2} \qquad (4.6).$$

In this equation $\bar{K}_{ve}$ is the average effective vertical permeability.

The length of the effective flow path must always exceed the height traversed if shales are present. In formula:

$$\Delta z_e = \Delta z + \text{additional tortuosity term} \qquad (4.7).$$

Equation 4.5 consists only of the additional tortuosity term, because the height of the traversed grid block is missing. Haldorsen and Lake (1984) state that their method is valid only for grid blocks with $\Delta z/\Delta x < 0.1$. They assume that when shale intercalations are numerous, the effect of the vertical term would be negligible.

Begg and King (1985) introduced four different methods for finding the effective vertical permeabilities of reservoirs containing stochastic shales. The first is based on numerical simulation, the second is an analytical method and the other two calculate lengths of effective vertical flow paths to determine K_{ve} (in fact based on the same idea as Haldorsen and Lake (1984)). In the numerical simulation method Begg and King constructed a fine grid model for a volume of sand containing discontinuous shales. The grid must be sufficiently fine to enable all shales to be modelled accurately. Then the effective vertical permeability is calculated:

$$K_{ve} = \frac{Z}{X\ Y\ (P_t - P_b)} \sum_{j=1}^{d_x} \sum_{k=1}^{d_y} K_{dz,j,k}\ \Delta X\ \Delta Y \left(\frac{P_t - P_{dz,j,k}}{\Delta Z}\right) \qquad (4.8).$$

The main disadvantage of this method is the long computing time, which limits the size of the fine grid. This in turn limits the ability to resolve detailed shale distributions, especially in three-dimensional problems.

To find the permeability with the analytical method, uniform flow through an ellipsoid surface encompassing a shale is considered. The pressure within the ellipsoid is computed. Then the ellipsoid is replaced by a homogeneous medium and the vertical permeability is calculate (for the mathematical background of this method see the original paper by Begg and King). The analytical method is of limited use, because the shale lengths must be constant.

In the explicit streamline method developed by Begg and King (1985), shales must be defined on a fine-meshed numerical grid. The

streamlines are traced through this grid by following a vertical line from each starting point until a shale is encountered. The streamline is then forced to go to the end of the shale closest to the horizontal home position of the streamline. The process is repeated until the top of the grid is reached (Figure 4.12). The effective vertical permeability is then calculated with:

$$K_{ve} = \frac{K_m \left(1 - F_s\right) Z^2}{Ps} \sum_{q=1}^{Ps} \frac{1}{\left(\Delta Z_e\right)_q^2} \qquad (4.9).$$

This method is only reliable when the shales are scarce. At dense concentrations of shales streamlines cannot be properly traced.

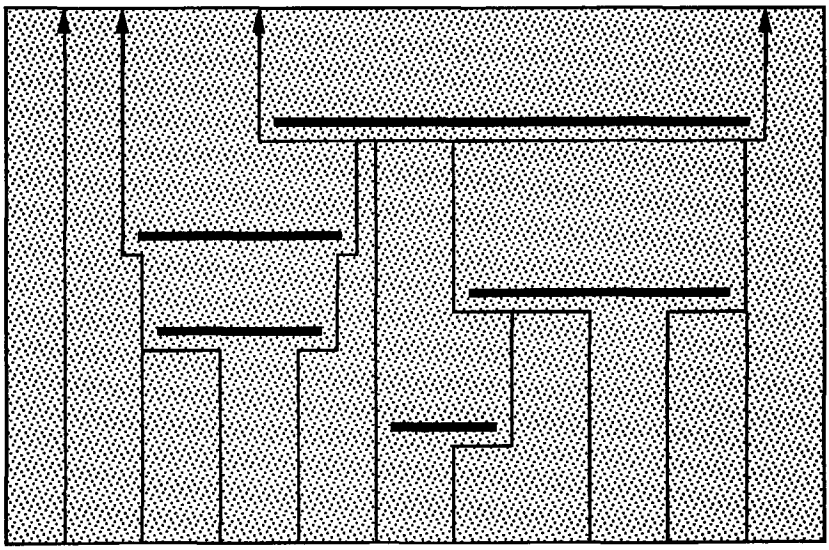

Figure 4.12 Tracing flowlines with the explicit streamline method of Begg and King (1985).

In the statistical streamline method an average number of shales encountered by each streamline is calculated from well data. Then, shale lengths are determined from cumulative frequency diagrams, and a step-out distance is calculated by multiplying the shale width by a

random number between 0 and 1. In two dimensions the average step-out will be half the shale length. By using such an average, Equation 4.9 can be written as:

$$K_{ve} = \frac{K_m \left(1 - F_s\right)}{\left(1 + f \frac{\overline{u_1}}{2}\right)^2} \qquad (4.10).$$

In this equation $\overline{u_1}$ is the average shale width. According to Begg and King, in three dimensions this equation must be written as:

$$K_{ve} = \frac{K_m \left(1 - F_s\right)}{\left(1 + f \frac{\overline{u_1}}{3}\right)^2} \qquad (4.11).$$

The statistical streamline method is the most suitable for practical use. It allows for varying shale lengths. Also the shale density is not limited by computational problems.

The model developed by Begg, Chang and Haldorsen (1985) takes the statistical streamline method of Begg and King (1985) and adapts it to the case of a layered medium with different anisotropic sand permeabilities and shale statistics in each layer. According to this method permeability anisotropy is given by:

$$k_{ve} = \frac{\left(1 - F_s\right) z^2}{p_s} \sum_{q=1}^{p_s} \frac{1}{\left(\Delta z_e\right)_q \left(\Delta z_{re}\right)_q} \qquad (4.12).$$

In this equation $(\Delta z_e)_q$ is given by:

$$\left(\Delta z_e\right)_q = \sum_{l=1}^{v} \left(z_l + \sum_{i=1}^{n_l} \left(\left(r_l\right)_{q,l,ik} \left(u_l\right)_{q,l,i} \right) \right) \qquad (4.13).$$

In this equation z_l is the thickness of layer l. In Equation 4.12 $(\Delta z_{re})_q$ is given by:

$$(\Delta Z_{re})_q = \frac{(\Delta Z_e)_q}{(K_e)_q} \qquad (4.14).$$

In Equation 4.14 $(K_e)_q$ is the effective permeability of stream tube q. Equation 4.14 can be rewritten as:

$$(\Delta Z_{re})_q = \sum_{l=1}^{v} \left(\frac{Z_l}{(K_{mz})_l} + \frac{1}{(K_{mx})_l} \left(\sum_{i=1}^{n_l} (r_l)_{q,l,i} \, (u_l)_{q,l,i} \right) \right) \qquad (4.15).$$

In this equation K_{mz} is the matrix permeability in the z direction and K_{mx} the matrix permeability in the y direction.

Equation 4.12 gives the vertical permeability for the two-dimensional case. This equation is also valid for three-dimensional cases. Only $(\Delta Z_e)_q$ and $(\Delta Z_{re})_q$ are different:

$$(\Delta Z_e)_q = \sum_{l=1}^{v} \left(Z_l + \sum_{i=1}^{n_l} b_{q,l,i} \right) \qquad (4.16),$$

and

$$(\Delta Z_e)_q = \sum_{l=1}^{v} \left(\frac{Z_l}{(K_{mv})_l} + \sum_{k=1}^{q} (b_e)_{q,l,i} \right) \qquad (4.17).$$

Where:

$$b_{q,l,i} = (r_l)_{q,l,i} \cdot (u_l)_{q,l,i} \qquad (4.18)$$

and

$$(b_e)_{q,l,i} = \frac{(r_l)_{q,l,i} \, (u_l)_{q,l,i}}{(K_{mx})_l} \qquad (4.19),$$

if:

$$\frac{\{(r_l)_{q,l,i} \, (u_l)_{q,l,i}\}^2}{(K_{mx})_l} < \frac{\{(r_2)_{q,l,i} \, (u_2)_{q,l,i}\}^2}{(K_{my})_l} \qquad (4.20).$$

Otherwise

$$b_{q,l,i} = (r_2)_{i,j,k} \cdot (u_2)_{q,l,i} \qquad (4.21)$$

and

$$(b_e)_{q,l,i} = \frac{(r_2)_{q,l,i}\,(u_2)_{q,l,i}}{(K_{my})_l} \qquad (4.22).$$

Desbarats (1987) constructed grids in which the grid blocks have either shale (low) or sandstone (high) permeabilities. For these grids the effective vertical permeability is determined through numerical simulation. The distribution of shale and sandstone permeabilities is based on shale statistics derived from outcrops. The generation scheme takes spatial correlation into account (for a detailed description of the generation scheme see the original paper by Desbarats).

In his paper Desbarats presents several experiments performed with his method. He considered grids with spatially uncorrelated permeabilities and compared calculated effective permeabilities for both two- and three-dimensional grids. This comparison shows that in the case of equal shale fractions, the two-dimensional grids will yield the lowest calculated effective permeabilities. Desbarats states that this is because poorly permeable zones are by-passed in the three-dimensional case. Desbarats also compared calculated effective permeabilities for grids with spatially uncorrelated and spatially correlated permeabilities. The comparison shows that effective permeabilities are highest for equal shale densities in the case of spatially correlated permeabilities. According to Desbarats this is because in the case of spatially correlated data the flow paths are more continuous.

Furthermore, Desbarats compared effective vertical permeabilities calculated with his method and effective vertical permeabilities calculated with the Begg and King (1985) method. He found that the effective permeabilities calculated with his method were much lower

than those calculated with Begg and King's method especially for large fractions of shale. Based on these results Desbarats concluded that Begg and King's method overestimates effective vertical permeability because it ignores the effect of a shale on streamlines that do not encounter that shale. However, the effective permeabilities calculated by Desbarats with his own method are too small, because the height of the grid blocks used in his simulation experiments is much larger than the vertical range of influence. As a result, the shale thicknesses are overestimated and it appears that potential flow paths are blocked (Figure 4.13). Desbarats noted this effect but did not further discuss it.

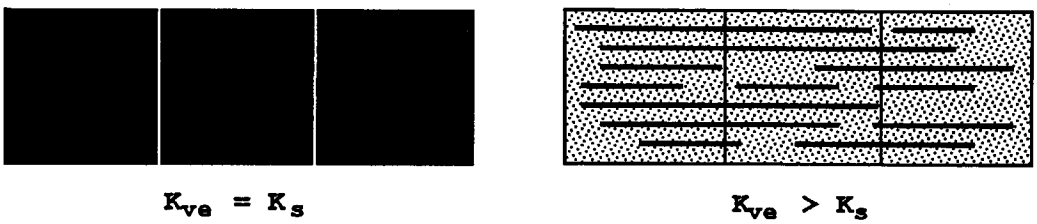

Figure 4.13 Effect of grid blocks whose vertical size is greater than the vertical range of influence: shale thickness is overestimated and hence vertical permeability is underestimated.

Deutsch (1989) calculated effective permeabilities by detailed numerical simulation with fine-meshed grids in which shales can be defined explicitly. He assumed that the shales were ellipsoids of equal size, positioned independently from other shales. He plotted calculated effective vertical permeabilities against the shale fraction. To obtain relationships between effective permeability and shale fraction he modelled the observed behaviour by power averaging and with a percolation model. These relations can be used for input preparation for conventional simulation studies in which the grid block dimensions are usually several times larger than the shale dimensions.

In the case of power averaging the effective permeability is given by:

$$K_e = \left[F_s K_s^{\omega} + \left(1 - F_s\right) K_m^{\omega}\right]^{1/\omega} \qquad (4.23).$$

Deutsch presented a graph in which the averaging power ω is plotted against the width/thickness ratio of the shales. This graph is based on detailed numerical simulation experiments for shales with different width/thickness ratios.

Deutsch also investigated the influence of the length/width ratio on ω. He found a slight increase of ω for increasing length/width ratios in the direction perpendicular to the shales as well as in the direction parallel to the long axis of the shales. Along the direction parallel to the short axis of the shales there is a sharp decrease of ω when the length/width ratio increases.

Deutsch states that Equation 4.23 can only be used for preparing input for conventional simulation studies if the grid block sizes used in these simulations are three times larger than the shale dimensions. If this is not the case ω must be corrected by:

$$\omega_c = \left(1 + a\, e^{L_b/L_s}\right) \omega \qquad (4.24).$$

In this equation L_b is the grid block dimension and L_s the shale dimension in the direction of flow.

If a percolation model is used, the effective permeability is given by:

$$\frac{K_e}{K_m} = c \left(F_{sc} - F_s\right)^t \qquad (4.25).$$

The parameter F_{sc} is the maximum amount of shale beyond which the flow rate will drop dramatically. According to Deutsch the physical significance of c and t is yet not well understood. Deutsch presents graphs in which the parameters c, t and F_{sc} are plotted against the width/thickness ratio of the shales. These graphs are based on

detailed numerical simulation experiments for different width/thickness ratios.

Deutsch's method deserves comment. First, all the shales are assumed to be equal size, but this is geologically improbable. Secondly, in the case of shales with length/width ratios larger than 1 it is assumed that all shales are oriented in the same direction. More important however, is the fact that the parameters needed to calculate the effective permeabilities have to be derived from numerical simulation experiments. In these simulation experiments the shales must be modelled explicitly. Therefore, in case of shales with large width/thickness ratios many grid blocks will be needed to determine the calculation parameters. However, computing costs will limit the number of blocks and therefore the width/thickness ratios of the shales for which the method is valid. In Deutsch's paper the maximum width/thickness ratios of the shales for which parameters are derived is 11. More realistic width/thickness ratios are usually much larger (Weber, 1982).

4.4.3.3 Comparison and application of shale models

The results of all but two of the shale models discussed above are presented in Figure 4.14. Desbarats's (1987) method was not included in this graph because it would require too many grid blocks. Deutsch's (1989) method was not included either, because Deutsch does not give modelling parameters for the shale width/thickness ratios used in Figure 4.14. The effective vertical permeability as a percentage of the horizontal permeability is plotted against the fractional aperture of a flow element containing two impermeable shales. The results of the models can be checked using two points only: when α=0 the plotted permeability ratio must be equal to zero and when α=1 the potted permeability ratio must equal unity. It appears that the methods of Prats (1972), Chirlin (1985), Brydges et al. (1975) and the statistical streamline method of Begg and King (1985) satisfy these conditions. When Equation 4.7 is used for the Haldorsen and Lake (1984) model instead of Equation 4.5 the results of this model also satisfy these conditions, because they are then

identical to the results obtained by Begg and King (1985). The method developed by Martin and Cooper (1984) and Brydges et al. (1975) give unrealistic results. The method of Martin and Cooper gives negative values for K_{ve} if $\alpha > 0.5$ and the method of Brydges et al. gives very low K_{ve} values (see also Table 4.11).

4.4.4 EVALUATION OF SHALE MODELS

4.4.4.1 Repetitive versus random patterns

Two types of shale models can be differentiated: models with a repetitive pattern and models with a random shale pattern. In shale models with a repetitive pattern the size and distribution of the shales is constant. Random models are more realistic in this respect, because both shale lengths and the distribution of the shales in space can be varied. However, models with a repetitive pattern are acceptable when the shales are very numerous and do not vary greatly in their lateral dimensions.

4.4.4.2 Permeability of shales

All the models except the Weber (1982) model, the Martin and Cooper (1984) model, the Desbarats (1987) model and the Deutsch (1989) model assume that the shales are impermeable. As this is often disputable Begg et al. (1985) calculated K_{ve} for two extreme shale distributions (a single shale and a dense distribution of long shales) where the shale permeability varied between zero and the sand permeability. They showed that if the effective vertical sand permeability is about 100 times that of the shale permeability, the difference in K_{ve} as a result of the permeable shales is only a few per cent (<5%). If the effective vertical permeability is about 1000 times greater than the shale permeability, the difference in K_{ve} as a result of the assumption of impermeable shales is reduced to almost zero. These results are valid for the two extreme shale distributions mentioned,

therefore it can be stated that as long as K_m is two or three orders of magnitude larger than the shale permeability, the K_{ve} calculated with a method that assumes impermeable shales is plausible.

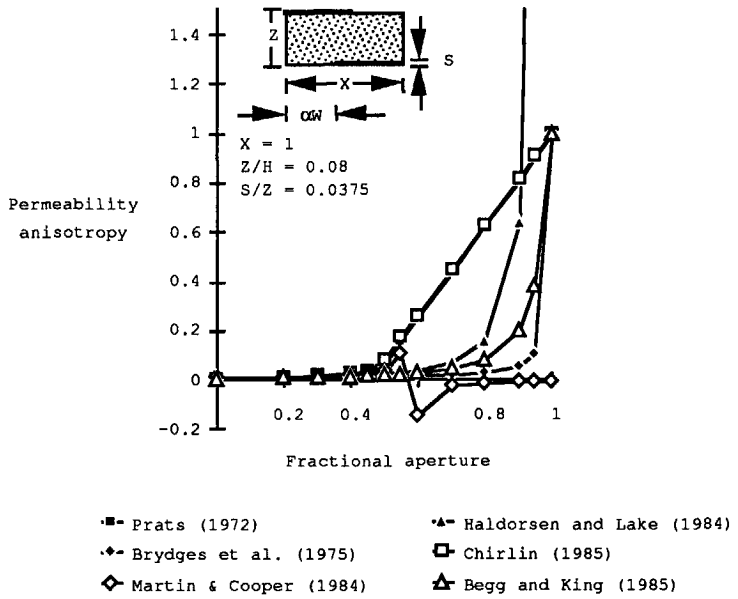

Figure 4.14 Quantitative comparison of shale models for a flow element containing two shales. Weber's method (1982) gives the same anisotropies as Prats' method (1972) for this configuration. The Begg et al. method (1985) gives the same results as the Begg and King method (1985).

4.4.4.3 Effect of vertically varying shale densities

Only the method of Begg et al. (1985) allows for a vertical variation in the density of shales. A variation can be introduced in the number of shales encountered by streamlines in different layers. However, the shale fraction is constant over the whole volume of rock under consideration. Therefore it would seem to be more appropriate to introduce different shale fractions in the different layers. Equation 4.12 may then be written as:

$$K_{ve} = \frac{Z}{\sum_{l=1}^{v} \frac{z_l}{(K_{ve})_l}} \qquad (4.26).$$

Here $(K_{ve})_l$ is the effective vertical permeability of Layer l and must be calculated with Equation 4.12. I compared the results of Equation 4.12 with Equation 4.13 for a two layered system (Figure 4.15). This comparison shows only minor differences (Figure 4.15).

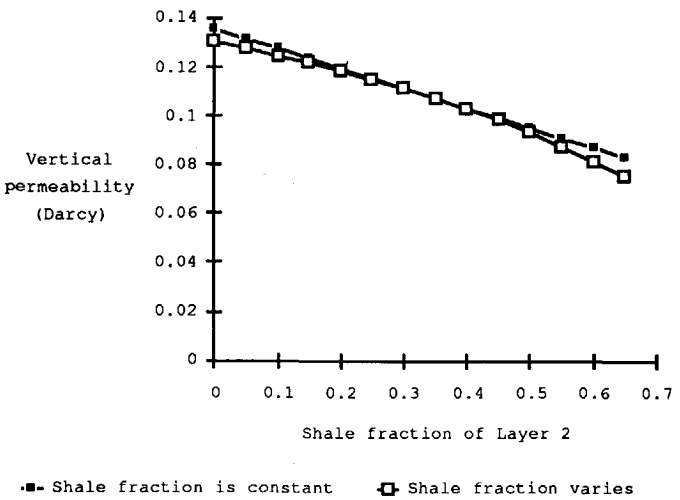

Figure 4.15 Comparison of vertical permeabilities calculated for a two-layer system if the shale fraction is kept constant (model of Begg et al., 1985) and if it varies between layers. The shale fraction in Layer 1 is kept constant at 0.33. Sand permeability is isotropic and equal to 1 Darcy. There are 0.33 shales per metre.

4.4.4.4 Introduction of a Poisson distribution

The techniques of Haldorsen and Lake (1984), Begg and King (1985) and Begg et al. (1985) result in all streamlines encountering an equal number of shales. In reality the number of shales that every streamline passes may be approximated by a Poisson distribution (Haak

and Elewaut, 1990). When there are only a few shales the vertical permeability is too small when calculated without the introduction of a Poisson distribution (Figure 4.16). When there are many shales this effect will diminish.

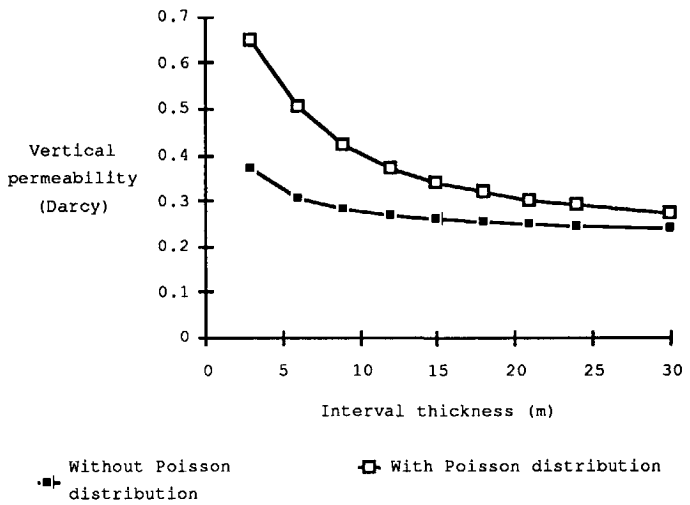

Figure 4.16 Comparison of vertical permeabilities without introduction of a Poisson distribution (model of Begg et al., 1985) and with introduction of a Poisson distribution. The sand permeability is isotropic and equal to 1 Darcy. There are 0.33 shales per metre.

4.4.4.5 Calculation of streamline lengths

Begg and King (1985) and Begg et al. (1985) stated that Equation 4.12 can be simplified by taking average stream tube lengths. Combination of Equations 4.12 and 4.14 gives:

$$K_{ve} = \frac{(1 - F_s)\, Z^2}{p_s} \sum_{q=1}^{p_s} \frac{(K_e)_q}{(\Delta Z_e)_q^2} \qquad (4.27).$$

Using the average stream tube length in this equation would mean that:

$$\frac{1}{p_s}\sum_{q=1}^{p_s}\frac{(K_e)_q}{(\Delta Z_e)_q^2} = \frac{K_e}{\overline{\Delta Z_e}^2} \qquad (4.28).$$

Rozendal (1989) proved that this is not correct, because the effect of small values of $(\Delta Z_e)_q$ is underestimated. From Figure 4.17 it can be concluded that this effect can be ignored if there are many shales.

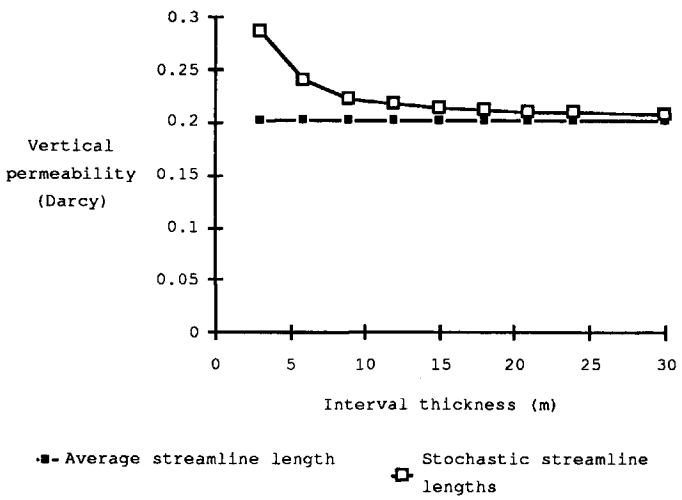

Figure 4.17 Comparison of calculated permeabilities using the average streamline length (model of Begg et al., 1985) and using stochastically determined streamline lengths. The sand permeability is isotropic and equal to 1 Darcy. There are 0.33 shales per metre.

4.4.4.6 2-D versus 3-D modelling

The Begg and King (1985) and Begg et al. (1985) models can be used in both two and three dimensions. In Figure 4.18 K_{ve} is plotted against the number of shales for several length/width ratios of the shales.

The 3-D model for a shale with an infinite length can be considered as a 2-D model. From Figure 4.18 it is apparent that a 2-D model is sufficient for length/width ratios greater than 3. This result can be understood if we consider the effect of larger length/width ratios on the average flow path parallel to a shale. For a square of shale the average flow path along each side is 1/8. For increasing length/width ratios the average flow path will quickly approximate 1/4 (Figure 4.19).

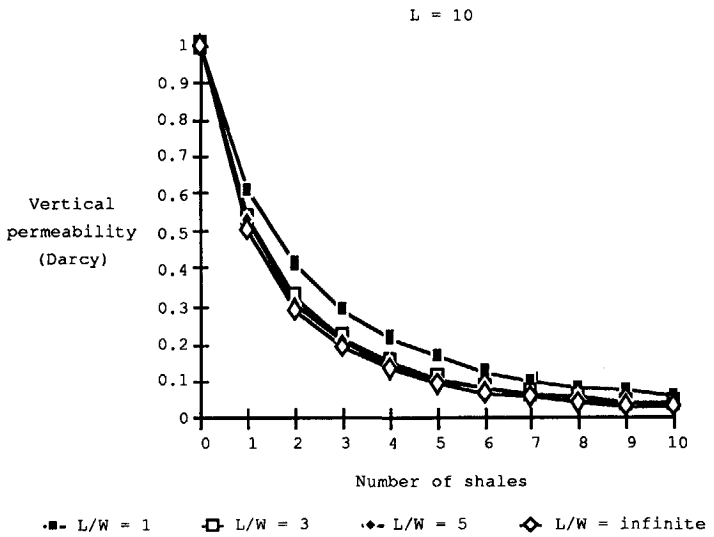

Figure 4.18 Vertical permeabilities for shales with increasing length/width ratios calculated with the method of Begg et al. (1985). Sand permeability is isotropic and equal to 1 Darcy.

In Figure 4.18 the matrix is considered to be isotropic. If the matrix is anisotropic the shale dimensions should be scaled according to:

$$u_2' = u_2 \sqrt{\frac{K_{mx}}{K_{my}}} \qquad (4.29).$$

The matrix can now be considered as isotropic with permeability K_{mx}. After the scaling process it can be judged whether a 3-D model is necessary, or if a 2-D model is sufficient.

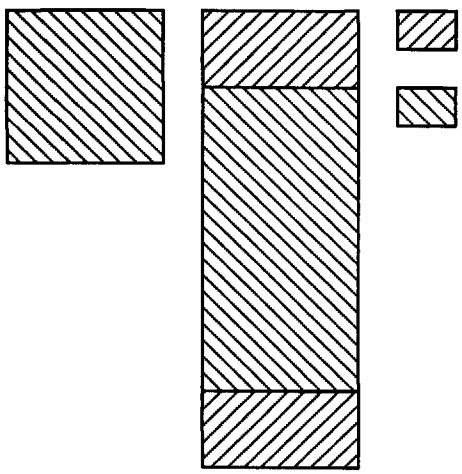

Average flow path parallel to each side of the shale is 1/8 times the width of the shale

Average flow path parallel to each side of the shale is 1/4 times the width of the shale

The average flow path parallel to a side of a shale $\bar{s}$ is given by:

$$\bar{s} = \frac{1}{n}\left(\frac{1}{4}\left(\frac{L}{W} - 1\right)W + \frac{1}{8}\right)$$

For L/W = 1, $\bar{s}$ is equal to:

$\bar{s}$ = 1/8 W = 0.125 W

For L/W = 3, $\bar{s}$ is equal to:

$\bar{s}$ = 1/3 (1/2 W + 1/8 W) = 5/24 W = 0.2083 W

For L/W = 5, $\bar{s}$ is equal to:

$\bar{s}$ = 1/5 (W + 1/8 W) = 9/40 W = 0.225 W

For L/W = ∞, $\bar{s}$ is equal to:

$$\bar{s} = \lim_{L/W \to \infty} \frac{1}{n}\left(\frac{1}{4}\left(\frac{L}{W} - 1\right)W + \frac{1}{8}\right) = \frac{1}{4} W = 0.25 W$$

Figure 4.19 Average flow path lengths around shales as calculated with 3-D streamline methods.

4.4.4.7 Comparison of calculated streamline lengths with numerical fluid flow simulation

Haldorsen and Lake (1984), Begg and King (1985) and Begg et al. (1985) approximated the flow path around a shale as in Figure 4.20A

(blocky flow path) but the actual flow path around a shale is, however, more likely to be as in Figure 4.20B. To test the error introduced, I simulated the flow around one shale with a finite difference approximation of the stream function; the result is shown in Figure 4.20B.

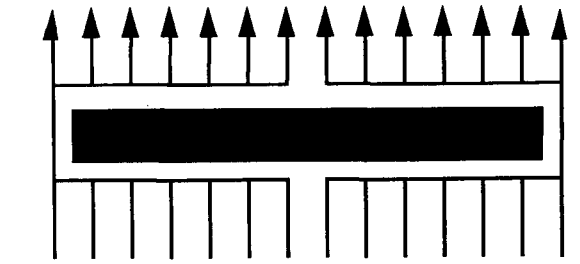

A.

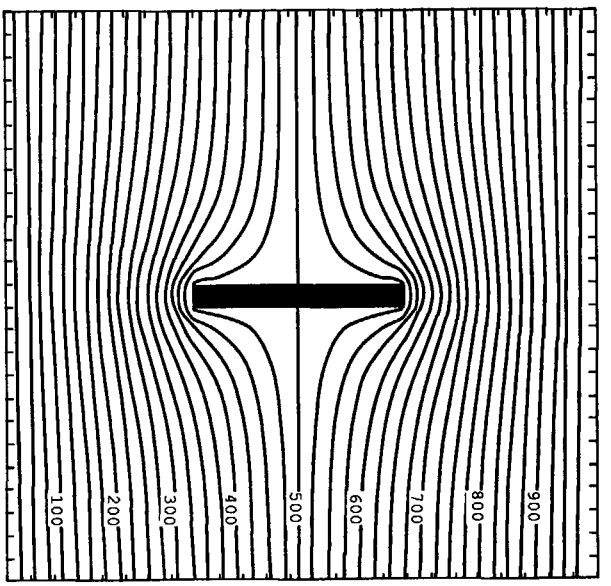

B.

Figure 4.20 A) Approximation of the flow path around a shale with streamline methods; B) more probable flow path.

I calculated streamline lengths based on the numerical simulation results and for the blocky flow path. When few shales are present, the assumption of a blocky flow path will result in most streamline lengths being overestimated (Figure 4.21). The results of the streamline methods give a curve with slope equal to 2. A better approximation of the simulation results is a curve with slope equal to 1. This means that streamline lengths calculated with methods assuming a blocky flow path are, on average, too large by a factor 2. This is also indicated by the results of Hazeu et al. (1988). They used the Begg and King (1985) model to calculate vertical permeabilities in a reservoir with few shales. Hazeu et al. (1988) had to divide the shale lengths by 2 to get a history match. I believe that the discrepancy between the streamline lengths I found with my numerical simulation experiments and the streamline lengths I calculated by assuming a blocky flow path are a good explanation for this discrepancy.

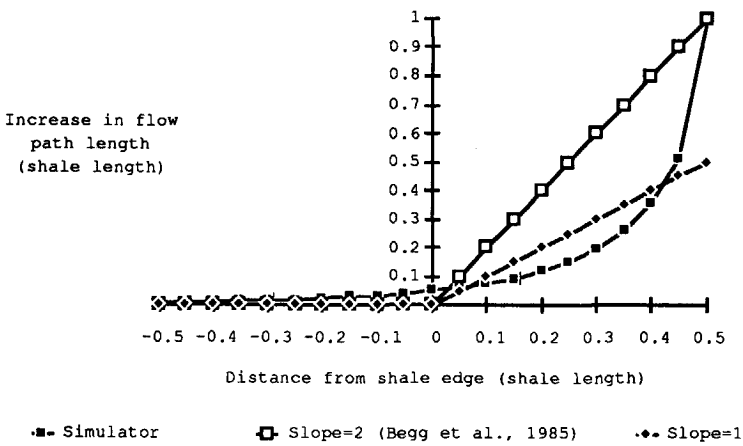

Figure 4.21 Streamline lengths derived with streamline methods compared with streamline lengths derived from numerical simulation. The definition of the parameters along the vertical and horizontal axis is given in Figure 4.22.

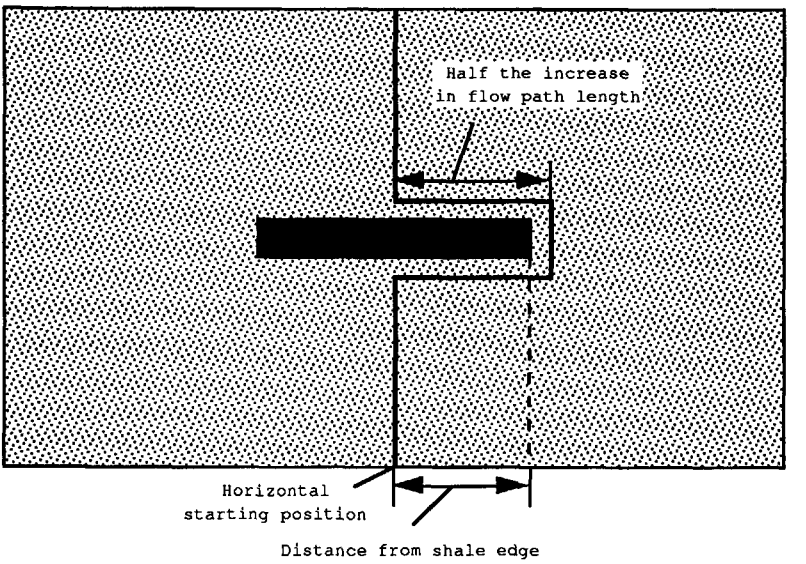

Figure 4.22 Increase in flow path length in relation to shale length according to the method of Begg et al. (1985).

4.4.5 VERTICAL PERMEABILITIES IN BIOTURBATED SAND/SHALE SEQUENCES

Some sedimentary environments contain sand-filled burrows, that pierce shale intercalations. Such burrows have a beneficial effect on the vertical permeability. The burrows are formed by organisms which dig through the fine-grained sediments during or shortly after deposition, and which fill the resulting holes with sand. Burrows of this type are virtually restricted to marine and transitional sediments. In marine sediments the intensity of bioturbation increases with increasing distance from the coast (Moore and Scrutton, 1957).

In shallow marine environments, especially barrier foot sediments a clear alternation of lithologies (sand and clay) often occurs. In cases where layer thickness ranges from 5 to 20 centimetres, burrows that penetrate the shales from sand to sand can be found, e.g.

Skolithos and *Ophiomorpha*. At present, not much attention is being paid to the effect of biogenetic structures on vertical permeability. Often the vertical permeability is assumed to be zero. However, measurements with a mini-permeameter have shown that the vertical permeability is probably significant in such bioturbated reservoirs (Weber, 1982; 1986).

4.4.5.1 Types of bioturbation

Seilacher (1967) differentiated six types of biogenetic structures (Figure 4.23). This differentiation is based on the biogenetic activity which formed the structures:

- Resting traces (*Cubichnia*)
- Crawling traces (*Repichnia*)
- Grazing traces (*Pascichnia*)
- Dwelling traces (*Domichinia*)
- Feeding traces (*Fodichnia*)
- Escape structures (*Fuchinia*)

Only vertical burrows have significant influence on the vertical fluid flow in heterogeneous reservoirs. Therefore, feeding, dwelling and escape traces are the most important biogenetic structures for the enhancement of vertical permeability.

4.4.5.2 Method for determining vertical permeability in bioturbated sand/shale sequences

Vertical permeabilities in bioturbated sand/shale sequences can be estimated in a core by assuming the shales as permeable. In principle one could try to assess the overall vertical permeability via whole core measurements. However these are expensive and require very well preserved cores. A less expensive method might be to use core derived burrow densities and detailed permeability distributions measured with the mini-permeameter. The permeability of the shales can then be given by:

$$K_s = K_b \cdot F_b \qquad (4.30).$$

In this equation K_b is the burrow permeability and F_b the relative burrow fraction in the horizontal plane. The relative burrow fraction can be estimated from the cores. Sand layer and burrow permeabilities can be measured with a mini-permeameter. The vertical permeability of the core is given by:

$$K_{ve} = Z_c \left(\frac{\sum_{l=1}^{v} Z_l}{K_m} + \frac{Z_c - \sum_{l=1}^{v} Z_l}{K_s} \right)^{-1} \qquad (4.31).$$

In this equation Z_l is the thickness of sand layer l, v the number of sand layers and Z_c the core length.

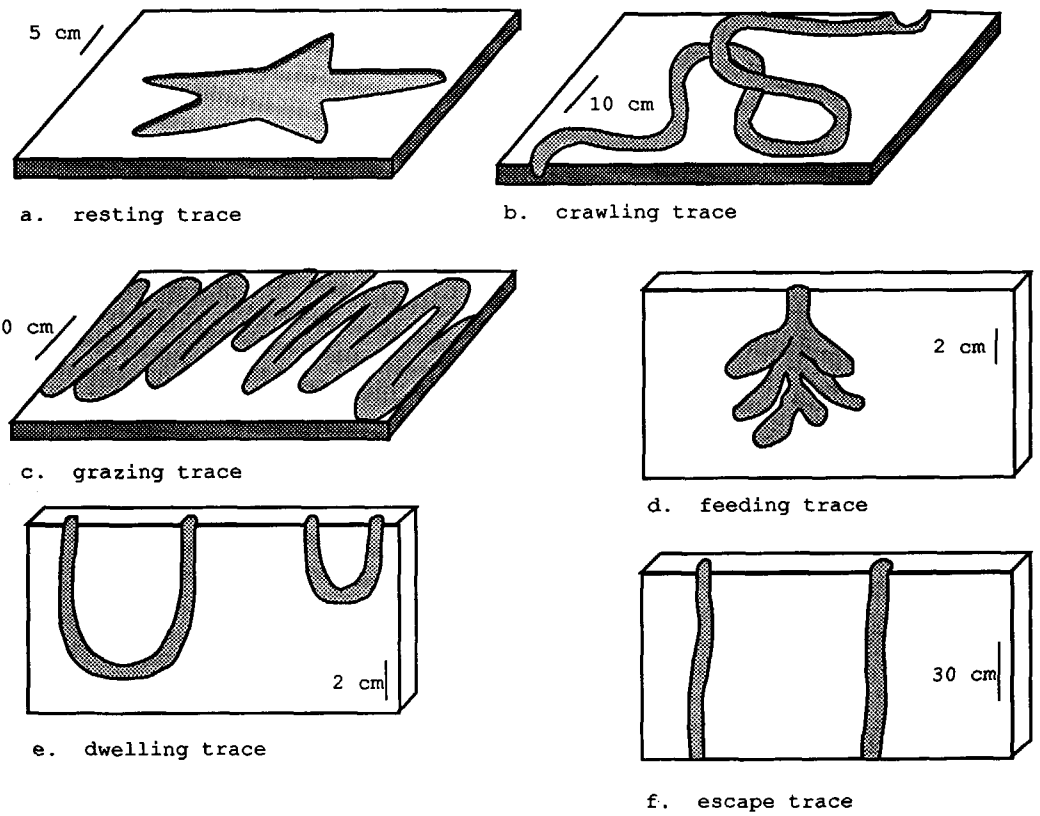

Figure 4.23 Different types of biogenic structures.

I have tested Equation 4.31 by numerical simulation using the stream function approach of Floris (in prep.). The results are given in Figure 4.24. In this example burrow permeability and sand permeability are equal. The length of the sands was varied as well as the burrow density. From Figure 4.24 it is apparent that the results of Equation 4.31 do not differ significantly from the simulated results if the sand is not extremely thin.

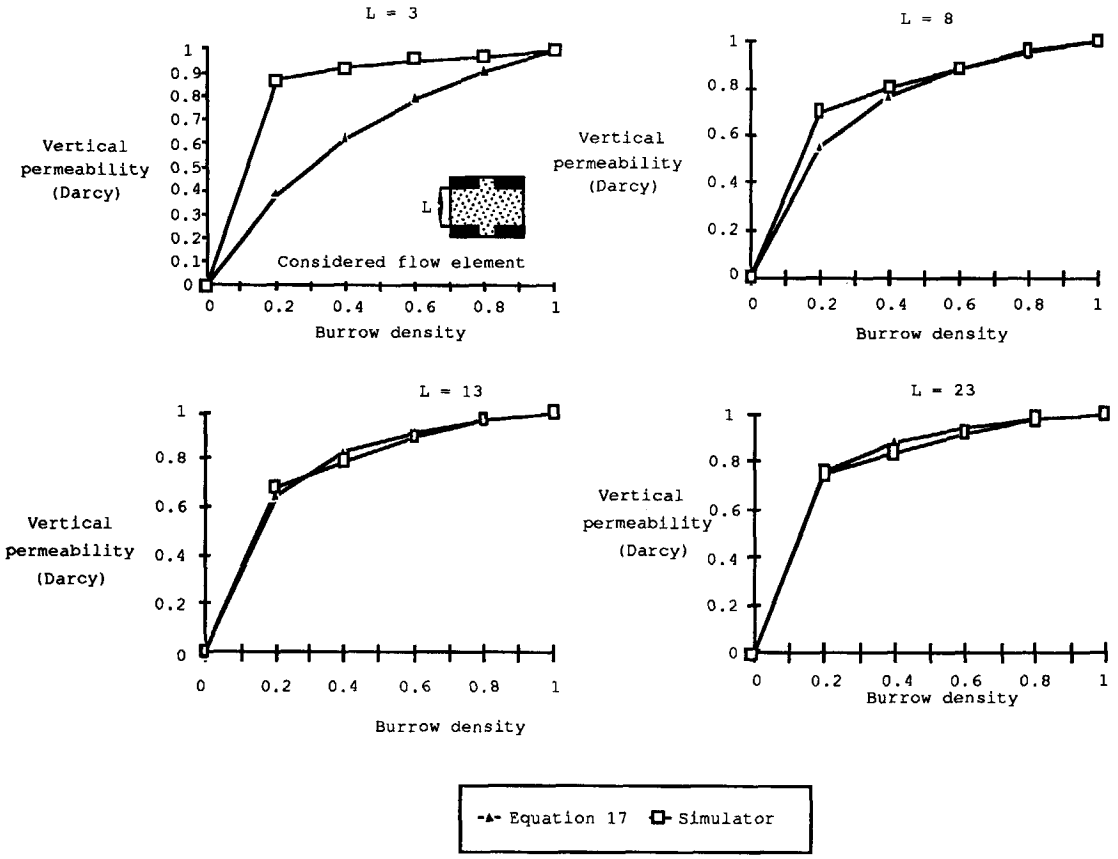

Figure 4.24 Vertical permeabilities calculated with Equation 4.31 compared with vertical permeabilities found by numerical simulation. Shale thickness is equal to 1. Sand thickness is equal to L.

4.5 Simulation experiments on configurations of common flow units

In § 4.1 eight sedimentologically defined flow unit configurations were differentiated within deltaic rocks. They were characterized by sedimentological properties that influence fluid flow. In the previous sections the influence of these properties was discussed separately. In this section an attempt will be made to approach averaging over grid block size units incorporating all sedimentological characteristics that influence fluid flow.

The incentive for averaging permeability is the impossibility of incorporating small-scale heterogeneities even into very detailed 3D reservoir simulations. The idea is to design detailed models of prototype units which are the building blocks of the reservoir as a whole. Genetic units with their characteristic heterogeneities are simulated with a grid that is sufficiently fine-meshed to allow small-scale features to be incorporated.

4.5.1 PREVIOUS WORK ON AVERAGING PERMEABILITY

Various papers have been published on the averaging problem. Haldorsen (1986) discusses the problem of averaging reservoir data on different scales to provide parameters for simulator input. He emphasizes the enormous difference in scale between core plugs and grid blocks. Lasseter, Waggoner and Lake (1986) give examples of detailed simulation studies for determining pseudo-properties when small-scale heterogeneities are present. Basically, this is the method I use in this section, applying it to realistic configurations of flow units.

Recently, Weber and Van Geuns (1990) discussed the problem of the construction of simulation grids in relation to reservoir architecture. They stipulate how the small-scale geological configuration of the reservoir should be incorporated into these

grids, and how the permeability should be averaged. Slatt and Hopkins (1990) give a case study of the Balmoral field turbidite reservoir in which they discuss the translation of a geological model into a flow unit model and give characteristic petrophysical parameters for each of the four different types of flow unit. This approach comes close to the one I use in this thesis as I will show in the next paragraphs.

Whereas there is little literature on permeability averaging via analogue geological models, much has been written on using geostatistical methods for this purpose. Guérillot et al. (1990) describe an outcrop with geostatistical methods and subsequently use the model to determine a matrix of effective permeability for flow calculations. This approach seems to be less generally applicable than the one I propose. Methods like those proposed by Guérillot et al. skip over a detailed depositional description, and only connect certain litho classes to a permeability range. The influence of sedimentary structures or specific length distributions of intercalated shales cannot be incorporated.

4.5.2 PERMEABILITY ANISOTROPIES

4.5.2.1 Fine grid simulations

I constructed detailed sedimentological models for each flow element (Figure 4.1). These models were translated into fine grid simulation models with grid blocks ranging in size from 10 x 4 centimetres to 100 x 20 centimetres. The overall size of each grid was 5 metres x 200 metres, the approximately minimum size of the conventional grid blocks used during reservoir simulation studies.

I incorporated several types of heterogeneity. The effect of sorting trends was inserted by a permeability profile reflecting this trend. Baffles were included in the models as zones of extremely poor

permeability, and the effect of sedimentary structures was incorporated by horizontal and vertical permeability anisotropies.

Four types of sedimentary structures were incorporated in the models: ripple lamination, cross-bedding, parallel lamination and parallel bedding. Based on the work of Mast and Potter (1963), Weber et al. (1972), Pryor (1973), and Weber (1982) horizontal and vertical permeability anisotropies were assigned to each type of sedimentary structure. These are listed in Table 4.12.

Table 4.12 Permeability anisotropies incorporated in the simulation studies for different sedimentary structures.

	horizontal permeability anisotropy	vertical permeability anisotropy
cross-bedding	0.8	0.9
parallel bedding	1.0	0.8
ripple lamination	0.6	0.8
parallel lamination	1.0	0.6

I used the fine grid simulation models to calculate permeability anisotropies for the sedimentologically defined flow unit configurations on a reservoir simulation grid block scale. This was done by calculating horizontal and vertical effective permeabilities for the sedimentologically defined flow unit configurations, both parallel and perpendicular to depositional dip. Horizontal and vertical permeability anisotropies were obtained from these effective permeabilities.

For the calculation of effective vertical permeabilities, only uni-directional, single phase and incompressible flow was considered. In this case the flow pattern will only reflect the influence of rock properties. The boundaries parallel to the flow direction are taken as no-flow boundaries. I solved the single phase incompressible flow

equations using the mixed hybrid finite element method described by Kaasschieter (1990). I was therefore able to obtain the effective permeability in the flow direction K_e from the calculated flow rates Q, using:

$$K_e = \frac{\mu Q}{\Delta P \Delta X} \qquad (4.32).$$

Here μ is the viscosity, ΔP the applied pressure drop and ΔX the width of the flow domain. The results of the simulations are given in Table 4.13 and are discussed in the next sub-section.

Table 4.13 Characteristic permeability anisotropies for the sedimentologically defined flow unit configurations.

sedimento-logically defined flow unit configura-tion	horizontal permeability anisotropy	vertical permeability anisotropy
A	0.6	0.009
B	0.9	0.4
C	0.9	0.7
D	0.7	0.003
E	2	0.09
F	0.5	0.3
G	3	0.3
H	1	0.4

4.5.2.2 Results of the simulations using a fine-meshed grid

Large horizontal permeability anisotropies occur in Type F (estuarine channel fills) and Type G (upper point bar deposits) flow units. This is the result of the inclined zones of poor permeability that occur in these flow units.

As expected, large vertical permeability anisotropies were found to occur in flow units with many continuous shales, like Type A (various shallow marine sediment body types) and D (low energy channel fill) flow units. By comparison with Type A and D flow units, the vertical permeability anisotropies in Type F flow units (levee and barrier foot deposits) are relatively small. This is caused by the relatively poor permeability of sand and good permeability of shale, which implies that the shales are not very effective barriers to flow by comparison with the sand layers.

For Type F and G flow units I found a difference for the vertical permeability anisotropies in sections parallel and perpendicular to the strike of the baffles. This is because the inclined shales appear as extensive horizontal baffles in the sections parallel to the strike direction of the shales. To be able to obtain a realistic vertical permeability value, the flow should be modelled in three dimensions. However, the vertical permeability anisotropy obtained from the sections perpendicular to the strike of the baffles is probably very close to the overall 3D anisotropy.

4.5.3 PSEUDO RELATIVE PERMEABILITY AND CAPILLARY PRESSURE CURVES

In Type A, D and G flow units there is a significant contrast in lithologies between the upper and lower parts (Figure 4.1). In Type A flow elements sands with abundant clay drapes are found at the base, with a transition to cleaner sands upward. Consequently permeabilities are larger in the upper parts of this type of flow element. In Type D flow elements abundant shales occur at the top. In this case permeabilities are greatest at the base of the unit. In

Type G flow units the grain size and sorting decrease upward. Because of the significant contrast in permeabilities in these flow units, pseudo-relative and capillary pressure curves are needed to represent the flow behaviour accurately (Table 4.14). The difference in the distribution of the phases in grid blocks and plugs for the same average saturations have to be represented in an equation by an unique relationship. Thus we have to compute relative permeability and capillary pressure curves at grid block scale.

Table 4.14 The need of pseudo relative permeability curves and pseudo capillary pressure curves for each sedimentologically defined flow unit configuration.

sedimentologically defined flow unit configuration	pseudo relative permeability curve	pseudo relative pressure curve
A	needed	needed
B	not needed	not needed
C	not needed	not needed
D	needed	needed
E	not needed	not needed
F	not needed	not needed
G	needed	needed
H	not needed	not needed

For simple cases with fairly homogeneous rock and conditions in which vertical equilibrium can be assumed the computations are straightforward (Coats, Dempsey and Henderson, 1971). However, for more complex reservoirs and flow processes the derivation of pseudo function often leads to restrictive results (Lake, Kasap and Shook,

1990). Standardized nomogram type sets of curves related to rock properties cannot be applied because the curves are dependent in many ways. Pseudo relative permeability curves can depend on flow rates and directions, rock distribution and characteristics (Kyte and Berry, 1975). If the saturation history plays a role one may end up needing directional pseudo functions for both drainage and imbibition. Control of numerical dispersion may impose the need for pseudo functions.

In this section the derivation will be treated qualitatively. Two situations can be differentiated:

- The less permeable parts are flushed first.
- The more permeable parts are flushed first.

The first situation occurs when a rising fluid contact enters a Type A flow unit. In this case the pseudo relative permeabilities have to be less than the clean sand permeabilities to give an accurate representation of the flow behaviour. The difference between pseudo and clean sand permeabilities has to decrease with increasing water saturations, because with increasing water saturations more sands will be flushed resulting in larger relative permeabilities (Figure 4.25A). Capillary pressures have to be greater than clean sand capillary pressures. This difference between pseudo and clean sand capillary pressures must also decrease with increasing water saturations (Figure 4.25B).

The second situation occurs when Type D and G flow units are flushed or when the most permeable parts of Type A flow units are flushed first. This latter case occurs for example in tilted reservoirs or when a waterflood takes place. The pseudo relative permeabilities have to be less than the clean sand permeabilities to give an accurate representation of the flow behaviour. The difference between pseudo relative permeabilities and clean sand relative permeabilities must increase with increasing water saturations, because with increasing water saturations more poorly permeable rocks will be flushed (Figure 4.26A). The pseudo capillary pressures will also have to increase with increasing water saturations to give an accurate representation of the flow behaviour (Figure 4.26B).

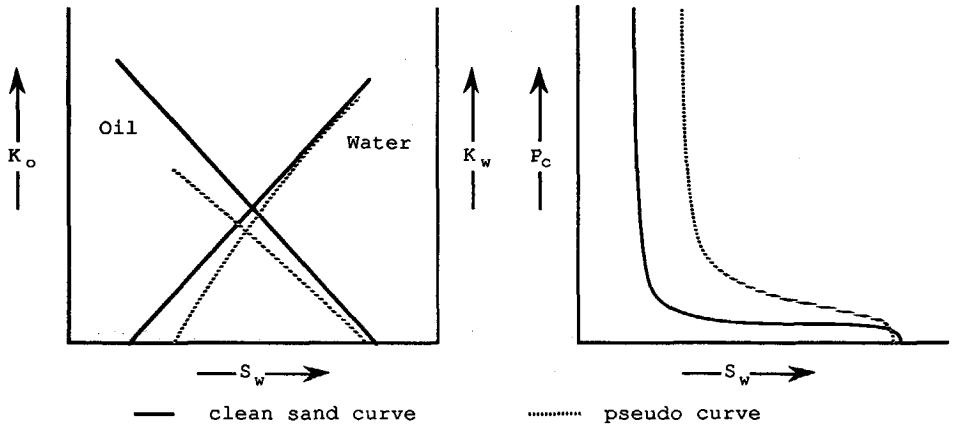

Figure 4.25 Qualitative comparison of pseudo relative permeability and capillary pressure curves and clean sand curves when the least permeable parts of flow unit types A, D and G are flushed first.

4.5.4 TWO-PHASE FLOW SIMULATIONS ON CONFIGURATIONS OF COMMON FLOW UNITS

The results of the fine grid simulations were used to simulate a waterflood through geological models of the delta types differentiated in Chapter 2. The geological models were constructed using the elementary flow elements differentiated in § 4.1 (Figures 4.28 to 4.34). Realistic input values for permeability and porosity were assigned to the grid blocks on the basis of data from Berg (1986) and using permeability anisotropies found with the fine grid simulations (Table 4.13). The simulations were based on a finite difference approximation of the stream function equation and a finite volume approximation of the saturation equation using the Godunov flux (Floris, in prep.). They were performed in the direction of greatest geological variability. The main characteristics of the simulator are given in Figure 4.27.

For fluvial-dominated deltas the simulations show that water influx is most rapid in Type B flow elements representing the central bar sediments (Figure 4.28C). The front advances mainly through the central bar. The distal bar sediments in the lower part of the delta

sequence are as well drained as the central bar sediments, even though the gravitational forces should favour downward flow of the water (Figures 4.28D and E). This downward flow is hampered by the poor vertical permeabilities in the Type A flow units representing the distal bar sediments.

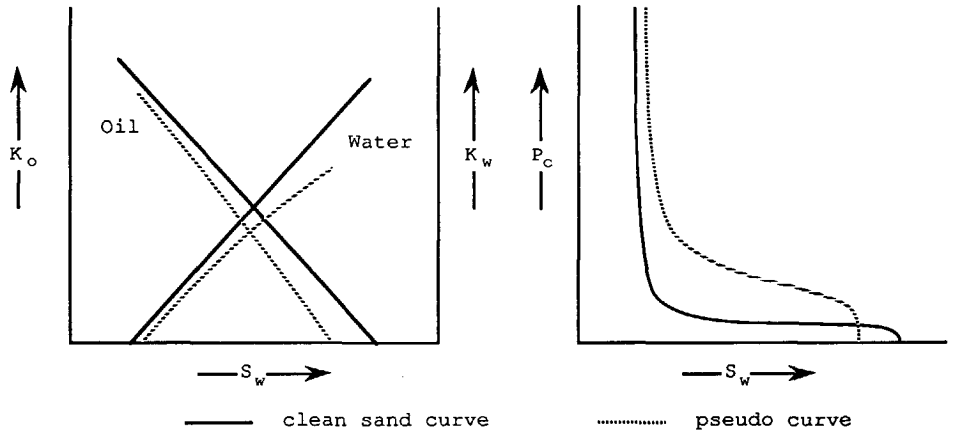

Figure 4.26 Qualitative comparison of pseudo relative permeability and capillary pressure curves and clean sand curves when the most permeable parts of flow unit types A, D and G are flushed first.

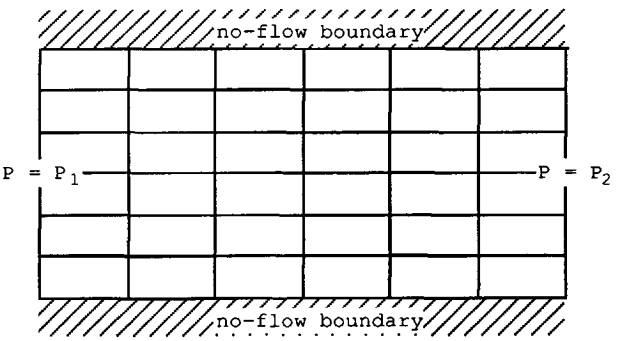

Figure 4.27 Boundary conditions of the fluid flow simulator used.

For tide-dominated deltas the simulation results show initial water influx in the distributary channel sands (Figure 4.29A). The basal

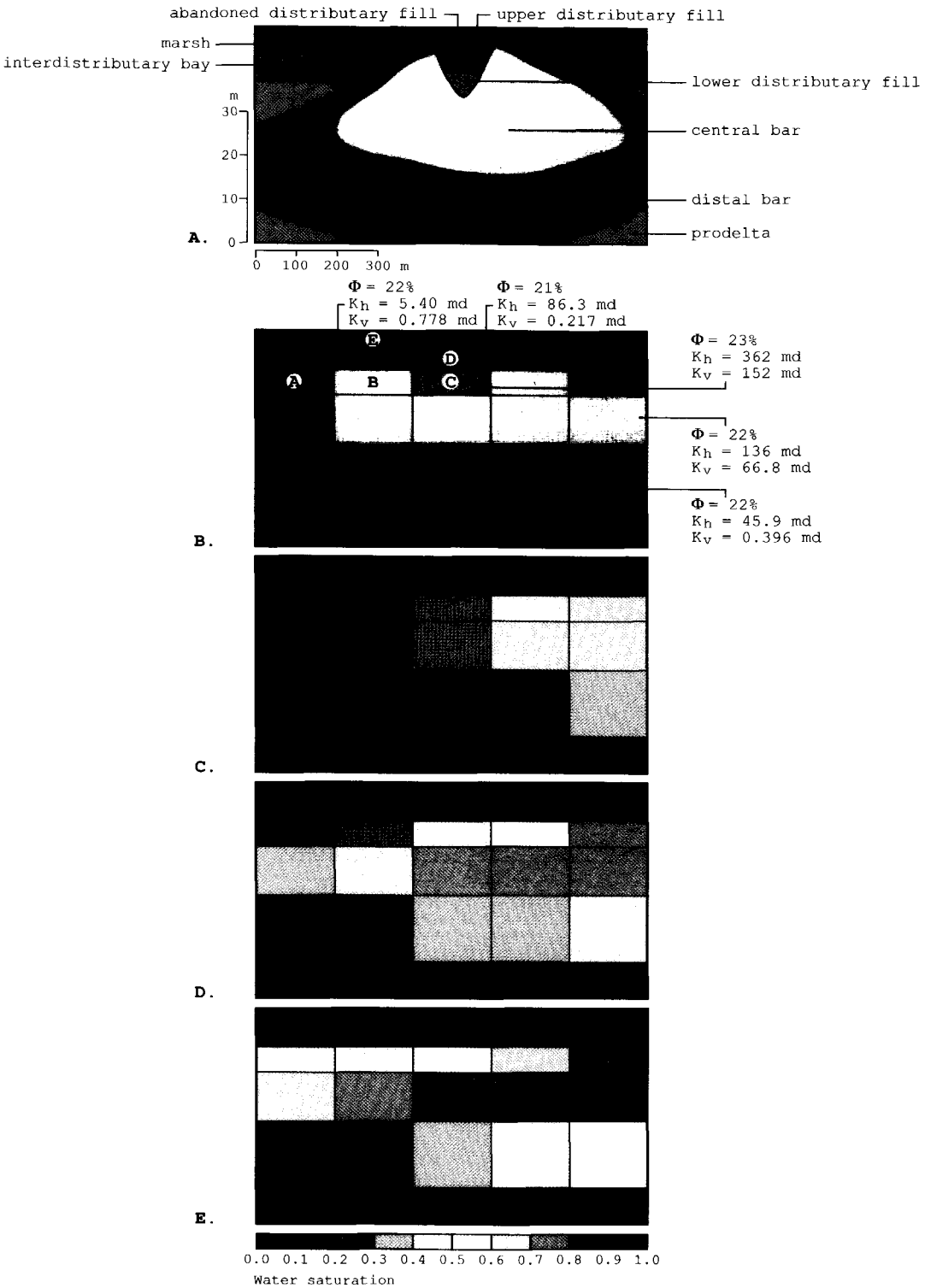

Figure 4.28 Waterflood through a fluvial dominated delta: A) geological model, B) simulation grid, C) t=500 days, D) t=1000 days, E) t=1500 days.

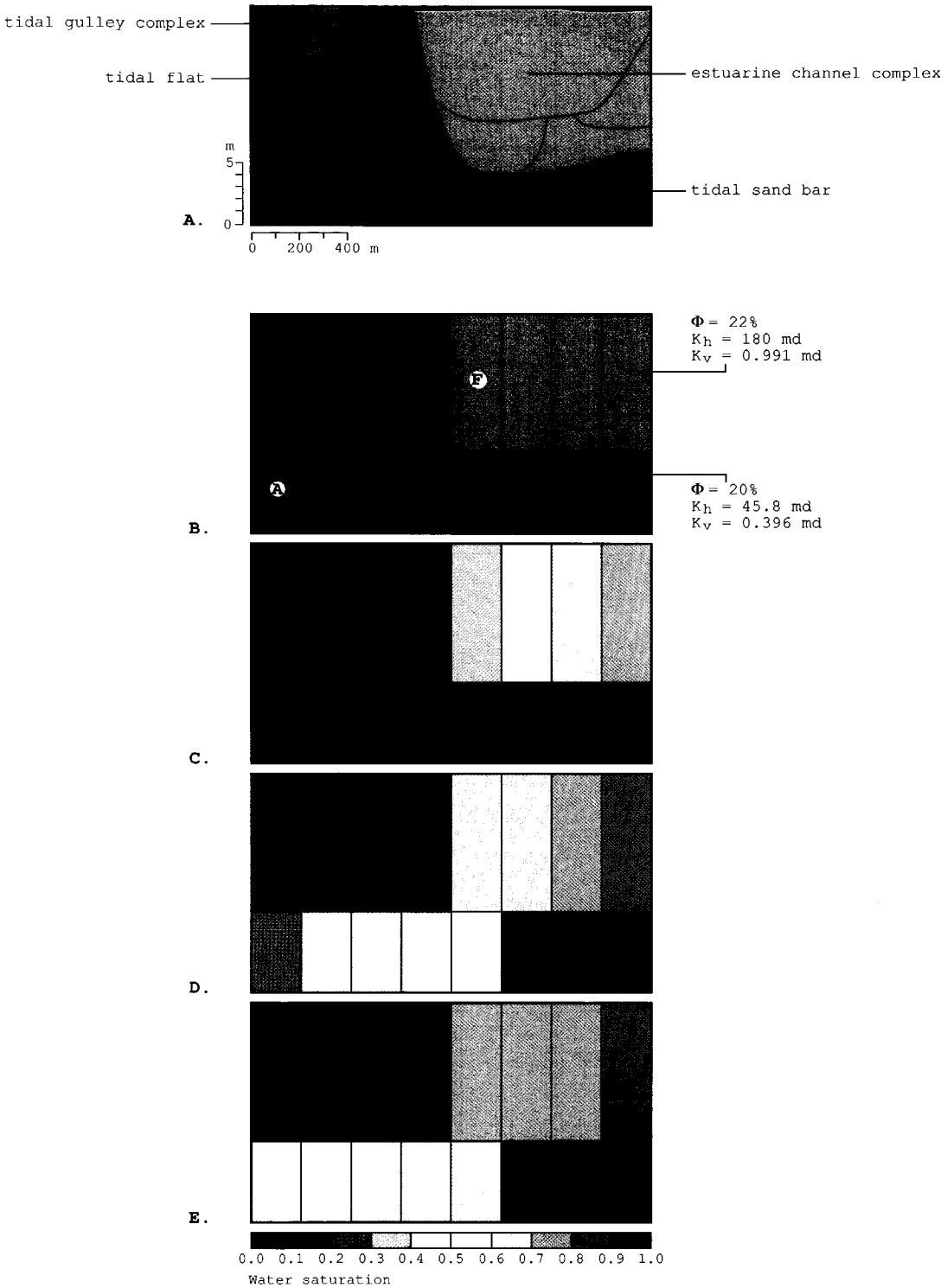

Figure 4.29 Waterflood through a tide dominated delta: A) geological model, B) simulation grid, C) t=500 days, D) t=1000 days, E) t=1500 days.

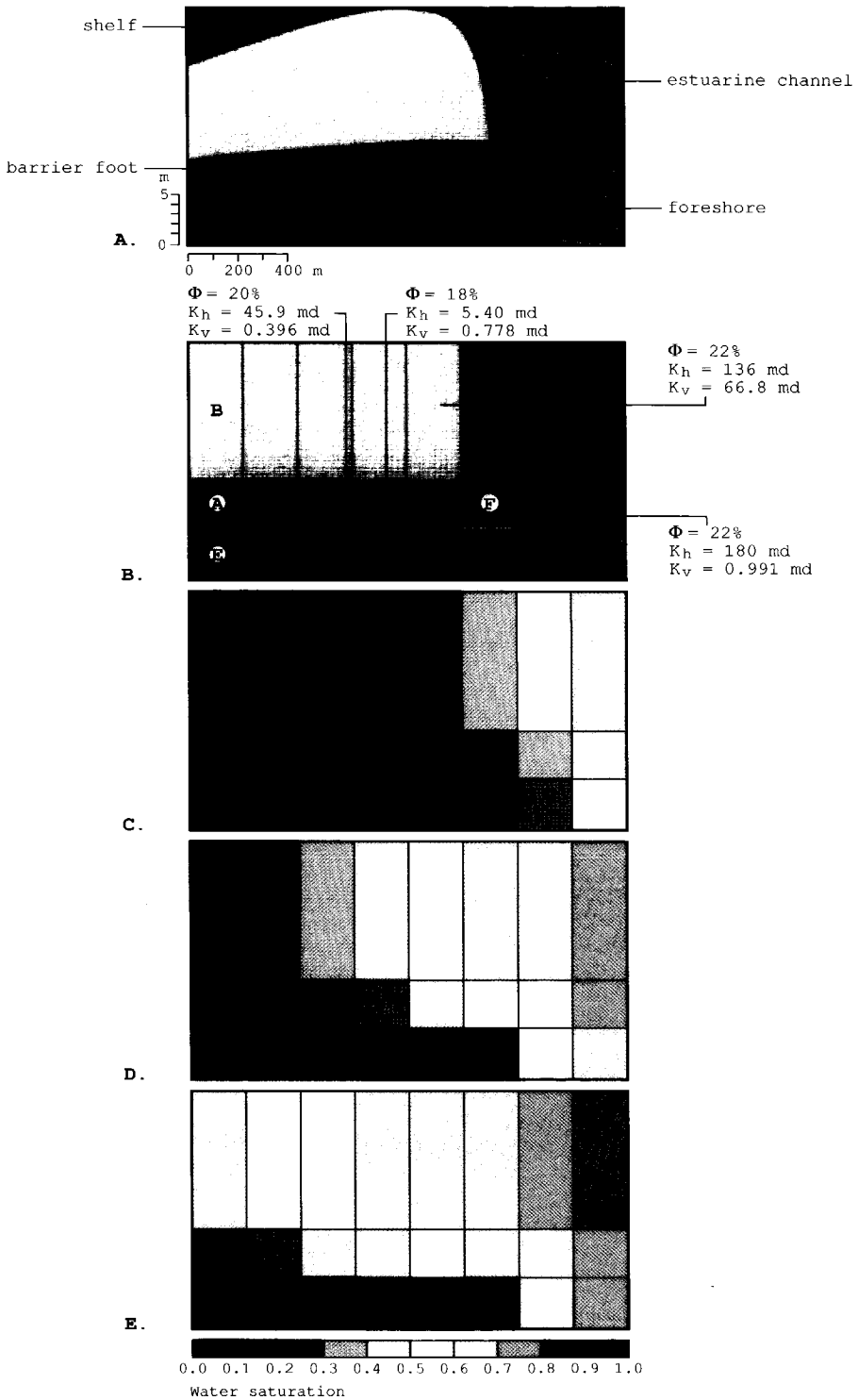

Figure 4.30 Waterflood through a delta with fluvial/wave/tide interaction: A) geological model, B) simulation grid, C) t=500 days, D) t=1000 days, E) t=1500 days.

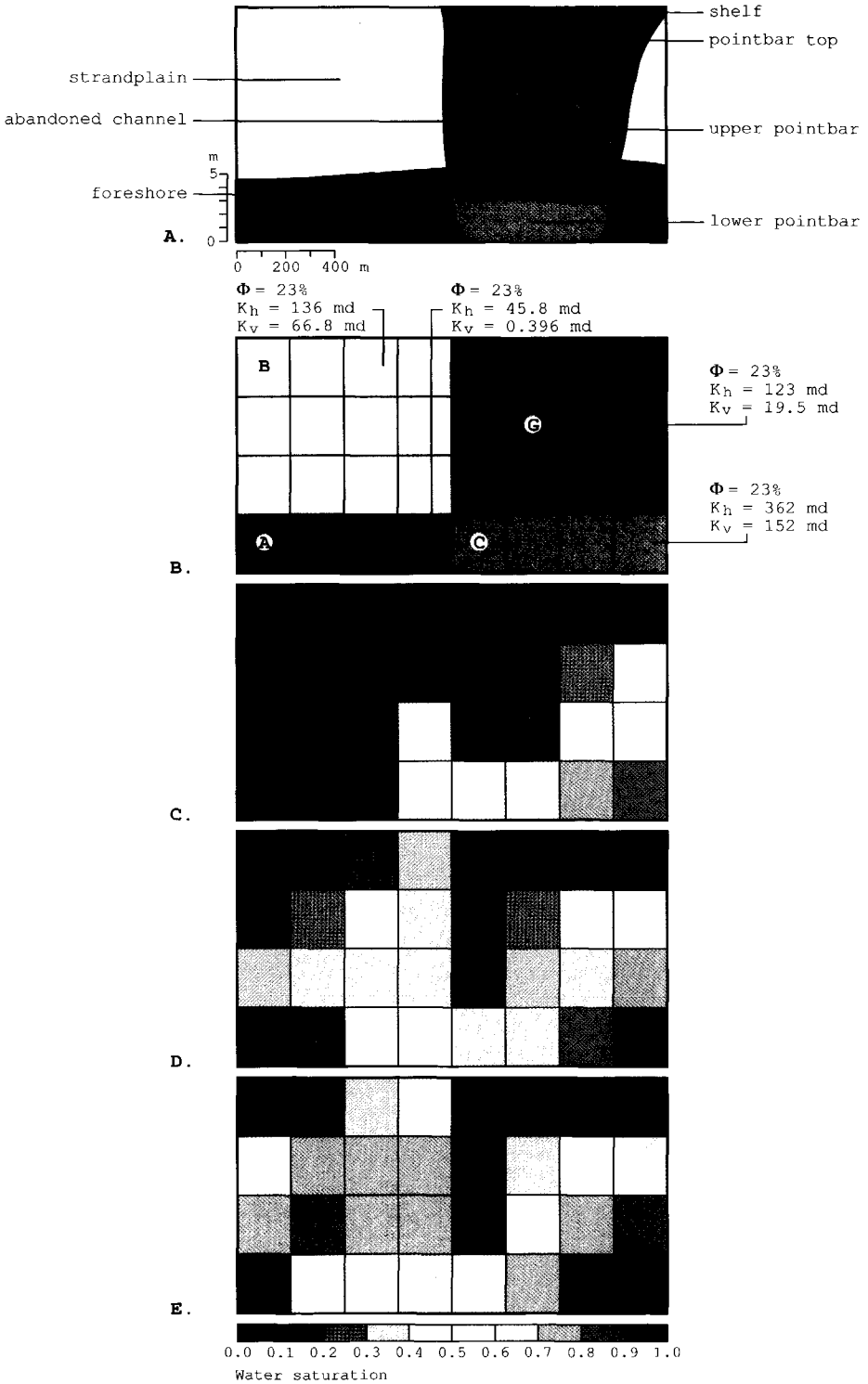

Figure 4.31 Waterflood through a wave dominated delta: A) geological model, B) simulation grid, C) t=500 days, D) t=1000 days, E) t=1500 days.

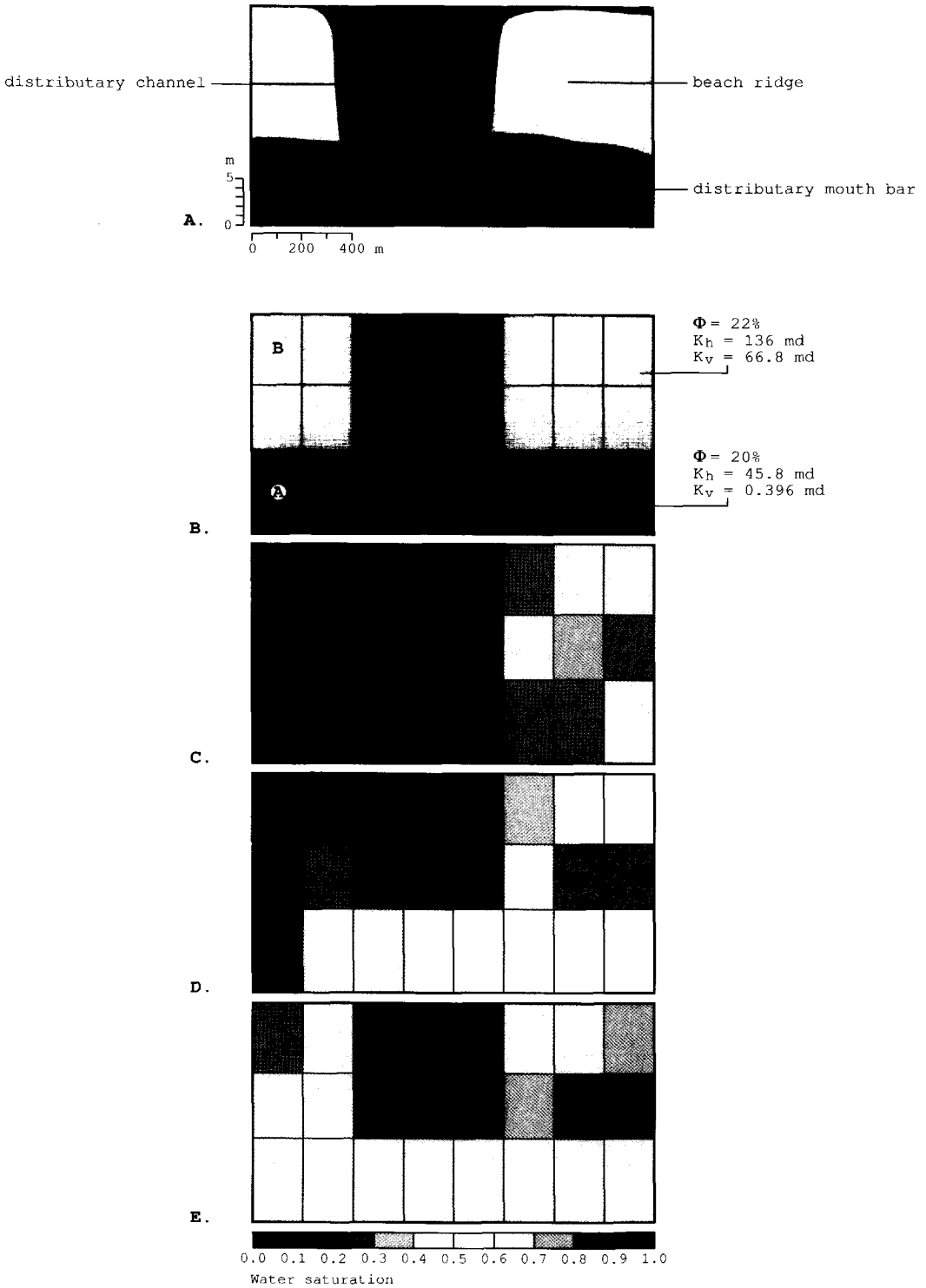

Figure 4.32 Waterflood through a delta with wave/current interaction: A) geological model, B) simulation grid, C) t=500 days, D) t=1000 days, E) t=1500 days.

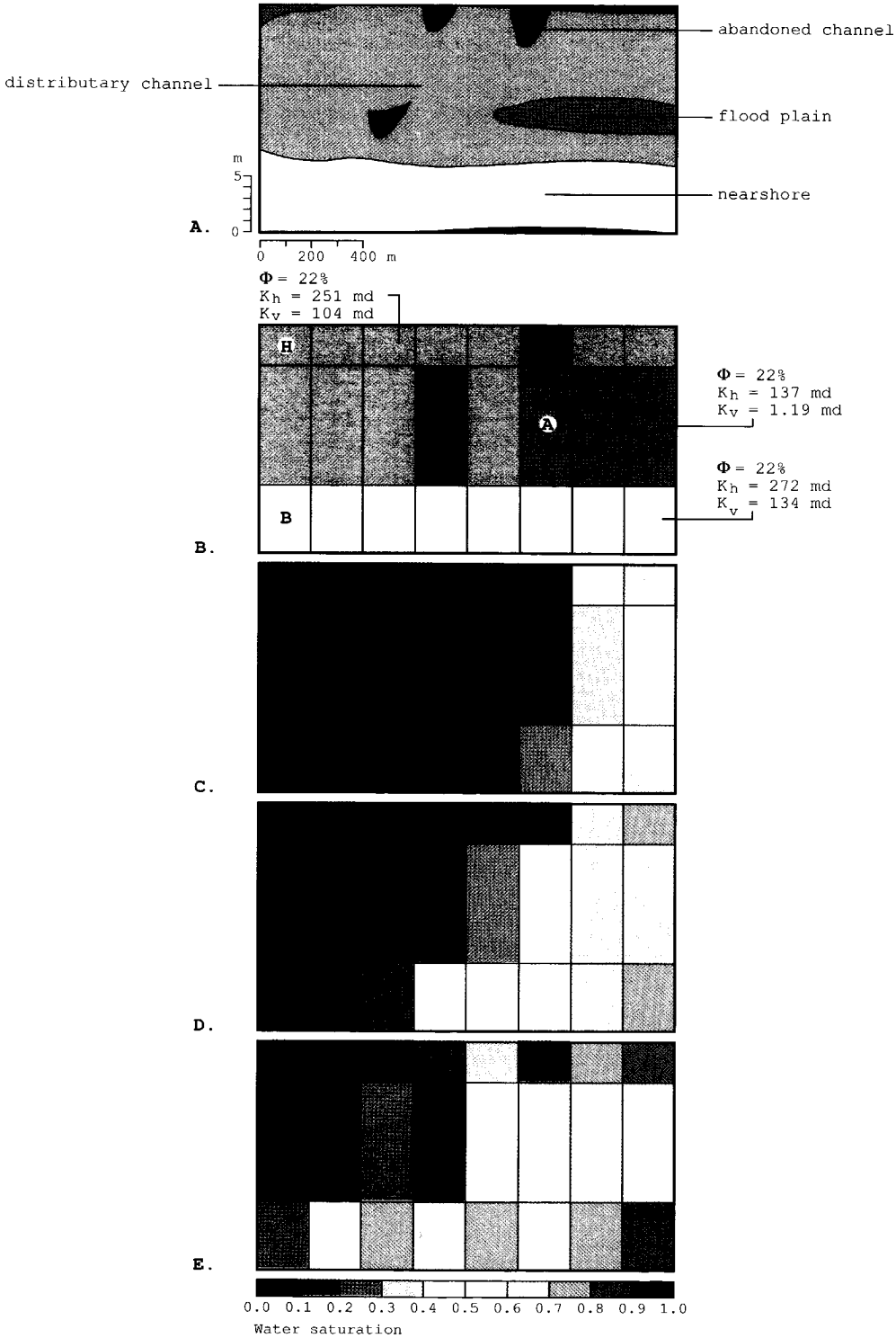

Figure 4.33 Waterflood through a fan delta: A) geological model, B) simulation grid, C) t=500 days, D) t=1000 days, E) t=1500 days.

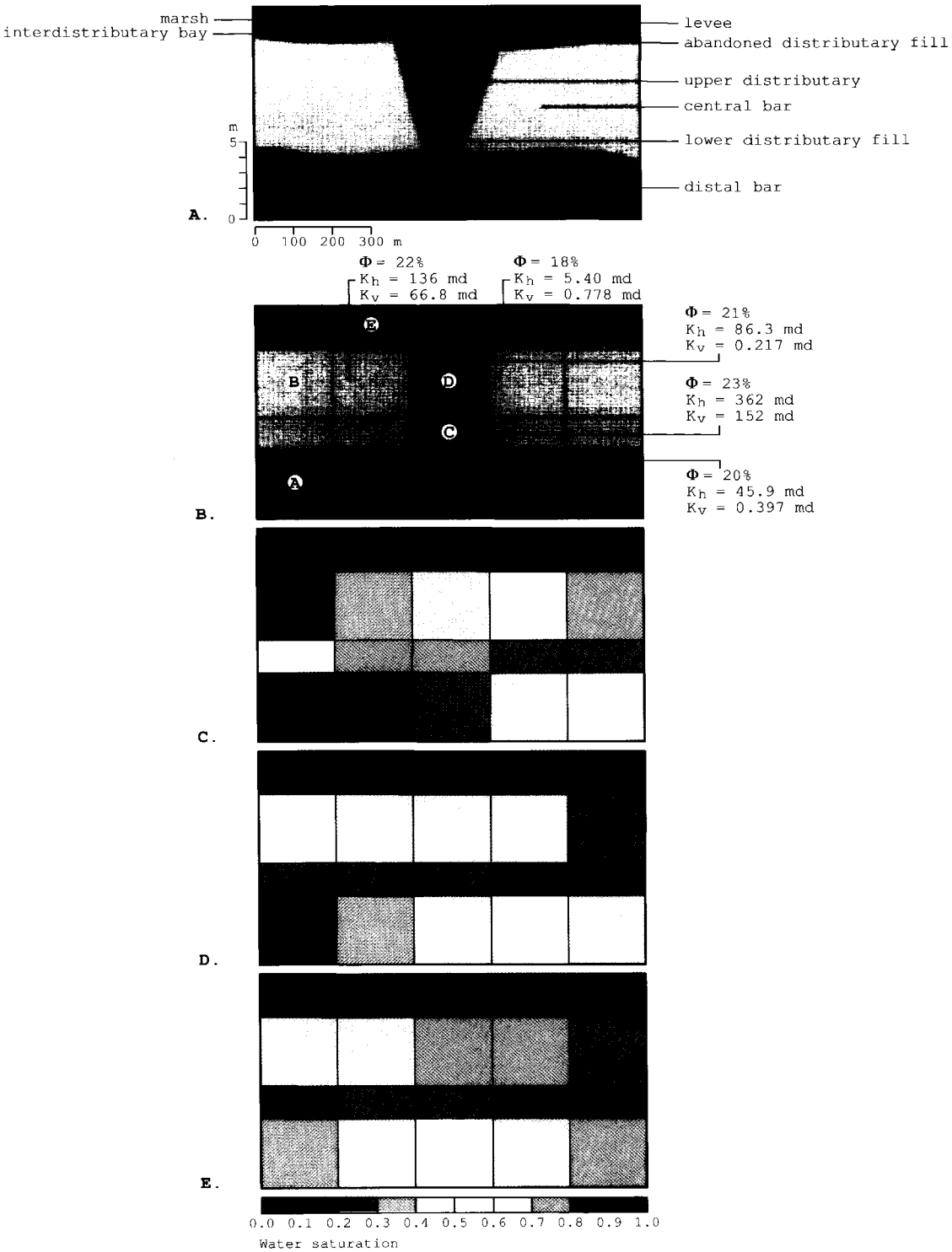

Figure 4.34 Waterflood through a lacustrine delta: A) geological model, B) simulation grid, C) t=500 days, D) t=1,000 days, E) t=1500 days.

zone consisting of tidal sand bar sediments is not drained as a result of the poor vertical permeabilities in this zone (Figure 4.29D). However, when the water front has reached the tidal flat sediments the flow is forced downwards resulting in an efficient sweep of the basal zone (Figure 4.29E).

The simulation results for deltas with fluvial/wave/tide interaction show an influx over the complete distributary channel interval (Figure 4.30A). Despite gravitational forces, the basal zone shows a less rapid influx than the upper parts of the distributary channel sequence. This is because the occurrence of intercalations of tidal flat sediments in the lower part of this sequence which block the flow and force it upward (Figure 4.30D). When the water front reaches the barrier bar sediments a rapid influx is visible in the barrier core sediments. The lower parts show little water influx, mainly as result of poor vertical permeabilities (Figure 4.30E).

Simulation of a waterflood in wave-dominated deltas shows that the main water flux is in the basal zone of the distributary channel (Figure 4.31C). This is because of the relatively poor horizontal permeabilities in the upper point bar sands of the distributary channel fill. These are characterized by inclined zones of poor permeability representing epsilon cross-bedding. Also the clay plugs representing the abandonment fill force the flow downward (Figure 4.31D). When the water front has a passed the channel plug the flow is forced upward as a result of the relatively poor permeabilities in the basal part of the strandplain sediments, resulting in a relatively good drainage of the upper strandplain deposits (Figure 4.31E).

In deltas with wave-current interaction the main inflow takes place in the beach ridge sediments (Figure 4.32C). When the water front reaches the distributary channel fill, the water is forced to flow through the distributary mouth bar sediments (Figure 4.32D). When it has passed the distributary channel fill some upward flow is visible. At t = 1500 days however, the upper part of the beach ridge is only partly drained (Figure 4.32E).

Waterflood simulation through the fan delta model shows that the main influx takes place in the basal and middle parts of the sequence (Figure 4.33C). Drainage of the middle zone is blocked when the water front reaches an abandoned channel plug (Figure 4.33D). In the upper part there is little water inflow. At t = 1500 days this part of the sequence is very badly drained (Figure 4.33E).

In lacustrine deltas a large influx of water takes place in the middle part of the sequence (Figures 4.34C and 4.34D). This zone is represented by Type B flow elements representing central bar sediments. At t = 1500 days the basal parts of the sequence are only partly drained, despite gravitational forces. This is caused by the poor vertical permeabilities in this zone (Figure 4.34E).

The results of the simulations of geological models of the most common delta types show that sedimentological heterogeneities have a large influence on the fluid flow. Most obvious in deltaic sequences are the occurrence of basal zones with poor vertical permeabilities resulting in only moderate drainage of these zones despite gravitational forces. On the other hand, many delta types contain clay plugs which force the water to flow into the poorly permeable basal zones.

4.5.5 DISCUSSION

The anisotropies given in this section are conceptual. My objective aim was to present a method for determining reservoir simulation parameters from a geological point of view. In actual cases, the properties derived in this chapter should be estimated via studies of the relevant reservoir. Also the sensitivity of the simulations should be tested by using a range of parameters commensurate with the uncertainties in the geological data.

Further refinements of this technique would probably yield ranges of rock parameters leading to specific anisotropy ranges. Three

dimensional simulations would have to be done, using the principles explained in this chapter, and the results would have to be tested against real reservoir data. Such anisotropy ranges would eliminate much unnecessary calculation and repetition for common cases.

The results obtained with the simulations through geological models of the most common delta types yield guidelines and considerations for proper evaluation of various completion lay-outs and production schemes for environments of deltaic deposition. Such simulations enable various production scenarios to be assessed, taking geological variability into account.

5. CONCLUSIONS

There are three main problems within reservoir characterization: 1) determining the geology from reservoir data, 2) describing the reservoir architecture, and 3) incorporating geological variability within numerical simulation grids.

The classification proposed by Coleman and Wright (1975) is the most appropriate for reservoir characterization because it characterizes the various delta types according to their vertical rock succession and sand distribution pattern. However, some adaptions are needed:

- Type 2 and 3 of Coleman and Wright can be combined, because they have very similar characteristics in terms of vertical facies succession and sand distribution pattern.

- Fan deltas and lacustrine deltas have to be included, because the sediments deposited in such deltaic settings can be important hydrocarbon reservoirs.

Reservoir data do often not yield sufficient information for an accurate description of the reservoir, because information from well logs and cores cannot be interpolated far into the interwell area and information from well tests and seismics is not detailed enough. Therefore, modelling techniques taking into account both reservoir data and geological knowledge have to be used to obtain an accurate description of the reservoir.

The case studies presented in the literature to date show that deterministic interpolation is possible when sufficient information is available on the formation structures. However, lateral homogeneity relative to the well spacing is essential for obtaining reliable results.

At the moment, geological process simulation is not very useful for describing reservoir architecture. Geological processes are often

very complex and are incompletely understood. This results in far too many input parameters and unreliable assumptions.

Papers dealing with sequence-based permeability modelling show that reliable results can only be obtained with 'large-scale' data (i.e. well test data). However, in the case of large-scale data a deterministic approach is more appropriate. With 'small-scale' data (i.e. data from wells) the use of sequence-based techniques for estimating permeability is limited, because of the small ranges of influence.

Sequence-based techniques used for modelling of lithofacies are better applicable. However, the range of influence still limits the use of these techniques to rocks that are relatively homogeneous in relation to the well spacing.

Object-based geostatistical techniques have the most potential for the modelling of reservoir architecture. However, at the moment often insufficient quantitative data are available on important geological phenomena to obtain a representative view of the reservoir architecture with such techniques.

Data-bases and knowledge bases must be created in order to fully use the potential of object-based modelling techniques. These data- and knowledge bases should contain quantitative geological information and should be based on areas where geological variation can be sampled adequately, such as outcrops, recent environments and densely drilled fields.

The three sedimentological parameters that are most important for fluid flow are sorting trend, sedimentary structures and baffles to flow. Based on these three parameters the 26 most common sandy genetic units occurring in deltaic systems can be represented by only eight typical flow unit configurations.

The most common baffles to flow that occur in sandy deltaic rocks are horizontal shales varying in length from 1 to 100 metres.

It is plausible that in histograms of shale lengths measured from outcrops one peak represents the average width and the other the length of the shales, when the shale lengths are measured arbitrary with respect to the shale bed orientation.

The most sophisticated model to calculate vertical permeabilities in sand/shale sequences to date is the one presented by Begg et al. (1985). However, their method underestimates effective permeabilities for small shale fractions. If there are few shales the introduction of a Poisson distribution and stochastic calculation of streamline lengths probably results in more reliable vertical permeabilities.

When using the method of Begg et al. (1985) it is not necessary to use three-dimensional models if the length/width ratio of the shales exceeds 3.

The methods of Haldorsen and Lake (1984), Begg and King (1985) and Begg et al. (1985) assume a blocky flow path. In the case of low shale fractions, this can result in an over-estimation of streamline lengths with a factor 2 and therefore in a significant underestimation of vertical permeability.

Comparison of the results of the method proposed in this thesis to calculate vertical permeabilities in bioturbated sand/shale sequences with numerical simulation results shows that the proposed method works well in case of high burrow densities.

6. RECOMMENDATIONS

Much work still needs to be done to improve the accuracy of simulator input parameters. Seven useful topics for further research are listed below:

- Developing an object-based modelling algorithm that is conditioned to geology.

- Developing a knowledge base containing quantitative geological information. This involves quantifying geological phenomena in areas where the variation of these phenomena can be adequately sampled, such as outcrops, recent environments and densely drilled fields.

- Establishing characteristic pseudo-parameters and pseudo-curves for the elementary flow elements using detailed outcrop and core data.

- Validating and refining the sedimentologically defined flow unit approach described in Chapter 4 by applying it in 3 dimensions to well studied reservoirs.

- Using three-dimensional models of the sedimentologically defined flow unit configurations to evaluate what is the minimal selected information that is sufficiently indicative for the overall permeability pattern within a flow unit.

- Extending the sedimentologically defined flow unit approach to other depositional environments.

- Extending the sedimentologically defined flow unit approach for application in multi-phase flow experiments.

NOMENCLATURE

A = permeability anisotropy

c = proportionality constant

d_x = number of grid blocks in the x direction

d_y = number of grid blocks in the y direction

d_z = number of grid blocks in the z direction

E = absolute percentage error

f = number of shales per metre [m^{-1}]

F_b = burrow fraction

F_s = shale fraction

H = vertical spacing of shales [m]

K = grid block permeability [m^2]

K_b = burrow permeability [m^2]

K_e = effective permeability [m^2]

K_h = horizontal permeability [m^2]

K_m = matrix permeability [m^2]

K_{mv} = vertical matrix permeability [m^2]

K_{mx} = matrix permeability in the x direction [m^2]

K_{my} = matrix permeability in the y direction [m^2]

K_s = shale permeability

K_v = vertical permeability [m^2]

K_{ve} = effective vertical permeability [m^2]

$(K_{ve})_{nw}$ = effective permeability of the non-wetting phase [m^2]

$(K_{ve})_w$ = effective permeability of the wetting phase [m^2]

L = half the distance between mid-points of two shales [m]

$\max(u)$ = maximum value of u

$\min(u)$ = minimum value of u

n = number of vertical barriers to flow

P = grid block pressures [Pa]

P_b = pressure at the bottom of the volume of rock under consideration [Pa]

p_s = number of stream tubes

P_t = pressure at the top of the volume of rock under consideration [Pa]

Q = flow rate [$m^3 \cdot s^{-1}$]

r = random number between 0 and 1

S = shale thickness [m]

s = stream tube length [m]

$\bar{s}$ = average flow path length parallel to one side of a shale [m]

t = percolation parameter

$\hat{u}$ = normalized value of u

u_1 = shale width [m]

u_2 = shale length [m]

v = number of layers

V_e = estimated value

V_t = measured value

X = width of a volume of rock [m]

Y = length of a volume of rock [m]

Z = height of a volume of rock [m]

Z_c = core length [m]

z = vertical coordinate

α = fractional aperture

γ = ratio of permeability barrier overlap to permeability barrier width

ΔP = pressure drop [Pa]

ΔX = width of a grid block [m]

ΔY = length of a grid block [m]

ΔZ = height of a grid block [m]

ΔZ_e = effective flow path length [m]

μ = viscosity [Pa·s]

$\xi(z)_i$ = sand fraction at z

ω = averaging power

Subscripts

i = shale index

j = location index in the x direction

k = location index in the y direction

q = stream tube index

l = layer index

REFERENCES

ALLEN, J.R.L. (1965) Late Quaternary Niger delta, and adjacent areas: sedimentary environments and lithofacies. *Bulletin of the American Association of Petroleum Geologists*, v. 49, p. 547-600.

ALLEN, J.R.L. (1970a) A quantitative model of grain size and sedimentary structures in lateral deposits. *Geological Journal*, **7**, 129-146.

ALLEN, J.R.L. (1970b) *Physical processes of sedimentation, An introduction*, 248 pp. Allen & Unwin, London.

ALLEN, J.R.L. (1978) Studies in fluviatile sedimentation: an exploratory quantitative model for avulsion-controlled alluvial suites. *Sedimentary Geology*, **21**, 129-147.

ALMON, W.R., FULLERTON, L.B. & DAVIES, D.K. (1976) Pore space reduction in Cretaceous sandstones through chemical precipitation of clay minerals. *Journal of Sedimentary Petrology*, **46**, 89-96.

ARNDORFER, D.J. (1973) Discharge patterns in two crevasses of the Mississippi delta. *Marine Geology*, **15**, 269-287.

AUGEDAL, H.O., OMRE, H. & STANLEY, K.O. (1986) SISABOSA, a program for stochastic modelling and evaluation of reservoir geology. Paper presented at the Seminar on Reservoir Description and Simulation held in Oslo, Norway, September 3-5.

BATES, C.C. (1953) Rational theory of delta formation. *Bulletin of the American Association of Petroleum Geologists*, **37**, 2119-2162.

BEARD, D.C. & WEYL, P.K. (1973) Influence of texture on porosity and permeability of unconsolidated sand. *Bulletin of the American Association of Petroleum Geologists*, **57**, 349-369.

BEGG, S.H., CHANG, D.M. & HALDORSEN, H.H. (1985) A simple statistical method for calculating the effective permeability of a reservoir containing discontinuous shales. Paper presented at the 60th Annual Technical Conference and Exhibition of the Society of Petroleum Engineers held in Las Vegas, Nevada, September 22-25.

BEGG, S.H. & KING, P.R. (1985) Modelling the effects of shales on reservoir performance: Calculation of effective vertical permeability. Paper presented at the Society of Petroleum Engineers 1985 Reservoir Simulation Symposium held in Dallas, Texas, February 10-13.

BELT, E.S. (1975) Scottish Carboniferous cyclothem patterns and their palaeoenvironmental significance. In *Deltas, models for exploration* (Ed. by M.L. Broussard), pp. 427-449. Houston, Houston Geological Society, Houston.

BERG, R.R. (1986) *Reservoir Sandstones*, 481 pp. Prentice-Hall, New Jersey.

BERNARD, H.A. (1965) A resumé of river delta types. *Bulletin of the American Association of Petroleum Geologists* (Abs.), **49**, 334-335.

BEUF, S., BIJU-DUVAL, B., DE CHARPAL, O., ROGNON, P., GARIEL, O. & BENNACEF, A. (1971) *Les grès du Paléozoïque inférieur au Sahara. Sédimentation et discontinuités évolution structurale d'un craton*, 465 pp. Publication du Institute Français du Pétrole **18**, Rueil Malmaison Cedex.

BLATT, H., MIDDLETON, G.V. & MURRAY, R.C. (1980) *Origin of Sedimentary Rocks* (2nd ed.), 766 pp. Prentice-Hall, New Jersey.

BONHAM-CARTER, G.F. & SUTHERLAND, A.J. (1968) *Mathematical model and FORTRAN IV program for computer simulation of deltaic sedimentation*, 55 pp. Kansas Geological Survey Computer Contributions **24**, Kansas.

BRIDGE, J.S. (1979) A FORTRAN IV program to simulate alluvial stratigraphy. *Computers and Geosciences*, **5**, 335-348.

BRIDGE, J.S. & LEEDER, M.R. (1979) A simulation model of alluvial stratigraphy. *Sedimentology*, **26**, 617-644.

BROWN, S. (1984) Jurassic. In *Introduction to the Petroleum Geology of the North Sea* (Ed. by K.W. Glennie), pp. 103-132. Blackwell, Oxford.

BRUMMERT, A.C., POOL, S.E., PORTMAN, M.E., HANOCK, J.S. & AMMER, J.R. (1989) Determining optimum estimation methods for interpolation and extrapolation of reservoir properties: A case study. Paper presented at the 64th Annual Technical Conference and Exhibition of the Society of Petroleum Engineers held in San Antonio, Texas, October 8-11.

BRYDGES, W.T., GULATI, S.T. & BAUM, G. (1975) Permeability of glass ribbon-reinforced composites. *Journal Material Sciences*, **10**, 2044-2049.

BURKE, K., DESSAUVAGIE, T.F.J. & WHITEMAN, A.J. (1971) Opening of the Gulf of Guinea and geological history of the Benue Depression and Niger delta. *Nature*, **233**, 51-55.

CHIRLIN, G.R. (1985) Flow through a porous medium with periodic barriers to flow or fractures. *Society of Petroleum Engineers Journal*, **25**, 358-362.

COATS, K.H., DEMPSEY, J.R. & HENDERSON, J.H. (1971) The use of vertical equilibrium in two-dimensional simulation of three-dimensional reservoir performance. *Society of Petroleum Engineers Journal*, **11**, 136-144.

COLEMAN, J.M. (1969) Brahmaputra river: Channel processes and sedimentation. *Sedimentary Geology*, **3**, 129-239.

COLEMAN, J.M. (1981) *Deltas: Processes and models of deposition for exploration*, 124 pp. Burgess Publication Company, CEPCO Division, Minneapolis.

COLEMAN, J.M. & GAGLIANO, S.M. (1964) Cyclic sedimentation in the Mississippi river deltaic plain. *Transactions of the Gulf Coast Association of Geological Societies*, **14**, 67-80.

COLEMAN, J.M., GAGLIANO, S.M. & SMITH, W.G. (1970) Sedimentation in a Malaysian high tide tropical delta. In *Deltaic Sedimentation: Modern and Ancient* (Ed. by J.P. Morgan and J.P. Shaver), pp. 185-197. Society of Economic Palaeontologists and Mineralogists Special Publication **15**, Tulsa.

COLEMAN, J.M. & PRYOR, D.B. (1981) Deltaic environments of deposition. In *Sandstone Depositional Environments* (Ed. by P.A. Scholle and D. Spearing), pp. 139-178. American Association of Petroleum Geologists Memoir **31**, Tulsa.

COLEMAN, J.M., SUHAYDA, J.N., WHELAN, T. & WRIGHT, L.D. (1974) Mass movement of Mississippi delta sediments. *Transactions of the Gulf Coast Association of Geological Societies*, **24**, 49-68.

COLEMAN, J.M. & WRIGHT, L.D. (1975) Modern River deltas: Variability of processes and sand bodies. In *Deltas, models for exploration* (Ed. by M.L. Broussard), pp. 99-149. Houston Geological Society, Houston.

CORSMIT, J., VERSTEEG, W.H., BROUWER, J.H. & HELBIG, K. (1987) High resolution 3D reflection seismics on a tidal flat: acquisition, processing and interpretation. *First Break*, **6**, 9-23.

CRAMER, P.W. (1988) Reservoir development using offset VSP techniques in the Denver-Julesberg basin. *Journal of Petroleum Technology*, **40**, 197-205.

CROSS, T.A. (1991) Field-scale reservoir characterization. In *Reservoir Characterization II* (Ed. by L.W. Lake, H.B. Carroll and T.C. Wesson), pp. 493-496. Academic Press, Orlando.

CURRAY, J.R., EMMEL, F.J., & CRAMPTON, P.J.S. (1969) Holocene history of a strandplain, lagoonal coast, Nayarit, Mexico. In *Coastal Lagoons: A Symposium* (Ed. by A.A. Castañares and F.B. Phleger), pp. 63-100. Universidad Nacional Autonoma, Mexico.

DA COSTA E SILVA, A.J. (1984) A new approach to the characterization of reservoir heterogeneities based on the geomathematical model and kriging technique. Paper presented at the 60th Annual Technical Conference and Exhibition of the Society of Petroleum Engineers held in Las Vegas, Nevada, September 22-25.

DALZIEL, I.W.D., DE WIT, H.J. & PALMER, R.F. (1974) A fossil marginal basin in the Southern Andes. *Nature*, **250**, 291-294.

DELHOMME, A.E.K. & GIANNESINI, J.F. (1979) New reservoir techniques improve simulation results in Hassi-Messaoud field - Algeria. Paper presented at the 54th Annual Fall Technical Conference and Exhibition of the Society of Petroleum Engineers held in Las Vegas, Nevada, September 23-26.

DESBARATS, A.J. (1987). Numerical estimation of effective permeability in sand-shale formations. *Water Resources Research*, **23**, 273-286.

DEUTSCH, C. (1989) Calculating effective permeabilities in sandstone/shale sequences. *Society of Petroleum Engineers Formation Evaluation*, **4**, 343-348.

DICKINSON, G. (1953) Geological aspects of abnormal reservoir pressures in Gulf Coast, Louisiana. *Bulletin of the American Association of Petroleum Geologists*, **37**, 410-432.

DICKINSON, W.R., BEARD, L.S., BRACKENRIDGE, G.R., ERJAVEC, J.L., FERGUSON, R.C., INMAN, K.F., KNEPP, R.A., LINDBERG, F.A. & RYBERG, P.T. (1983) Provenance of North American Phanerozoic sandstones in relation to tectonic setting. *Bulletin of the Geological Society of America*, **94**, 222-235.

DICKINSON, W.R. & SUCZEK, C.A. (1979) Plate tectonics and sandstone composition. *Bulletin of the American Association of Petroleum Geologists*, **63**, 2164-2182.

DICKINSON, W.R. & VALLONI, R. (1980) Plate setting and provenance of sands in modern ocean basins. *Geology*, **8**, 82-86.

DONALDSEN, A.C., MARTIN, R.H. & KANES, W.H. (1970) Holocene Guadeloupe delta of the Texas Gulf Coast. In *Deltaic Sedimentation: Modern and Ancient* (Ed. by J.P. Morgan and J.P. Shaver), pp. 107-137. Society of Economic Palaeontologists and Mineralogists Special Publication **15**, Tulsa.

DREYER, T., SCHEIE, A. & WALDERHAUG, O. (1990) Mini-permeameter based study of permeability trends in channel sand bodies. *Bulletin of the American Association of Petroleum Geologists*, **74**, 359-374.

DUBRULE, O. (1989) A review of stochastic models for petroleum reservoirs. In *Geostatistics (Volume 2)* (Ed. by M. Amstrong), pp. 493-506. Kluwer, Dordrecht.

DUBRULE, O. & HALDORSEN, H.H. (1986) Geostatistics for permeability estimation in reservoir characterization. In *Reservoir Characterization* (Ed. by L.W. Lake, L.W. and H.B. Carroll H.B.), pp. 223-248. Academic Press, Orlando.

DUPUY, M. & LEFEBVRE DU PREY, E. (1968) L'anisotrpie d'écoulement en milieu poreux présentant des intercalations horizontales discontinues. *Communication Troisième Colloque de l'A.R.T.F.P.*, **33**, 643-676.

ELLIOTT, T. (1974) Interdistributary bay sequences and their genesis. *Sedimentology*, **21**, 611-622.

ELLIOTT, T. (1986) Deltas. In *Sedimentary environments and facies* (2nd ed.) (Ed. by H.G. Reading), pp. 113-154. Blackwell, Oxford.

ETHRIDGE, F.G. (1970) *Quantitative petrographic criteria for recognition of environments of deposition*, 169 pp. Ph.D. Thesis, Texas A & M University, College Station.

FISHER, W.L., BROWN, L.F., SCOTT, A.J. & MCGOWEN, J.H. (1969) *Delta systems in the exploration for oil and gas: A research colloquium*, 210 pp. Bureau of Economic Geology, University of Texas at Austin, Austin.

FISK, H.N. (1961) Bar-finger sands of Mississippi delta. In *Geometry of sandstone bodies - A symposium* (Ed. by J.A. Peterson and J.C. Osmond), pp. 29-52. American Association of Petroleum Geologists, Tulsa.

FLINT, S.S., VAN ROSSEM, S.J. & WILLIAMS, H. (1989) Quantitative outcrop analysis of coastal plain sequences from eastern

Kentucky: Example of high quality data input to three dimensional reservoir modelling (Abs.). *Bulletin of the American Association of Petroleum Geologists*, **73**, 356.

FLORIS, F.J.T. (in prep.) *Two-phase flow of newtonian and non-newtonian fluids in a porous medium applied to water coning.* Ph.D. Thesis, Delft University of Technology, Delft.

FÜCHTBAUER, H. (1967a) Der Einfluss des Ablagerungsmilieus auf die Sandsteindiagenese im mittleren Buntsandstein. *Sedimentary Geology*, **1**, 159-179.

FÜCHTBAUER, H. (1967b) Influence of different types of diagenesis on sandstone porosity. *Proceedings of the 7th World Petroleum Congress Mexico*, **2**, 353-369.

FÜCHTBAUER, H. (1974) Zur Diagenese fluviatiler Sandsteine. *Geologische Rundschau*, **63**, 904-925.

GALLAGHER, J.G., JR. (1991) Maximum entropy litho-porosity volume fraction predictions from Vp/Vs ratio measurements. In *Reservoir Characterization II* (Ed. by L.W. Lake, H.B. Carroll and T.C. Wesson), pp. 382-401. Academic Press, Orlando.

GALLOWAY, W.E. (1975) Process framework for describing morphologic and stratigraphic evolution of deltaic depositional systems. In *Deltas, Models for Exploration* (Ed. by M.L. Broussard), pp. 87-98. Houston Geological Society, Houston.

GALLOWAY, W.E. & CHENG (1985) *Reservoir facies architecture in a microtidal barrier system - Frio Formation, Texas Gulf Coast*, 36 pp. Bureau of Economic Geology, The University of Texas at Austin Report of Investigations **144**, Austin.

GALLOWAY, W.E. & HOBDAY, D.K. (1983) *Terrigeneous Clastic Depositional Environments*, 423 pp. Springer-Verlag, New York.

GEEHAN, G.W., LAWTON, T.F., SAKURAI, S., KLOB, H.K., CLIFTON, T.R., INMAN, K.F. & NITZBERG, K.E. (1986) Geologic prediction of shale continuity, Prudhoe Bay field. In *Reservoir Characterization* (Ed. by L.W. Lake and H.B. Carroll, Jr.), pp. 63-82. Academic Press, Orlando.

GEEHAN, G. & UNDERWOOD, J. (1990) The use of length distributions in geological modelling. Paper presented at the 13th International Sedimentological Congress held in Nottingham, UK, August 26-31.

GOGGIN, D.J., CHANDLER, M.A., KOCUREK, G. & LAKE, L.W. (1988) Patterns of permeability in aeolian deposits: Page sandstone (Jurassic),

northeastern Arizona. *Society of Petroleum Engineers Formation Evaluation*, **4**, 287-306.

GUÉRILLOT, D., RUDKIEWICZ, J.L., RAVENNE, C., RENARD, G. & GALLI, A. (1990) An integrated model for computer aided reservoir description: from outcrop study to fluid flow simulations. *Revue de l'Institut Français du Pétrole*, **45**, 71-77.

GUGGENHEIM, E.A. (1967) *Thermodynamics* (5^{th} ed.), 390 pp. Elsevier, Amsterdam.

HAAK, A.M. & ELEWAUT, E.F.M. (1990) Hybrid modelling of heterogeneity to improve 3-D simulation results: Case studies 1 and 2 on a North Sea gas field. In *North Sea Oil & Gas Reservoirs-II* (Ed. by A.T. Buller, E. Berg, O. Hjelmeland, J. Kleppe, O. Torsaeter and J.O. Aasen), 415-424. Graham & Trotman, London.

HALDORSEN, H.H. (1983) *Reservoir characterization procedures for numerical simulation*, 556 pp. Ph.D. Thesis, University at Austin, Austin.

HALDORSEN, H.H. (1986) Simulator parameter assignment and the problem of scale in reservoir engineering. In *Reservoir characterization* (Ed. by L.W. Lake and H.B. Carroll Jr.), pp. 293-340. Academic Press, Orlando.

HALDORSEN, H.H. (1989) On the modelling of vertical permeability barriers in single-well simulation models. *Society of Petroleum Engineers Formation Evaluation*, **4**, 349-358.

HALDORSEN, H.H., BRAND, P.J. & MACDONALD, C.J. (1988) Review of the stochastic nature of reservoirs. In *Mathematics in Oil Production* (Ed. by S. Edwards and P.R. King), pp. 109-210. Claredon, Oxford.

HALDORSEN, H.H. & LAKE, L.W. (1984) A new approach to shale management in field-scale models. *Society of Petroleum Engineers Journal*, **24**, 447-457.

HARBAUGH, J.W. & WAHLSTEDT, W.J. (1967) *FORTRAN IV Program for mathematical simulation of marine sedimentation with IBM 7040 and 7094 computers*, 40 pp. Kansas Geological survey Computer Contributions **9**, Kansas.

HAZEU, G.J.A., KRAKSTAD, O.S., RIAN, D.T. & SKAUG, M. (1988) The application of new approaches for shale management in a three-dimensional study of the Frigg field. *Society of Petroleum Engineers Formation Evaluation*, **3**, 493-501.

HERODOTUS (454 B.C.) *The histories of Herodotus of Halicarnasus* (Translation by H. Carter, 1962), 617 pp. Oxford University Press, Oxford.

HOLMES, A (1965) *Principles of Physical Geology*, 1288 pp. Ronald Press, New York.

HYNE, N.J., COOPER, W.A. & DICKEY, P.A. (1979) Stratigraphy of intermontane, lacustrine delta, Catatumbo River, Lake Maracaibo, Venezuela. *Bulletin of the American Association of Petroleum Geologists*, **63**, 2042-2057.

INMAN, D.L. & NORDSTROM, C.E. (1971) On the tectonic and morphologic classification of coasts. *Journal of Geology*, **79**, 1-21.

JOHNSON, H.D. & KROL, D.E. (1984) Geological modelling of a heterogeneous sandstone reservoir: Lower Jurassic Statfjord Formation, Brent Field. Paper presented at the 55th Annual Technical Conference and Exhibition, held in Houston, Texas, September 16-19.

JOHNSON, M.J. (1990) Tectonic versus chemical-wheatering controls on the composition of fluvial sands in tropical environments. *Sedimentology*, **37**, 713-726.

KAASSCHIETER, E.F. (1990) *Preconditioned conjugate gradients and mixed-hybrid finite elements for the solution of potential flow problems*, 151 pp. Ph.D. Thesis, Delft University of Technology, Delft.

KANES, W.H. (1970) Facies development of the Colorado river delta in Texas. In *Deltaic Sedimentation: Modern and Ancient* (Ed. by J.P. Morgan and J.P. Shaver), pp. 78-106. Society of Economic Palaeontologists and Mineralogists Special Publication **15**, Tulsa.

KITTRIDGE, M.G., LAKE, L.W., LUCIA, F.J., AND FOGG, G.E. (1989) Outcrop-subsurface comparisons of heterogeneity in the San Andres Formation. Paper presented at the 64th Annual Technical Conference and Exhibition of the Society of Petroleum Engineers held in San Antonio, Texas, October 8-11.

KORTEKAAS, T.F.M. (1985) Water/oil displacement characteristics in cross-bedded reservoir zones. *Society of Petroleum Engineers Journal*, **25**, 917-926.

KRAUS. M.J. & MIDDLETON, L.T. (1987) Contrasting architecture of two alluvial suites in different structural setting. In *Recent*

developments in fluvial sedimentology (Ed. by F.G. Ethridge, R.M. Flores and M.D. Harvey), pp. 253-262.

KRIGE, D.G. (1951) A statistical approach to some basic mine valuation problems on the Witwatersrand. *Journal of Chemical Metallurgy and Mining Society of South Africa*, **52**, 119-138.

KYTE, J.R. & BERRY, D.W. (1975) New pseudo functions to control numerical dispersion. *Society of Petroleum Engineers Journal*, **15**, 269-276.

LAKE, L.W. & CARROLL, H.B., JR. (Eds) (1986) *Reservoir Characterization*, 659 pp. Academic Press, Orlando.

LAKE, L.W., KASAP, E. & SHOOK, M. (1990) Pseudofunctions - The key to practical use of reservoir description. In *North Sea Oil and Gas Reservoirs - II* (Ed. by A.T. Buller, E. Berg, O. Hjelmeland, J. Kleppe, O. Torsaeter and J.O. Aasen), 297-308. Graham & Trotman, London.

LASSETER, T.J., WAGONNER, J.R. & LAKE, L.W (1986) Reservoir heterogeneities and their influence on ultimate recovery. In *Reservoir characterization* (Ed. by L.W. Lake and H.B. Carroll Jr.), pp. 545-560. Academic Press, Orlando.

LAWSON, D.A. (1991) Interwell geology from geophysical data. In *Reservoir Characterization II* (Ed. by L.W. Lake, H.B. Carroll and T.C. Wesson), pp. 442-459. Academic Press, Orlando.

LEEDER, M.R. (1978) A quantitative stratigraphic model for alluvium with special reference to channel deposit density and interconnectedness. In *Fluvial Sedimentology* (Ed. by A.D. Miall), pp. 587-596. Canadian Association of Petroleum Geologists Memoir **5**, Calgary.

LOWRY, P. & RAHEIM, A. (1991) Characterization of delta front sandstones from a fluvial dominated delta system. In *Reservoir Characterization II* (Ed. by L.W. Lake, H.B. Carroll and T.C. Wesson), pp. 665-676. Academic Press, Orlando.

MACGOWEN, J.H. (1970) *Gum Hollow fan delta, Nueces bay, Texas*, 91 pp. Bureau of Economic Geology, University of Texas at Austin, Report of Investigation **69**, Austin.

MACPHERSON, J.G. & MILLER, D.D. (1990) A subsurface study of fluvial sand-body geometries and connectedness (Abs.). In *13th International Sedimentological Congress: Abstracts - Papers*, pp. 349-350. International Association of Sedimentologists, Utrecht.

MARTIN, J.H. & COOPER, J.A. (1984) An integrated approach to the modelling of permeability barrier distribution in a sedimentological complex reservoir. Paper presented at the 59th Annual Technical Conference and Exhibition of the Society of Petroleum Engineers held in Houston, Texas, September 16-19.

MARTIN, J.H. & EVANS, P.F. (1988) Reservoir modelling of marginal aeolian/sabkha facies, southern North Sea (U.K. Sector). Paper presented at the 63rd Annual Technical Conference and Exhibition of the Society of Petroleum Engineers held in Houston, Texas, October 2-5.

MAST, R.F. & POTTER, P.E. (1963) Sedimentary structures, sand shape fabrics, and permeability: II. *Journal of Geology*, **71**, 448-565.

MATHERON, G. 1963 Principles of geostatistics. *Economic Geology*, **58**, 1246-1266.

MATHERON, G., BEUCHER, H., DE FOUQUET, C., GALLI, A., GUÉRILLOT, D. & RAVENNE, C. (1987) Conditional simulation of the geometry of fluvio-deltaic reservoirs. Paper presented at the 62nd Annual Technical Conference and Exhibition of the Society of Petroleum Engineers held in Dallas, Texas, September 27-30.

MAYNARD, J.B. (1984) Composition of plagioclase feldspar in modern deep-sea sands: relationship to tectonic setting. *Sedimentology*, **31**, 713-726.

MECKEL, L.D. (1975) Holocene sand bodies in the Colorado delta area, northern Gulf of California. In *Deltas, Models for Exploration* (Ed. by M.L. Broussard), pp. 239-265. Houston Geological Society, Houston.

MIDDLETON, G.V. & SOUTHARD, J.B. (1978) *Mechanics of Sediment Movement*, 246 pp. Society of Economic Palaeontologists and Mineralogists Short Course **3**, Tulsa.

MINTER, W.E.L. (1978) A sedimentological synthesis of placer gold, uranium and pyrite concentrations in Proterozoic Witwatersrand sediments. In *Fluvial Sedimentology* (Ed. by A.D. Miall), pp. 801-829. Canadian Association of Petroleum Geologists Memoir **5**, Calgary.

MONDT, J.C. (1990) The use of dip and azimuth horizon attributes in 3D seismic interpretation. Paper presented at EUROPEC 90 held in The Hague, The Netherlands, October 22-24.

MOORE, T.C. & SCRUTTON, P.C. (1957) Minor internal structures of some recent unconsolidated sediments. *Bulletin of the American Association of Petroleum Geologists*, **41**, 2723-2751.

MORGAN, J.P. & MCINTIRE, W.G. (1959) Quaternary geology of the Bengal Basin, East Pakistan and India. *Bulletin of the Geological Society of America*, **70**, 319-342.

NAGTEGAAL, P.J.C. (1978) Sandstone-framework instability as a function of burial diagenesis. *Journal of the Geological Society of London*, **135**, 102-105.

NAMI, M. & LEEDER, M.R. (1978) Changing channel morphology and magnitude in the Scalby Formation (M. Jurassic of Yorkshire, England. In *Fluvial Sedimentology* (Ed. by A.D. Miall), pp. 431-440. Canadian Association of Petroleum Geologists Memoir **5**, Calgary.

NEASHAM, J.W. (1977) The morphology of dispersed clay in sandstone reservoirs and its effect on sandstone shaliness, pore space and fluid flow properties. Paper presented at the 52nd Annual Fall Technical Conference and Exhibition of the Society of Petroleum Engineers of the American Institute of Mining, Metallurgical, and Petroleum Engineers, Inc. held in Denver, Colorado, October 9-12.

NORTH, F.K. (1985) *Petroleum Geology*, 607 pp. Allen & Unwin, London.

OOMKENS, E. (1970) Depositional environments and sand distribution in the post-glacial Rhône delta complex. In *Deltaic Sedimentation: Modern and Ancient* (Ed. by J.P. Morgan and J.P. Shaver), pp. 198-212. Society of Economic Palaeontologists and Mineralogists Special Publication **15**, Tulsa.

OOMKENS, E. (1974) Lithofacies relationships in the Late Quaternary Niger delta complex. *Sedimentology*, **21**, 195-222.

PANNEKOEK, A.J. (1973) Verwering en bodemvorming. In *Algemene Geologie* (Ed. by A.J. Pannekoek), pp. 179-202. Tjeenk Willink, Groningen.

PAULSSON, B.N.P. (1991) Cross well seismology - A toll for reservoir geophysics. In *Reservoir Characterization II* (Ed. by L.W. Lake, H.B. Carroll and T.C. Wesson), pp. 460-477. Academic Press, Orlando.

PELT, E.J. (1990) *A review of the modelling techniques for the prediction of reservoir architecture and reservoir properties*, 68 pp. M.Sci. Thesis, Delft University of Technology, Delft.

PETTIJOHN, F.J., POTTER, P.E. & SIEVER, R. (1987) *Sand and Sandstone* (2nd ed.), 553 pp. Springer-Verlag, New York.

POTTER, P.E. (1984) South America modern beach sand and plate tectonics. *Nature*, **311**, 493-501.

PRATS, M. (1972) The influence of oriented arrays of thin impermeable shale lenses or of highly conductive natural fractures on apparent permeability anisotropy. *Journal of Petroleum Technology*, **22**, 1219-1221.

PRYOR, W.A. (1973) Permeability-porosity patterns and variations in some Holocene sand bodies. *Bulletin of the American Association of Petroleum Geologists*, **57**, 162-189.

QUINT, E.N.M. (1990) Improving lateral and vertical resolution in geotomography. Paper presented at EUROPEC 90 held in The Hague, The Netherlands, October 22-24.

RAILROAD COMMISSION OF TEXAS (1983) *Annual report of the Oil and Gas Division for 1982*, 733 pp. Railroad Commission of Texas, Austin.

RAVENNE, C, & BEUCHER, H. (1988) Recent developments in description of sedimentary bodies in a fluvio-deltaic reservoir and their 3D conditioned simulation. Paper presented at the 63rd Annual Technical Conference and Exhibition of the Society of Petroleum Engineers held in Houston, Texas, October 2-5.

RAVENNE, C., ESCHARD, R., GALLI, A., MATHIEU, Y., MONTADERT, L., AND RUDKIEWICZ, J.L. (1989) Heterogeneities and geometry of sedimentary bodies in a fluvio-deltaic reservoir. *Society of Petroleum Engineers Formation Evaluation*, **5**, 239-246.

ROBERTSON, J.D. (1991) Reservoir management using 3-D seismic data. In *Reservoir Characterization II* (Ed. by L.W. Lake, H.B. Carroll and T.C. Wesson), pp. 340-354. Academic Press, Orlando.

ROSE, W. (1983) A note on the role played by sediment bedding in causing permeability anisotropy. *Journal of Petroleum Technology*, **35**, 330-332.

ROZENDAL, S. (1989) Numerieke experimenten met modellen voor de bepaling van de effectieve verticale permeabiliteit op basis van stroomlijnlengtes, 60 pp. M.Sci. thesis, Delft University of Technology, Delft.

SCHMIDT, V. & MACDONALD, D.A. (1979a) The role of secondary porosity in the course of sandstone diagenesis. In *Aspects of Diagenesis* (Ed. by P.A. Scholle and P.R. Schluger), pp. 175-207. Society of

Economic Palaeontologists and mineralogists Special Publication **26**, Tulsa.

SCHMIDT, V. & MACDONALD, D.A. (1979b) Texture and recognition of secondary porosity in sandstones. In *Aspects of Diagenesis* (Ed. by P.A. Scholle and P.R. Schluger), pp. 209-225. Society of Economic Palaeontologists and mineralogists Special Publication **26**, Tulsa.

SCHUILING, R.O., DE MEYER, R.J., RIEZEBOS, H.J. & SCHOLTEN, M.J. (1985) Grain size distributions of different minerals in a sediment as a function of their specific density. *Geologie en Mijnbouw*, **64**, 199-203.

SEILACHER, A. (1967) Bathymetry of trace fossils. *Marine Geology*, **5**, 413-128.

SHEPERD, R.G. (1987) Lateral accretion surfaces in ephemeral-stream point bars, Rio Puerco, New Mexico. In *Recent developments in fluvial sedimentology* (Ed. by F.G. Ethridge, R.M. Flores and M.D. Harvey), pp. 93-98.

SILVA, R.J., NIKO, H. & VAN DEN BERGH, J.N. (1988) Numerical modelling of gas and water injection in a geologically complex volatile oil reservoir in the Lake Maracaibo area, Venezuela. Paper presented at the 63rd Annual Technical Conference and Exhibition of the Society of Petroleum Engineers held in Houston, Texas, October 2-5.

SLATT, R.M. & HOPKINS, G.L. (1990) Scaling geologic reservoir description to engineering needs. *Journal of Petroleum Technology*, **42**, 202-210.

SNEIDER, R.M., RICHARDSON, F.H., PAYNTER, D.D., EDDY, R.E. & WYANT, I.A. (1977) Predicting reservoir rock geometry and continuity in Pennsylvanian reservoirs, Elk City Field, Oklahoma. *Journal of Petroleum Geology*, **29**, 851-866.

SNEIDER, R.M., TINKER, C.N. & MECKEL, J.D. (1978) Deltaic environment reservoir types and their characteristics. *Journal of Petroleum Technology*, **30**, 1538-1546.

STALKUP, F.I. (1986) Permeability variations observed at the faces of cross-bedded sandstone outcrops. In *Reservoir Characterization* (Ed. by L.W. Lake and H.B. Carroll), pp. 141-175. Academic Press, Orlando.

STANLEY, K.O., JORDE, K., RAESTAD, N. & STOCKBRIDGE, C.P. (1990) I. Stochastic modelling of reservoir sand bodies for input to reservoir simulation, Snorre Field, northern North Sea, Norway. In *North Sea Oil & Gas Reservoirs-II* (Ed. by A.T. Buller, E. Berg, O. Hjelmeland, J. Kleppe, O. Torsaeter and J.O. Aasen), 91-101. Graham & Trotman, London.

STONECIPHER, S.A., WINN, R.D. & BISHOP, M.G. (1984) Diagenesis of the Frontier Formation, Moxa Arch: A function of sandstone geometry, texture and composition, and fluid flux. In *Clastic Diagenesis* (Ed. by D.A. MacDonald and R.C. Surdam), pp. 289-316. American Association of Petroleum Geologists Memoir **37**, Tulsa.

SUTTNER, L.J., BASU, A. & MACK, G.H. (1981) Climate and the origin of quartz arenites. *Journal of Sedimentary Petrology*, **51**, 1235-1246.

SWETT, K.G., KLEIN, V. & SMITH, D.E. (1971) A Cambrium tidal sand body - the Eriboll sandstone on northwest Scotland: An ancient - recent analog. *Journal of Geology*, **79**, 400-415.

TOMUTSA, L., JACKSON, S.R., AND SZPAKIEWICZ, M. (1986) Geostatistical characterization and comparison of outcrop and subsurface facies: Shannon shelf sand ridges. Paper presented at the 56th California Regional Meeting of the Society of Petroleum Engineers held in Oakland, California, April 2-4.

TYLER, N. & AMBROSE, W.A. (1983) *Facies Architecture and Production Characteristics of Strandplain Reservoirs in the Frio Formation, Texas*, 42 pp. Bureau of Economic Geology, University of Texas at Austin, Report of Investigations **146**, Austin.

VAIL, P.R., MITCHUM, R.M., JR. & THOMPSON, S., III (1977) Seismic stratigraphy and global changes of sea level, Part 4: cycles of relative changes of sea level. In *Seismic stratigraphy - applications to hydrocarbon exploration* (Ed. by C.E. Payton), pp. 83-97. American Association of Petroleum Geologists Memoir **26**, Tulsa.

VALLONI, R. & MAYNARD, J.B. (1981) Detrital modes of recent deep-sea sands and their relation to tectonic setting: a first approximation. *Sedimentology*, **28**, 75-83.

VAN HEERDEN, I.L. & ROBERTS, H.H. (1988) Facies development of Atchafalaya delta, Louisiana: a modern bayhead delta. *Bulletin*

of the American Association of Petroleum Geologists, **72**, 439-453.

VAN STRAATEN, L.M.J.U., NAGTEGAAL, P., REIJERS, T.J.A., DUNOYER DE SEGONZAC, G., ROTHE, P. & PERCONIG, E. (1980) Diagenesis of non-carbonaceous deposits. In *Geological Nomenclature* (Ed. by W.A. Visser), pp. 246-253. Bohn, Scheltema & Holkema, Utrecht.

VAN VEEN, F.R. (1977) Prediction of permeability trends for water injection in a channel-type reservoir, Lake Maracaibo, Venezuela. Paper presented at the 52nd Annual Fall Technical Conference and Exhibition of the Society of Petroleum Engineers of the American Institute of Mining, Metallurgical, and Petroleum Engineers held in Denver, Colorado, October 9-12.

VAN WAGONER, J.C., MITCHUM, R.M., CAMPION, K.M. & RAHMANIAN, V.D. (1990) *Siliciclastic Sequence Stratigraphy in Well Logs, Cores, and Outcrops: Concepts for High-Resolution Correlation of Time and Facies*, 55 pp. American Association of Petroleum Geologists Methods in Exploration Series **5**, Tulsa.

VERRIEN, J.P., COURAUD, G. & MONTADERT, L. (1967) Applications of production geology methods to reservoir characteristics analysis from outcrops observations. *Proceedings 7th World Petroleum Congress, Mexico*, pp. 425-446.

VISSER, M.J. (1980) Neap-spring cycles reflected in Holocene subtidal large-scale bedform deposits: A preliminary note. *Geology*, **8**, 543-546.

WALDERHAUG, O., AND MJOS, R. (1991) Sandbody geometry in fluvial systems - An example from the Jurassic of Yorkshire, England. In *Reservoir Characterization II* (Ed. by L.W. Lake, H.B. Carroll and T.C. Wesson), pp. 701-703. Academic Press, Orlando.

WEBER, K.J. (1971) Sedimentological aspects of oilfields of the Niger delta. *Geologie en Mijnbouw*, **50**, 559-576.

WEBER, K.J. (1982) Influence of common sedimentary structures on fluid flow in reservoir models. *Journal of Petroleum Technology*, **34**, 665-672.

WEBER, K.J. (1986) How heterogeneity affects oil recovery. In *Reservoir Characterization* (Ed. by L.W. Lake and H.B. Carroll), pp. 487-544. Academic Press, Orlando.

WEBER, K.J. (1987) Hydrocarbon distribution pattern in Nigerian growth fault structures controlled by structural style and

stratigraphy. *Journal of Petroleum Science and Engineering*, **1**, 91-104.

WEBER, K.J., EIJPE, R., LEIJNSE, D. & MOENS, C. (1972) Permeability distribution in a Holocene distributary channel-fill near Leerdam (The Netherlands). *Geologie en Mijnbouw*, **51**, 53-62.

WEBER, K.J. & DAUKORU, E. (1975) Petroleum geology of the Niger delta. *Proceedings 9th World Petroleum Conference*, pp. 209-221.

WEBER, K.J., KLOOTWIJK, P.H., KONIECZEK, J. & VAN DER VLUGT, W.R. (1978) Simulation of water injection in a barrier-bar-type, oil-rim reservoir in Nigeria. *Journal of Petroleum Technology*, **30**, 1555-1565.

WEBER, K.J. & VAN GEUNS, L.C. (1990) Framework for constructing clastic reservoir simulation models. *Journal of Petroleum Technology*, **34**, 439-453.

WEISE, B.R. (1980) *Wave-dominated delta systems of the Upper San Miguel Formation, Maverick Basin, South Texas*, 33 pp. Bureau of Economic Geology, University of Texas at Austin, Report of Investigations **146**, Austin.

WESCOTT, W.A. & ETHRIDGE, F.G. (1980) Fan-delta sedimentology and tectonic setting - Yallahs fan delta, Southeast Jamaica. *Bulletin of the American Association of Petroleum Geologists*, **64**, 374-399.

WHITBREAD, T. & KELLING, G. (1982) Mrar Formation of western Libya - Evolution of an Early Carboniferous delta system. *Bulletin of the American Association of Petroleum Geologists*, **66**, 1091-1107.

WINKER, C.D. (1982) Cenozoic shelf margins, northwestern Gulf of Mexico. *Transactions of the Gulf Coast Association of Geological Societies*, **32**, 427-448.

WRIGHT, L.D. & COLEMAN, J.M (1973) Variations in morphology of major river deltas as functions of ocean wave and river discharge regimes. *Bulletin of the American Association of Petroleum Geologists*, **57**, 370-398.

WRIGHT, L.D., COLEMAN, J.M. & THOM, B.G. (1975) Sediment transport and deposition in a high tide range environment: Cambridge Gulf Ord delta, western Australia. *Journal of Geology*, **81**, 15-41.

YURETICH, R.F (1986) Controls on the composition of modern sediments, Lake Turkana, Kenya. In *Sedimentation in African Rifts* (Ed. by

L.E. Frostick, R.W. Renaut, I. Reid and J.J. Tiercelin), pp. 141-152. Blackwell, Oxford.

ZHIWU, W., QINING, W., BOHU, L., CHENGJING, L. & XIANGZHONG, L. (1982) Ways to improve development efficiency of Daqing oil field by flooding. In *Oil field Development Techniques: Proceedings of the Daqing International Meeting, 1982* (Ed. by J.F. Mason and P.A. Dickey), pp. 49-62. American Association of Petroleum Geologists Studies in Geology **28**, Tulsa.

ABSTRACT

Numerical simulation models are used to predict the production behaviour of hydrocarbon reservoirs. The reliability of these models largely depends on the accuracy of the description of the reservoir architecture and the spatial variability of rock properties. More needs to be known about these factors, so that the accuracy of the simulations can be improved. The research described in this thesis investigated the reservoir architecture and spatial variability of deltaic rocks, a lithological category which frequently contains hydrocarbons and for which much data are available.

The sedimentation in deltaic rocks is considered in relation to tectonic setting and the characteristics of the hinterland and receiving basin. Classification schemes for deltaic rocks are evaluated. Some modifications are proposed, resulting in a classification scheme specifically for reservoir characterization. This scheme recognizes seven delta types, according to vertical rock succession and sand distribution pattern. The mineralogy of deltaic sediments and the most common diagenetic processes are discussed.

The use of reservoir data in the description of reservoir architecture is examined and the modelling techniques most commonly used to characterize reservoirs are critically evaluated. It is concluded that the object-based modelling of reservoir architecture has the most potential. However, at the moment too few geological data are available to condition such models. A methodology for building knowledge bases for quantitatively predicting reservoir architecture and permeability distribution is developed. It uses data from recent environments, outcrops and densely drilled fields. Examples of data collection are shown from the Recent Atchafalaya delta (Louisiana) and the Oligocene Frio Formation of the North Markham-North Bay City field (Texas).

A study of the sedimentology of reservoir rocks that influence fluid flow shows that sorting trends, sedimentary structures and shales are most important. Characterization of sandy genetic units based on

these three parameters shows that the 26 genetic sandy units recognized in deltaic rocks can be represented by only 8 models that differ with respect to fluid flow. The relation between sorting and permeability is analysed. Methods for the calculation of permeability anisotropy caused by sedimentary structures are evaluated and techniques for calculating vertical permeabilities in sand/shale sequences are critically reviewed. The combined effect of the different types of heterogeneity is also considered. Detailed geological models are constructed for each of the 8 basic flow elements. The scale of these models is comparable with the size of reservoir simulation grid blocks commonly used. Characteristic horizontal and vertical permeability anisotropies are established for each type of sedimentologically defined flow unit configuration. To illustrate the use of these parameters, they are used as input in a waterflood simulation in the seven most common delta types. The results give characteristic sweep patterns for each delta type.

SAMENVATTING

Om het produktiegedrag van koolwaterstofreservoirs te voorspellen wordt gebruik gemaakt van numerieke simulatie-modellen. De betrouwbaarheid van deze modellen hangt voor een groot deel af van de nauwkeurigheid van de beschrijving van de gesteenteëigenschappen in het reservoir. Op dit moment is de kennis over deze fenomenen nog zo gering dat de uitkomsten van deze simulaties vaak onbetrouwbaar zijn. Dit proefschrift richt zich op het verbeteren van bestaande technieken voor het beschrijven van gesteenteëigenschappen. Het proefschrift richt zich met name op delta-afzettingen omdat er al veel onderzoek naar deze afzettingen is uitgevoerd dat als basis gebruikt kan worden voor deze studie. Verder bevatten delta-afzettingen regelmatig koolwaterstoffen.

Sedimentatie in deltamillieus is beschouwd in relatie tot het tectonische kader en de karakteristieken van het achterland en het ontvangende bekken. Klassifikatieschemas voor delta-afzettingen zijn geëvalueerd. Enkele wijzigingen op bestaande schemas zijn voorgesteld. Dit resulteert in een klassificatieschema specifiek voor reservoirkarakterisatie-doeleinden. In dit klassifikatieschema worden 7 deltatypen onderscheiden welke gekarakteriseerd zijn op basis van de vertikale gesteente-opeenvolging en laterale zandverdeling. De mineralogische samenstelling van delta-afzettingen en de meest voorkomende diagenetische processen zijn bestudeerd.

Het nut van gegevens uit het reservoir voor de beschrijving van de reservoirarchitektuur is onderzocht en de meest gebruikte modelleringstechnieken zijn besproken. Er wordt geconcludeerd dat 'object-based' technieken voor het modelleren van de reservoirarchitektuur waarschijnlijk de meeste mogelijkheden bieden. Op het moment is er echter een gebrek aan kwantitatieve geologische informatie voor het konditioneren van deze modellen. Een methode voor het opbouwen van een kwantitatief geologisch gegevensbestand is ontwikkeld. Deze methode gebruikt gegevens van recente afzettingen, ontsluitingen en dichtbeboorde velden. Voorbeelden van het verzamelen van gegevens worden gegeven voor de Recente Atchafalaya delta

(Louisiana) en de Oligocene Frio Formatie in het North Markham-North Bay City veld (Texas).

De sedimentologische parameters zijn beschouwd die het meest van belang zijn voor vloeistofstroming. Deze parameters zijn de korrelgrootte trend, sedimentaire structuren en de verbreiding van schalies. Karakterisatie op basis van deze parameters laat zien dat de 26 zandige genetische eenheden die binnen deltas zijn te onderscheiden gerepresenteerd kunnen worden door 8 basiseenheden in relatie tot vloeistofstroming. De relatie tussen sorteringstrend en permeabiliteitstrend is onderzocht. Methodes voor de bepaling van permeabiliteitsanisotropie tengevolge van sedimentaire structuren zijn geëvalueerd en technieken voor de bepaling van vertikale permeabiliteit in zand/schalie opeenvolgingen zijn kritisch bekeken. Ook is het gecombineerde effect van deze parameters beschouwd. Gedetailleerde modellen zijn geconstrueerd voor de 8 elementaire vloeistofeenheden. Voor elk van deze eenheden zijn karakteristieke permeabiliteitsanisotropieën berekend. Om het nut van deze parameters te illustreren is een aantal simulaties uitgevoerd van het verdringen van olie door water in modellen van de 7 meest voorkomende delta types. De resultaten geven karakteristieke verdringingspatronen voor elk delta type.

CURRICULUM VITAE

Name : Mijnssen, Frans Christiaan Jacobus

Born : January 1, 1963

Nationality : Dutch

EDUCATION

1969 - 1975 : Primary school, Hildebrand School, Amsterdam

1975 - 1981 : Secondary School, (Buitenvelderts Lyceum, Amsterdam; Nassau Veluwe College, Harderwijk)

1981 - 1987 : State University of Utrecht, Department of Geology and Geophysics (doctoral degree)

1987 - 1991 : Delft University of Technology, Department of Mining and Petroleum Engineering (doctorate degree)